

EFFECT OF MORPHOLOGY AND MINERALOGY ON COMPRESSIBILITY OF SANDS

by

RAHIM ABEDINZADEH

EE
1989
D
9BE
EFF

TH
DC/1989/D
Ab. 3c



DEPARTMENT OF CIVIL ENGINEERING

INDIAN INSTITUTE OF TECHNOLOGY KANPUR

MAY 1989

25 FEB 2009 / CE

दुर्घटनाकारी सेवक पुस्तकालय

दृष्टिकोणीय संस्थान ब्राह्मण

141992

अंकार्धि क्र० A



A141992

Dedicated

To

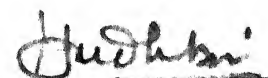
my guides

and

my wife

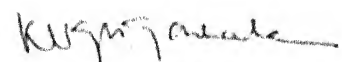
CERTIFICATE

This is to certify that the thesis entitled, "EFFECT OF MORPHOLOGY AND MINERALOGY ON COMPRESSIBILITY OF SANDS", by Mr. Rahim Abedinzadeh, for the award of the Degree of Philosophy, of Indian Institute of Technology, Kanpur is a record of bonafide research work carried out by him under our supervision and guidance. The result embodied in this thesis have not been submitted to any other university or institute for the award of any degree or diploma.



(YUDHBIR)

Professor

Department of Civil Engineering
Indian Institute of Technology, Kanpur

(K.V.G.K. GOKHALE)

Professor

Department of Civil Engineering
Indian Institute of Technology, Kanpur

April, 1989

ACKNOWLEDGEMENTS

The author feels immense gratitude and indebtedness to Professor Yudhbir, who provided invaluable guidance, inspiration, numerous suggestions and took keen interest in the progress of the research work and preparation of the manuscript of the thesis.

In the same breath the author expresses his deep gratitude to Professor K.V.G.K. Gokhale for his ceaseless encouragement and critical interest at every stage of the work. Without the active involvement of both of them the many hurdles faced during the research work could hardly have been overcome and the thesis endeavour brought to its fruition.

Special thanks are due to Professor T.R. Ramachandran and Dr. Sanjay Gupta of Material Science Department and Dr. P.K. Basudhar, Dr. A.K. Mittal, Dr. B. Rath, Dr. G. Barua and Dr. A.P. Shukla for their help.

The author is grateful to his friends Dr. S. Bhargava and G. Roy for their immense help during the last stage of the work. The author would also like to sincerely thank his friends Dr. A.K. Nayak, Dr. A. Sanyal, Dr. I.K. Bhat, Mr. Saeid Fattahi, Mr. G. Bhattacharya and others for their help.

The author wishes to acknowledge the day to day help of Mr. A.K. Srivastava, Mr. R.P. Trivedi, Mr. Gulab Chand and Parasuram of Geotechnical Laboratory and Mr. B.K Jain of Material Testing Laboratory (ACMS).

The assistance of Mr. S.V. Kapoor, Mr. Siddiqui and Mr. R.V. Verma in fabricating the experimental set up and Mr. M.L. Srivastava and Mr. S.D. Dubey for their helpful co-operation is sincerely acknowledged.

The neat typing work of Mr. A.C. Pandey and careful tracing work of Mr. B.K. Jain is very much appreciated.

Finally, the author places in record his indebtedness and high appreciation for the patience and endurance shown by his beloved wife, Shahnaz.

AUTHOR

LIST OF CONTENTS

	PAGE NO.
TITLE PAGE	i
DEDICATION	ii
CERTIFICATE	iii
ACKNOWLEDGEMENT	iv
TABLE OF CONTENTS	vi
LIST OF TABLES	x
LIST OF FIGURES	xi
LIST OF PLATES	xxi
NOTATIONS	xxii
SYNOPSIS	xxiv
 CHAPTER I INTRODUCTION	 1
1.1 General	1
1.2 Organisation of Thesis	2
 CHAPTER II LITERATURE REVIEW	 4
2.1 General	4
2.2 Morphology of Sands	7
2.2.1 Grain Shape	8
2.2.1.1 Surface Texture	8
2.2.1.2 Roundness	8
2.2.1.3 Sphericity	13
2.2.2 Classification of Shape Type	16
2.2.3 Effect of Morphology of Sand on its Engineering Properties	20
2.3 Behaviour of Sands at Low and High Confining Pressure	22
2.4 Compressibility	25

2.5	Particle Crushing	34
2.5.1	Types of Crushing	36
2.5.1.1	Shearing of Asperities	34
2.5.1.2	Splitting of Soil Grains	36
2.5.1.3	Breakdown of Shear Asperities	37
2.5.1.4	Breakdown of Asperities due to the stress Reversals	38
2.5.2	Quantitative Expressions for Degree of Crushing	38
2.5.3	Particle Crushing and its Effect on Engineering Properties of Granular Soil	42
2.6	Scope of Work	46
 CHAPTER III MATERIAL AND METHODS		49
3.1	General	49
3.2	Material Used	49
3.2.1	Ganga Sand	49
3.2.2	Calcareous Sand	50
3.2.3	Kalpi Sand	53
3.2.4	Standard Sand	53
3.3	Experimental	56
3.3.1	Preparation of Samples of Specific Relative Densities Values	56
3.3.2	Mineralogical Characterization	56
3.3.3	Compressibility	58
3.3.4	Particle Shape Analysis	60
3.3.4.1	Microscope and Scanner	60
3.3.4.2	Basic Module	61
3.3.4.3	Display Unit	61
3.3.4.4	Entire Field Count Unit	61
3.3.4.5	Measurement Unit	61
3.3.4.6	Particle Measurement	61
3.3.4.7	Quantification of Particle shape	67
3.3.4.7.1	Sphericity and Shape Factor	67
3.3.4.7.2	Roundness (Angularity)	69
 CHAPTER IV EXPERIMENTAL DATA		74
4.1	General	74
4.2	Mineralogical Composition	74
4.3	Physical Characteristics	79

4.4	Morphological Characteristics	90
4.5	Compressibility	90
4.6	Crushing	116
CHAPTER V	INTERPRETATION AND DISCUSSION OF TEST DATA	146
5.1	Grain Morphology	146
5.1.1	Sphericity and Shape Factor	147
5.1.2	Particle Angularity	148
5.1.3	Shape Factor versus Sphericity	151
5.1.4	Average Roundness versus Average Number of Tangents	155
5.1.5	Distribution of Tangents	156
5.1.6	Typical Distributions of Shape Characteristics of Sands	166
5.1.7	Main Observations	174
5.2	Particle Modification and Crushing During Compression	177
5.2.1	General	177
5.2.2	Modification of Size and Shape of Grains	178
5.2.3	Particle Breakage	180
5.2.4	Variation of B_T with Stress	185
5.2.5	Variation of B_T with d_{50}	193
5.2.6	Particle Modifications	195
5.2.6.1	Changes in Grain Shape	196
5.2.6.2	Changes in Grain Angularity	198
5.2.7	Particle Crushing	209
5.2.7.1	Variation of B_r with stress	210
5.2.8	Hardin's Model for Particle Crushing	222
5.3	Compressibility and Constrained Modulus of Sands	239
5.3.1	Compressibility	239
5.3.1.1	General	239
5.3.1.2	Test Results	243
5.3.2	Constrained Modulus	253
5.3.2.1	Analysis of Experimental Results	264
5.3.2.2	Effect of Grain Mineralogy on the Relationship between Modulus and Stress	273
5.3.3	Application of Test Results to the Estimation of Cone Penetration Resistance in Sands	277
5.3.3.1	Calculation of q_c for sands with Varying Degree of Compressibility	277

5.3.3.2 Comparison between Predicted and Measured Modulus versus Stress Relationships for Sands	283
5.3.3.3 Relationship Between q_c and Angle of Shearing Resistance	294
5.3.3.4 Relationship Between M and q_c	294
CHAPTER VI CONCLUSIONS	304
REFERENCES	314

LIST OF TABLES

Table No.	Page
2.1 Roundness Grades	10
2.2 Roundness Grades (Powers, 1953)	12
2.3 Zingg Classification of Particle Shape	17
3.1 Experimental Programme	57
4.1 Mineral Contents of Different Sands	87
4.2 Percentage of Carbonate Fraction (Acid Dissolution Method)	88
4.3 Various Physical Properties of Sands	94
5.1 Percentage of Particles in Each Quadrant	149
5.2 Weighted Average of Shape Factor, Sphericity, Number of Tangent, $h/$ and Roundness Index	154
5.3 Gradation, Size, Mineralogy and Grain Breakage Parameters for Variety of Sands	183
5.4 Values of d_{50} , B_T , and B_r for Different Sands at Effective Stress of 80 Kg/cm^2	217
5.5 Value of Shape Number, Roundness Index and Tangent for Different Particle Shapes	241
5.6 Classification of Sands According to Their Compressibility	254
5.7 Model Parameters for Constrained Modulus (M) of Variety of Sands	265
5.8 Suggested Model Parameters for Modulus (M) and Cone Penetration Resistance (q_c)	284
5.9 Range of Value for Sands with Ranging Compressibility	300

LIST OF FIGURES

Fig.No.		Page
2.1	Zingg Diagram with Lines of Equal Sphericity	18
2.2	Different Types of Crushing	37
3.1	Block Diagram of Material Testing System	59
3.2	Block Diagram of Image Analyzer	63
3.3	Different Types of Single Feature Measurement	65
3.4	Lower Positive and Negative Tangents and Two Features Engaged in Each Other	68
4.1	X-ray Diffraction Pattern of Ganga Sand	75
4.2	X-ray Diffraction Pattern of Kalpi Sand	77
4.3	X-ray Diffraction Pattern of Calcareous Sand	78
4.4	X-ray Diffraction Pattern of Standard Sand	80
4.5	X-ray Diffraction Pattern of Ganga Sand with Enhanced Mica	81
4.6	X-ray Diffraction Pattern of Ganga Sand with Mica Removed	82
4.7	X-ray Diffraction Pattern of Coarse Ganga Sand	83
4.8	X-ray Diffraction Pattern of Artificial Calcareous Sand	84
4.9	X-ray Diffraction Pattern of Kalpi 1 Sand	85
4.10	X-ray Diffraction Pattern of Kalpi 2 Sand	86
4.11	Particle Size Distribution of Ganga, Standard, Calcareous and Kalpi Sands	89
4.12	Particle Size Distribution of Kalpi 1, Kalpi 2, Ganga with Mica Enhanced, Ganga with Mica Removed, Coarse Ganga and Artificial Calcareous Sands	89
4.13	Relative Density versus Height of Fall	91
4.14(a)	Relative Density versus Height of Fall	92

4.14(b) Variation of Relative Density with Rate of Pouring for Different Sands	93
4.15 Shape Classification Using Zingg Diagram for Ganga Sand	95
4.16 Shape Classification Using Zingg Diagram for Ganga Sand Subjected to 22.04 Kg/cm ²	96
4.17 Shape Classification Using Zingg Diagram for Ganga Sand Subjected to 176.32 Kg/cm ²	97
4.18 Shape Classification Using Zingg Diagram for Coarse Ganga Sand	98
4.19 Shape Classification Using Zingg Diagram for Kalpi Sand	99
4.20 Shape Classification Using Zingg Diagram for Kalpi Sand Subjected to 22.04 Kg/cm ²	100
4.21 Shape Classification Using Zingg Diagram for Kalpi Sand Subjected to 176.32 Kg/cm ²	101
4.22 Shape Classification Using Zingg Diagram for Kalpi 1	102
4.23 Shape Classification Using Zingg Diagram for Kalpi 2	103
4.24 Shape Classification Using Zingg Diagram for Calcareous Sand	104
4.25 Shape Classification Using Zingg Diagram for Calcareous Sand Subjected to 22.04 Kg/cm ²	105
4.26 Shape Classification Using Zingg Diagram Calcareous Sand Subjected to 176.32 Kg/cm ²	106
4.27 Shape Classification Using Zingg Diagram for Artificial Clacareous	107
4.28 Shape Classification Using Zingg Diagram for Standard Sand	108
4.29 Shape Classification Using Zingg Diagram for Ottawa Sand	109

4.30	Shape Classification Using Zingg Diagram for San Fernando # 5 Sand	110
4.31	Shape Classification Using Zingg Diagram for San Fernando # 6 Sand	111
4.32	Shape Classification Using Zingg Diagram for San Fernando # 7 Sand	112
4.33	Shape Classification Using Zingg Diagram for Leighton Buzzard Sand	113
4.34	Shape Classification Using Zingg Diagram for Lagunillas (94A-M19) Sand	114
4.35	Shape Classification Using Zingg Diagram for Lagunillas (94A+94B) Sand	115
4.36	Range of Shape Factor for Ganga Sand	117
4.37	Range of Shape Factor for Ganga Sand Subjected to 22.04 Kg/cm ²	118
4.38	Range of Shape Factor for Ganga Sand Subjected to 176.32 Kg/cm ²	119
4.39	Range of Shape Factors for Coarse Ganga Sand	120
4.40	Range of Shape Factors for Kalpi Sand	121
4.41	Range of Shape Factors for Kalpi Sand Subjected to 22.04 Kg/cm ²	122
4.42	Range of Shape Factors for Kalpi Sand Subjected to 176.32 Kg/cm ²	123
4.43	Range of Shape Factors for Kalpi 1	124
4.44	Range of Shape Factors for Kalpi 2	125
4.45	Range of Shape Factors for Calcareous Sand	126
4.46	Range of Shape Factors for Calcareous Subjected to 22.04 Kg/cm ²	127
4.47	Range of Shape Factors for Calcareous Subjected to 176.32 Kg/cm ²	128

4.48	Range of Shape Factors for Artificial Calcareous	129
4.49	Range of Shape Factors for Standard Sand	130
4.50	Range of Shape Factors for Ottawa Sand	131
4.51	Range of Shape Factors for San Fernando # 5 Sand	132
4.52	Range of Shape Factors for San Fernando # 6 Sand	133
4.53	Range of Shape Factors for San Fernando # 7 Sand	134
4.54	Range of Shape Factors for Leighton Buzzard Sand	135
4.55	Range of Shape Factors for Lagunilla (94A-M19) Sand	136
4.56	Range of Shape Factors for Lagunillas (94A+94B) Sand	137
4.57	One Dimensional Compression Behaviour of Sands	138
4.58	One Dimensional Compression Behaviour of Sands	139
4.59	One Dimensional Compression Behaviour of Sands	140
4.60	Particle Size Gradation Before and after Loading for Ganga Sand	141
4.61	Particle Size Gradation Before and After Loading for Calcareous Sand	141
4.62	Particle Size Gradation Before and After Loading for Kalpi Sand	142
4.63	Particle Size Gradation Before and After Loading for Standard Sand	142
4.64	Particle Size Gradation Before and After Loading for Kalpi 1 Sand	143
4.65	Particle Size Gradation Before and After Loading for Kalpi 2 Sand	143

4.66	Particle Size Gradation Before and After Loading for Artificial Calcareous Sand	144
4.67	Particle Size Gradation Before and After Loading for Coarse Ganga Sand	144
4.68.	Particle Size Gradation Before and After Loading for Ganga with Mica Removed and Ganga with Enhanced Mica	145
5.1(a)	Relationship Between Particle Angularity and Particle Size	152
5.1(b, c)	Relationship Between Tangent Count and Roundness Index as well as Sphericity and Shape Factor	153
5.2	Tangent Count Distribution for Standard Sand	157
5.3	Tangent Count Distribution for Calcareous Sand	158
5.4	Tangent Count Distribution for Ganga Sand	159
5.5	Tangent Count Distribution for Kalpi Sand	160
5.6	Tangent Count Distribution for Kalpi 1 Sand	162
5.7	Tangent Count Distribution for Kalpi 2 Sand	163
5.8	Tangent Count Distribution for Coarse Ganga Sand	164
5.9	Tangent Count Distribution for Artificial Calcareous Sand	165
5.10	Tangent Count Distribution for Ottawa Sand	167
5.11	Tangent Count Distribution for Leighton Buzzard Sand	168
5.12	Tangent Count Distribution for Lagunillas (94A-M19) Sand	169
5.13	Tangent Count Distribution for Lagunillas (94A+94B) Sand	170
5.14	Tangent Count Distribution for San Fernando Mix #5 Sand	171
5.15	Tangent Count Distribution for San Fernando Mix # 6 Sand	172

5.16	Tangent Count Distribution for San Fernando Mix # 7 Sand	173
5.17	Typical Distribution of Surface Characteristics for Subrounded to Rounded and Subangular to Subrounded Sands	175
5.18	Typical Distribution of Surface Characteristics for Angular and Very Angular Sands	176
5.19	Definition of Potential and Total Breakage	179
5.20	Grain Size Distribution of Different Sands Used for Calculating Total Potential Breakage	181
5.21	Grain Size Distribution of Variety of Sands Used for Calculating Total Potential Breakage	182
5.22	Relationship Between Potential Breakage and Particle Size	184
5.23	Relationship Between Total Breakage and Stress Level for Variety of Sands	186
5.24	Particle Size Distribution Before and After Loading for Mol and Tayoura Sands	187
5.25	Particle Size Distribution Before and After Loading for Chattahoochee River and Ottawa Sands	188
5.26(a)	Relationship Between Total Breakage and Grain Angularity for Different Sand at Relative Density of 0.25 and Stress Level of 22.04 Kg/cm^2	192
5.26(b)	Relationship Between Average Particle Size and Total Breakage	194
5.27	Relationship Between Flatness and Elongation Ratios Showing the Particle Degradation Under Stress for Standard, Ganga, Calcareous and Kalpi Sands	197
5.28	Distribution of Tangents at Stress Level of 22.04 and 176.32 Kg/cm^2	199
5.29	Distribution of Tangents at Stress Level of 22.04 and 176.32 Kg/cm^2 for Calcareous Sand	200

5.30	Distribution of Tangents at Stress Level of 22.04 and 176.32 Kg/cm ² for Kalpi Sand	201
5.31	Smooth Edge Distribution at Stress Level of 22.04 and 176.32 Kg/cm ² for Ganga Sand	203
5.32	Smooth Edge Distribution at Stress Level of 22.04 and 176.32 Kg/cm ²	204
5.33	Smooth Edge Distribution at Stress Level of 22.04 and 176.32 Kg/cm ² for Kalpi Sand	205
5.34	Relationship Between Average Grain Angularity and Average Tangent Count at Stress Level of 22.04 and 176.32 Kg/cm ² for Variety of Sands	206
5.35	Relationship Between the Relative Breakage and Grain Angularity for Variety of Sands	208
5.36	Relationship Between Relative Breakage and Vertical Effective Stress	211
5.37	Relationship Between Relative Breakage and Vertical Effective Stress	212
5.38	Variation of Relative Breakage at Low Stress and Model Prediction	213
5.39	Variation of Relative Breakage at High Stresses	214
5.40	Variation of Relative Breakage with Mineral Content of Sands	219
5.41	Relationship Between Relative Breakage and Breakage Effective Stress	223
5.42	Relationship Between Relative Breakage and σ_1/P_a for Crushed Granite (Based on Data from Lee and Farhoomand, 1967)	226
5.43	Relationship between σ_1/P_a and Relative Breakage (Based on Data from Hardin, 1985)	227
5.44	Relationship Between b/σ_1 and K	229
5.45	Relationship Between Relative Breakage and Breakage Effective Stress	231
5.46	Relationship Between Relative Breakage and Breakage Effective Stress	233

5.47	Relationship Between Relative Breakage and Breakage Effective Stress	234
5.48	Gradation Curve Before and After Loading for Ganga, Ganga Enhanced Mica 1 Kalpi 1 Kalpi 2 Sands	238
5.49	Relationship Between Shape Number and Roundness	240
5.50	Stress-Straion Relationship for the Loose Sands at High Stress Level	244
5.51	Stress-Strain Relationship at Low Confining Stress for Loose Sands	245
5.52(a)	Stress-Strain Relationship at Low Confining Stress for Loose Sands	246
5.52(b)	Model Plate Load Tests at Constant Relative Density for Four Sands	249
5.53	Stress-Strain Relationship for Variety of Sands at High Confining Stress	252
5.54	Relationship Between Constrained Modulus and Relative Density at Different Stress Levels for Standard Sand	256
5.55	Relationship Between Constrained Modulus and Relative Density at Different Stress Levels for Calcareous Sand	257
5.56	Relationship Between Constrained Modulus and Relative Density at Different Stress Level for Ganga Sand	258
5.57	Relationship Between Constrained Modulus and Relative Density at Different Stress Level for Ganga Sand	259
5.58	Evaluation of m_0 , m_1 and m_2 Coefficients for Standard Sand	260
5.59	Evaluation of m_0 , m_1 and m_2 Coefficients for Calcareous Sand	261
5.60	Evaluation of m_0 , m_1 and m_2 Coefficients for Ganga Sand	262
5.61	Evaluation of m_0 , m_1 and m_2 Coefficients for Ganga Sand	263
5.62	Relationship Between Constrained Modulus Effective Confining Stress for Standard Sand	266

5.63	Relationship Between Constrained Modulus and Effective Confining Stress for Calcareous Sand	267
5.64	Relationship Between Constrained Modulus and Effective Confining Stress for Kalpi and Calcareous Sands	268
5.65	Relationship Between Constrained Modulus and Effective Confining Stress for Kalpi 2 Sand	269
5.66	Relationship Between Constrained Modulus and Effective Confining Stress for Ganga Sand	270
5.67	Comparison of Modulus versus Effective Confining Stress at Low Stress Level for Ganga, Kalpi, Calcareous and Standard Sands	274
5.68	Relationship Between Critical Stress and Relative Density for Different Sands	275
5.69	Dependence of Critical Stress and m_0 on Mineral Content	276
5.70	Effect of Mica on Modulus versus Effective Confining Stress Relationship for Ganga Sand	276
5.71	Relationship Between Bearing Capacity Number and Peak Friction Angle	278
5.72	Relationship Between Peak Friction Angle and Relative Density for Standard Sand at Different Stress Levels	280
5.73	Relationship Between Peak Friction Angle and Relative Density for Ganga and Kalpi at Different Stress Levels	281
5.74	Relationship Between and Void Ratio (or Relative Density)	282
5.75	Effect of Relative Density and Effective Stress on Modulus for Standard Sand	285
5.76	Effect of Relative Density and Effective Stress on Modulus for Calcareous Sand	286
5.77	Effect of Relative Density and Effective Stress on Modulus for Kalpi Sand	287
5.78	Effect of Relative Density and Effective Stress on Modulus for Ganga Sand	288

5.79	Effect of Relative Density and Effective Stress on Modulus for Ganga, Kalpi, Standard and Calcareous Sands	289
5.80	Comparison of Modulus versus Effective Stress for Three Types of Sands at Two Relative Densities	291
5.81	Comparison of q_c versus Effective Stress for Three Types of Sands at Two Relative Densities	292
5.82(a)	Relationship Between Model Parameters for Modulus, q_c and Particle Roundness	293
5.82(b)	Relationship Between q_c and Angle of Shearing Resistance	295
5.83	Relationship Between Modulus and q_c for Sands of Low Compressibility	297
5.84	Relationship Between Modulus and q_c for Sands of Moderate Compressibility	298
5.85	Relationship Between Modulus and q_c for Sands of High Compressibility	299
5.86	Relationship Between Relative Density for Sands	301

LIST OF PLATES

Plate No.		Page No.
3.1	Ganga Sand	51
3.2	Calcareous Sand	52
3.3	Ralpi Sand	54
3.4	Standard Sand	55
3.5	Image Analyzer Set Up	62
3.5	Projected Image of Particle with Edge Protrusions	71

NOTATIONS

K	=	Roundness value
A	=	Area measured by a Planimeter
P	=	Perimeter measured by a map measurer
R_j	=	Average roundness value for the sieve fraction
R_i	=	Roundness value assigned to the particle i
R	=	Roundness for sand specimen
	=	Sphericity
a, d_L	=	Longest diameter
b, d_I	=	Intermediate diameter
c, d_S	=	Shortest diameter
P	=	Flatness ratio
q	=	Elongation ratio
S.F.	=	Shape Factor
M	=	Constrained modulus
m_o, M_{SW}	=	Modulus number
m_1	=	Exponent indicating rate of change of M with stress
m_2	=	Exponent indicating rate of change of M with Relative Density
'	=	Effective normal stress
e_{max}	=	Maximum void ratio
e_{min}	=	Minimum void ratio
n	=	Porosity
B_g	=	Percentage by weight of the solid phase that has undergone breakage
q	=	Volume of broken particles
C_c	=	Crushing coefficient

b_p	=	Potential breakage for a particle
B_p	=	Potential breakage for sand
B_T	=	Total breakage for sand
B_r	=	Relative breakage
T_j	=	Average value of Tangents for each sieve fraction
T_i	=	Total number of Tangent counts for particle i
T	=	Average value of Tangents for sand
d_p	=	Diameter of an equivalent circle
h	=	Amplitude of the Grain Protrusion
	=	Wave length of the surface protrusion
PA	=	Particle angularity
b	=	Breakage effective stress
r	=	Breakage reference effective stress
n_b	=	Breakage number
n_s	=	Shape number
h	=	Crushing hardness
K	=	Coefficient of subgrade reaction
c	=	Critical stress
	=	Angle of shearing resistance
q_c	=	Cone penetration resistance
	=	

EFFECT OF MORPHOLOGY AND MINERALOGY ON
COMPRESSIBILITY OF SANDS

A Thesis Submitted
in Partial Fulfilment of the Requirements
for the Degree of

DOCTOR OF PHILOSOPHY

by
RAHIM ABEDINZADEH

to the

Department of Civil Engineering
Indian Institute of Technology, Kanpur

April 1989

SYNOPSIS

Mechanical behaviour of a granular material is controlled by its constituent particle characteristics. The particle size, gradation, shape and angularity together with the relative density play an important role in the deformation characteristics of sands. Although classification of a sand for engineering purposes is based on the size attributes, the presence of mineral constituents with compositional differences such as quartz, feldspar, mica and carbonates results in significant changes in the engineering behaviour of the system. While the importance of all these parameters in understanding the behaviour of granular material has been recognized earlier, adequate attention has not been bestowed to study in detail the

influence of all these parameters on the system behaviour. Further, not enough attempts have been made to quantify some of these aspects. There is also a need to study the particle modification at low stress levels prior to particle crushing especially with reference to the liquefaction potential of sands. Available literature on this aspect is scanty. In the present study, an attempt has been made to investigate all these aspects.

Three natural sands of differing mineral composition and an artificially prepared quartz sand were chosen. In addition, six more samples have also been prepared using these four sands through size fractionation, mineral separation and selective mixing. Seven samples of sands as obtained from RPI New York were also used in the study. All these samples have been characterized in terms of their sphericity, shape factor, and angularity. The quantification of particle shape has been achieved using these three parameters. Compressibility tests were carried out for the ten samples under differing relative density conditions and varying stress levels. A scheme for classification of sands on the basis of compressibility was evolved using the results from the present study and test data available from different sources in the literature. For the different classes of compressibility as proposed in the present work, studies on constrained modulus (M) have enabled the estimation of coefficients in the constrained modulus expression. In addition, the modifications in particle size and shape have been systematically monitored for specimens subjected to compression. The stress levels within which the particle

modification takes place for different sands, prior to crushing have been established. Role of particle size, angularity, shape, relative density and mineral composition on compressibility, constrained modulus, modification and crushing has been established. Predictions of cone penetration resistance (q_c) for sands of different compressibility on the basis of results in the present study and available theoretical models (Janbu 1974) are shown to be in complete agreement with the trends reported.

The work contained in the thesis has been organized into six chapters. In chapter one, the topic has been introduced and the scope of the present study has been outlined. The available literature on the characterization of shape of particles, its influence on, stress-strain-dilatancy behaviour, compressibility characteristics, and mechanism of grain modification as well as crushing under different stress conditions has been reviewed in Chapter Two. The materials and methods involved are described in detail in Chapter Three. The four sands (Ganga, Calcareous, Kalpi and Standard samples) have been characterized for their mineralogical composition using X-ray diffraction. Particle shape analysis has been carried out using an image analyzer system. Details of this equipment and procedures of measurements are presented in this chapter. The various expressions used for the quantification of particle shape such as sphericity, shape factor and angularity are explained. Sample preparation and the test procedure for compression test has also been outlined. Chapter four deals with the experimental data concerning mineralogical

composition, physical characteristics, morphology, compressibility and crushing. While the Ganga Sand is composed of quartz (60-65%), feldspar (20-25%) and mica (8 to 10%) with minor amount (upto about 3%) of chlorite and kaolonite, Kalpi sand has calcite upto around 18% with quartz and feldspar in equal proportion (40% each) together with minor quantity of mica (upto 2%). The calcareous sand has carbonate upto 95% with subordinate quartz (upto 5%). Aragonite and calcite are the main minerals. The standard sand is a pure quartz sand. Grain size distribution and morphological characteristics for all these sands have been presented. Data on compressibility for dry sands with loose and dense relative densities were obtained upto a confining pressure of 176.32 Kg/cm^2 and deformation characteristics are presented. Grain size distributions for sand samples on completion of compression tests are contrasted with the original gradation. In Chapter Five, the test data obtained are interpreted in terms of various operative parameters and the details are presented on morphological classification and role of grain modification and crushing on compressibility and constrained modulus. The role of mineralogical composition in the behaviour of sand under stress has also been brought out. Interrelationships between various parameters used for the description of surface characteristics are established. It has been brought out that for the classification of sands, in addition to the usual tests (e_{\max} , e , e_{\min} , grain size distribution etc.), shape and angularity characteristics of sand grains should also be evaluated and this has been accomplished using a

technique proposed in the present study. It is shown that based on grain size, shape, angularity, mineralogy, gradation and relative density natural sands experience particle degradation to a varying degree under stress. On the basis of particle gradation characteristics before and after compression, an expression for total potential for particle degradation as related to d_{50} has been established. It has also been brought out that there exists a critical stress level at which the grain modification of an alluvial sand is initiated. This stress is much less than the stress level required for actual grain crushing. It has been indicated that critical stress value is of the order of $8-9 \text{ kg/cm}^2$ for Ganga and calcareous sands whereas it is around 16 kg/cm^2 for Kalpi sand; the standard sand showing no modification at all even upto stress level of 176 Kg/cm^2 . It has been indicated that the compressibility of sands is strongly controlled among other factors by mineralogy and angularity. At a low stress level, the stress-strain behaviour of sands with significant amount of mica and or carbonates is mainly governed by grain inter-locking. At high stresses, the stress-strain behaviour is significantly different from that at low stress due to grain modification and crushing. Depending on mineral composition, particle size, shape, angularity and gradation, grouping of sands into three broad categories - sands of low, moderate and high compressibility, has been proposed on the basis of their compressibility characteristics. The power laws governing variation of constrained modulus with effective confining stress and relative density as reported in the literature, tacitly

assume that the sand remains unchanged during loading to high stress. It has been established in the present study that particle modification and crushing at high stress level (greater than the critical stress) influence the stress-strain behaviour of sand. Hence, these power laws are strictly applicable for stress levels less than the critical stress. The power laws of the type proposed by Belotti et al. (1985) between q_c and effective stress as well as M and effective stress, for a given relative density, has been observed to be strongly controlled by the compressibility of sands. The coefficients in these power laws have been quantitatively correlated with grain mineralogy and angularity. The predicted trends for q_c are in agreement with those reported by Robertson et al. (1983). Based on these relationships for q_c and M , the value of $\alpha = q_c/M$ is shown to vary between 3 and 11 as generally reported.

The conclusions arrived at on the basis of the present study are highlighted in Chapter Six.

CHAPTER I

INTRODUCTION

1.1 General

It is known that the mechanical behaviour of granular material is controlled by the characteristics of its constituent particles. Considerable work has been done on the material characterization in terms of particle size, gradation, and relative density as well as on the effect of these parameters on mechanical characteristics such as liquefaction potential, penetration resistance, shearing resistance, dilatancy, compressibility and crushing. While the importance of grain shape, angularity and mineral composition in understanding the mechanical behaviour of granular material has been recognized (Holubec and D'Appolonia, 1973; National Research Council, 1985), enough attempts have not been made to quantify these aspects and also to study their influence on the mechanical behaviour of sands. A detailed review of available literature as outlined in Chapter II, has clearly brought out several aspects of granular materials that deserve an immediate and a greater attention. Particle shape and angularity, which have hitherto been specified in a descriptive manner, need to be quantified. No systemic details are available on grain morphology and mineralogy as related to their mechanical behaviour. No attempt seems to have been made by earlier workers to recognize the particle modification, in contrast to particle crushing, and also to systematically monitor the same at different stress levels. For sands of dominant carbonate composition, possibility of

modification and crushing at relatively lower stress levels exists compared to quartz sands and the available information is scarce. In fact, there is a need to classify sands in regard to their compressibility taking into consideration the size, shape angularity and mineral composition of constituent particles.

In the present study, an effort has been made to develop quantitative procedures for describing particle shape and angularity. Experimental programmes were designed on a systematic basis to examine the influence of grain morphology and mineralogy on the compressibility, modification, crushing and constrained modulus for a variety of sands.

1.2 ORGANISATION OF THE THESIS

In Chapter I, an introduction indicating the need of the present study is given with a discussion on the and the presentation of the material in the thesis.

Available literature on the characterization of particle shape and its influence on mechanical behaviour of sands, stress-strain dilatancy behaviour of sands under varied confining pressures, compressibility of sands, and the mechanisms of grain modification and crushing under different stress conditions and their influence on engineering properties of sands has been reviewed in Chapter II.

The characteristics of the starting materials and the test procedures adopted together with the details of the equipment involved are dealt in Chapter III.

Results of experimental investigations carried out to characterize all the sand samples involved in the present study in terms of their mineralogy, physical and morphological characteristics form the theme of Chapter IV.

In Chapter V, test data in terms of particle sphericity, shape factor and angularity have been interpreted. The classification of sands in terms of grain angularity has been presented. Results of compressibility, grain modification and crushing have been correlated with grain size, angularity, mineralogy and stress levels. The influence of grain angularity and mineralogy on cone penetration resistance (q_c) as well as constrained modulus (M) have been reported for different stress levels.

The conclusions arrived at in the present study are highlighted in Chapter VI. Relevant references pertaining to the present study are given at the end of the thesis.

CHAPTER II

LITERATURE REVIEW

2.1 General

The significant effect of confining pressure on behaviour of granular material has been recognized since the earlier days of Soil Mechanics. Yet, until recent years, the entire knowledge of mechanical behaviour of such material has been based on observations limited to stress levels that could be achieved in conventional triaxial apparatus (mean normal stresses not exceeding 10 Kg/cm^2). Even from a practical point of view, this situation has frequently led to unjustified extrapolations. For example, the stresses under deep foundations as in the case of very high earth and rockfill dams may be of the order of 100 Kg/cm^2 . In recent years intensive use of the principles of Soil and Rock Mechanics in geological and geophysical analyses, and interest in evaluating response of geologic materials under blast loads, have extended the range of pressures of practical interest to well above $10,000 \text{ Kg/cm}^2$.

The term high pressure obviously has only a relative meaning. For most physicists it would mean pressures exceeding 1000 Kg/cm^2 , whereas for practising geotechnical engineers it may mean any pressure that exceeds the capacity of ordinary triaxial apparatus (about 10 Kg/cm^2). The terminology for range of pressure used by different investigators, has been varied, depending on the nature of problems dealt with. Bishop (1965) and

Leps (1970) used the following terminology for pressure ranges dealing with response of soils under high dams:

Low Pressure	0.0 to 0.7	Kg/cm^2
Medium Pressure	0.7 to 7.0	Kg/cm^2
High Pressure	7.0 to 70.0	Kg/cm^2
Very High Pressure	> 70.0	Kg/cm^2

whereas the pressure range terminology used by Vesic and Clough (1968) was:

Low Pressure	0.0 to 10	Kg/cm^2
Elevated Pressure	10 to 100	Kg/cm^2
High Pressure	100 to 1000	Kg/cm^2
Very High Pressure	1000 to 10000	Kg/cm^2
Ultra High Pressure	beyond 10000	Kg/cm^2

In civil engineering, in some situations the range of pressure can be as high as several hundred Kg/cm^2 . Several investigations on the material properties of soils subjected to high pressures have been made by earlier workers using elevated cell pressure apparatus (Bridgman, 1918; Robert and De Souza, 1958; Lee and Seed, 1967; Vesic and Clough, 1968; Agar et al, 1987). Available data clearly point out to a need for differentiating the mechanical properties of soil under high pressures from those determined at low confining pressures.

At low pressure there is hardly any significant amount of particle modification or crushing and the sand particles being relatively free to move with respect to each other, the dilatancy effect can be quite significant. As the mean normal stress

increases, crushing becomes more pronounced and the dilatancy effect gradually disappears. Crushing appears to be most intense in the elevated pressure range (10 - 100 Kg/cm²) until the so-called "break down stress" (Vesic and Clough 1969) is reached (this stress is defined as the stress needed to eliminate the entire effect of initial void ratio of sand). The main effects of grain crushing on properties of granular materials (Vesic and Clough 1969) are:

1. Principal effective stress ratio at failure decreases with increasing confining pressure due to the suppression of dilatancy, but it does not tend towards a lower limiting constant value.
2. Large volume reduction occurs.
3. Particle breakage and crushing produces fine material (powder) with consequent reduction of the permeability and dilatancy and increase the density, and resulting in further additional settlement due to reorientation of the grains.
4. Much of the grain crushing occurs among the coarse and medium size particles in a specimen.
5. The strength and stress-strain behaviour of an element of soil is affected greatly by the extent of crushing or particle breakage during loading and deformation.

While most of the studies at high pressures have concentrated on total grain-crushing, the minor modification in the grain boundary characteristics have not received adequate attention.

In this study, the available literature has been reviewed under the following heads:

1. Morphology of sands (physical characteristics of soil).
2. Behaviour of sand at low and high confining pressures.
3. Compressibility.
4. Grain modification and crushing.

2.2 MORPHOLOGY OF SANDS

General

Size classification of particles is commonly based on either the arithmetic or the geometric mean of the greatest, intermediate and least diameters. The values obtained in both cases are dependent upon two factors -the shape and the volume of the particle. Two particles, one irregular having varying diameters and the other a sphere with the three diameters of the same length, may both have the same "size" value as a result of the arithmetic or geometric mean of their diameters, although they may differ distinctly in respect to both shape and volume.

Engineering classification of sands is generally based on particle size distribution and relative density without much regard to the particle morphology. For example, two sands at the same relative density and with similar gradation curves may have widely different maximum and minimum void ratio values depending upon the grain shape. Thus the maximum volume change potential (liquefaction under undrained cyclic loading) of a sand deposit will be significantly governed by the shape of the grains

(Burmister, 1938, 1962; Kilbuzewski, 1963; Ishihara and Watanabe, 1976; Castro, 1969).

2.2.1 Grain Shape

Shape is a complex property of a grain and it is difficult to describe shape precisely except for grains that approximate regular geometrical shapes. The following aspects of shape are generally adopted by sedimentologists to characterize the shape of particle (Blatt et al, 1971):

- I Surface texture
- II Roundness
- III Sphericity

2.2.1.1 Surface Texture

Surface texture is used to describe the type of surfaces of particle that are so small to affect the overall shape. Terminology commonly adopted for distinguishing surface textures includes terms such as polished surface, greasy surface and frosting of the grain.

2.2.1.2 Roundness

Roundness refers to the sharpness of the corners and edges of the grain. It therefore refers to those aspects of the grain surface that are on a larger scale than those classed as surface texture, but still smaller than the overall dimension of the grain. Wentworth (1919) was the first to quantify roundness. He defined roundness as the ratio of radius of sharpest corner to the radius of largest inscribed circle.

Pentland (1922) was the first to express roundness of individual sand grains as a ratio of percentage area of the grain projection to that of a circle with equal diameter of the grain. The area of the grain projection was determined from camera lucida drawings.

Cox (1927), on the basis of measurements made on the image of grains as projected on a screen, calculated the roundness or circularity as

$$K = \frac{4A\pi}{p^2} \quad (2.1)$$

where A - area measured by a planimeter

p - perimeter measured by a map measurer

K - roundness value.

Tickell (1931) used ratio of the area of the projected grain to the area of the smallest circumscribed circle to express "roundness".

Wadell (1932) was the first to show that the commonly used terms "shape" and "roundness" were not synonymous, but really included two geometrically distinct concepts. He defined roundness as the ratio of the average of radii of corners of the grain image and the maximum radius of the inscribed circle. This definition is a modification of the Wentworth roundness. Russel and Taylor (1937) placed particles into classes based on comparison with photographs of type grains using five grade terms (Table 2.1). The class limits for the grade terms are based on

Table 2.1 Roundness Grades

Grade	Russel and Taylor		Pettijohn	
terms	Class limits	Arithmatic Mid-Point	Class limits	Geometric Mid-Point
Angular	0.00 to 0.15	0.075	0.00 to 0.15	0.125
Subangular	0.15 to 0.30	0.225	0.15 to 0.25	0.200
Subrounded	0.30 to 0.50	0.400	0.25 to 0.40	0.315
Rounded	0.50 to 0.70	0.600	0.40 to 0.60	0.500
Well Rounded	0.70 to 1.00	0.850	0.60 to 1.00	0.800

the roundness estimates using Wadel's method. These roundness grades are subsequently modified by Pettijohn (1949) using "geometric scale" and rounding off the class limits (Table 2.1). Pettijohn used Silhouettes of the grains rather than their photographs (as used earlier) for the grouping of particles into classes.

Powers (1953) has further modified the roundness scale by adding another descriptive term, "very angular" to Pettijohn's and Russel and Taylor's set of roundness terms, which would provide an additional division of the lower classes. The interval from 0.12 to 1.00 has been subdivided into six intervals in such a way that the ratio of the upper to the lower limit of any interval is 0.70 (Table 2.2). The characteristic point of each interval is the geometric mean of the class limits.

Folk (1955) suggested a logarithmic transformation of roundness analogous to the ϕ scale for size. In this scale, designated as the ρ scale, the ρ values extend from 0.0 (perfectly angular) to 6.0 (perfectly rounded) with each unit corresponding to one class on the Powers' scale of roundness.

Pobkins and Folk (1970) suggested use of the radius of the largest corner divided by the radius of the largest inscribed circle as a measure of roundness. For precise measurement of small particles, the projected image of the grain must be enlarged to a standard size and the radii measured using a set of circles engraved on a plastic template.

Table 2.2 Roundness Grades Powers (1953)

Grade Terms	Class Interval	Geometric Mean
Very Angular	0.12 - 0.17	0.14
Angular	0.17 - 0.25	0.21
Sub Angular	0.25 - 0.35	0.30
Sub Rounded	0.35 - 0.49	0.41
Rounded	0.49 - 0.70	0.59
Well Rounded	0.70 - 1.00	0.84

Youd (1973) adopted the procedure as suggested by Powers but with the modification to consider particles from each size fraction rather than the specimen as a unit. The procedure used for his study consisted of examining under a microscope a representative number of sand particles (at least 50) from each sieve fraction and visually assigning each particle to a category listed by Powers (Table 2.2). The average roundness value for the sieve fraction (R_j) was then calculated from the equation

$$R_j = (\sum_{i=1}^n R_i)/n \quad (2.2)$$

where R_i is the roundness value assigned to the particle i , and n is the number of particles examined. The average value of roundness for the sand specimen was then calculated from

$$R = (\sum P_j R_j)/100 \quad (2.3)$$

where P_j is the percent (by weight) of particles retained in each sieve fraction.

2.2.1.3 Sphericity

The shapes of objects may be classified in a number of ways. The geometrician has defined a series of regular shapes such as cube, prism, sphere, cylinder, cone. The crystallographer likewise uses a classification of solids bounded by plane surface. Neither system is adequate for the natural sediments. At best, pebble shapes only approximate the regular solids of the geometrician. Terms such as prismoidal, bipyramidal, pyramidal,

wedge-shaped and parallel-tabular may be used to describe particle shape (Wentworth, 1936). Such a classification however, is at best a qualitative description only. Instead a single number index of shape would be desirable which is amenable to mathematical or graphic analysis and by means of which a shape distribution or frequency curve can be constructed.

A quantitative or numerical index of shape requires some standard of reference. Wadell (1932) was the first to choose sphere as a standard. A sphere is not only the limiting shape eventually assumed by many rock and mineral fragments upon prolonged abrasion during transportation, but it has certain unique properties which make it an acceptable standard of reference.

Ideally, the property of sphericity might be defined as s/S (Wadell 1932) where "s" is the surface area of a sphere of the same volume as the fragment in question and S is the actual surface area of the object. For practical purposes this ratio is difficult to measure and the actual measurement is expressed in terms of a ratio of the volume of particle to the volume of its circumscribed sphere. The cube root of this ratio is called the sphericity of the particle.

Wadell expressed the volume of the particle in terms of a sphere having the same volume, the diameter of the corresponding sphere is the "nominal particle diameter" (d). On this basis volume of particle is $(\pi/6)d^3$. The volume of the circumscribed

sphere is in general based on the longest diameter (a) of the particle, so that the volume of this sphere is $\pi/6 a^3$. Therefore, the Wadell's sphericity reduces to the ratio of the nominal diameter of the particle to its longest diameter (d/a).

As a further improvement, Krumbein (1941) used the concept of intercept sphericity, wherein the volume of particle is expressed in terms of a triaxial ellipsoid having the three diameters, a, b, c with $a>b>c$. The volume of such an ellipsoid is $\pi abc/6$ and sphericity is given as

$$\psi = \sqrt[3]{\frac{bc}{a^2}} \quad (2.4)$$

Sneed and Folk (1958) have objected to the use of sphericity as defined by Wadell on the ground that although it accurately measures the degree to which a particle approaches a sphere, it does not correctly express the dynamic behaviour of the particle in a fluid. This is because particles tend to orient themselves with their maximum projection area normal to the flow and this is true both for particles settling in a fluid and for particles resting on the bottom. In either case, the fluid drag is almost the same as the force on a sphere with the same projection area as the particle, whereas the gravity force is the same as on a sphere with the same volume of the particle. Defining the "maximum projection sphericity" as a ratio of the diameters of these two spheres, Sneed and Folk (1958) expressed sphericity as:

$$\psi = \sqrt[3]{\frac{c^2}{ab}} \quad (2.5)$$

Based on a measure of flatness and elongation ratios (p and q respectively), Aschenbrenner (1956) and Lees (1964), proposed the following relationship for particle sphericity:

$$\Psi = \frac{12.8(p^2q)^{1/3}}{1+p(1+q)+6 [(1+p^2(1+q^2))^{1/2}]} \quad (2.6)$$

2.2.2 Classification of Shape Type

"Definition of roundness and sphericity of a particle does not define the shape uniquely, even for the case of ideal ellipsoids" (Blatt et al 1971). Several other indices have been proposed and used by sedimentologists to define other aspects of shape.

Zingg (1935) proposed the use of two shape indices, d_L/d_I and d_S/d_I , where d_L, d_I and d_S represent the longest, intermediate and the shortest particle dimensions. These indices are used to construct a diagram, commonly called the Zingg diagram (Fig. 2.1), which is divided into four quadrants defining four main shape classes - tabular (oblate spheroid or disk shape), equant, bladed and prolate spheroid (rod or roller shaped). The boundaries for each region are indicated in Table 2.3.

Equant particles have highest sphericity but oblate, bladed and prolate particles may all have comparable sphericity values.

Krumbein (1941) superimposed the Wadell sphericity fields on the Zingg diagram (Fig. 2.1).

Heywood (1947) defined the two indices B/T and L/B as flakiness and elongation respectively, where L, B and T are

Table 2.3 Zingg Classification of Particle Shape

Quadrant	d_I/d_L	d_S/d_I	Shape
I	$> 2/3$	$< 2/3$	Oblate (disk-like)
II	$> 2/3$	$> 2/3$	Equant
III	$< 2/3$	$> 2/3$	Bladed
IV	$< 2/3$	$< 2/3$	Prolate (roller, Rod-like)

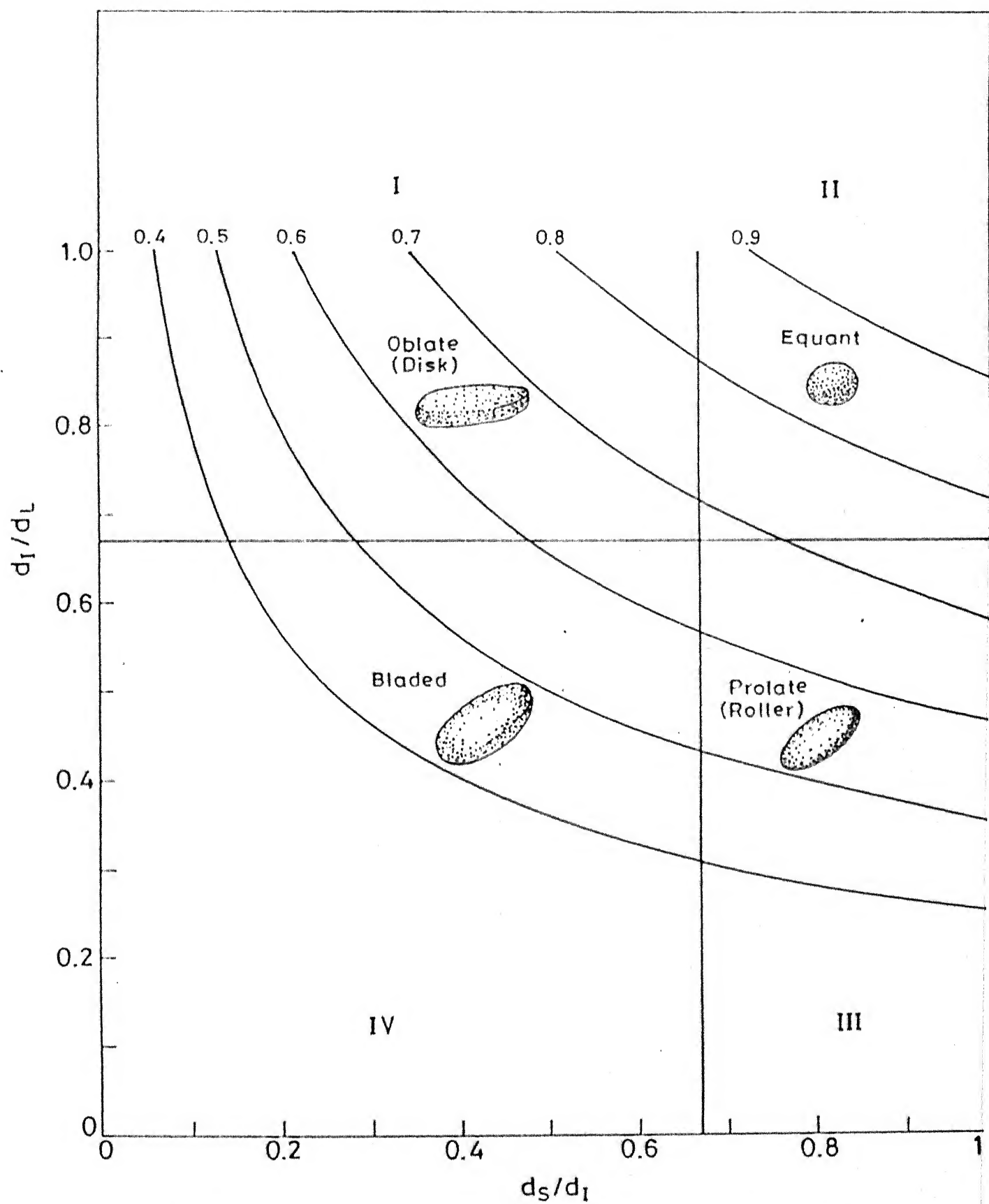


Fig. 2.1 Zingg diagram with lines of equal sphericity.

analogous to d_L , d_I and d_S). He further pointed out that if approximately $B=L=T$ the particle is said to be bulky. The particle is said to be flaky, platey, scale-like if $L=B>T$ and rod or needle-like when $L>B=T$.

Sneed and Folk (1958) presented triangular diagram combining the two indices d_S/d_L and $(d_L-d_I)/(d_L-d_S)$. The diagram is divided into a number of shape fields and line of equal maximum projection sphericity may be drawn on it.

Lees (1964) defined the flatness (p), elongation (q) and shape factor respectively as

$$p = \frac{c}{b} \quad (2.7)$$

$$q = \frac{b}{a} \quad (2.8)$$

$$F = \frac{p}{q} = \frac{c}{b^2} \quad (2.9)$$

where $a > b > c$ (analogous to d_S , d_I , d_L).

It may be noted that for a given value of F, the grain shape can vary considerably depending upon either flatness or elongation ratio. For example when $F=1$, $c/b=b/a = k$ (say) the particles will be equidimensional only for variation of k as $2/3 \leq k < 1.0$. Particles with larger elongation ratio (compared to flatness ratio) are disc or blade like in shape. Whereas grains having flatness ratio greater than elongation ratio are

dominantly rod or roller like in shape. Accordingly to Blatt et al (1971) equation 2.5 for sphericity is similar to the expression given below for shape factor (SF) as used earlier by engineers to express the main effect of shape on settling velocity:

$$SF = \frac{d_S}{\sqrt{d_L \cdot d_I}}$$

2.2.3. Effect of Morphology of Sand on Its Engineering Properties

Burmister (1938, 1962) observed that the range of particle sizes is the most important factor controlling maximum and minimum densities. The density increases with the increase in the range of particle sizes. Other factors he considered important were the type of gradation curve and particle shape.

Smith (1965) found a 3 percent decrease in $n_{\max} - n_{\min}$ (maximum porosity range) as grains increased in roundness from very angular (crushed basalt) to rounded (Erith sand), which is consistent with the trend observed by El Sobby (1964) who reported a 5.7 percent difference between the values of porosity interval for crushed feldspar and glass ballotini.

Dickin (1973) studied the influence of grain shape and size upon the limiting porosities of quartz sands (5 different sands) and glass ballotini and concluded that both the maximum and minimum porosities decrease with increasing sphericity for the fine sands chosen for their study. In the case of natural quartz sands, limiting porosities decrease with increasing grain size

for any one sand as a result of the inherent increase in sphericity with grain size.

Ishihara and Watanabe (1976) proposed use of the term volume decrease potential, $e_{\max} - e_{\min}$ (maximum void ratio range) for assessing liquefaction potential of sands. They suggested progressive decrease in $(e_{\max} - e_{\min})$ values with increasing average particle size (d_{50} , mm). It may be pointed out that in case of sedimentary sand deposits, larger particle size would be approaching high values of roundness due to abrasion during transportation as compared to finer sand grains which are likely to be angular in shape for the same distance of transportation. Data for Fuji river sand given by Ishihara and Watanabe supports this conclusion (Dicken 1973). Thus it is evident that volume decrease potential is also governed by the particle shape. Youd (1973) observed that the particle size has very little effect on e_{\max} and e_{\min} .

The $(n_{\max} - n_{\min})$ values for $d_{50} = 0.11$ mm is 15% for Fuji River sand and 8% for glass beads, giving a decrease of 7% as the roundness of the particle increases. This trend is in conformity with the results of El Sohby (1964) and Smith (1965).

Charles and Watt (1980) have carried out large scale drained triaxial compression tests on rockfill and found that the maximum principal stress ratio at failure is related to the rate of dilation which is itself a function of particle shape, strength and relative density.

Usesugi and Kishida (1986) examined the effect of significant factor on the frictional coefficient using three different sands and found that the particle shape, mineral ingredients and surface roughness of the particles have considerable influence on the frictional coefficient.

2.3 BEHAVIOUR OF SANDS AT LOW AND HIGH CONFINING PRESSURES

Considerable amount of research work has been published on the behaviour of granular materials, based on oedometer and triaxial shear tests. Many of such studies have been limited to low to elevated cell pressure range. Research work carried out under high confining pressures was restricted mainly to small size specimens (typical volume being equal to a few cubic centimeters or a fraction of a cubic inch). Available information on large size particulate materials tested at high pressures is very limited. In this review, the behaviour of sands under cyclic loading is not considered.

One of the earliest investigations concerning the compressibility of sand was by Terzaghi (1925). On the basis of a number of confining pressure tests on sand and clay soils, Terzaghi observed that the compressibility of both types of soil was similar. However, the volume changes in sand were not as great as those which occurred in clay soil when tested under the same magnitude of load. Nevertheless, the sand was found compressible even at pressures of the order of 3 Kg/cm^2 . An extension of this work is quoted by Terzaghi and Peck (1948). Several sands

and sand mica mixtures were subjected to one dimensional compression, and the particle crushing that was observed was suggested to be responsible for the compressibility of the sand at high pressures.

Bridgman (1918) was able to compress an angular sand (grounded quartz) to 30000 Kg/cm^2 , reducing its porosity to about 2 per cent.

Robert and De-Souza (1958) tested different sands and observed that at moderately low pressure, crushing and consequent compression are more in angular sands compared to the rounded ones. However, at very high pressure little difference was observed between the behaviour of angular and rounded sands.

Hardin, Borg, Fredman and Higgs (1960) and Griggs, Turner and Heard (1960) conducted triaxial tests on small samples of sand at very high pressure (upto 5000 Kg/cm^2) combined with high temperature and reported the ductile failure at large strains in most samples with no visible effect of temperature upto 600°C .

Hirschfeld and Poulas (1963) on the basis of tests on silt and sand at different confining pressures concluded that while there is a net increase in volume during shear at low confining pressure, a net decrease in volume results at high confining pressure.

Vesic and Barksdale (1963) investigated the mechanical behaviour of sand in the high pressure range on samples of dense sand (2.2 cm diameter) at all pressures upto 630 Kg/cm^2 and found

that the curvature of the Mohr envelope of the sand tested was restricted to an initial pressure range. They showed by a limited number of volume change measurement in shear at constant mean normal stress that the effect of dilatancy of the material and the curvature of its strength envelope disappeared at high pressure.

Lee and Farhoomand (1967) tested crushed granitic material (angular to subangular) upto confining pressures of 140 Kg/cm^2 under isotropic and anisotropic conditions and reported increase in compressibility with increase in confining pressures.

Lee and Seed (1967), in the case of an intially loose specimen of fine uniform Sacramento river sand subjected to confining pressure greater than 100 Kg/cm^2 , were able to obtain a final void ratio that was less than the minimum void ratio obtained under normal tests conditions in the laboratory.

Vesic and Clough (1968) studied the behaviour of granular material at high pressures extending beyond the mean normal stresses of 1000 Kg/cm^2 . Data reported by them on Chattahoochee river sand revealed the existance of a mean normal stress beyond which the curvature of strength envelope for all initial void ratio vanishes, and the shear strength of sand is not affected by its initial void ratio. This stress is designated as the crushing stress or breakdown stress as it represents the stress level at which all dilatancy effects disappear and particle crushing becomes the only mechanism, in addition to shearing displacement due to simple slip along the slip planes. It appears that this

stress is affected by gradation and shape of particles of the granular material as well as the mineral composition.

Lee and Seed (1970) conducted drained and undrained triaxial test on fine, uniform clean graded Sacramento river sand ($e_{max} = 1.03$, $e_{min} = 0.61$) with relative density varying from loose to dense (dense having relative density of 78%), and concluded that, for the granular soils the volume changes which occur during consolidation appear to depend only on the magnitude of the major principle stress and to be entirely independent of the minor principal stress during consolidation.

Miura and Yamanouchi (1973) conducted isotropic consolidation tests on "Toyoura Standard Sand" for two relative densities of 24 percent and 90 percent. Tests were performed upto isotropic pressure of 500 Kg/cm^2 . At 300 Kg/cm^2 isotropic pressure, two samples showed 21 and 10 percent volumetric compression respectively. They also concluded that void ratio of the two samples approaches a certain value at a pressure of 500 Kg/cm^2 .

Agar et al (1987) investigated the strength and stress deformation behaviour of Athabasca oil sand at elevated temperature ($25 - 200^\circ\text{C}$) and confining pressure of 800 Kg/cm^2 using triaxial compression test and concluded that the shear strength of dense sand increases non-linearly with effective confining pressure.

2.4 COMPRESSIBILITY

The compressibility of granular materials has been studied both in anisotropic (i.e. in oedometer) and in isotropic (i.e.

in triaxial) conditions. From these studies it is concluded that the compressibility of granular media is a consequence of complex phenomena resulting from displacements between particles combined with particle breakage. The deformation of granular soils under loading is a result of three main mechanisms (Loung 1982).

1. Consolidation mechanism - Change in shape and compressibility of the particle assemblies.
2. Distortion mechanism - Bending of the flat particles, sliding and rolling of rounded grains.
3. Attrition mechanism - Particle crushing and breakage, modification of the soil fabric and packing.

Stress-strain behaviour of sands as studied in oedometer test (Hendron, 1963; Roberts, 1964) has been considered by Lambe and Whitman (1969) to be in three stages as detailed below:

1. Locking behaviour during which sand gets stiffer and stiffer as the level of stress increases "upto 150 Kg/cm^2 , and finally, a stage is reached in which already dense arrays (of particles) are being squeezed more tightly together as contact points crush, thus allowing a little more sliding".
2. Yield behaviour as a "result of fracturing of individual sand particles which permits large relative motions between particles" at stresses equal to and greater than 150 Kg/cm^2 . Considerable particle degradation takes place during this stage.

3. Fracturing and crushing leading to tighter packing of particles and increase of number of particle contacts and "thus the sand once again becomes stiffer and stiffer as the stress increases still further".

These distinct stages of compression were observed for medium to coarse, well rounded quartz sand. However, actual stress level at which compression behaviour of sand changes from locking to yielding depends on many factors such as mineralogy, particle size, shape, roughness, angularity, gradation and relative density, composition, cementation, average stress level, prestressing, stress path and ageing.

Effect of the different factors such as particle size, shape, roughness, angularity, relative density and mineralogy on the compressibility has been studied earlier. In the succeeding paragraphs, a brief review of the available literature pertinent to the present study is made.

One of the earliest investigations concerning the compressibility of sand was by Terzaghi (1925). He reported the increase in compression with confining pressure. Many such experiments have since been performed by investigators interested in compressibility of different granular materials.

Burmister (1948) reported that the deformation increases with increasing void ratio and that different soils with 0% relative density are not equally compressible.

Schultz and Mousa (1961) reported that compressibility of a sand is considerably increased when a small quantity of cohesive soil is mixed with the same.

The study of compressibility on Leighton Buzzard sand by Kolbuszewski and Fredrick (1963) has shown slight increase in compressibility as roughness of particle increases when samples are dense, and a large increase in compressibility as roundness of particle decreases for loose samples.

De Beer (1963) reported that the compressibility and crushing of particles are accelerated by the addition of water and increase with increase in angularity and grain size of uniform soil, and decrease in strength of individual grains.

Kjaernsli and Sande (1963) showed that for a given material, compressibility is low for well-graded material in comparison to uniformly graded material. For example, the compressibility of crushed angular particles of syenite increased from 4.75 to 16 percent with a decrease in the coefficient of uniformity from 2.5 to 1.4. They also observed that the material with weakest particles show the greatest amount of compression and particle breakage.

Marshal (1967) performed drained triaxial test on coarse gravel and broken rock upto 20 cm in diameter, with confining pressures upto 25 Kg/cm^2 and showed that compressibility is related to the nature of the soil. The material with weakest particles showed the greatest amount of compressibility.

Koerner (1968) reported that deformation increases with decreasing coefficient of uniformity and decreases with increasing roughness.

El Sohby (1969) studied the effect of stress on resulting axial deformation and volume change for three different materials- Silver Sand ($D_{60} = .25$, $D_{10} = .14$), Glass Bollotini ($D_{50} = 0.1$ mm), fine sand and found that the total deformation of a mass of sand subjected to a constant stress ratio can be divided into two main components i.e. sliding deformation and elastic deformation. He further reported that deformation increases with increasing void ratio.

Koerner (1970) conducted tests on quartz, feldspar and calcite and reported more compressibility and degradation for uniform soils in comparison to the well graded soil having same maximum particle size.

Charles Moore (1971) performed two series of tests on Chattahoochee river sand (with addition of mica upto 1, 5, 10, 50 and 100 percent) and residual silt from Atlanta. Results of tests on Chattahoochee river sand conducted with relative density values of 25, 30 and 57 percent indicated that the compressibility increases appreciably with increasing mica content (5 percent of mica will double the relative compressibility).

Bordon and Proctor (1971) performed a series of tests on river Willand sand using triaxial compression test with cell pressure of 703 Kg/cm^2 and showed that the dense sample is highly dilatant with insignificant crushing whereas loose sample

shows no dilatancy but has significant amount of particle crushing.

El-Sohby and Andrews (1972) have reported results from an experimental study on variety of granular materials using confining pressure upto 6.33 Kg/cm^2 only, and showed that the compressibility of granular material is mainly governed by the properties of its individual particles and geometry of its internal structure, i.e. the deformation increases with increasing void ratio, decreasing coefficient of uniformity and decreasing mineral strength.

Ramamurthy and Kanitkar (1972) conducted isotropic consolidation test on four fractions of Badarpur sand. Larger volume changes were observed for the coarsest material tested ($d_{50} = 1.7 \text{ mm}$). The volumetric compression during isotropic consolidation in the pressure range of 8.5 to 84 Kg/cm^2 varied from 1.00 to 4.2 percent for mean particle size of 0.096 mm, 1.9 to 7.00 percent for size of 0.5 mm, 2.4 to 11.3 percent for size of 1.00 mm, and 3 to 15.5 percent for size of 1.7 mm.

D'Appolonia and Holubec (1973) showed that the particle shape has minor influence on the minimum void ratio, but has a major influence on the maximum void ratio. Since the maximum void ratio increases considerably with angularity than in the case of the minimum void ratio, the void ratio difference increases markedly with increase in angularity. They suggested that the deformability of sands having the same gradation and

relative density increases with increasing angularity. Also, strength, as measured by friction angle, increases with increasing angularity.

Cornforth (1974) reported that deformation of granular material increases with increasing void ratio.

Haruyama (1977) studied the deformation characteristics of highly compressible angular, uniformly graded volcanic deposit (Shirasu sand) with different relative densities, using triaxial test and the results were compared with uniformly graded Toyoura standard sand. It was revealed that Shirasu sand showed higher compressibility as much as three times compared to that for Toyoura standard sand.

Oberoi (1983) performed oedometer tests on dune sand, Chao-parya river sand and micaceous sand upto 30 Kg/cm^2 and reported volumetric strains of 4.5, 7.8 and 34 percent respectively.

Al Hussiani (1983) conducted drained triaxial compression and plane strain tests at 31 Kg/cm^2 using crushed basalt and found that compressibility decreases as the uniformity coefficient increases.

Clayton et al (1985) have reviewed factors affecting compressibility of sands. Following Daramala (1978) they have grouped these factors into two categories - the material-dependent factors and the stress-dependent factors. According to them all the factors in both categories, angularities of particles and void ratio have the maximum effect on compressibility of sands. It has been shown that the compressibility of an uniform fine sand is strongly dependent on its previous stress path.

Kapoor (1985) tested four different sands with different relative densities, using oedometer and triaxial compression test and showed that dense samples are highly dilatant with insignificant amount of particle breakage whereas loose samples show no dilatancy but have significant amount of particle breakage.

Belotti et al (1985) observed the variation of tangent modulus with relative density and normal stress and suggested the following equation

$$M = m_0 P_0 \left(\frac{\sigma'}{P_0} \right)^{m_1} \exp (m_2 \times D_R) \quad (2.10)$$

where

P_0 = reference stress (1 Kg/cm^2),

σ' = effective normal stress, and

m_0, m_1, m_2 are experimental constants.

Yudhbir and Rahim (1987) have reviewed the factors controlling compressibility. Based on available data, it was shown that "in general the compressibility is high when the sand is loose, the grains are angular, the coefficient of uniformity, C_u , is low, the average particle size is small, particle surface is smooth, the grain mineral strength is small, interparticle cementation is weak and the ageing effects are insignificant. Stress history, stress level and stress path have significant influence on compressibility of sands". It was also concluded that the angular well-graded sands attain closer packing of particles compared to poorly graded and rounded sands for same height of fall in a raining technique of sample preparation. Also angular well graded sands are more compressible than poorly graded

sand. It was further pointed out that in case of angular sands, the grain boundaries are modified at a stress level less than the critical stress, and at stress levels greater than the critical stress, sands behave like normally consolidated clay, exhibiting compressibility.

Phool Chand (1988) investigated the response of three sands, namely standard rounded quartz sand, angular micaceous Ganga sand and angular Kalpi sand (having quartz, feldspars and carbonates as major minerals), under one-dimensional compression and unloading. The modulus during unloading was shown to follow the relationships as proposed by Janbu (1985):

$$M = M_{sw} \sigma' \quad (2.11)$$

$$M = \frac{d \sigma'}{d e} \quad (2.12)$$

where

M_{sw} is a modulus number,

and σ' = effective vertical stress.

He observed that for standard sand practically one value of M_{sw} was obtained for samples with two different relative densities (25 % and 55 %), whereas for angular Kalpi and Ganga sand distinct values of M_{sw} were obtained for each density. Also M_{sw} was shown to be independent of the past maximum pressure in case of rounded standard sand whereas these values varied with past maximum pressure (higher value for lower past maximum pressure) in case of angular Ganga and Kalpi sands.

Janbu (1985) suggested M_{sw} approximately equal to $(5 - 10)m_0$ (where m_0 is modulus number for normally consolidated states for sands). Phool Chand's results indicate $M_{sw} = (2 - 10) m_0$, the lower values being for rounded sand and the highest for very angular flaky micaceous sand. This ratio M_{sw}/m_0 appears to be independent of relative density (he studied only two relative densities).

2.5 PARTICLE CRUSHING

When soil grains are hard, tough and well - rounded, they may take up reasonably high stresses without crushing. Angular particles of freshly quarried material undergo fragmentation under ordinary pressures due to breakdown of sharp angularities (grain modification). The decomposed particles split under ordinary pressures in addition to breakdown of angularities.

The Hertz theory of contact stresses between elastic spherical particles can be used to estimate the radius of zone of particle contact and the magnitude and distribution of contact stress in this zone. The load per particle will obviously depend on the mode of particle packing and the particle shape (Marsal, 1963). Marsal's theory brings out the influence of void ratio (packing), particle shape factor (sphericity), particle diameter and the average number of contacts per particle.

Grivas and Harr(1980) have investigated particle contacts in discrete materials and suggested that, for all practical purposes, the product of number of contacts per particle, and the

porosity (n) is a constant equal to three. The response of sand particles at their contacts would be governed by the magnitude of both normal and tangential contact stress.

Mindlin and Deresiewks (1953) after introducing tangential stress component suggested that higher stress is developed in the anulus of the slip on the periphery of contact area. Smith and Liu (1953) have investigated the distribution of stresses due to normal and tangential forces on the contact between rolling bodies. They have shown that a rolling contact leaves behind it a tensile stress, while introducing a compressive stress ahead of it.

In addition to the existence of normal and tangential forces at the contacts of particles during reorientation, the contacts may also be subjected to twist due to the movement of neighbouring particle. Studies of Hentengi and Mc-Donald (1958) and others revealed that spheres, when subjected to combined effect of pressure and twist, experience severe stresses on the contact surface resulting in rapid destruction and failure of material.

In the presence of sharp angularity and asperities, the stress concentrations are likely to be higher than that the points could possibly bear. The soil grains experience crushing under direct loading or shearing of angularities and asperities under shear stresses. Under increasing stresses, the asperities are likely to undergo progressive crushing until the contact area is sufficiently increased to withstand the stresses without any

further crushing, or the interference of the sheared material may restrict the development of resistance between the contacts.

2.5.1 Types of Crushing

The different types of crushing (Ramamurthy, 1966) occurring in granular soils during shear may be classified as follows:

1. Crushing or shearing of asperities on the contact surface.
2. Splitting of soil grains.
3. Breakdown of sharp asperities.
4. Breakdown of asperities due to the stress reversal.

2.5.1.1 Shearing of Asperities

The frictional resistance between soil grains depends on their surface properties and mineral constituents. Locally stronger asperities act as indentors on the contact surface and develop resistance to plastic deformation of material. When shear stresses are applied, these asperities plough through or scratch the surface indentation and increase the resistance. An asperity can scratch a surface if the surface hardness of an asperity is at least equal to 1.2 times the hardness of the surface to be scratched (Tabor, 1956). The resistance developed during scratching and indentation is essentially the plastic property of a material. Bridgeman (1953) using a high pressure equipment has demonstrated that under hydrostatic pressures, a material which is brittle under ordinary conditions can be prevented from fracture and made to deform plastically.

The proportion of the crushed material is very small, since it involves only the asperities in regions of high shear stresses. The degree of crushing varies according to the magnitude of the stress and movement of particle. Even though the magnitude of crushing may be of the order of a few per cent of the entire sample, its effect on the strength will be disproportionately large.

2.5.1.2 Splitting of Soil Grains

Splitting of soil grains takes place under high compressive stresses. Splitting is encountered during field/laboratory compaction of granular soils, particularly in clayey sand and clayey gravel type of soils. Its extent depends upon the shape, size and strength of individual grains and also on contact pressures. Splitting may be limited to the contact region or may extend across whole grain. In the preparation of laboratory specimens of coarse grained soil, large local voids tend to develop during deposition. If these specimens are compressed statically in a mould to achieve the desired density (especially if the movement occurs at one end only), the particle will split at the contact.

The fragments formed due to grain splitting are coarser than those formed due to the shearing or crushing of the surface asperities. The broken fragments are generally angular and may offer greater surface frictional resistance on the newly formed surfaces. The magnitude of crushing in static compaction varies

with the difference between the density achieved during deposition and that after compaction. And, therefore, a very open initial soil structure experiences greater crushing while statically compacting the specimen to a given density.

2.5.1.3 Breakdown of Sharp Asperities

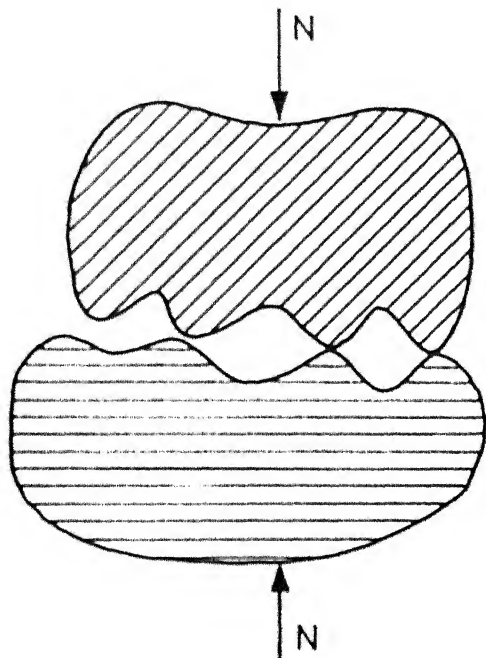
In quarried materials and residual soils, sharp corners of particles break during compaction or shear, producing extra blunt corners, though reducing the overall angularities. The newly formed surface and corners are relatively stronger. The asperities on the newly formed surfaces are stronger at low pressures and may not exhibit crushing, but they may behave differently under different stress ranges.

2.5.1.4 Breakdown of Asperities due to the Stress Reversals

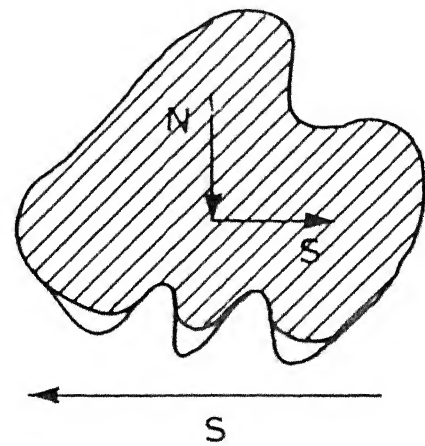
This category of crushing occurs when hard soil grains are subjected to stress release at their contact points. Under high contact stresses, the angularities and asperities of particles experience elastic and plastic deformations. When shear strains are induced, some of the initial contacts may be unloaded; when the load is transferred to new contacts such stress reversals results in fragmentation. Different kinds of crushing are indicated in Fig. 2.2.

2.5.2 Quantitative Expressions for Degree of Crushing

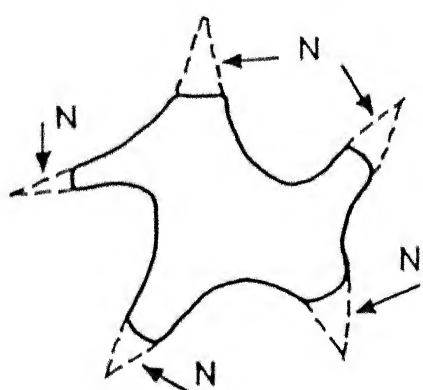
The degree of crushing has been expressed quantitatively by several investigators.



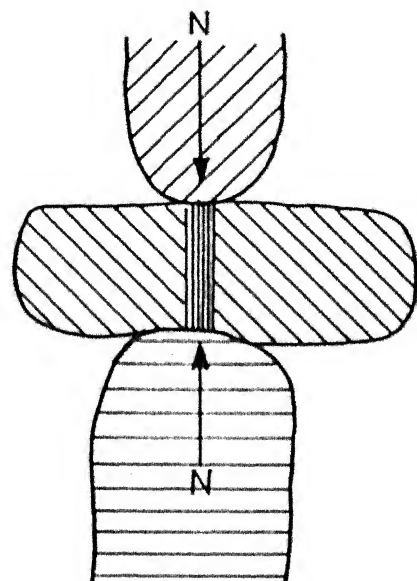
(a) Crushing of asperities
(introduces lubrication effect)



(b) Shearing of asperities
(introduces smoother surface)



(c) Breaking of angularities
(introduces more corners and stronger surfaces)



(d) Splitting of particle
(introduces more fragmentation and stronger surfaces)

Fig. 2.2 Different types of crushing (Ramamurthy, 1966)

Leslie (1963) used the percent passing the sieve on which the original material was 100 % retained.

Marsal (1965) has selected as a measure of grain breakage a parameter B_g equal to the sum of the positive Δ_{Wk} , where Δ_{Wk} is the difference between the percentages of the total sample contained in each grain size fraction before and after the test. Hence B_g is the percentage by weight of the solid phase that has undergone breakage. The parameter B_g (expressed as a ratio) multiplied by the concentration of solid (q), is the volume of the broken particles per unit total volume

$$B_g \cdot q = \frac{B_g}{1 + e} \quad (2.13)$$

Lee and Farhoomand (1967) studied crushing of material under anisotropic compression and defined a parameter designated as relative crushing which is equal to D_{15i}/D_{15a} , where D_{15i} is the diameter through which 15 % of particles of the original material pass and D_{15a} is the diameter through which 15 % of the particle pass after being subjected to anisotropic compression.

Ramamurthy and Lal (1970) have expressed quantitatively the degree of crushing as the area between the grading curves of a sand obtained before and after it has been subjected to shear.

Lowrison (1974) suggested that the amount of crushing can be estimated by evaluating the increase in surface area of the particles after crushing.

Leslie (1975) modified his earlier method and used the increase in percent passing the sieve on which 90% of the original sample was retained.

Datta, Gulhati and Rao (1980) expressed the magnitude of crushing in terms of a crushing coefficient, C_c defined as:

$$C_c = \frac{\text{Percentage of particle of sand after being subjected to stress finer than } D_{10} \text{ of the original sand}}{\text{Percentage of particle of the original sand finer than } D_{10} \text{ of the original sand.}} \quad (2.14)$$

Hardin (1985) has critically reviewed the factors affecting crushing of sands. He has proposed a numerical measure of degree of crushing in terms of "potential breakage", "total breakage" and "relative breakage", and developed equations that can be used to evaluate the above mentioned terms for a given soil subjected to a specified loading. The potential for breakage of a particle of a given size D , may be represented by:

$$b_p = \log_{10} \frac{D \text{ in mm}}{0.074 \text{ mm}} \quad \text{for } D \geq 0.074 \text{ mm.} \quad (2.15)$$

= 0 for $D \leq 0.074 \text{ mm}$ (because extremely large stresses will be required to produce crushing of particles with $D < 0.074 \text{ mm}$).

If b_p represents the potential for breakage that is significant to soil behaviour for a given size fraction, df , in an element of soil, where df is a differential of "percent passing" divided by 100, then the potential breakage is given by,

$$B_p = \int_0^1 bp df \quad (2.16)$$

The amount of crushing that is significant to soil behaviour is given by

$$B_t = \int_0^1 (bp_0 - bp_1) df \quad (2.17)$$

where bp_0 --- the original value of bp

bp_1 --- the values of bp after loading.

The relative breakage is given by

$$B_r = \frac{B_t}{B_p} \quad (2.18)$$

2.5.3 Particle Crushing and its Effect on Engineering Properties of Granular Soil

The strength and stress-strain behaviour of an element of granular soil is affected greatly by the degree to which crushing or particle breakage takes place during loading and deformation. For the type of deformation that primarily produces volume change, such as one dimensional strain or isotropic compression, particle breakage adds to the reduction in volume. For the type of deformation where particles are moving past or around one another, such as triaxial compression or simple shear, crushing at sliding contacts or breakage of particles decreases the rate of dilation corresponding to a given principal stress ratio. Sliding between particles is usually present at all stress levels.

The stress level at which crushing and fracturing of particle becomes significant is called the "critical stress".

This critical stress is smallest when the particle size is large, the soil is loose, the particles are angular, the strength of individual mineral particles is low, and the soil has a uniform gradation (Lambe and Whitman, 1969).

Terzaghi (1925) reported an increase of 4.6% fines (dust content) of a loose quartz sand (made by grinding grain size 0.7 to 0.25 mm) loaded in consolidometer under a stress of 50 Kg/cm^2 . He cited this increase in dust content as a proof that the compaction of structure (of sand grains under stress) was accompanied by breaking of corners and edges (grain modification).

Hilf (1957) observed that the residual and coarse-grained soils exhibited field dry density values higher than laboratory densities by about 32.04 to 48.05 Kg/cm^2 due to breakdown of soil grains. Robert and De Souza (1958), Rowel (1955), Mousa (1961), Vesic and Borkdale (1963), Dee Beer (1965) have described the significant amount of particle crushing and increase in compressibility of natural sands at pressures beyond about 150 Kg/cm^2 .

Hardin (1953), Borg et al (1960), and Griggs et al (1960) have carried out a certain number of triaxial tests on small samples of sand at very high pressure (upto 5000 Kg/cm^2) combined with high temperature. Elaborate data were presented on structural breakdown of the material, as well as on the fracture phenomenon of individual sand particles.

Leslie (1963) reported on testing of large samples of several poorly-graded to well-graded gravelly materials at all pressure upto 47.5 Kg/cm^2 . Marsal (1967) tested large samples of

coarse gravel and rockfill (45.72 cm diameter) at confining pressure upto 25 Kg/cm².

Bishop, Webb and Skinner (1965) tested loose sand samples by applying all pressures upto 10 Kg/cm². Lee and Fahroo mand (1967) performed triaxial tests on six different sand (fine and gravel size) samples under a confining pressure of 140 Kg/cm². All these investigators reported the structural breakdown of the tested material and also concluded that uniformly-graded soil undergoes more particle crushing compared to well-graded one.

Hall and Gordon (1963) performed drained triaxial compression test on gravelly soil and observed considerable amount of crushing especially during the shearing stage. They too observed more crushing for uniformly-graded soil than for well-graded soil.

Bishop (1966) showed that considerably more crushing occurs during the shearing stage of triaxial test than during the consolidation stage.

Lee and Seed (1967) showed increasing degradation of Sacramento river sand (having 4% material finer than 75 microns) with increasing confining pressure. It increased to 14%, 22%, 40% and 52% under confining pressure of 10, 40, 80 and 140 Kg/cm². In case of well-rounded Ottawa sand, they reported that it was much less compressible than fine sub-angular to sub-rounded sand, and the energy required for crushing of Ottawa sand was shown to make up to a significant component of the total observed shear strength of granular soil under high pressure.

Vesic and Clough (1968) performed triaxial tests on 50 samples of fine Chattahoochee river sand (medium, uniform micaeous sand, composed of subangular quartz grains, $d_{50} = 0.37$ mm, $e_{max} = 1.1$, $e_{min} = 0.61$) and reported that at very low pressure there is very little crushing. However, the sand particles were relatively free to move with respect to each other and the dilatancy effect could be quite significant. As the mean normal stress increased, the crushing became more pronounced and the dilatancy effect gradually disappeared and the crushing was more intense in the elevated pressure range ($10 - 100$ Kg/cm^2) until a "breakdown stress" was reached beyond which the sand behaved essentially as a linear deformable sand.

Ramamurthy (1970) studied the influence of fragmentation of particles of Badarpur sand with two different gradings, in triaxial compression test with confining pressures upto 70 Kg/cm^2 and showed that the magnitude of crushing increased with mean principal stress during isotropic consolidation and shear, but major crushing occurred during shear and in the coarser fraction of sands. This crushing produced major changes in the properties of sand like effective principal stress ratio, effective angle of shearing resistance, dilatancy ratio and coefficient of earth pressure at rest.

Koerner (1970) conducted tests on quartz, feldspar and calcite and reported more compressibility and degradation for uniform soils in comparison with well-graded soils having same maximum particle size.

Billan (1971) shows that some aspects of high pressure behaviour are strongly influenced by the tensile strength of the grain substance. Grain strength may be easily estimated and used as a scale factor for comparing the behaviour of initially dense granular materials sheared at high pressures.

Oda and Minami (1976) tested residual soil derived from weathering of granitic rock (called Masado) using direct shear tests and found that, due to effect of particle breakage, the failure envelope derived from direct shear tests under constant volume and constant normal stress is never a straight line.

Miura and Sukeo-o-Hara (1979) studied the effect of particle crushing on shear characteristics of a decomposed granite soil, using a series of triaxial compression tests under drained and constant confining pressure conditions and found that the particle crushing phenomena, under low stress, of a soil consisting of breakable particles is substantially the same as the particle crushing phenomena under very high pressure of soil consisting of strong particles. Further they showed that the particle breakage rate has a close relationship with volume change characteristics of the sample tested.

Datta, Gulhati and Rao (1980) studied the crushing of calcareous sands during drained shear, using triaxial compression test and confining pressure of 64 Kg/cm^2 , and found that calcareous sands with skeletal particles are significantly more susceptible to crushing than terrigenous quartzitic material. The extent of crushing is influenced by particle characteristics and void ratio. They further pointed out that

there is significant reduction in maximum principal effective stress ratio due to particle crushing.

Datta, Gulhati and Rao (1982) studied the engineering behaviour of carbonate soils of India and reported that crushing of carbonate particles and cementation by carbonate material are the two most dominating factors which influence the engineering behaviour of carbonate soils.

Vaid and Chern (1985) studied the effect of pressure and angularities on liquefaction of Ottawa and mine tailing sands and showed that there is some particle breakage in case of mine tailing sand (this implies that both consolidation and shearing of angular sands results in some breakage of sharp edges of particles, with no gross particle crushing under the level of confining pressure used) whereas no particle breakage could be observed for the Ottawa sand even at a stress of the 40 Kg/cm^2 .

Phool Chand (1988) performed direct shear test on angular sands (Ganga and Kalpi) and well rounded quartz sand (standard sand) and observed significant amount of particle crushing for the angular sands with no crushing for uniformly-graded rounded quartz sand.

2.6 SCOPE OF WORK

The foregoing review covered the following aspects of response of granular materials subjected to both normal and shear stresses:

- 1) Characterization of particle shape and its influence on mechanical behaviour of sands.

- 2) Stress-strain dilatancy behaviour of sands under low and high confining pressures.
- 3) Compressibility of sands and the significant controlling factors.
- 4) Mechanisms of grain modification and crushing under normal and shear stress and its influence on engineering properties of sands.

The review reveals that while geologists, dealing with large size particles, have successfully developed methods to quantify particle morphology, the same has not been done in case of sands in a standardized way. Highly descriptive and therefore subjective descriptions of particle shape are usually given. In this study, an attempt is made to develop a quantitative procedure to describe particle morphology. This is considered necessary since it is well recognized that particle morphology has significant effect on compressibility, particle degradation, liquefaction potential etc.

Literature review also reveals that data on natural sands demonstrating the effect of grain morphology and mineralogy is rather limited, and no systematic study involving a variety of natural sands is available. Most of the results reported relate usually to quartz sands with subrounded to subangular particles. In this study three natural sands with different mineralogy and mode of formation along with an artificial standard rounded quartz sand, have been used to investigate compressibility behaviour upto a normal stress of 176.32 Kg/cm^2 . In addition,

different mixtures/gradations of sands were prepared by intermixing the four main sands and morphological and mineralogical characteristics and their compressibility were investigated. The relationship between relative density and height of free fall (using raining technique) were investigated for all the sands.

The compression tests were also utilized to examine the nature and degree of grain modification/crushing. These results have been critically examined in terms of stress level, grain size and the nature of minerals present. The grain morphology after degradation was also quantified and compared with the unstressed natural sand particles. Nature of the laws governing variation of constrained modulus (M) with effective confining stress and relative density has been investigated for sands of varying compressibilities. Based on the influence of grain angularity on the angle of shearing resistance and the effect of sand compressibility on the mode of failure under the penetration cone tip, the laws governing the variation of ultimate cone tip resistance (q_c) with effective confining stress and relative density have been examined.

CHAPTER III

MATERIALS AND METHODS

3.1 General

Strength and compressibility are influenced significantly by the size and shape of the particles and the mineral composition of the soil constituents. While mechanical analysis and optical techniques are adopted for characterizing the size and shape, microscopic and X-ray difraction investigations have been resorted to for the mineralogical analysis. In the present Chapter, the materials chosen for the study are described in terms of their characteristics and the test procedures adopted together with the details of the equipment involved are presented.

3.2 Materials Used

In the present study four sands have been chosen of which three are natural sands while the fourth one is of an artificial type. In addition to the bulk samples of these four sands, six samples have also been prepared by size fractionation, mineral separation and also by selective mixing of the same.

Few samples of sands as obtained from sources abroad (Rensselaer Polytechnic Institute, New York) have also been studied in terms of their size and morphological characteristics. The data obtained were used for evaluation in the present case.

3.2.1 Ganga Sand

The sand from the flood plains of Ganga near Kanpur, chosen for the present investigation has uniform grain size

distribution. Examination with binocular microscope and image analyzer (Plate 3.1) revealed that this sand was predominantly angular with minor amounts of flaky as well as rounded grains. The mineral composition is dominantly of quartz and feldspar with subordinate amounts of mica and calcite (carbonate). Fragments of gneiss and quartzite also occur in minor quantity. The quartz grains are quite transparent and often noticed to be fractured, and some times coated with iron oxide. The feldspars are not as transparent as quartz and are partly altered. Presence of mica reflects the contribution of phyllitic material from the foothills of Himalayas as one of the possible sources. The carbonate constituent was possibly from associated carbonate formation in the Himalayan sequence.

Ganga sand used here is similar in many respects to the Chattahoochee river sand (Vesic, 1968) which is also uniformly graded and consists of subangular quartz grains with subordinate mica.

3.2.2 Calcareous Sand

Calcareous sand used in the present study was obtained from the area in vicinity of Okhla light house (Gujarat). The sand is well-graded with subrounded to subangular grains mostly composed of sea shells (Plate 3.2). The X-ray diffraction pattern for the same revealed dominant presence of carbonate (aragonite and calcite) with subordinate amount of quartz. The source for this carbonate material is from the oolites and also from the skeletal remains of marine organisms. The thin-walled skeletal calcareous grains are characterized by the typical presence of intra-particle voids that increase the tendency of the material to

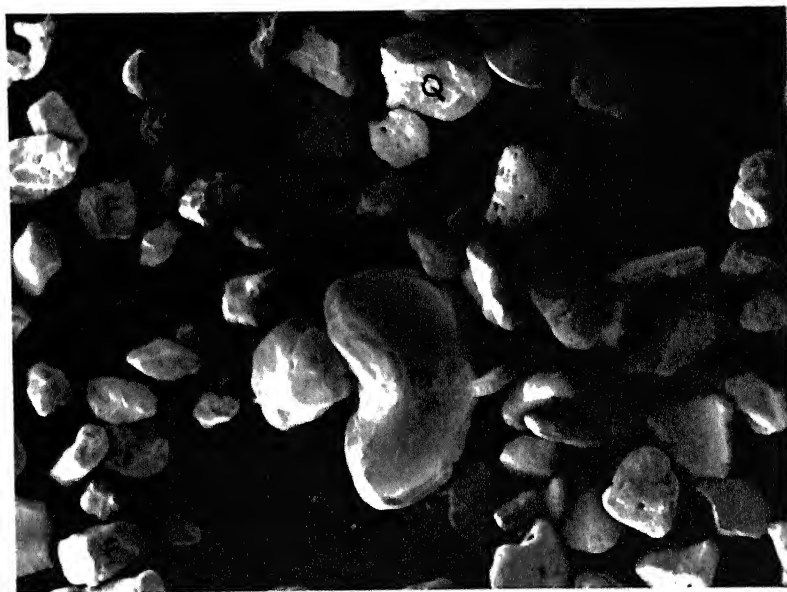


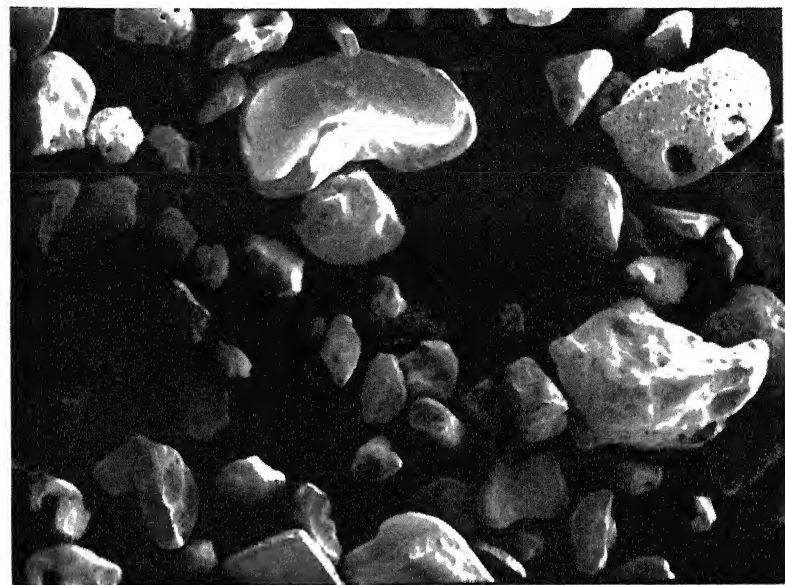
Plate 3.1

Micrograph of Angular grains of quartz (Q), feldspar (F) and flakes of mica(M) in ganga sand. (x 200)

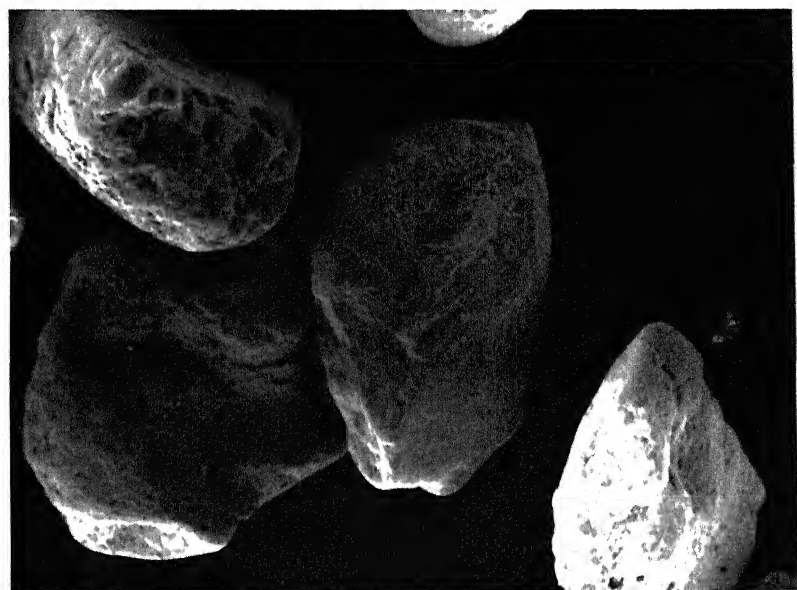
(SEM)

गंगा नदी की धूप वाली धूप कर पुस्तकालय
गंगा नदी की धूप की लक्षण काग्यव

अवधिक्रम A141992



a. Typical morphology of shells. (x 36)



b. Subrounded and Pitted Carbonate grains. (x 190)

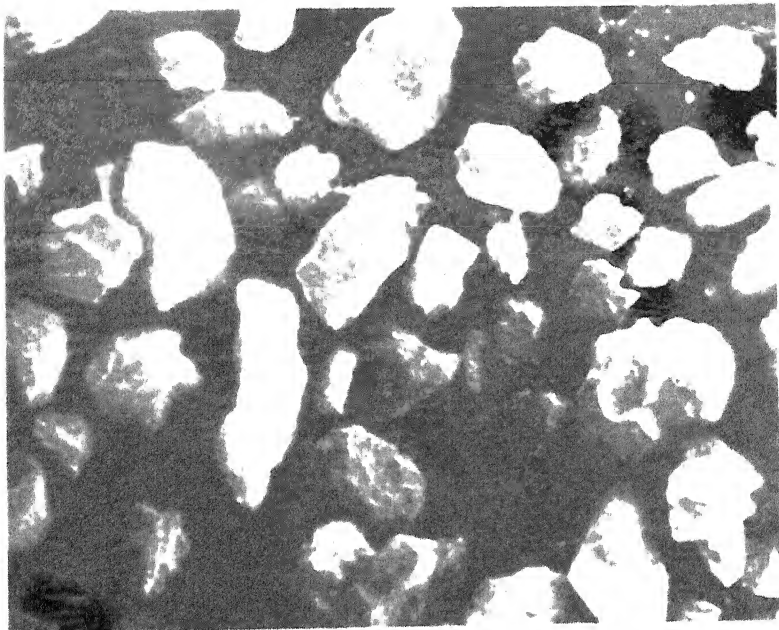
crush under stress.

3.2.3 Kalpi Sand

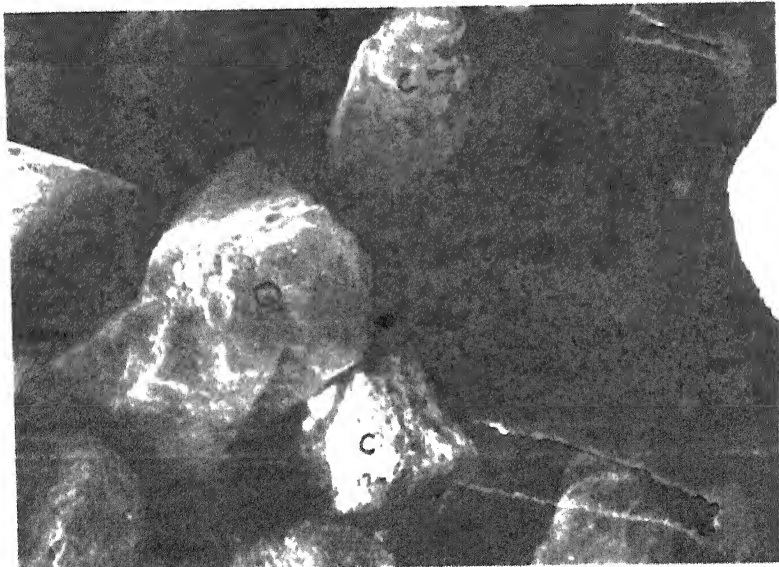
The sand from Kalpi used in this study is from Yamuna river system. In the region west of Kalpi, two tributaries (Kanchamalanga and Non) of Yamuna have their confluence at Gorakalon. The sand from the flood plain of river is very characteristic in its features and is distinctly different from the Ganga sand. The particles are well-graded, relatively coarse and very angular in outline (Plate 3.3). Quartz and feldspar are present in equal proportion (40% each). The carbonate fraction, composed of calcite, is present in considerable quantity (upto about 18%) rendering the sand calcareous as compared to the Ganga sand in which the carbonate fraction is in minor amount only. The carbonate material is present largely as matrix agglomerated with quartz and feldspar grains. When treated with mild acid, this matrix dissolves leaving the silicate particles that constituted the nucleus for the growth of carbonate. In addition, carbonate is also present in minor amount in the form of limestone grains.

3.2.4 Standard Sand

This sand, obtained from Ottawa (USA), is uniformly graded and is entirely of quartz. The grains are coarse, nearly spherical and highly rounded in outline (Plate 3.4). While the quartz grains in Ganga sand are very transparent, the grains in this sand are opaque with frosted surface possibly acquired during the process of its preparation.



a. Angular grains of quartz, feldspar and Carbonate grains. (x 70)



b. Typical Carbonate grain (c) and quartz (Q) coated with Carbonate. (x 150)

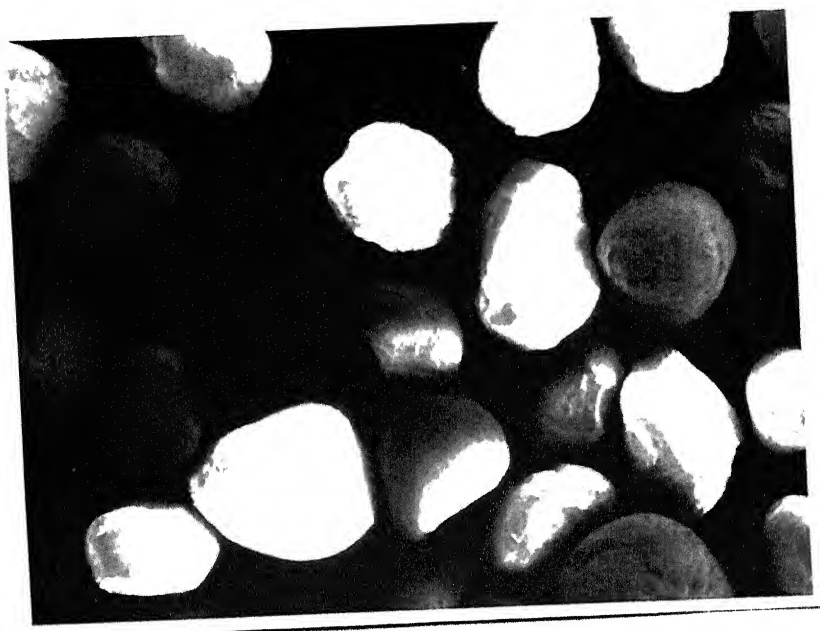


Plate 3.4

Micrograph of Standard Sand
indicating rounded grains of
quartz. (x 46)

(SEM)

3.3 Experimental

Estimation of grain size distribution, void ratios and specific gravity have been carried out adopting standard procedures using the conventional test facilities in soil engineering practice. Using sieves of 4.75, 2.00, 1.00, 0.600, 0.425, 0.212, 0.150, 0.075 and 0.045 mm, sand specimens were analyzed for their grain size before and after loading. For the estimation of maximum and minimum void ratios as well as specific gravity, tests were conducted on four specimens of each of the sand samples to obtain consistency of results.

3.3.1 Preparation of Samples at Specific Relative Density Values

For compressibility and crushing, test specimens with relative density values of 20, 25, 40 and 65% were used for different sands. For this purpose calibration charts have been prepared for relative density as a function of the height of fall using the raining technique. The sand was poured from a container (funnel) at a fixed height and corresponding relative density was calculated. The relative density of sand is a unique function of height of free fall of sand as long as a constant rate of flow is maintained. Details of experimental programme are given in Table 3.1.

3.3.2 Mineralogical Characterization

Mineralogical composition of the sands used in the present study was determined using X-ray diffraction technique. This analysis has been carried out on the General Electric Unit, operated at 30 KVA with 20 ma current, fitted with XRD-5 diffractometer using nickel-filtered Copper radiation. Scanning was done between 5 and 50 degrees (2⁰) at 2⁰ (2⁰) per cm.

Table 3.1 Experimental Programme

Sl. No.	Type of Tests	No. of Sand Samples	Particles per sample	Total	Remarks
1.	Morphology	23	100	2300	Particles
2.	Mineralogy				Tests
	a) without acid treatment	10	--		18
	b) with acid treatment	8	--		
3.	Gradation				"
	a) before loading	10	--		62
	b) after loading	52	--		
4.	Maximum void ratio	10	--	10	"
5.	Minimum void ratio	10	--	10	"
6.	Specific gravity	10	--	10	"
7.	Density (Raining technique)	9	--	9	"
8.	Compression				"
	a) relative density 25 %	25	--		42
	b) relative density 65 %	17	--		"

Identification was done by converting the "2 0" values of the peaks into the corresponding "d" values using Bragg's equation and comparing the "d" values and intensities of the peaks with the data reported in the standard file.

3.3.3 Compressibility

The test specimen prepared with different relative density values in oedometer were subjected to varying stress levels upto 176.32 Kg/cm². For this purpose Material Testing System (MTS 810) was used. This test facility has the following special features:

- i) Servo-hydraulic controls for smooth running
- ii) Electronic programming and read out.
- iii) Modular construction with the advantages of stroke, strain and lead controls.
- iv) Hydraulically operated grips for easy insertion and removal of test piece.
- v) X-ray recorders to suit various types of test output.
- vi) Large capacity of 10 tonnes with load cell having foil type strain guage bridge bonded to high strength metal-column. The bridge provides an output voltage proportional to applied load.

The system operates on a close loop principle. A command signal in the form of analog programme voltage, representing the desired load, stroke or strain to be applied to the specimen is compared with a feedback signal that represents the actual load. Stroke or strain is measured by transducer. Any deviation between the command and feedback causes a correction of the control signal to be applied to a servo-valve which in response to the control signal causes the actuator to move in a direction

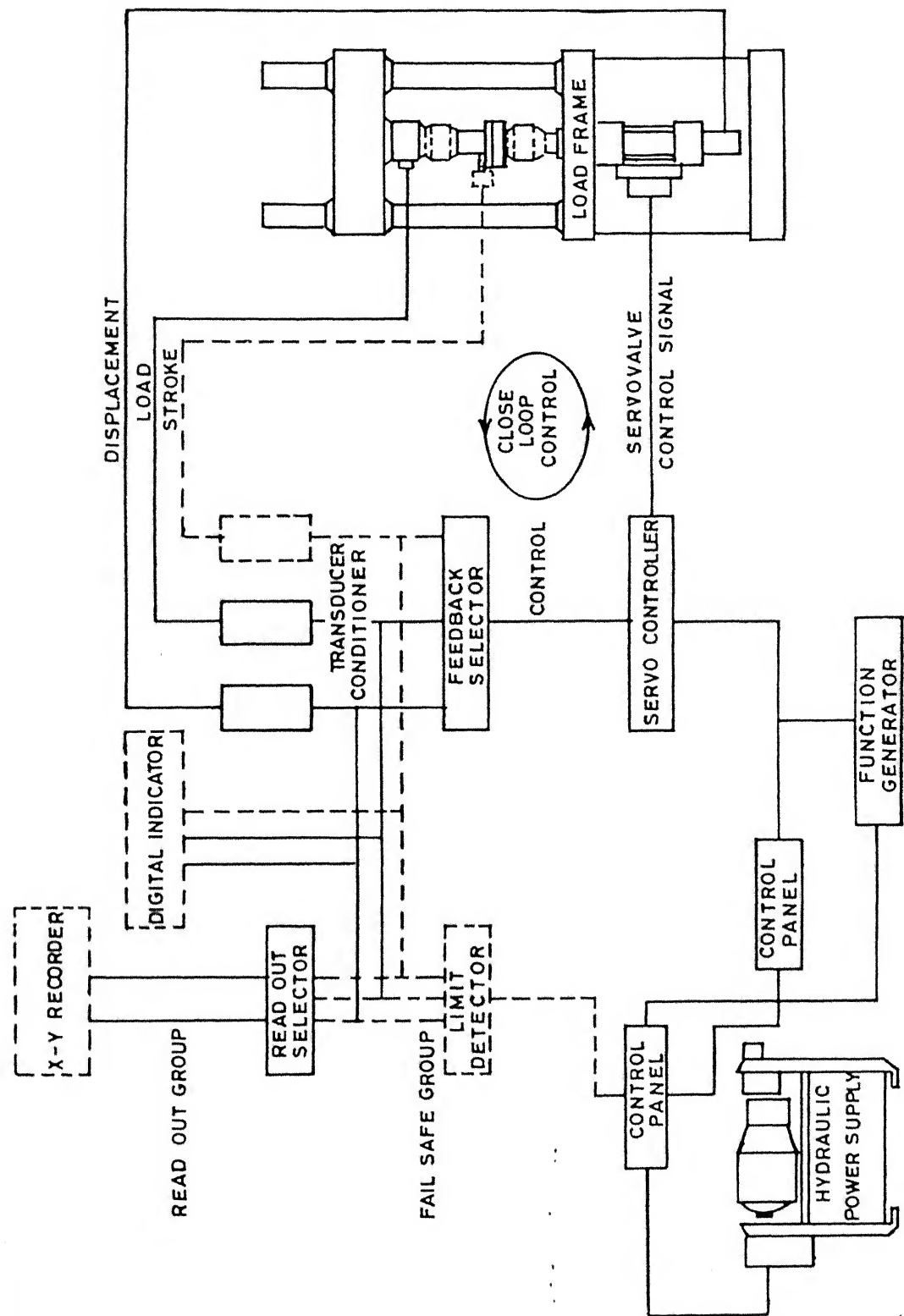


Fig. 3.1 Block diagram of Material Testing System - Model 810.

required to reduce the deviation to zero. Block diagram of the Material Testing System is given in Fig.3.1.

3.3.4 Particle Shape Analysis

The particles in each of the sand specimens before and after the compressibility tests were analyzed for shape in terms of their sphericity, shape factor and angularity. This involved estimation of long, intermediate and short diameters as well as tangent counts and projected surface area for different grains in each of the specimens. Using these parameters, quantitative evaluation of shape has been carried out.

An image Analyzer System of Bousch and Lamb make (Omnicon Alpha 500) has been used for this purpose. A brief description of the system is given in the succeeding paragraphs. The system is versatile and is capable of providing full field measurements or measurements of individual single feature in addition to the tangents and intercept counts. The system consists of two major assemblies --- the microscope with the scanner and the rack of modules - basic , display, control and measurement modules.

3.3.4.1 Microscope and Scanner

A microscope is essentially an optical image forming device used in conjunction with the analyzer. The scanner resolves the optical image presented to it by scanning along parallel lines, producing an analog signal (as a function of position) which corresponds to the intensity profile of the image along each line. The overall function of scanner is therefore, essentially similar to that of television camera, but with a different design for obtaining excellent linearity, stability, shading and noise performance, as well as an ability to accommodate rapid changes

In the level of illumination depending on the specimens.

3.3.4.2 Basic Module

The basic module supplies power to the Measurement Module and generates count tags, bright outline demarcating boundaries of the various features and the alpha-numeric characters that indicate the counts. After processing the video signal from the scanner, this module feeds the same into display.

3.3.4.3 Display Unit

The Display Unit is an instrumentation type television monitor with a diagonal screen size of 229 mm.

3.3.4.4 Entire Field Count Unit

The entire field count unit counts the selected features or their components in the image. It receives its input in the form of binary video signal from the Basic Module and provides Binary Coded-Decimal (BCD) output back to the Basic Module. (Plate 3.5).

3.3.4.5 Measurement Unit

The Measurement Unit measures the desired dimension of detected features. Measurement of full field or any single feature is possible with this unit. In the present study the latter has been adopted. Block diagram of the image analyzer is presented in Fig. 3.2.

3.3.4.6 Particle Measurement

The measurement of diameters, projected surface area and tangent counts have been made using the image analyzer system. These data were used for the quantitative analysis of the particle shape. For determination of diameter and surface area (area excluding hole), single feature measurement mode of the image analyzer was used. These measurements are possible on features selected by the operator using either the light pen or

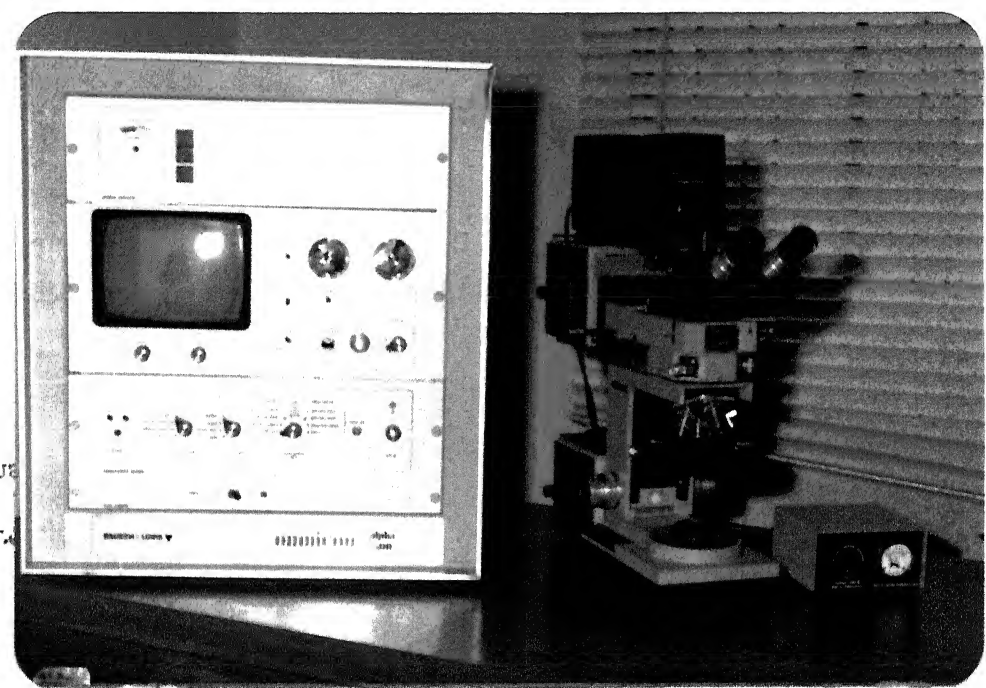


Plate 3.5

Image Analyzer Set Up

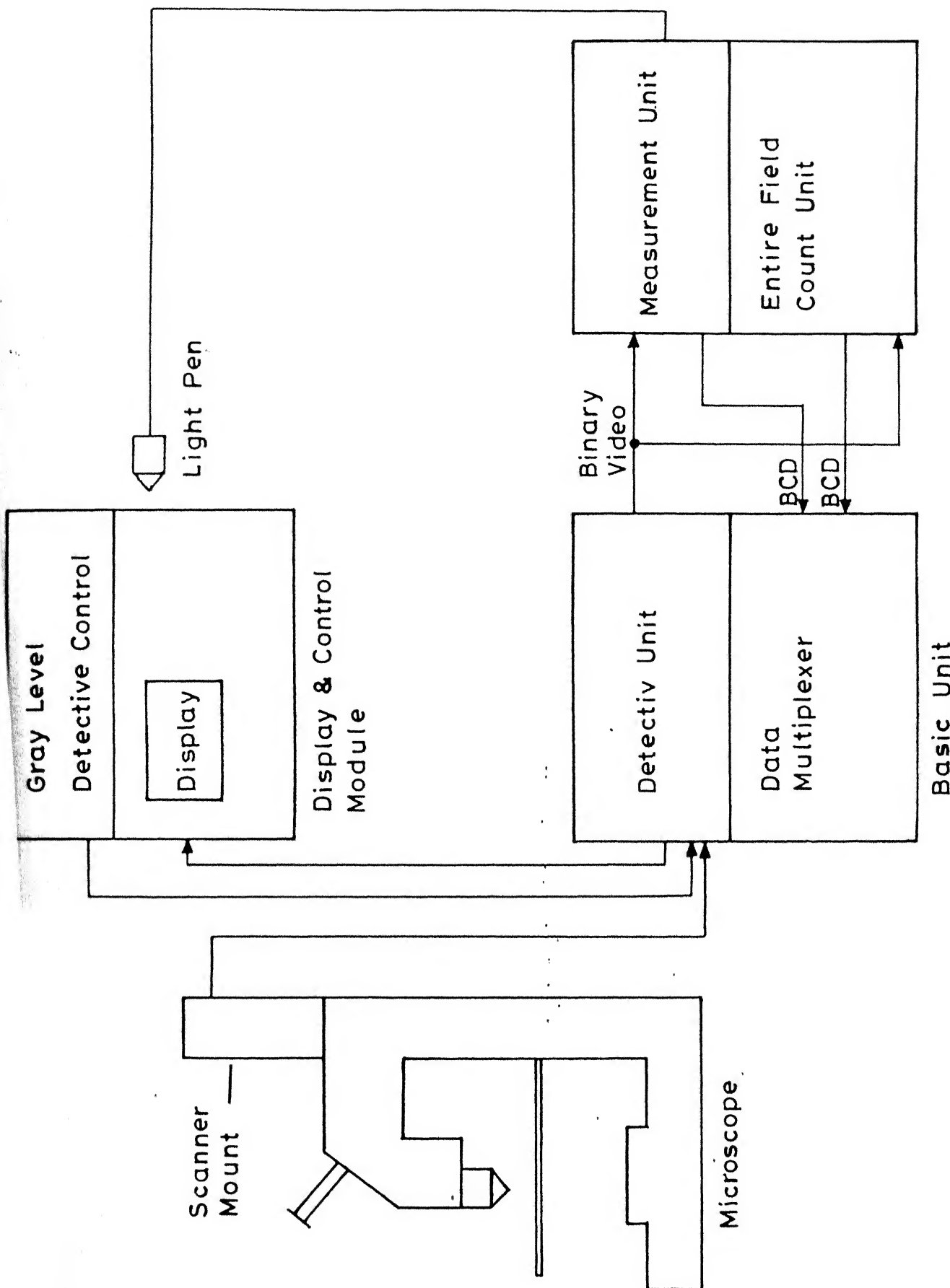


Fig. 3.2 Block diagram of the Omnican Alpha Image Analyser with Microscope.

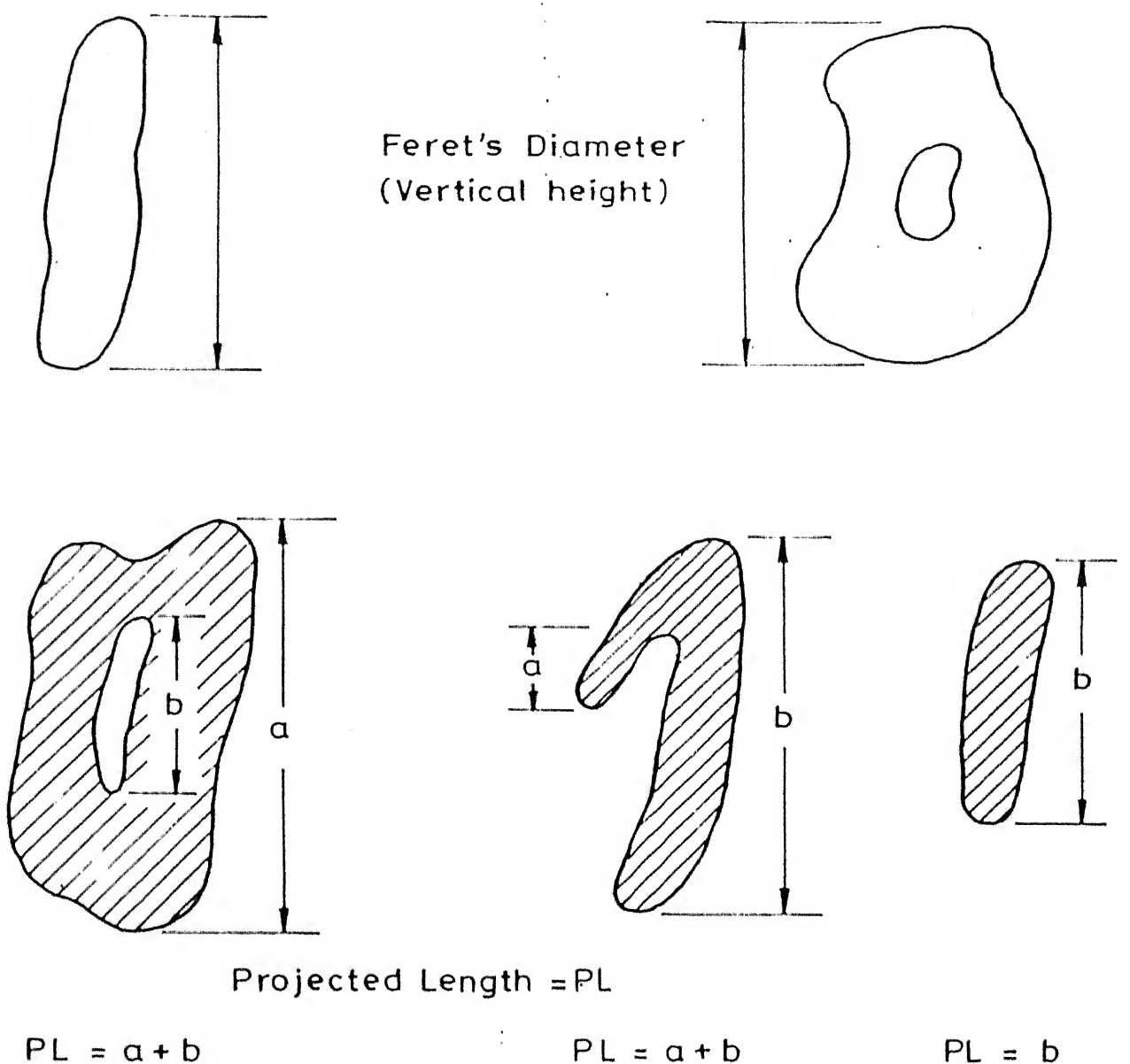
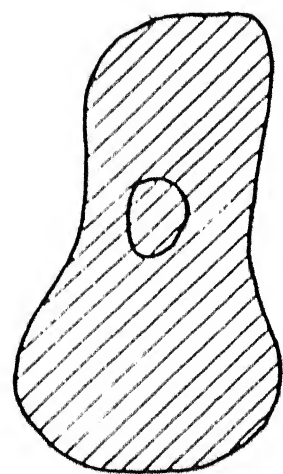
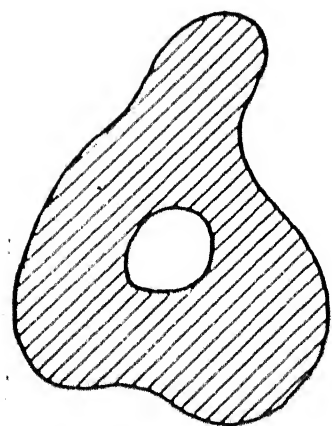


Fig. 3.3 Different types of single feature measurement.



Area including hole



Area excluding hole

Fig. 3.3 (Continued)

made to rest on their respective maximum projected area.

iii) The sample was placed on the movable stage under the microscope.

iv) An average of 25 to 30 particles from each sieve fraction were randomly chosen for the analysis.

v) The shortest diameter (d_S) for each grain was determined by focussing alternately on the glass plate and the top of grain (using the Vernier reading of the microscope) and measuring the differential deviation.

vi) Using the movable frame facility, "tangent rectangular" for each individual grain was constructed. The long side of the tangent rectangular measured in vertical direction was taken as long diameter (d_L).

vii) For determination of intermediate diameter (d_I) the movable stage along with the glass slide was rotated through 90 degrees and the short side of already constructed tangent rectangular was measured in the vertical direction.

The Count Mode of the image analyzer was used to determine the tangent count. Four types of counts are possible - total feature (particle) count, lower positive tangent, lower negative tangent and the intercept count. In this study, the lower positive tangent (the sum of all tangent points formed at the lower convex boundaries of the particle with horizontal scan line) and lower negative tangent (the sum of all tangent points formed at the lower concave boundaries of the particle with the horizontal scan line) were counted. The negative tangent count acted as a check because its value is equal to positive tangent count minus

two. For the determination of total number of protrusions on the upper portion of the grain can be counted by using either the dark mode of the image analyzer or by rotating the movable stage of microscope along with the glass slide by 90 degrees. Lower positive and negative tangents and features engaged in each other are shown in Fig. 3.4.

3.3.4.7 Quantification of Particle Shape

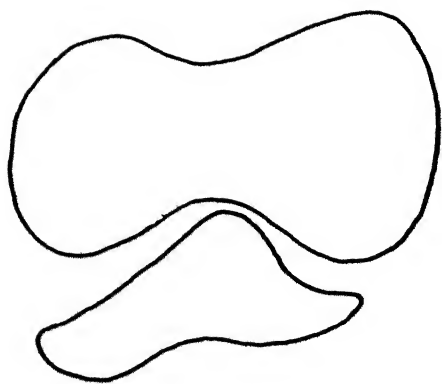
Shape is a complex property of a grain and it is difficult to define shape properly except for grains that approximate regular geometrical shapes. As already indicated, roundness (angularity) and sphericity (shape factor) aid in quantifying the particle shape. In the present work, detailed investigations were undertaken for the quantification of shape.

3.3.4.7.1 Sphericity and Shape Factor

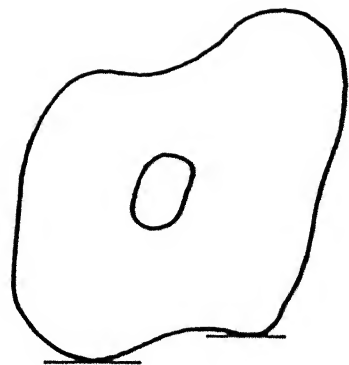
Krumbein (1941) expressed sphericity in terms of the three diameters (d_L , d_I , d_S) of a triaxial ellipsoid. A sphericity value of one implies a perfect sphere, and the sphericity value decreases with the irregularity of the particle shape. Based on measurements of d_L , d_I and d_S particle sphericity may be computed as:

$$\begin{aligned}\psi &= \frac{\text{Volume of particle}}{\text{Volume of circumscribed sphere}} \\ &= \frac{3}{4} \sqrt{\frac{d_I d_S}{d_L^2}} \quad (3.1)\end{aligned}$$

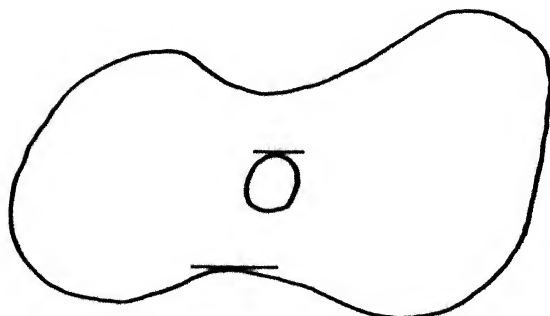
Shape factor is another index used as a measure of particle shape. Lees (1964) proposed a shape factor (F) in terms of flatness ratio P ($\frac{c}{b} = d_S/d_I$) and elongation ratio q ($b/a = d_I/d_L$).



Two features engaged
in each other are
counted as one



Lower Positive Tangent



Lower Negative Tangent

Fig. 3.4 Lower positive and negative tangents and two features engaged in each other.

In this study, shape factor was calculated using the expression (Blatt et al. 1972):

$$SF = \frac{d_S}{\sqrt{d_L d_I}} \quad (3.2)$$

where d_S is the short diameter,

d_I is the intermediate diameter, and

d_L is the long diameter

Procedure for the measurement of d_S , d_I and d_L has already been presented.

3.3.4.7.2 Roundness (Angularity)

Roundness refers to the sharpness of the corners and edges of the grain. It therefore refers to aspects of the grain surface that are on larger scale than those covered under surface texture but still smaller than the overall dimension of the grain. Wadell (1932) defined roundness (angularity) as the ratio of the average radius of curvature of the corners to the radius of largest inscribed circle. Powers (1953) proposed a procedure for estimating particle roundness by visual comparison of grains with standard images of grains of known roundness. The roundness index assigned as per Powers' classification is given in Table 2.2.

The procedure (Youd, 1973) used for the determination of particle roundness index (R) is as follows:

1. Separate the sand (<2mm) into different sieve fractions.
2. Examine under microscope a representative number of particles (at least 50) from each sieve fraction.

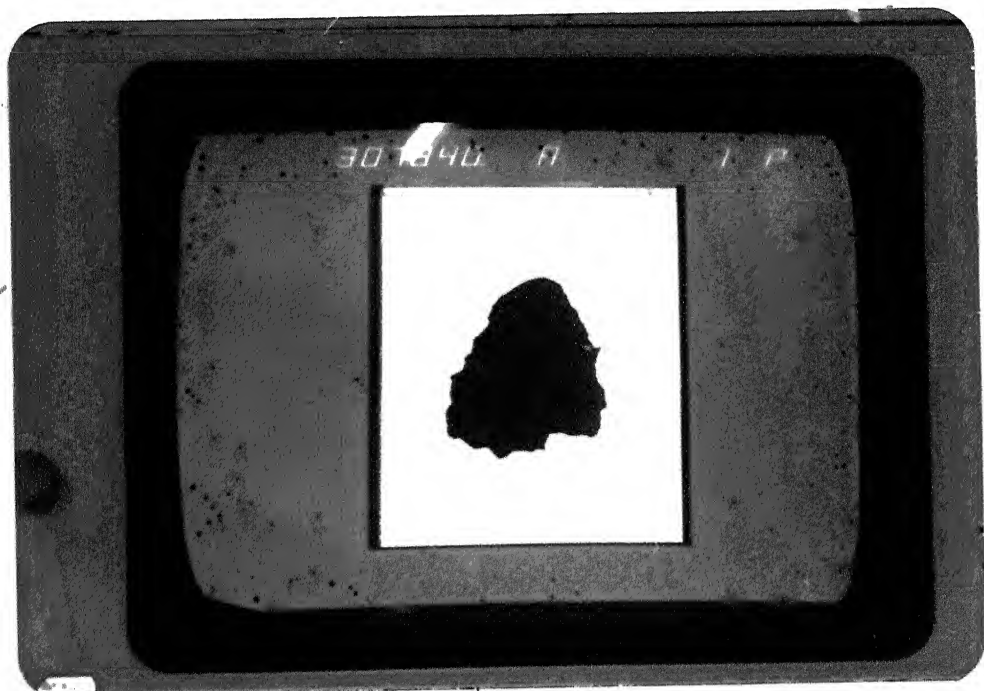


Plate 3.6

Projected Image of a Particle
Indicating Edge Protrusions

3. Visually compare shape of each particle with the shape classes and assign the value of roundness index (R) according to the classification scheme listed in Table 2.2.

4. The average value for each sieve fraction (R_j) was then calculated as

$$R_j = (\sum R_i)/n \quad (3.3)$$

where R_i is the R value assigned to particle i, and

n is the total number of particles examined.

5. After computing R_j for each sieve fraction, an average value of R_j for the sand under study was computed from the relationship

$$R = (\sum R_j P_j)/100 \quad (3.4)$$

where P_j is the percent (by weight) of the particles in the applicable sieve fraction.

The estimation of roundness index (R) by visual comparison of shape would appear to be some what subjective and therefore an independent approach was adopted to quantify roundness (angularity). Using the image analyzer, a count of total number of corners or protrusions was obtained on the boundary of the particle image, projected on the display screen (Plate 3.6). The image analyzer provides a total tangent count for both convex and concave features on the grain boundary. Tangent count was taken as a measure of grain angularity. The procedure involved in the estimation is as follows:

1. Sieve analysis of each sand sample was carried out.
2. Sufficient number of particles (25-30), from each size fraction were placed on a glass slide which after enough tapping (to ensure that the particle rests on the plane of its maximum projected area) was put on the movable stage under the microscope.
3. Each grain on the display screen is boxed in the "tangent rectangular" (by movable frame facility) and using the count mode of the image analyzer, the number of tangents on the lower and upper grain boundary is recorded.
4. The stage was then rotated through 90 degrees and the tangent counts were recorded for the other two sides.
5. Sum of tangent counts obtain in steps 3 and 4, provide a tangent count value for each particle.
6. The average value of tangents for each sieve fraction was then calculated as

$$T_j = (\sum T_i)/n \quad (3.5)$$

where T_i is the total number of tangent count for particle i , and n is the total number of particles examined.

7. After computing T_j for each sieve fraction, an average value of tangent count for the sand under study was determined from the relationship

$$T = (\sum T_j P_j/n)/100 \quad (3.6)$$

where P_j is the percent (by weight) of the particle in the corresponding sieve fraction.

The average value of tangent count thus obtained was directly used for comparing different sands. However, for comparing particle angularity for different sieve fraction of a given sand, the average tangent count for each fraction was normalized with the average circumference of the grains in that fraction.

It is important to note that both roundness index and tangent count are obtained by observing the grain images in two dimensions. A procedure similar to the one adopted here for tangent count has also been used for averaging the values of particle sphericity and shape factor.

CHAPTER IV

EXPERIMENTAL DATA

4.1 General

Experimental investigations have been carried out to characterize all the sand samples involved in the present study in terms of their mineralogical, physical and morphological characteristics. The samples subjected to the compressibility tests have been analyzed for their particle size and shape to enable an understanding of their role in the compressibility and also the extent of crushing the particles in the system undergo. In this Chapter, the experimental results are presented. Interpretation of these results along with the discussion of the interrelationship between various parameters involved during compressibility and crushing of the sands is dealt in the succeeding chapter.

4.2 Mineralogical Composition

X-ray diffraction analysis has been carried out for the different sands used in the present study. Various mineral constituents have been identified on the basis of their characteristic peaks. Semi-quantitative estimation of the mineral constituents has been made which has been confirmed to be fairly within the range on the basis of microscopic examination as well with the acid dissolution method in the case of carbonate fraction.

Typical diffraction pattern for the Ganga sand is presented in Fig. 4.1. Quartz is the dominant mineral constituent (60 to 65%) associated with feldspar (20-25%). In addition, presence of mica (8-10%) is confirmed to be present from the occurrence of

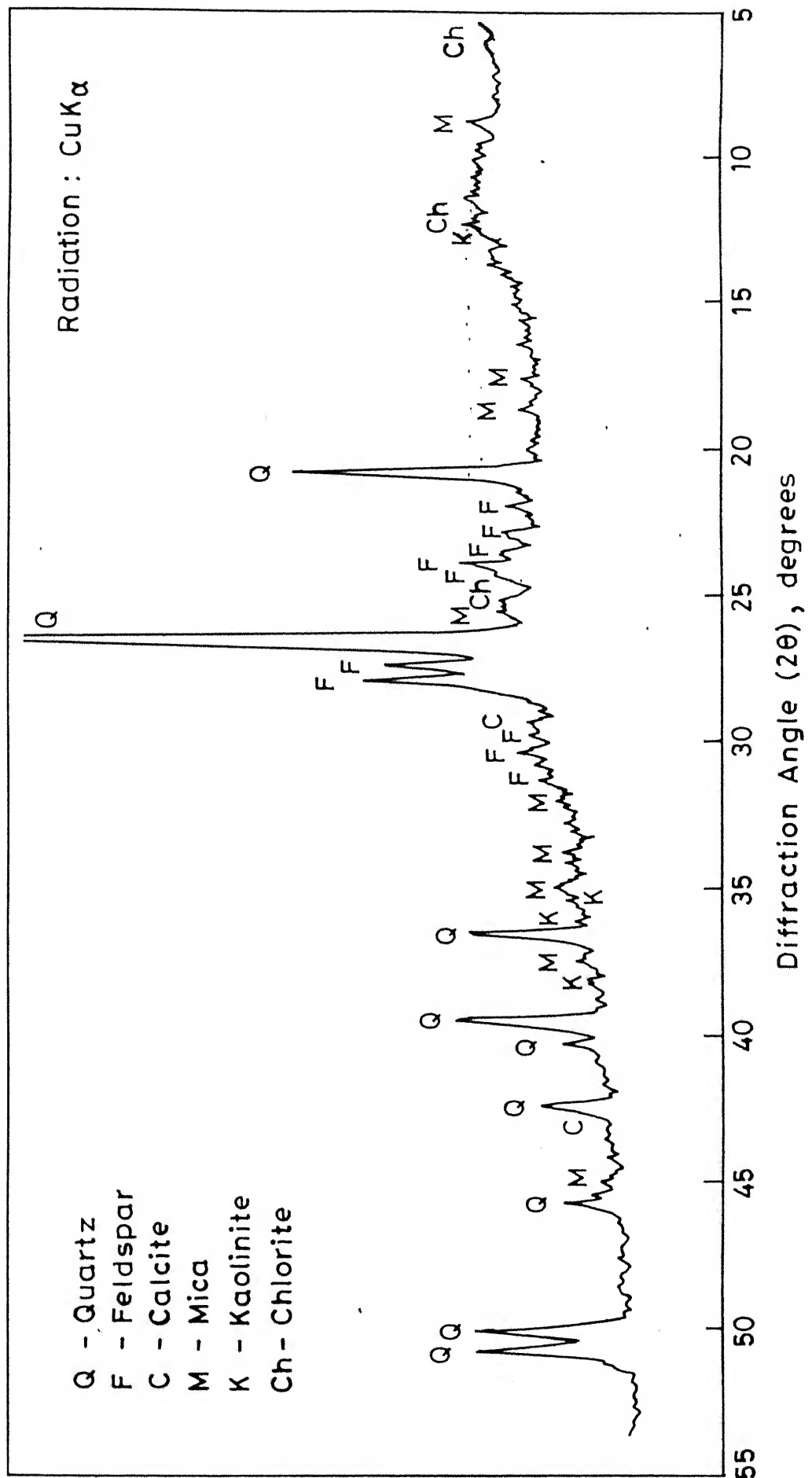


Fig. 4.1 X-ray diffraction pattern of Ganga sand.

the peaks around 10 \AA and 5 \AA as well as others marked in the pattern. Minor amount of carbonate in the form of calcite is also present. The peak around 12.4° (2θ) could either be of kaolinite or chlorite or both. From the presence of peaks around 36.1° and 38.2° (2θ), it has been confirmed that kaolinite is present in a very minor amount. On the other hand, the peak at 6.1° (2θ) corresponding to 14.2 \AA confirms minor amount of chlorite also. Thus chlorite and kaolinite are both present upto about 3% within the sand.

The X-ray diffraction pattern for Kalpi sand (Fig. 4.2) reveals distinct mineralogical composition as compared to Ganga sand. This sand is relatively rich in calcite with the carbonate fraction estimated to be around 18%. Quartz and feldspar are in equal proportion (around 40% each). In this sand, the feldspar however is of two varieties (alkali and potash types) indicating a distinctly different source for the sand as compared to that of Ganga. The occurrence of mica is in minor quantity (upto 2%) in this case.

The diffraction pattern for calcareous sand (Fig. 4.3) has confirmed the presence of carbonate upto 95% of its composition with quartz as the associated mineral (upto 5%). X-ray analysis has very clearly established the presence of two carbonate minerals namely aragonite and calcite. As already indicated, the association of aragonite reflects contribution of carbonate from marine organisms. Electron microscopic examination of carbonate particles in this sand has revealed a distinct morphological pattern for the grains typical of a sea shell surface.

The standard sand used is a commercially prepared one. It is a pure quartz sand without any other mineral constituents as

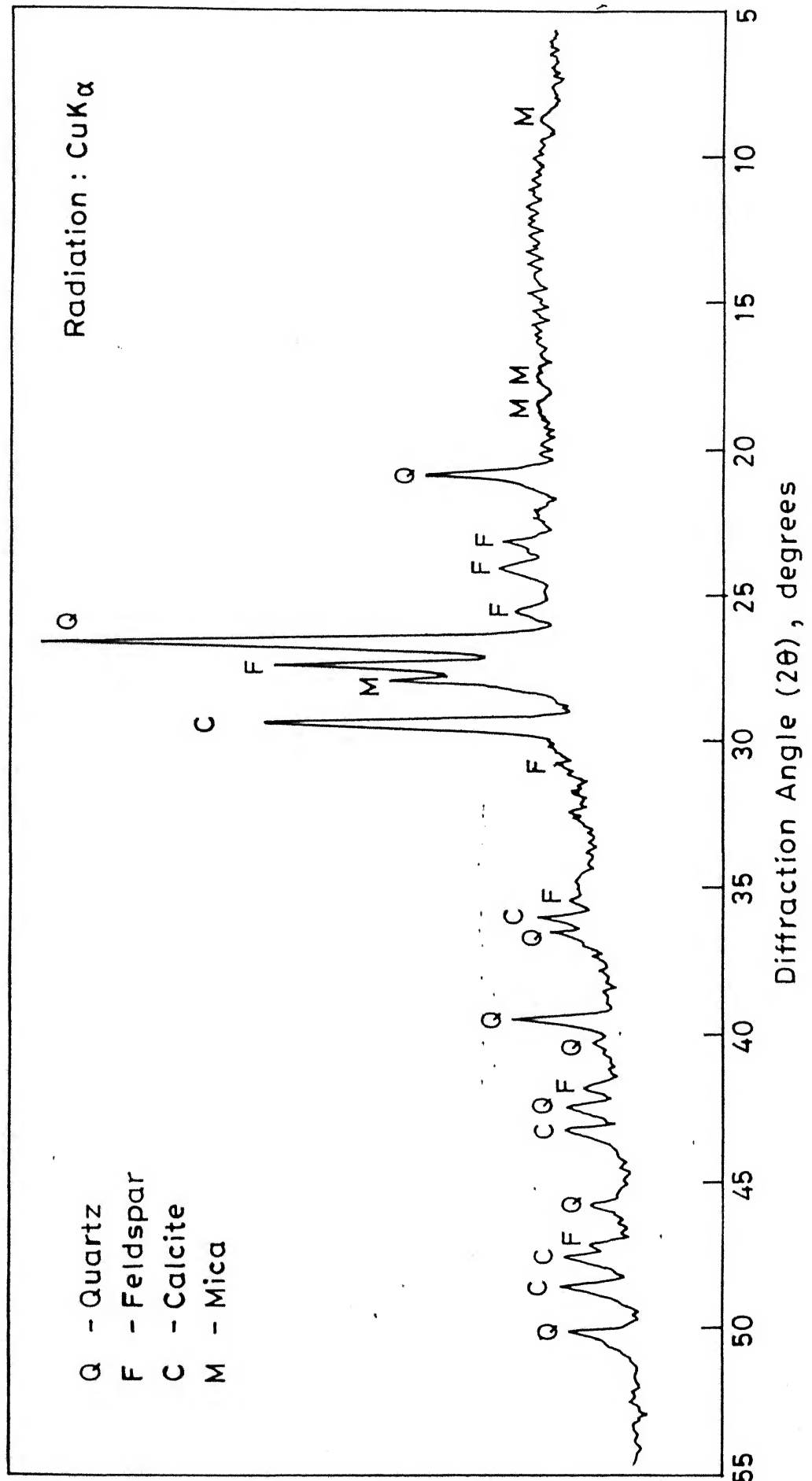


Fig. 4.2 X-ray diffraction pattern of Kalpi sand.

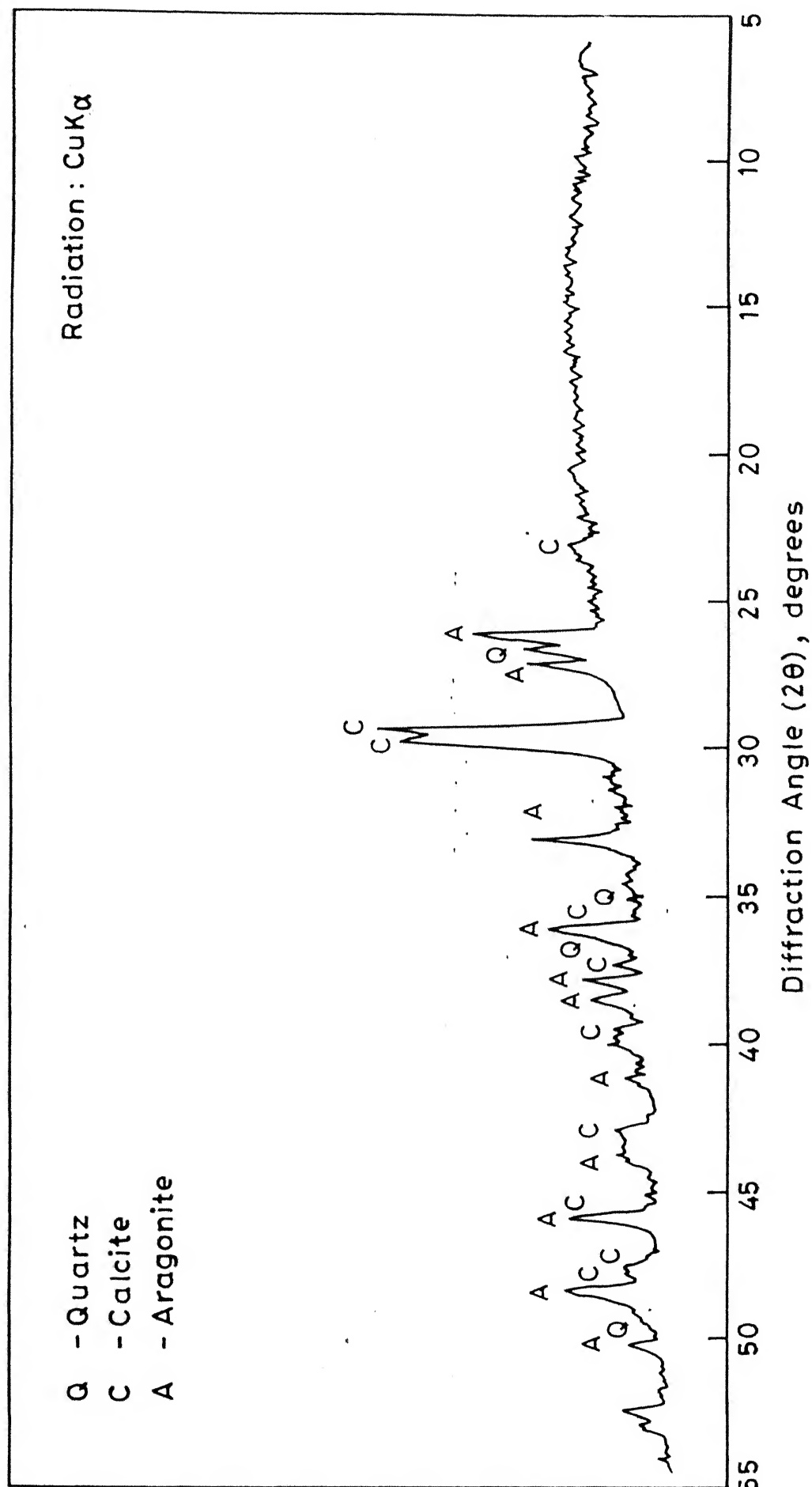


Fig. 4.3 X-ray diffraction pattern of Calcareous sand.

confirmed from its X-ray diffraction pattern (Fig. 4.4).

X-ray analyses have also been carried out for estimating the mineralogical composition of other sand samples namely the Ganga sand after removal of mica, Ganga with enhanced mica, the sand obtained by mixing Ganga, calcareous and Standard (referred to as coarse Ganga), artificial calcareous sand, prepared by mixing Ganga, Kalpi, and Standard sands and the two fractions of Kalpi sands with different grain size distribution (designated as Kalpi 1 and Kalpi 2). The respective X-ray diffraction patterns for these sands are presented in Figs 4.5 - 4.10. Estimated mineral composition for each of these sands is summarized in Table 4.1 and 4.2. The estimation has been fairly within the range as has been checked using the acid dissolution technique as in the case of carbonate fractions.

4.3 Physical Characteristics

The grain size distributions for four main sands (Ganga, Kalpi, Calcareous and Standard) are shown in Fig. 4.11, whereas Fig. 4.12 shows the gradation curves for Ganga with enhanced mica, Ganga with mica removed, Coarse Ganga, artificial calcareous, Kalpi 1 and Kalpi 2 sands. The grain size distribution for Kalpi sand (Fig. 4.11) is distinctly different compared to the other sands. It may be indicated that Kalpi sand has its source from the Yamuna with a relatively shorter distance of transport.

The relation between the relative density versus height of all using raining technique for Ganga, Kalpi, Calcareous and Standard Sands is shown in Fig. 4.13. For a comparison data for the Chattahoochee river sand (Vesic 1963) is also represented on

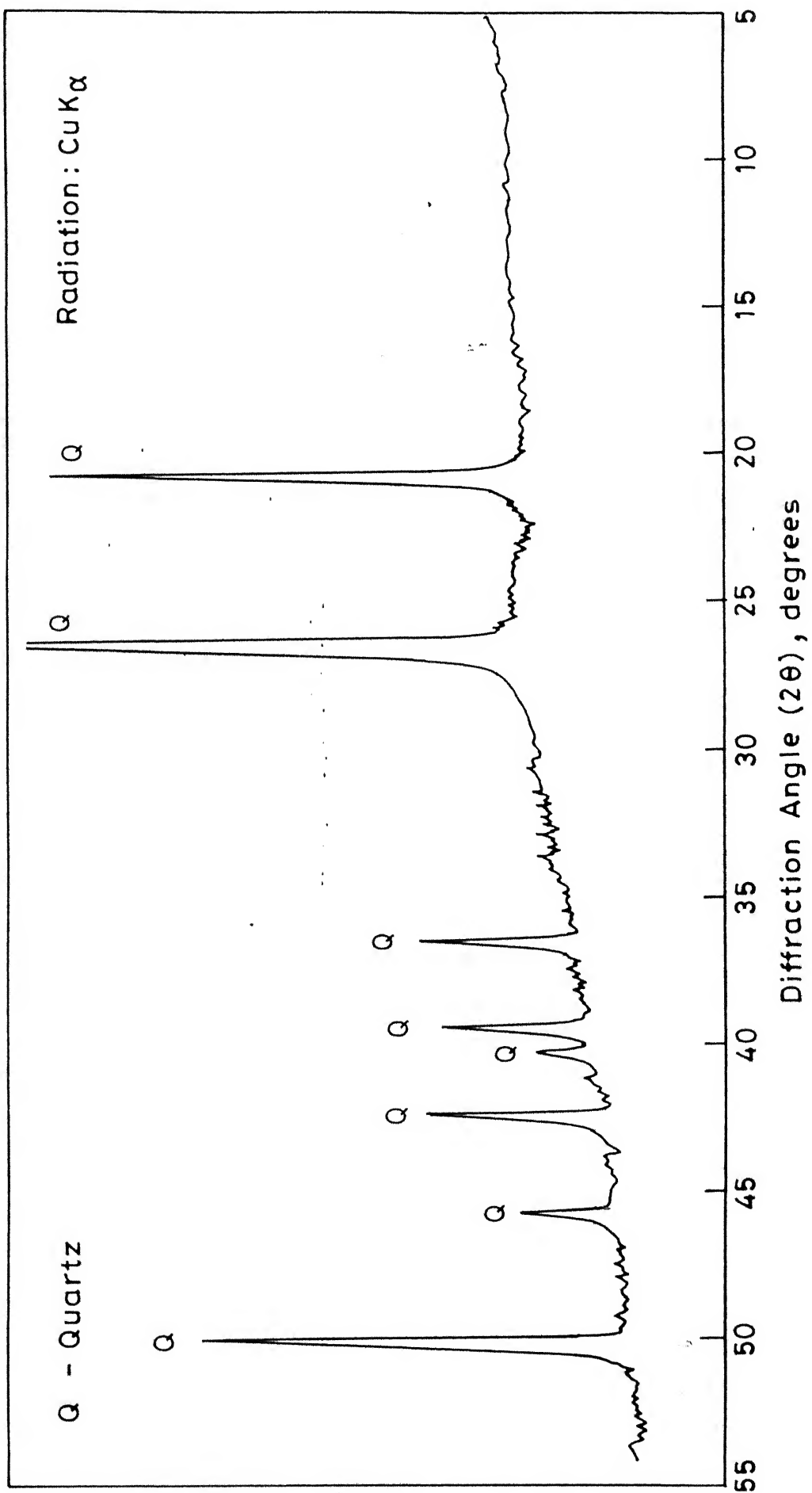


Fig. 4.4 X-ray diffraction pattern of Standard sand.

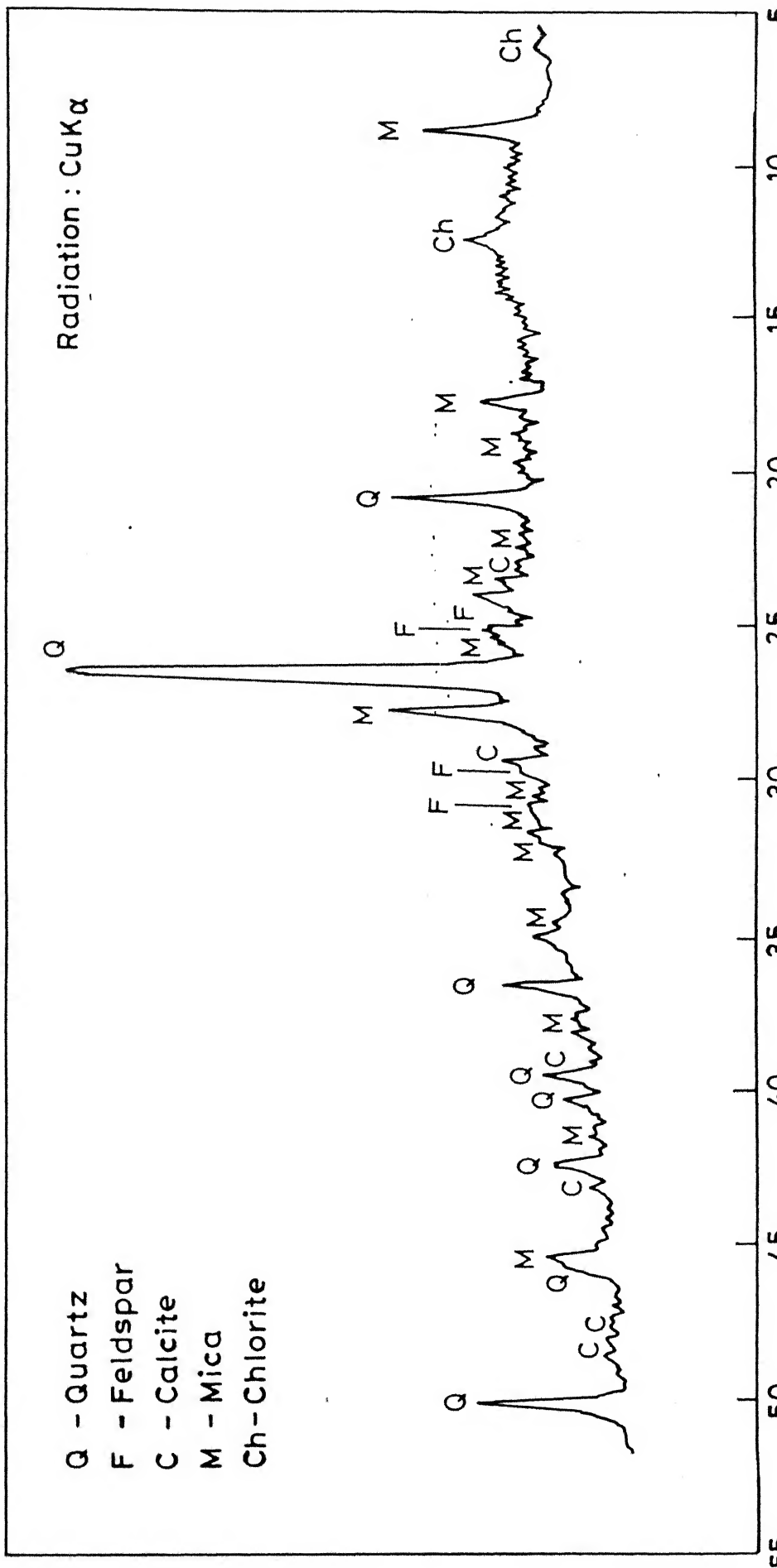


Fig. 4.5 X-ray diffraction pattern of Ganga sand with enhanced mica.

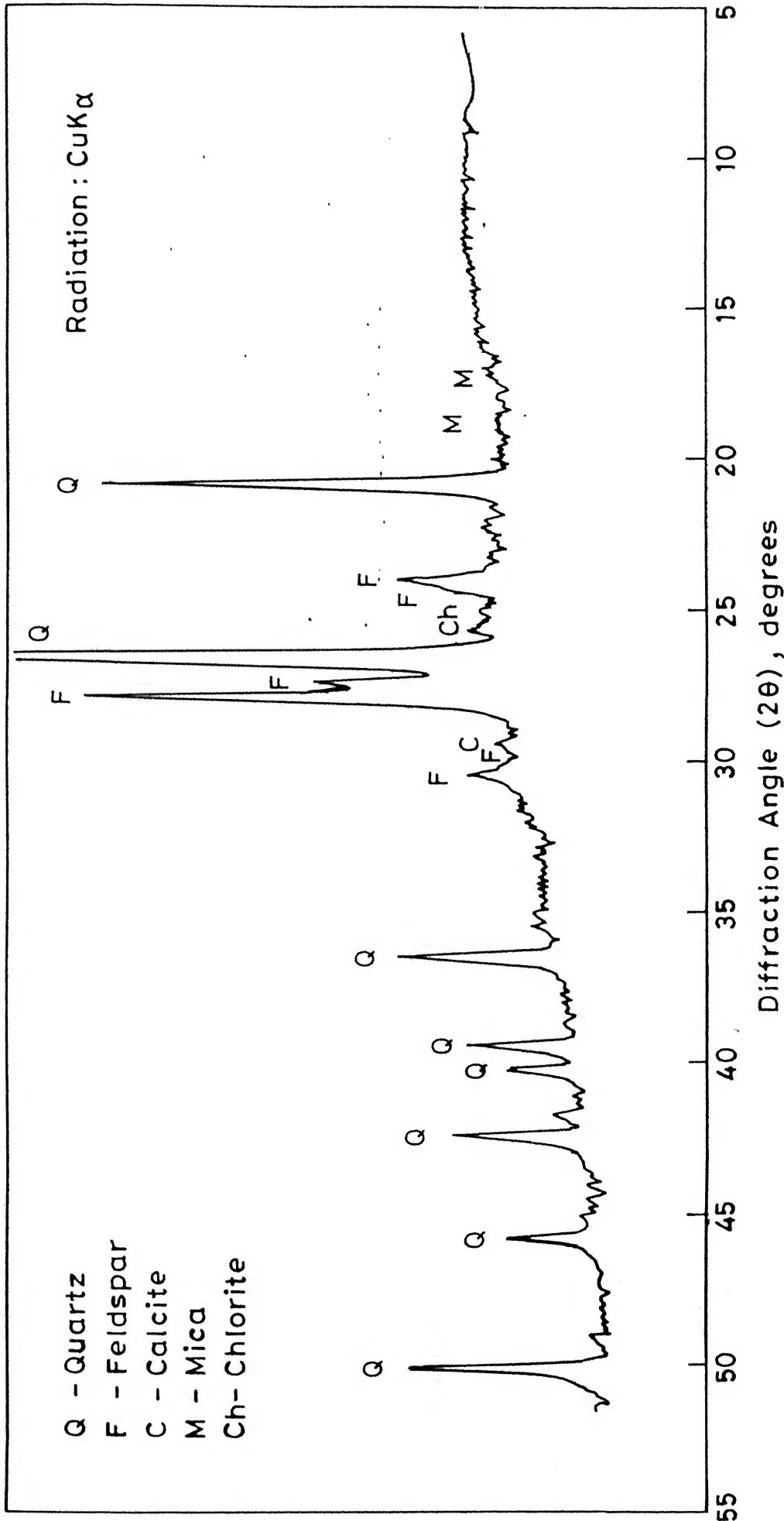


Fig. 4.6 X-ray diffraction pattern of Ganga sand with mica removed.

Radiation : CuK α

- Q - Quartz
- F - Feldspar
- C - Calcite
- M - Mica
- A - Aragonite

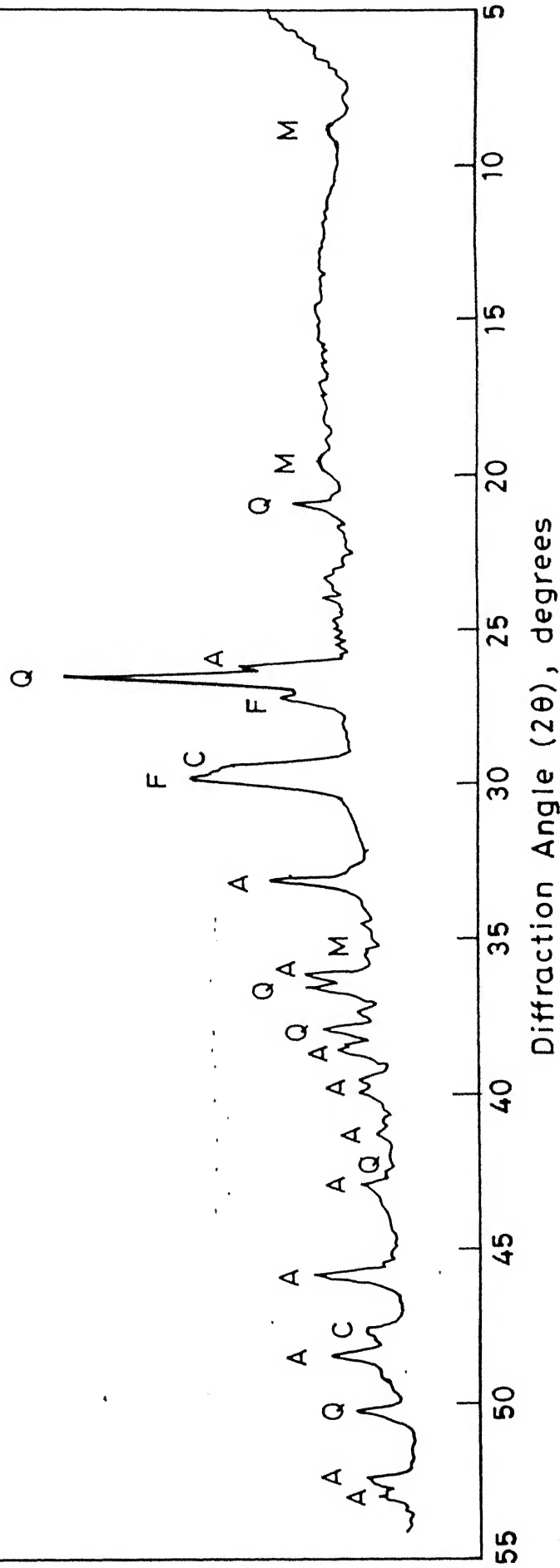


Fig. 4.7 X-ray diffraction pattern of Coarse Ganga sand.

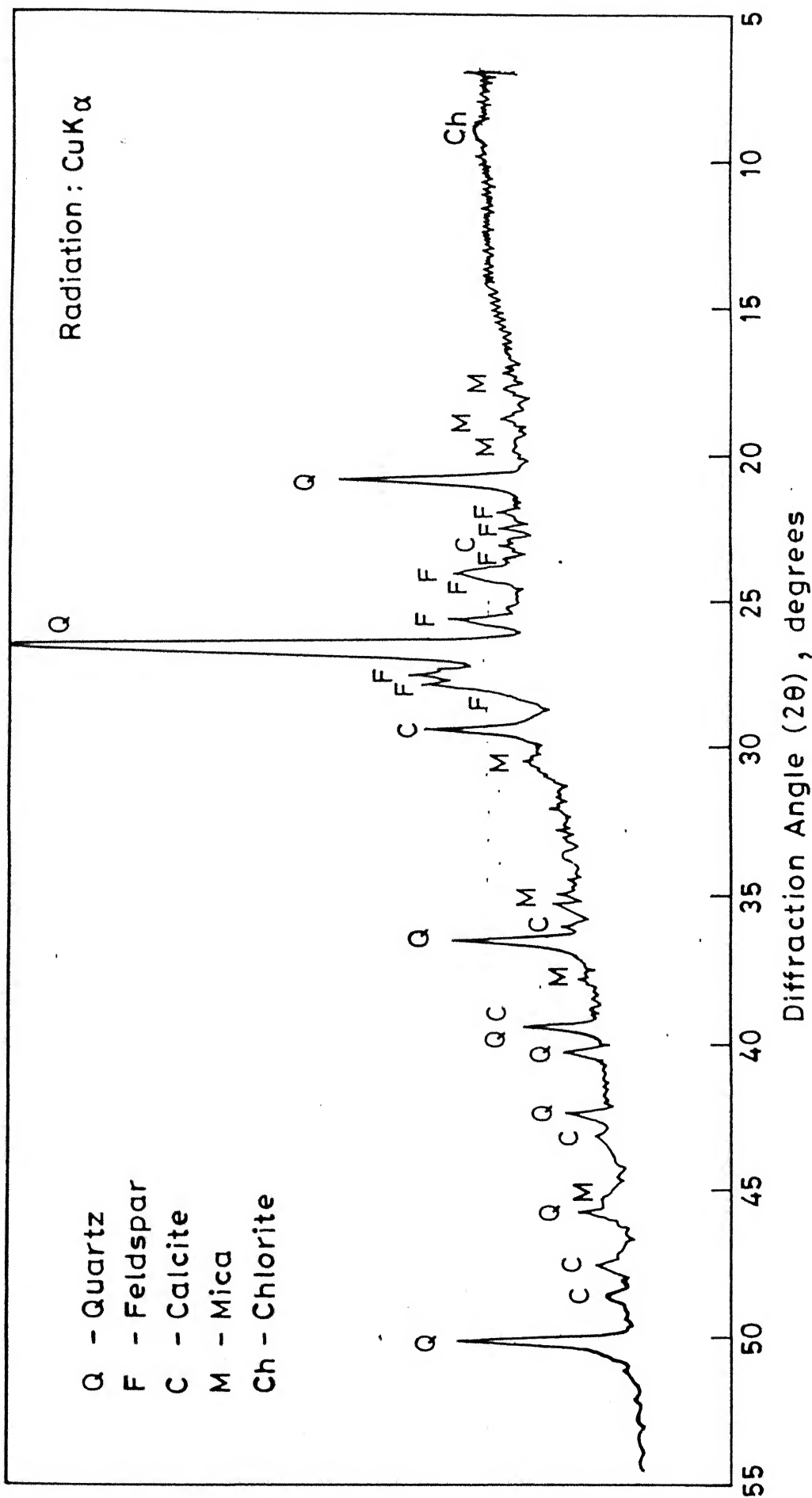


Fig. 4.8 X-ray diffraction pattern of Artificial Calcareous sand.

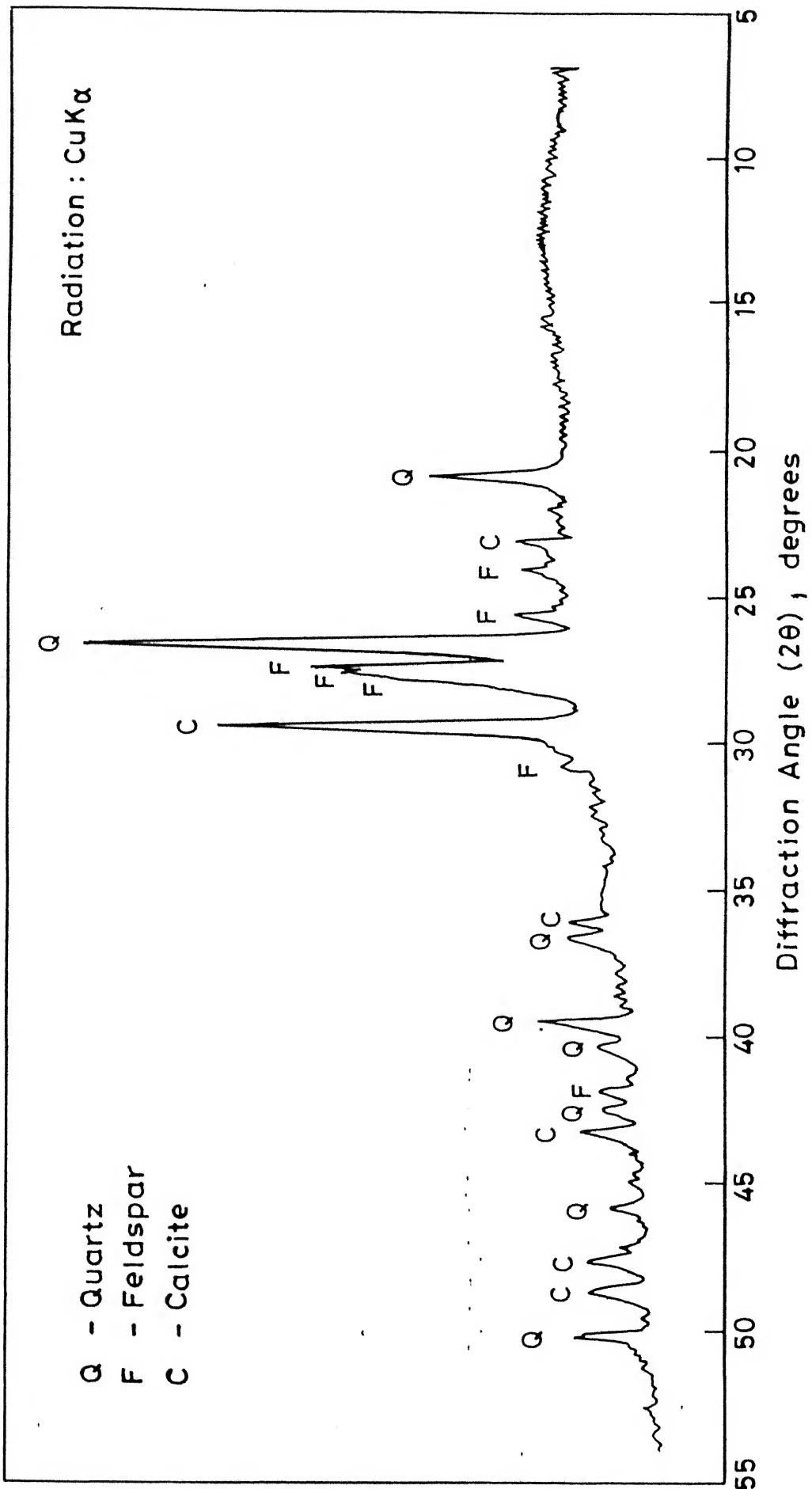


Fig. 4.9 X-ray diffraction pattern of Kalpi 1 sand.

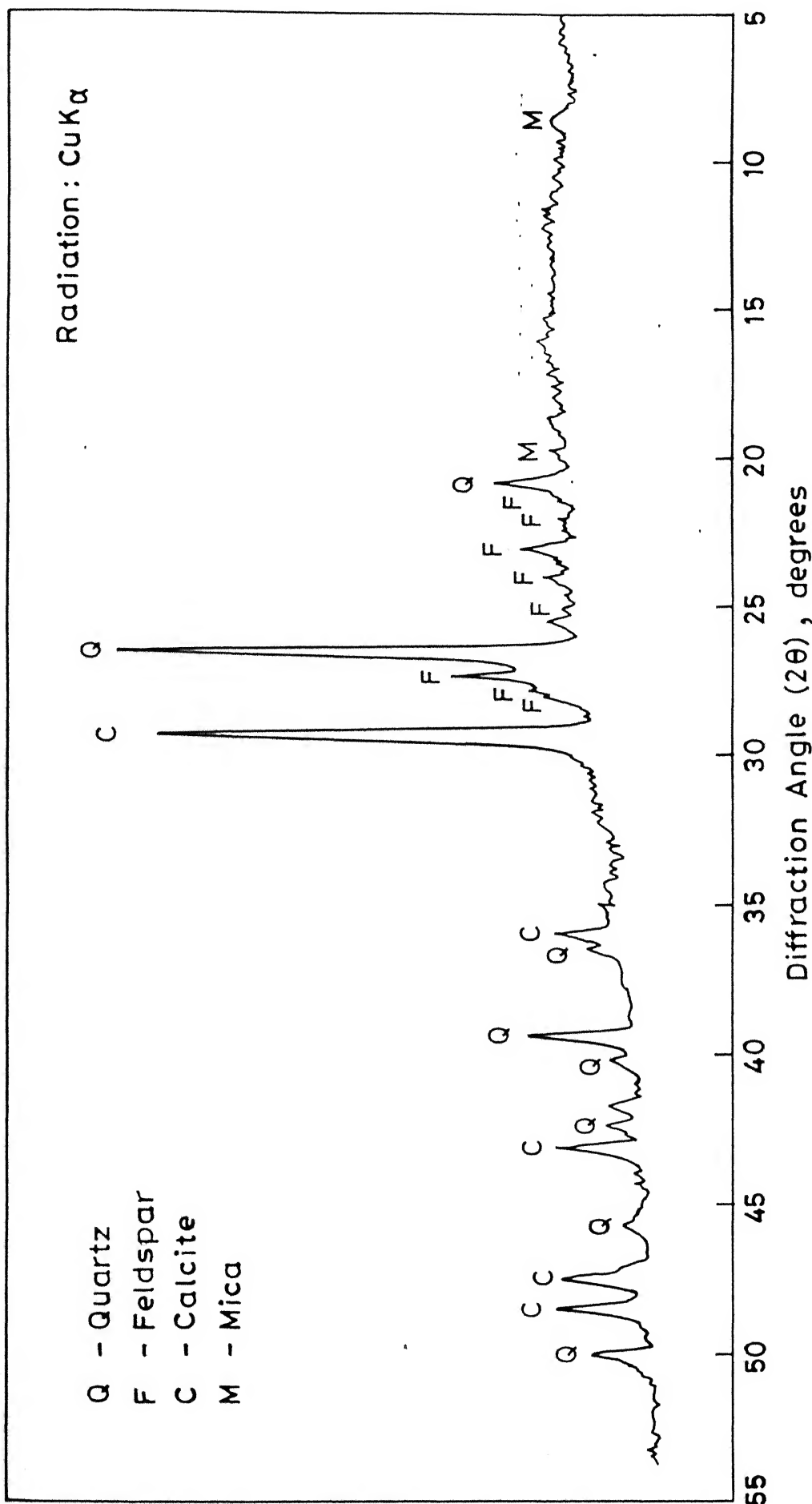


Fig. 4.10 X-ray diffraction pattern of Kalpi 2 sand.

Table 4.1 Mineralogical Composition of the Test Samples

S1. No.	Sand Sample	Quartz %	Feldspar %	Mica %	Carbonate %	Chlorite and Kaoli- nite, %
1	Ganga	60-65	20-25	8-10	2-3	2-3
2	Ganga with enhanced mica	30-40	6	50-60	4	3
3	Ganga with mica removed	65	30	1-2	3-4	-
4	Coarse Ganga	26-27	2-3	71		-
5	Kalpi	40	40	1-2	18	-
6	Kalpi 1	45	30	-	25	-
7	Kalpi 2	50	18-20	1-2	30	-
8	Calcareous	5	-	-	95 (aragonite and calcite)	-
9	Artificial calcareous	50	20	5	25	-
10	Standard	100	-	-	-	-
11	Kalpi (after Acid Treatment)	50	48	-	2	-
12	Kalpi 1 (After Acid Treatment)	55	40	-	5	-
13	Kalpi 2 (After acid treatment)	55	40	-	5	-

Table 4.2: Estimates of Carbonate and Noncarbonate Mineral Contents (on the basis of acid dissolution method)

Sl.No.	Sand	Carbonate %	Other minerals %
1	Ganga	5	95
2	Coarse Ganga	71	29
3	Kalpi	20	80
4	Kalpi 1	26	74
5	Kalpi 2	29	71
6	Calcareous	91	9
7	Artificial Calcareous	20	80
8	Standard	0	100

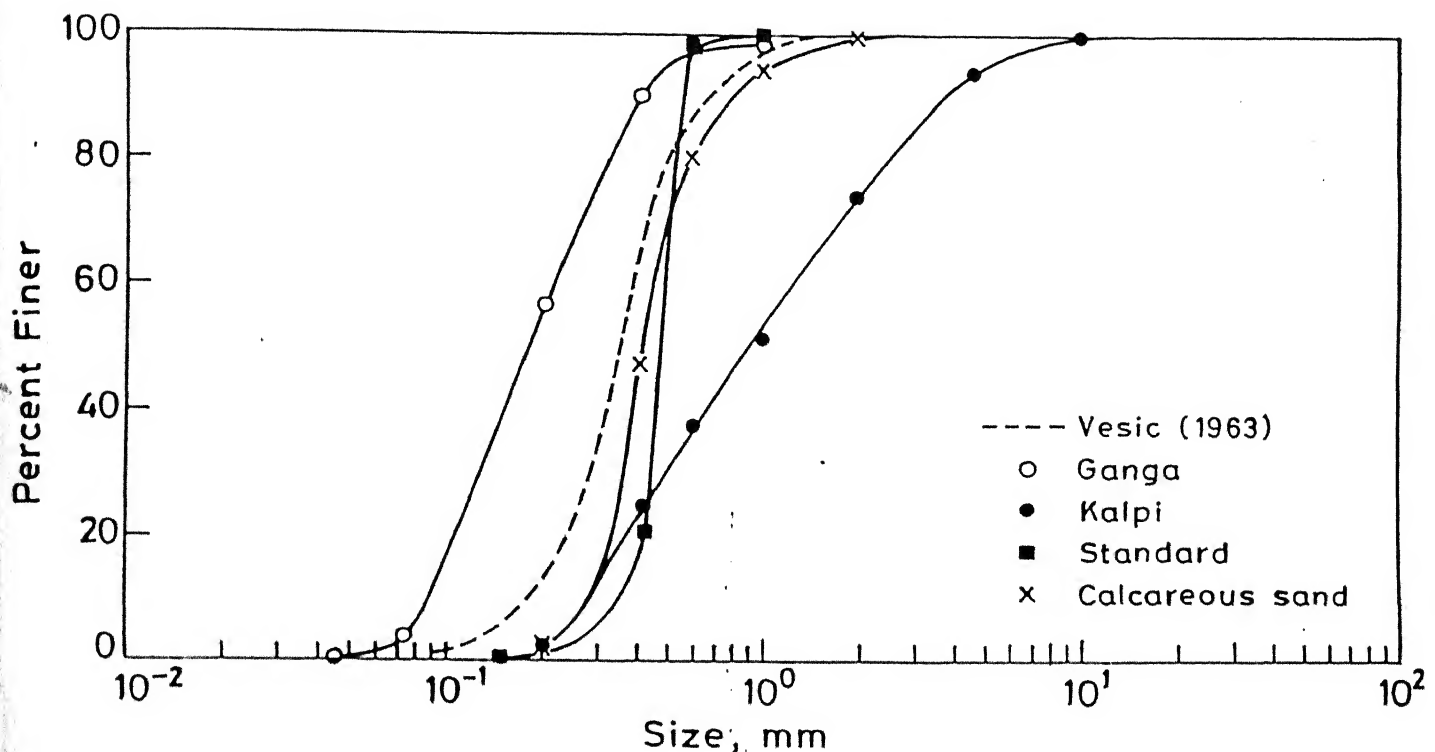


Fig. 4.11 Particle size distribution.

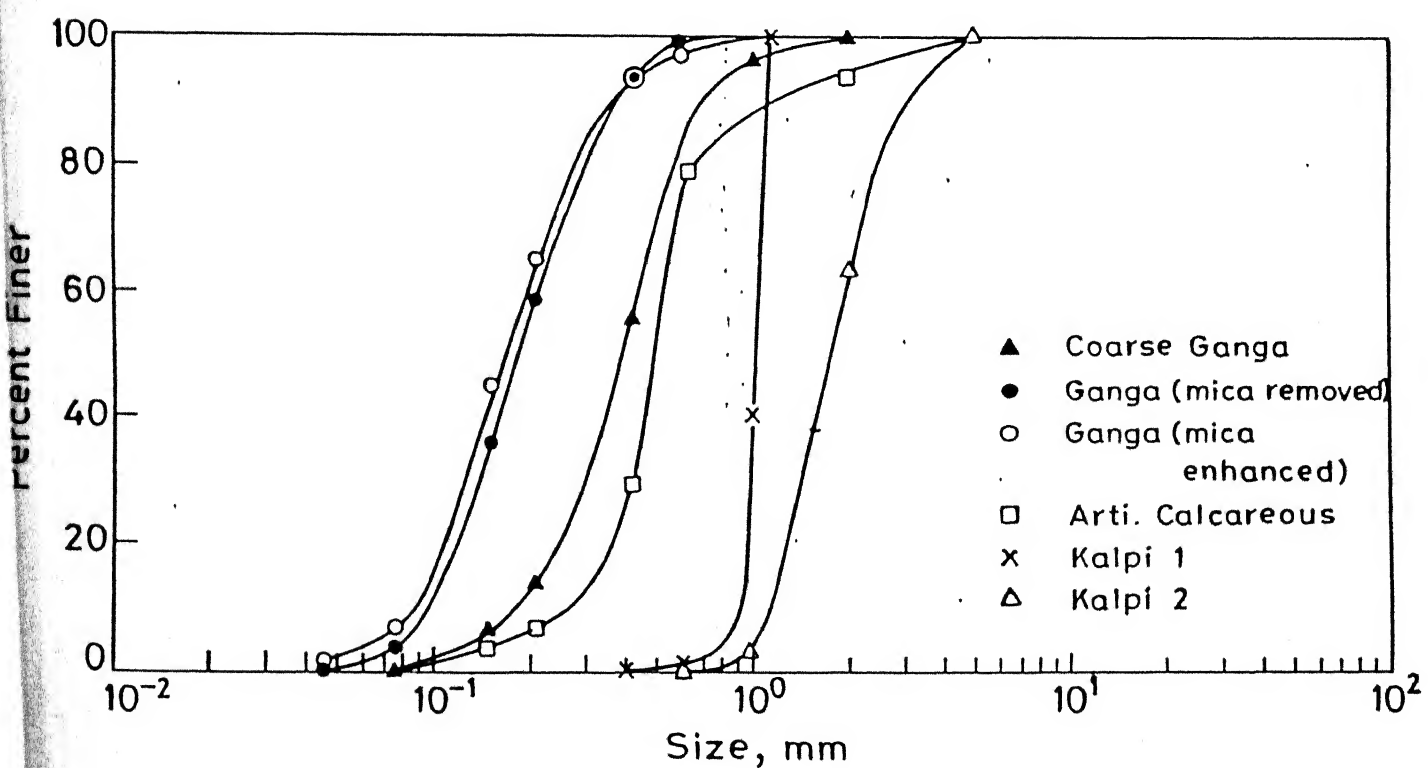


Fig. 4.12 Particle size distribution.

this Figure. The relationships for the rest of the sands are represented on Fig. 4.14a. As indicated earlier, the density of the sand is a unique function of height of free fall of sand as long as the rate of flow remains constant and beyond about 20 cm of height of fall, the rate of increase of relative density drastically varies. Effect of rate of flow has also been reported by Sahu (1988) and his results are presented in Fig. 4.14b. These relationships show that the particle gradation has a strong influence on the degree of compaction of sands. Various physical properties of sands is summarized in Table 4.3.

4.4 Morphological Characteristics

Image Analyzer System was used to find out the three diameters the long (d_L), the intermediate (d_I) and the short (d_S) diameters respectively. Using these three values, ratios of the intermediate to the long diameter (elongation ratio) (d_I/d_L) and the short to the intermediate diameter (Flatness ratio) (d_S/d_I) are determined for individual particles pertaining to each of the different size fractions. The particle shape classification for the sands, before and after loading, was done based on the Zingg shape concepts (Figs. 4.15 to 4.35). The relation between the shape factor and the flatness ratio (d_S/d_I) for sands before and after loading is indicated in Figs. 4.35 to 4.56. In addition to the study of particle shape, data were also obtained for each sieve fraction in term of number of tangents which reflect the surface characteristics of the edges of the particles.

4.5 Compressibility

To evaluate the compression characteristics, tests on dry sands at loose and dense relative densities (desired relative

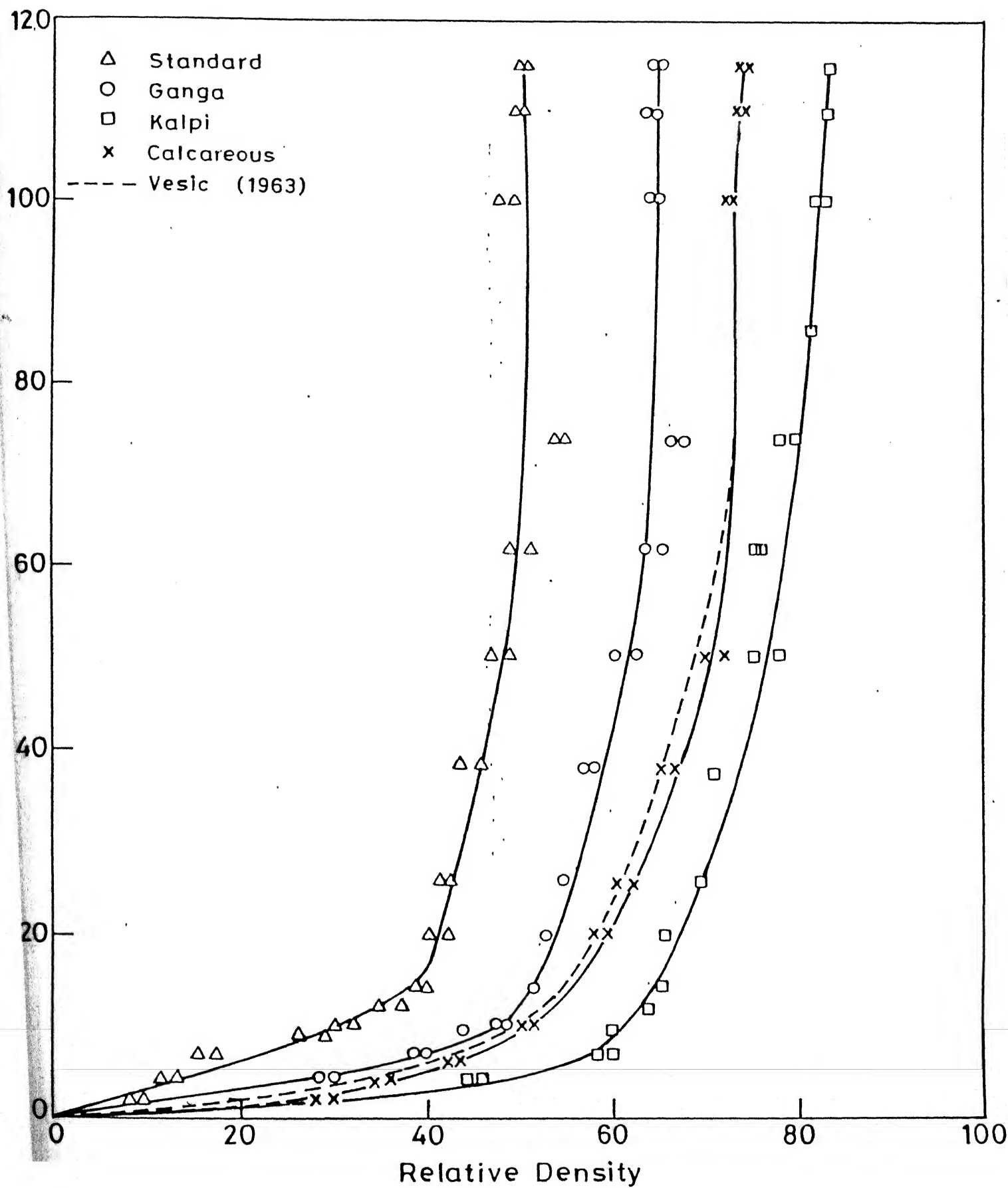


Fig. 4.13 Relative density vs height of fall.

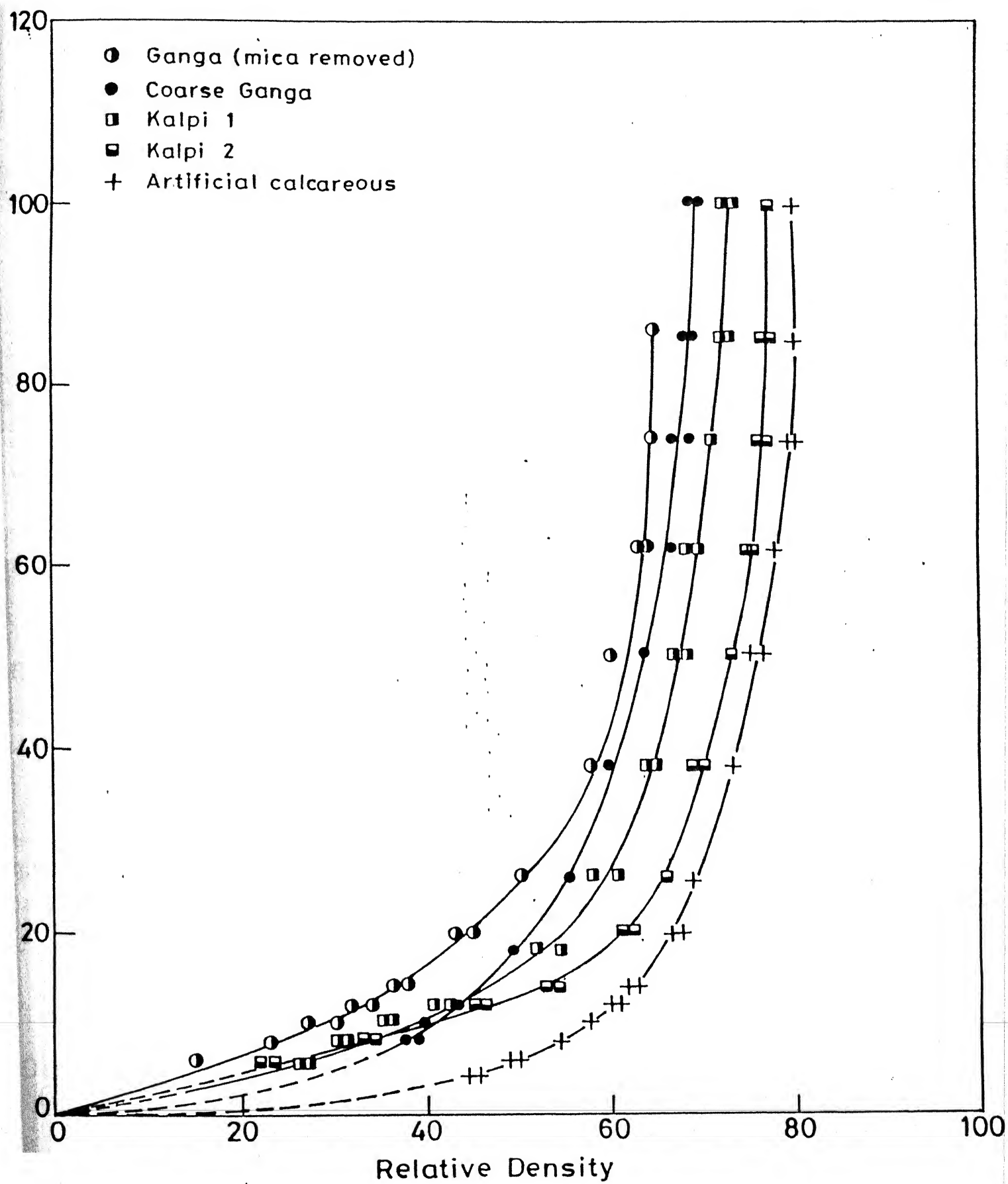


Fig. 4.14(a) Relative Density vs height of fall.

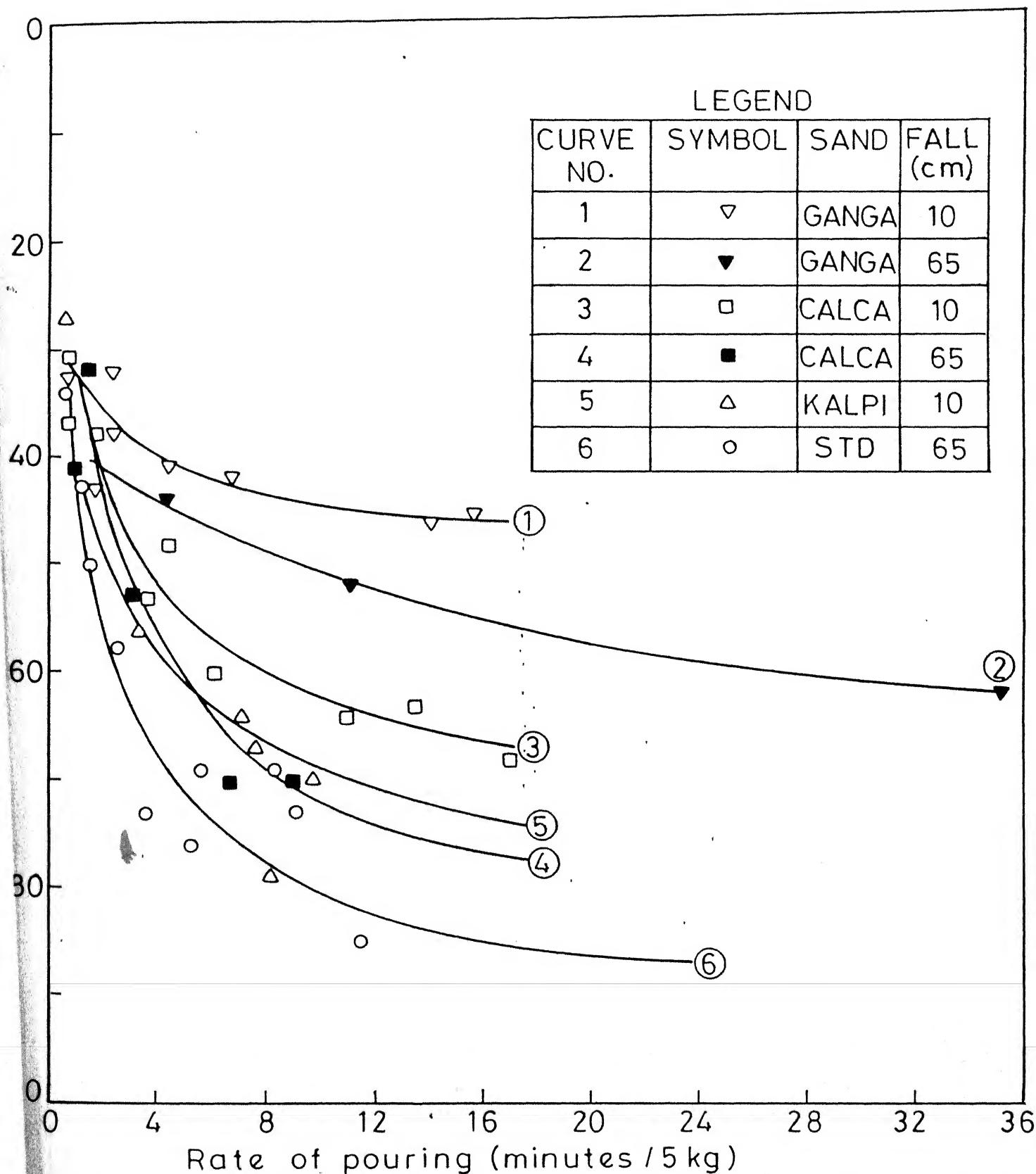


Fig. 4.14(b) Variation of relative density with rate of pouring for all sands (Sahu, 1988)

Table 4.3: Physical Properties of the Sands

S1.	Sand	G	d_{60}	d_{50}	d_{10}	C_u	e_{max}	e_{min}
1	Ganga	2.691	0.218	0.18	0.085	2.565	1.250	0.577
2	Kalpi	2.676	1.300	1.00	0.270	4.814	0.910	0.480
3	Calcareous	2.700	0.480	0.43	0.270	1.778	1.050	0.570
4	Standard	2.650	0.500	0.475	0.360	1.389	0.810	0.490
5	Ganga with mica	2.730	0.199	0.200	0.080	2.488	1.229	0.557
6	Ganga without mica	2.670	0.218	0.180	0.100	2.180	1.110	0.718
7	Coarse Ganga	2.675	0.460	0.400	0.180	2.565	0.773	0.485
8	Artificial Calcareous	2.669	0.500	4.800	0.280	1.780	0.904	0.516
9	Kalpi 1	2.695	1.050	1.020	0.950	1.073	0.932	0.540
10	Kalpi 2	2.710	1.950	1.700	1.180	1.613	0.989	0.576

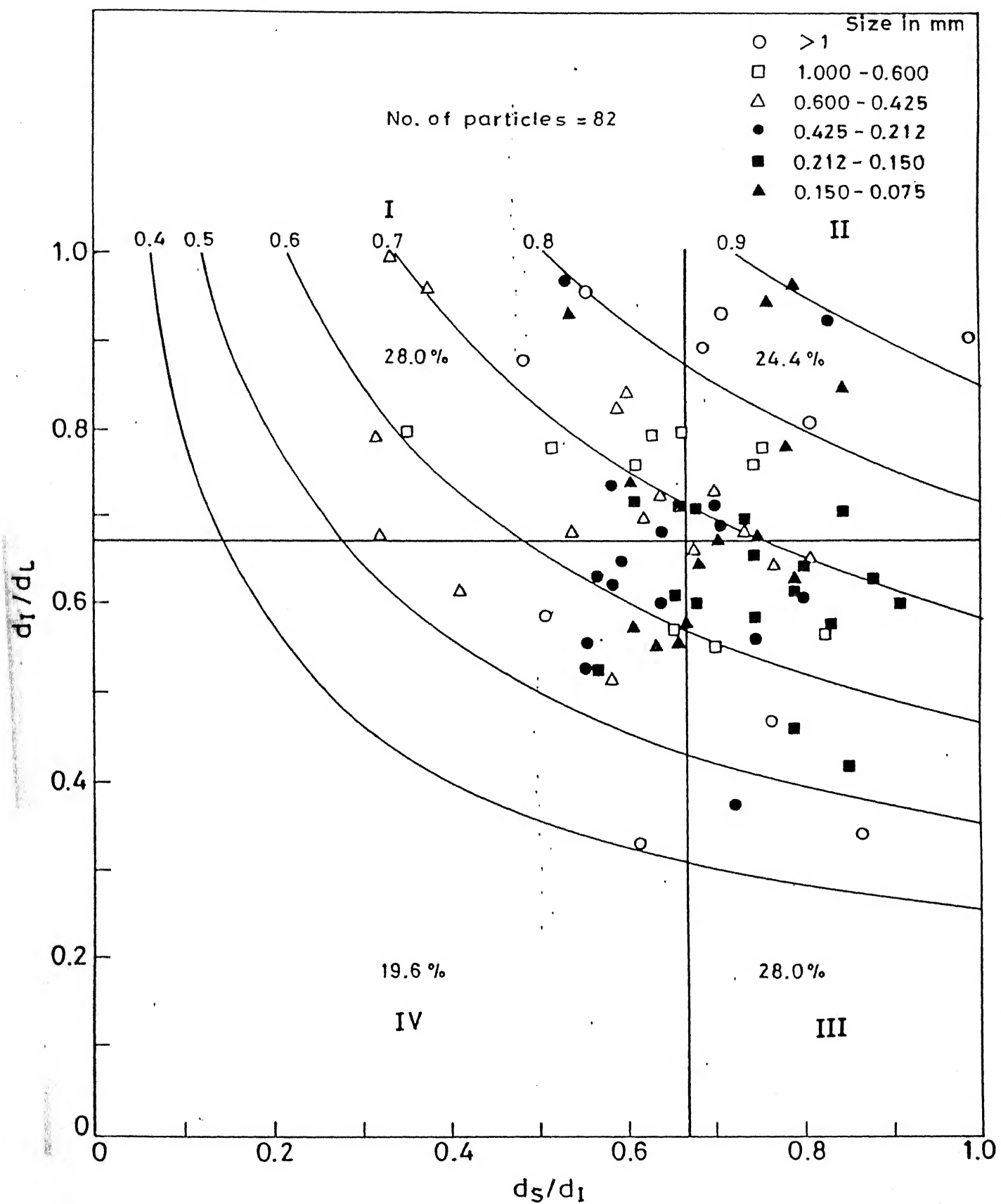


Fig. 4.15 Shape classification using Zingg diagram for Ganga sand.

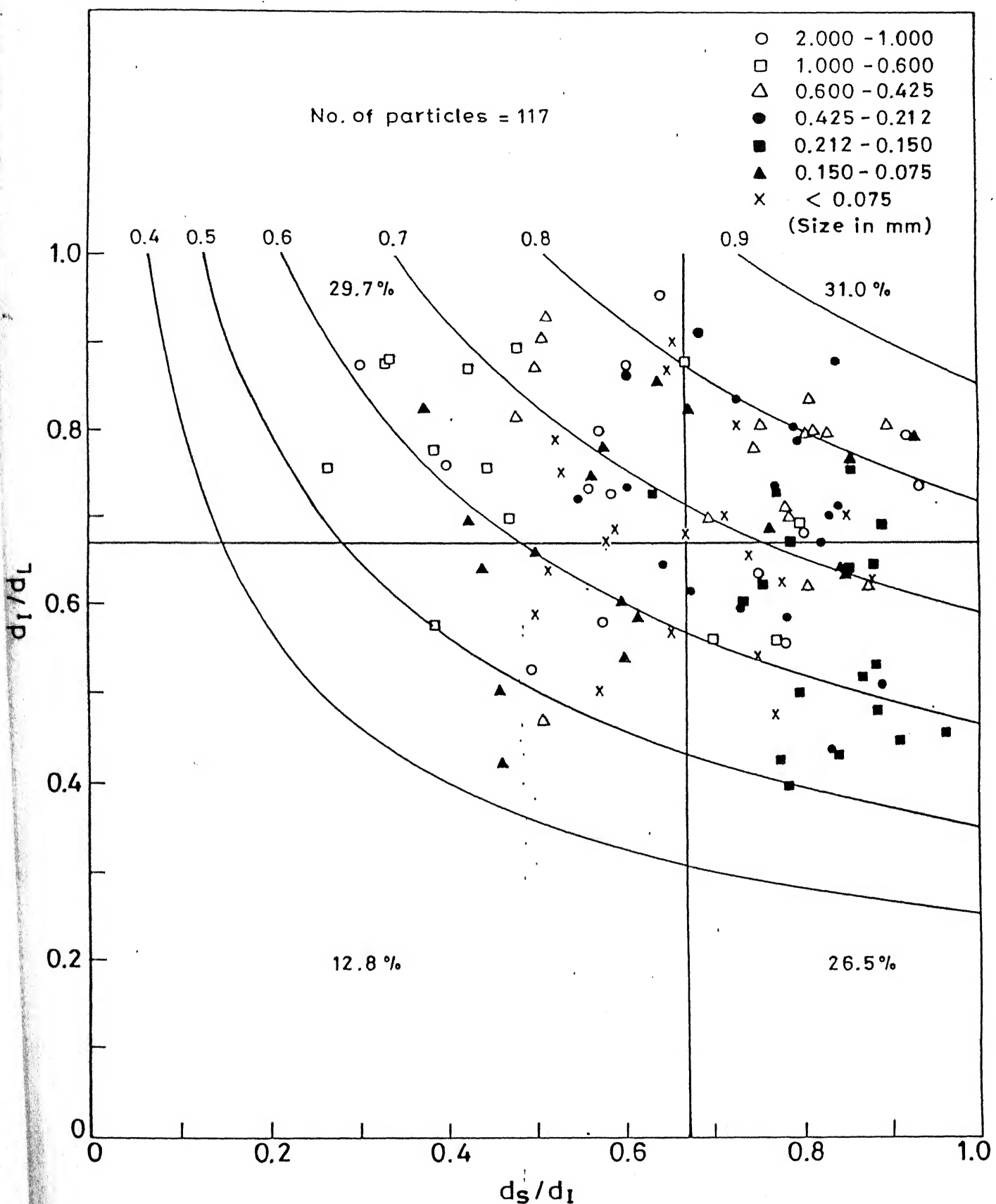


Fig. 4.16 Shape classification using Zingg diagram for Ganga sand subjected to 22.04 kg/cm^2 .

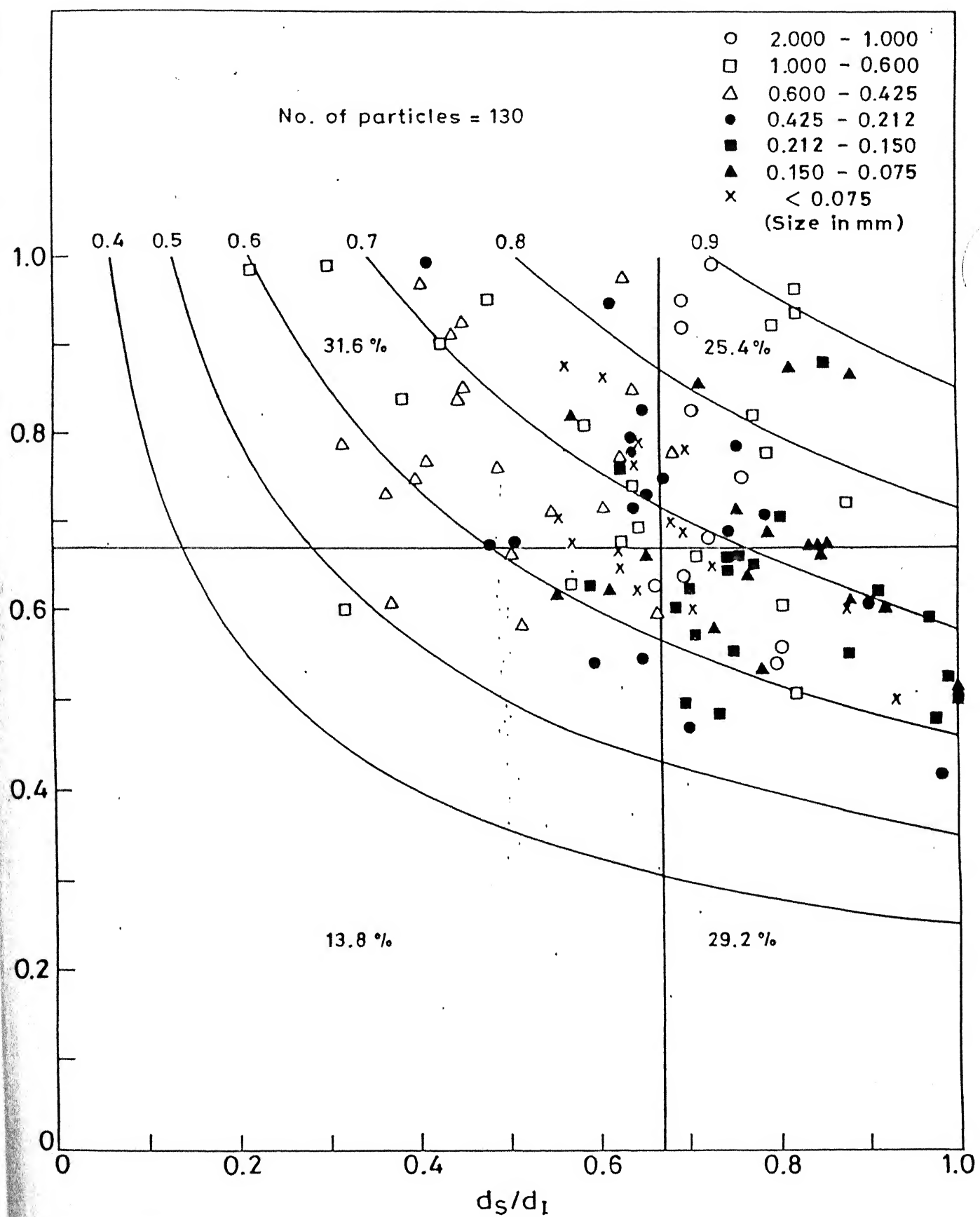


Fig. 4.17 Shape classification using Zingg diagram for Ganga sand subjected to 176.32 kg/cm².

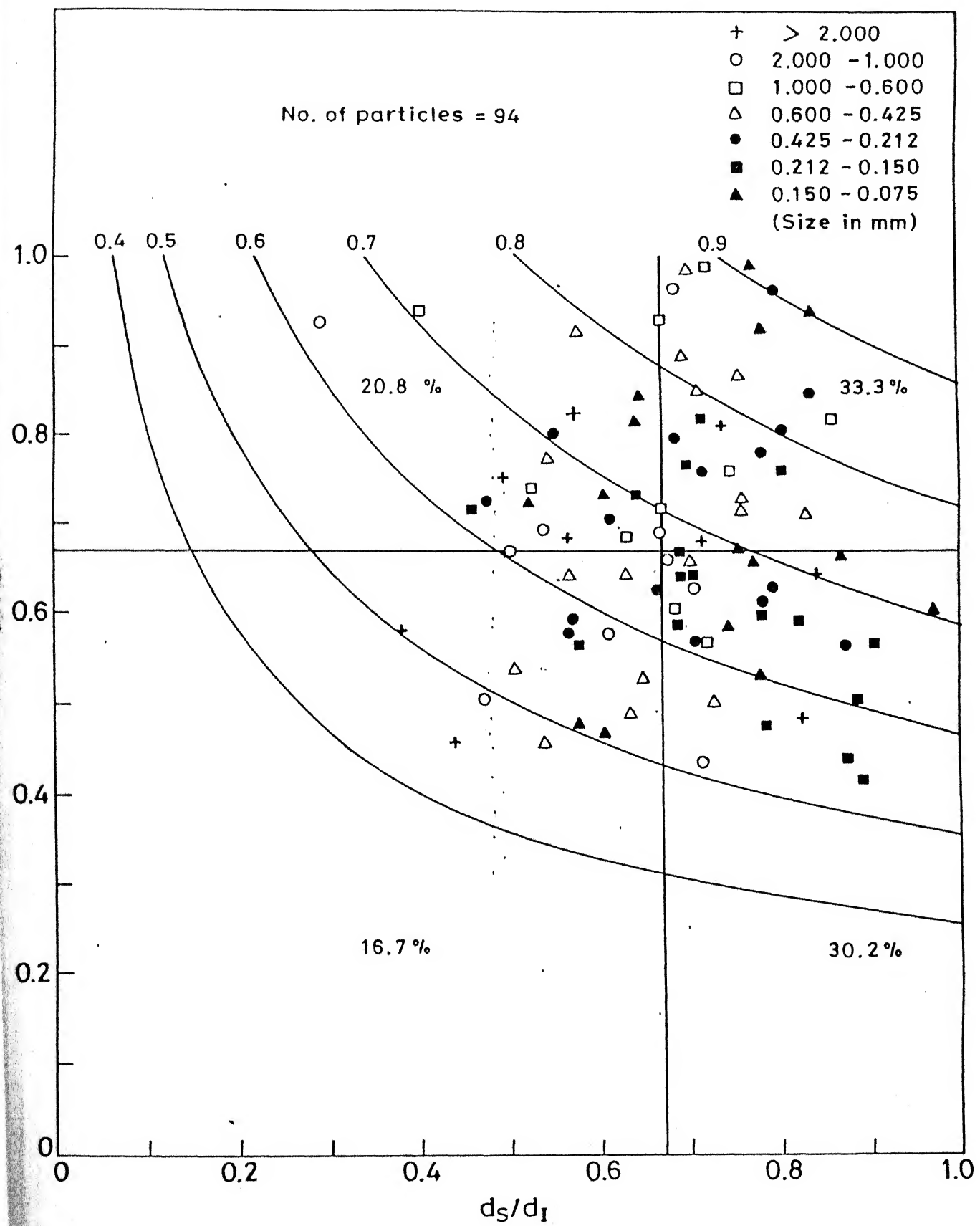


Fig. 4.18 Shape classification using Zingg diagram for coarse Ganga sand.

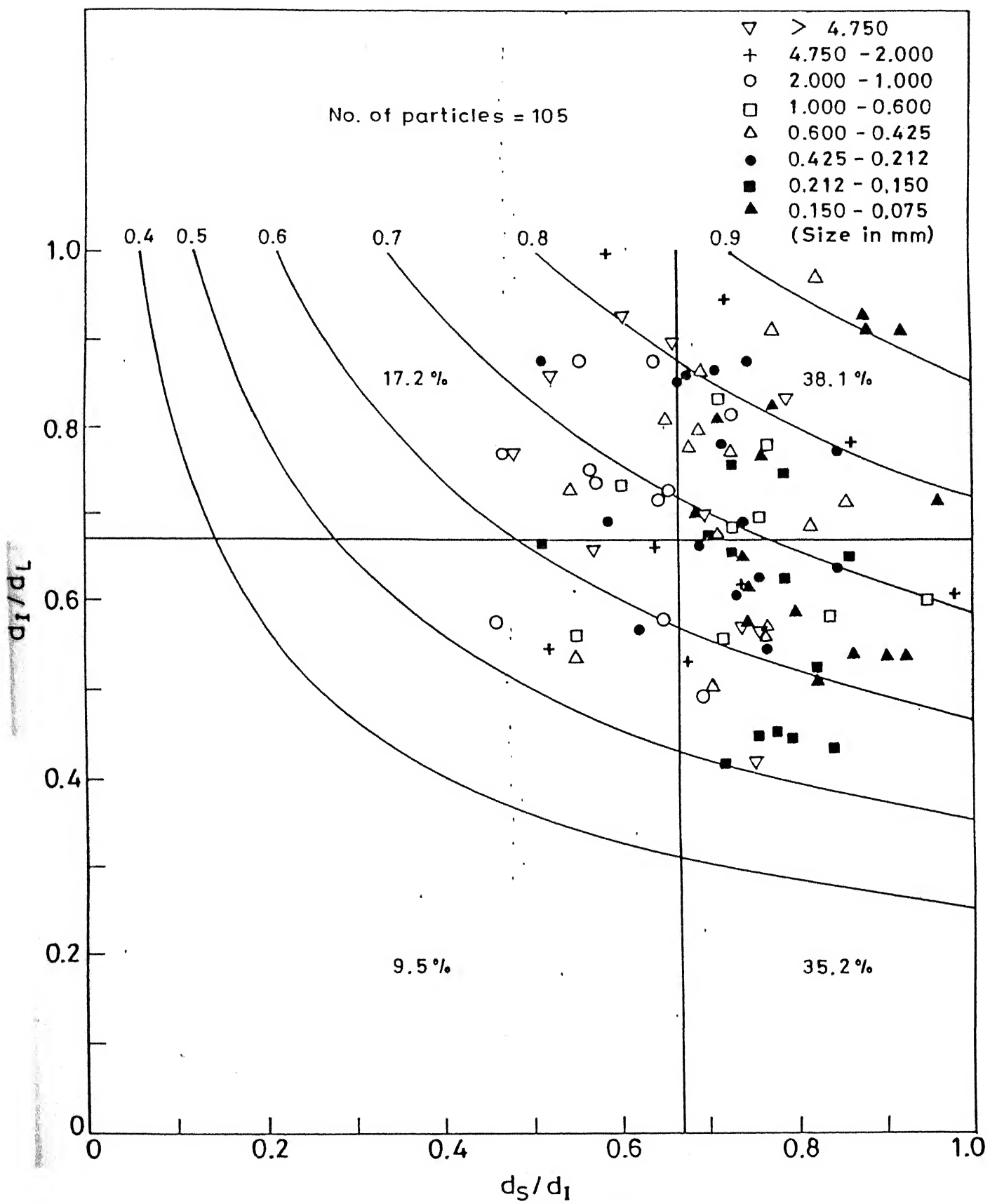


Fig. 4.19 Shape classification using Zingg diagram for Kalpi sand.

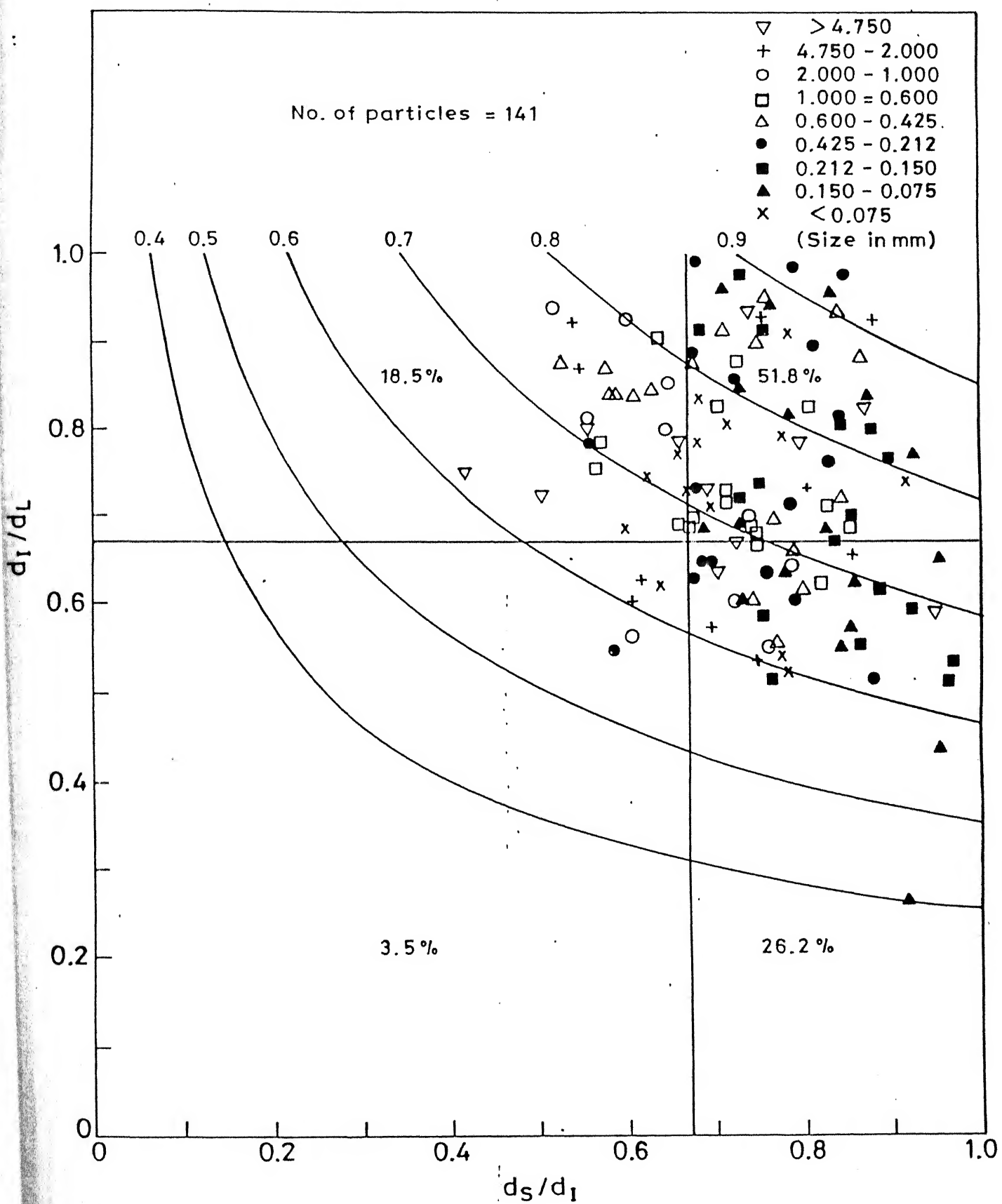


Fig. 4.20 Shape classification using Zingg diagram for Kalpi sand subjected to 22.04 kg/cm².

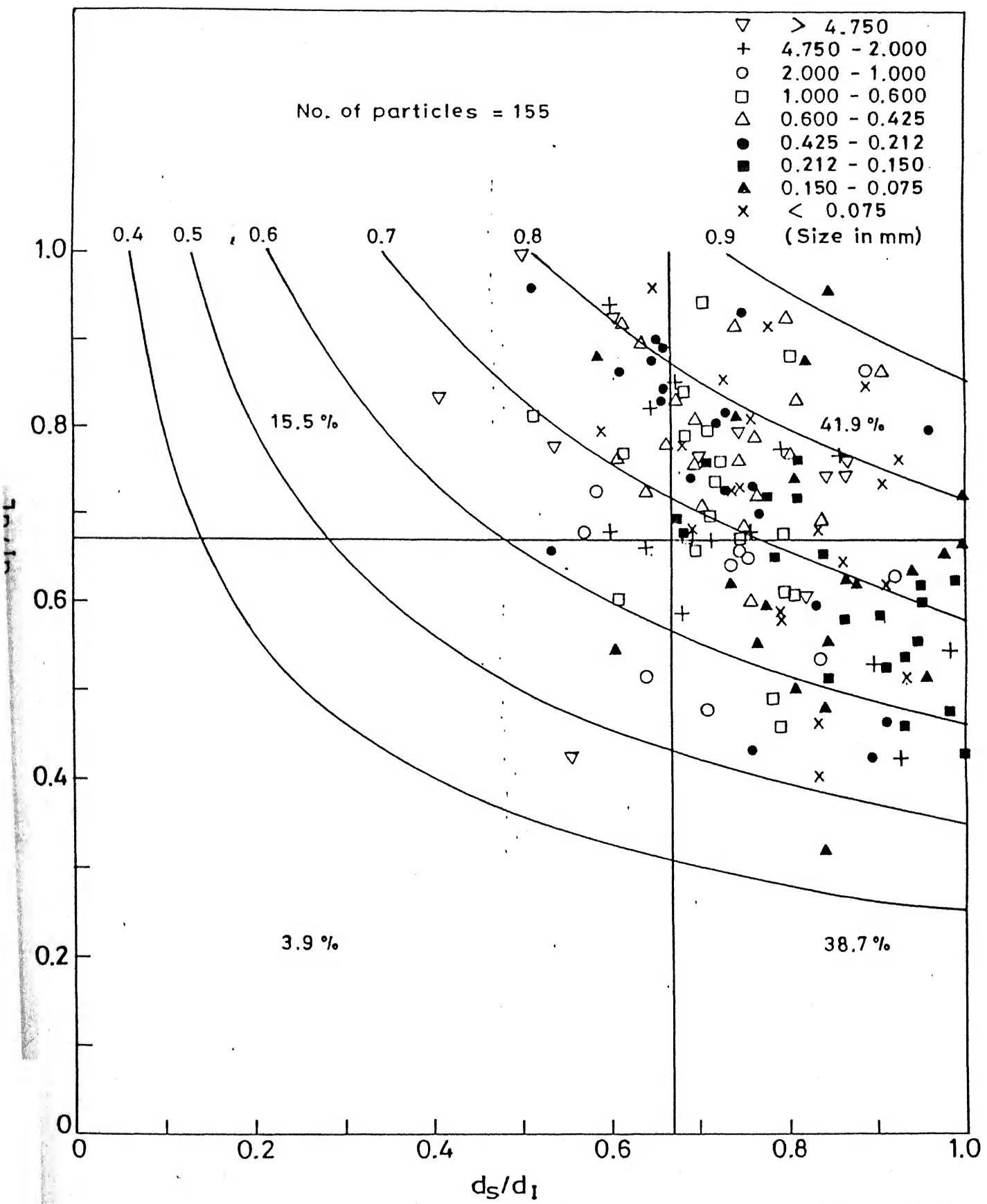


Fig. 4.21 Shape classification using Zingg diagram for Kalpi sand subjected to 176.32 kg/cm².

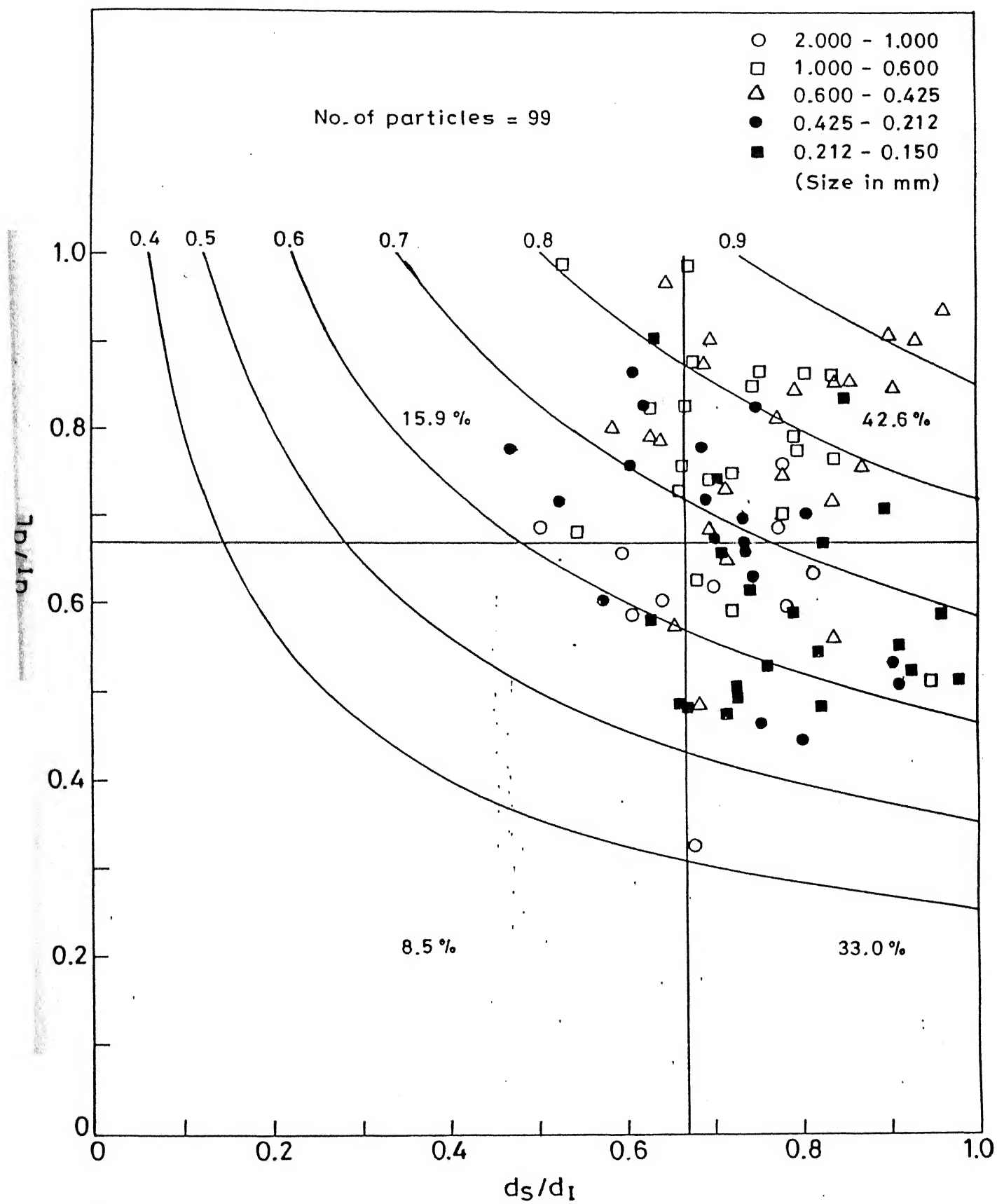


Fig. 4.22 Shape classification using Zingg diagram for Kalpi-1

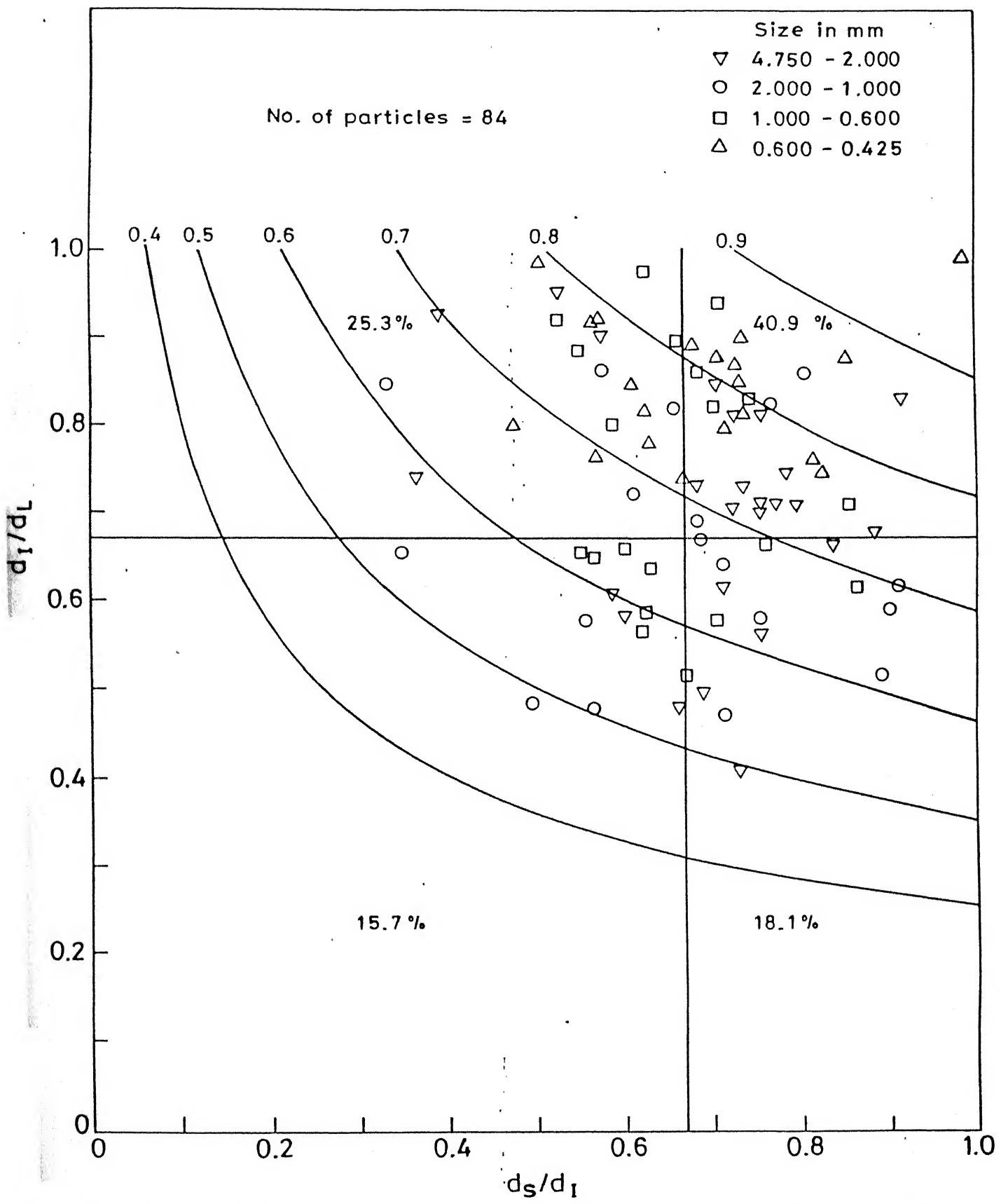


Fig. 4.23 Shape classification using Zingg diagram for Kalpi 2.

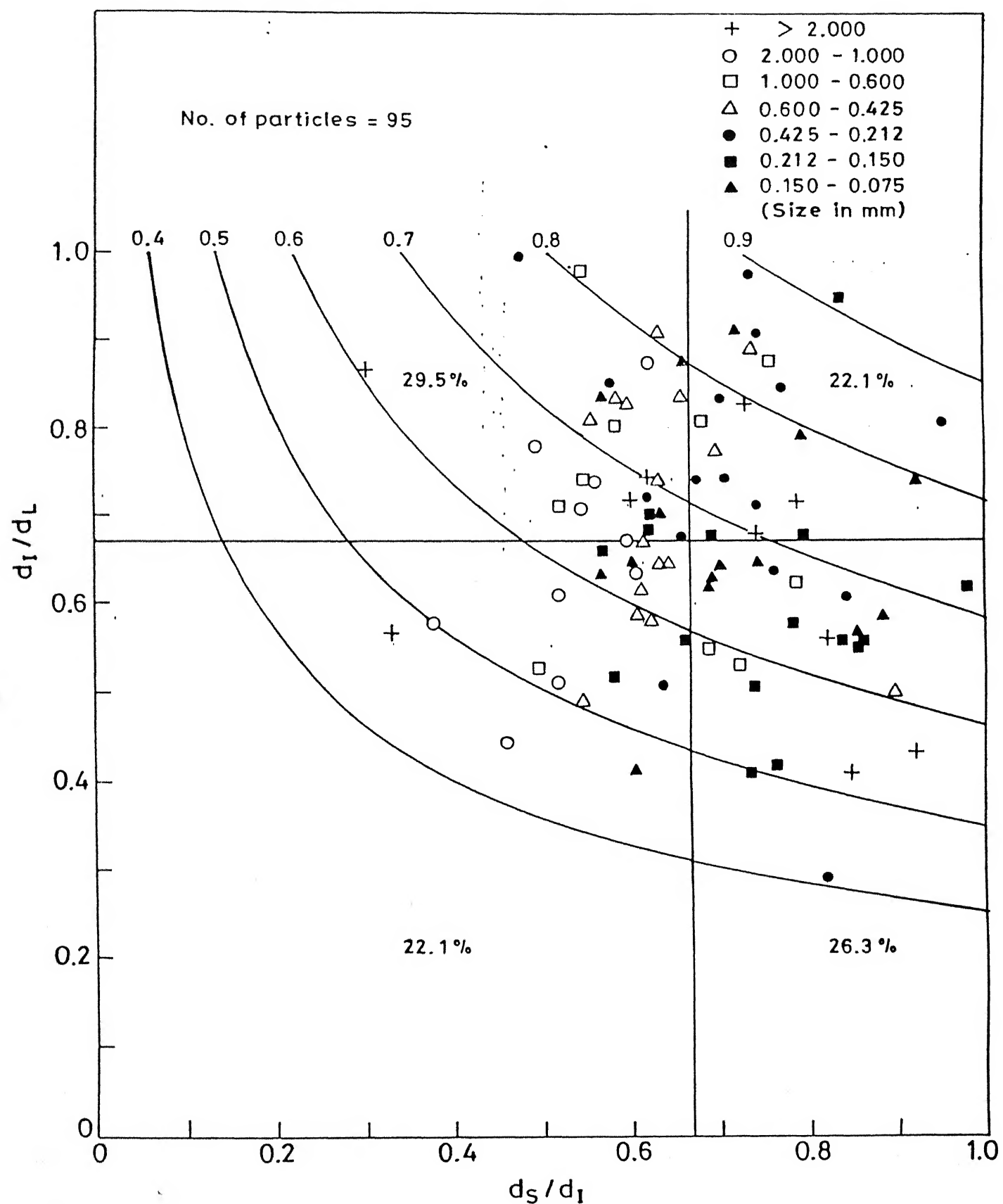


Fig. 4.24 Shape classification using Zingg diagram for calcareous sand.

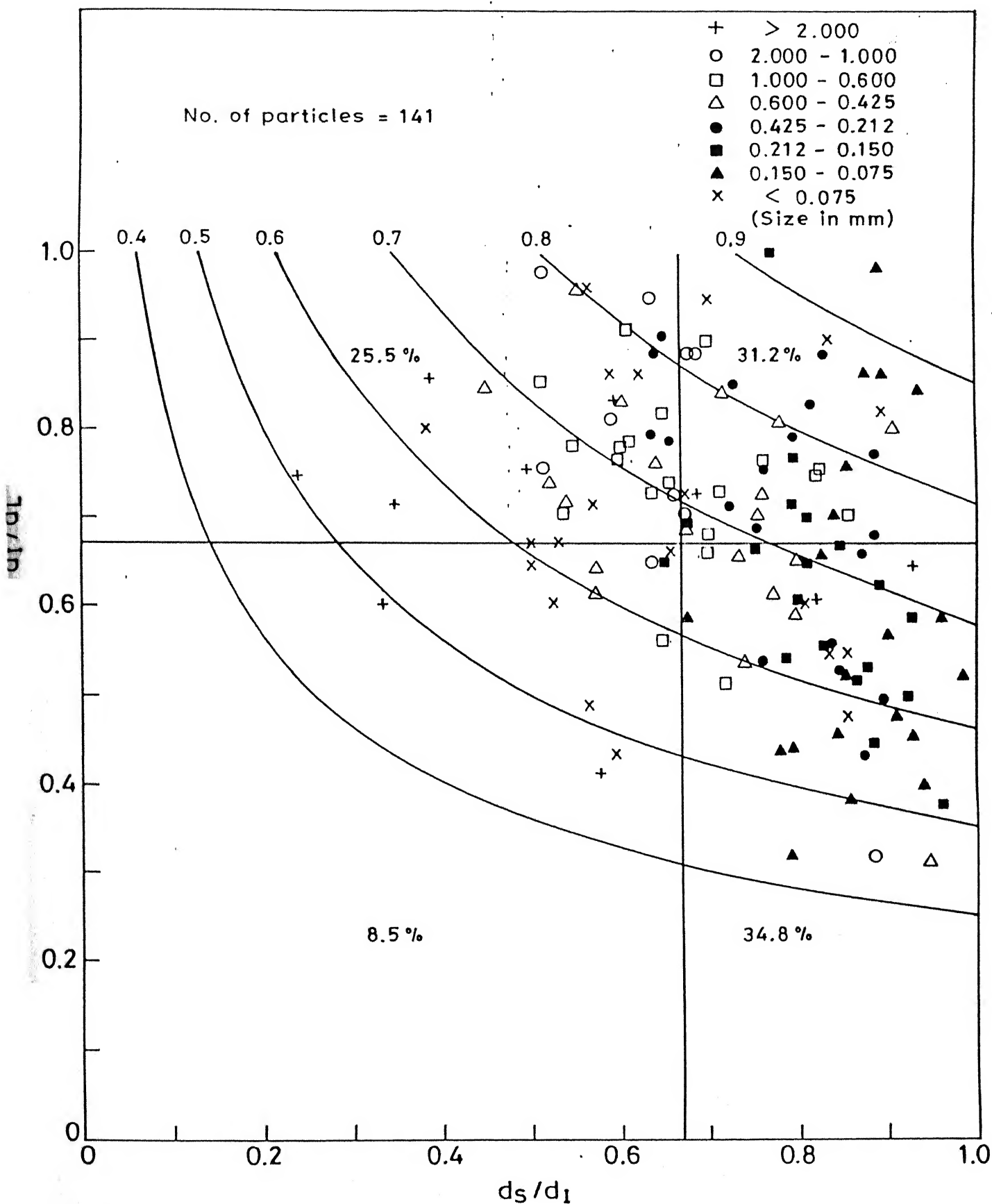


Fig. 4.25 Shape classification using Zingg diagram for calcareous sand subjected to 22.04 kg/cm^2 .

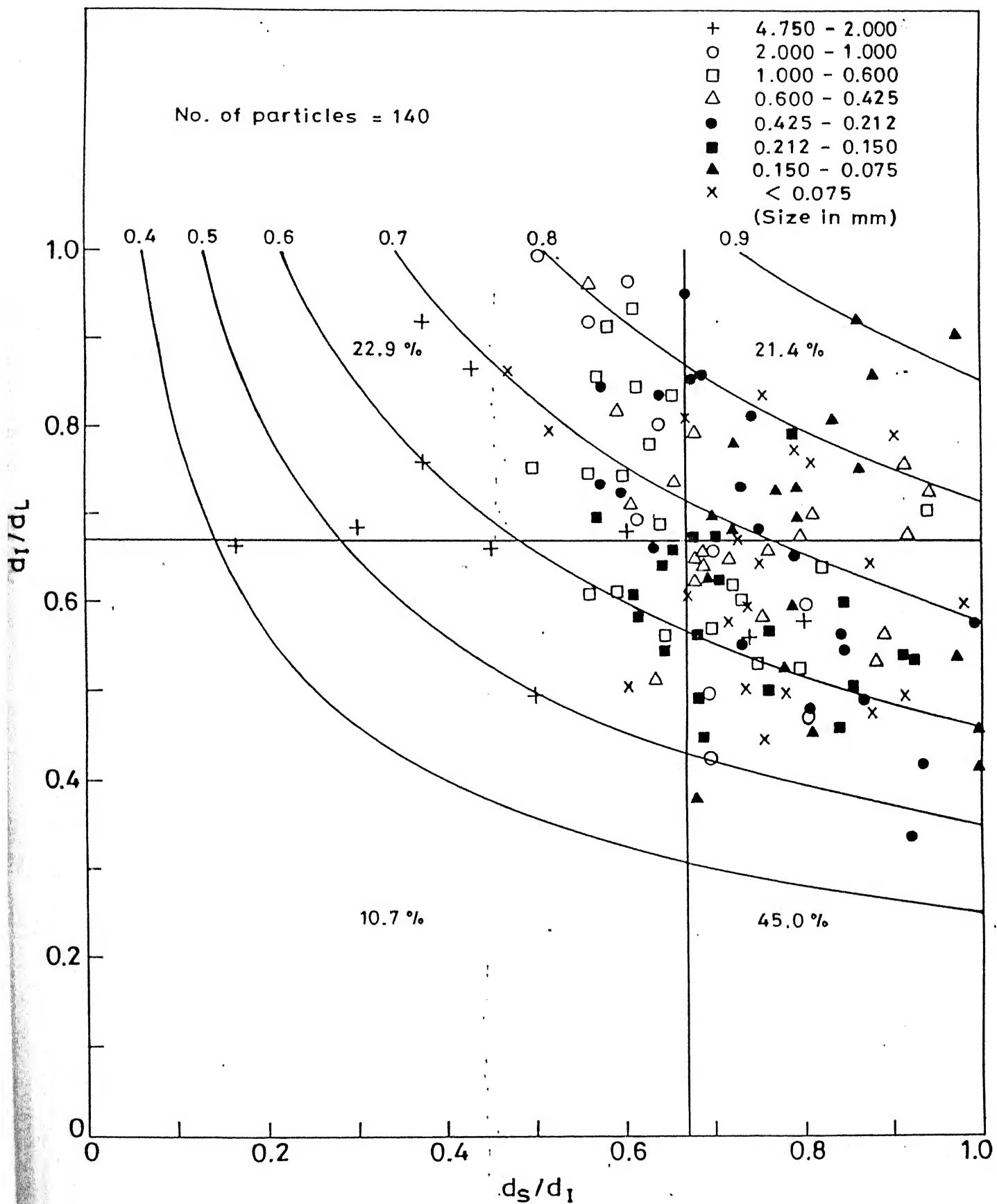


Fig. 4.26 Shape classification using Zingg diagram for calareous sand subjected to 176.32 kg/cm².

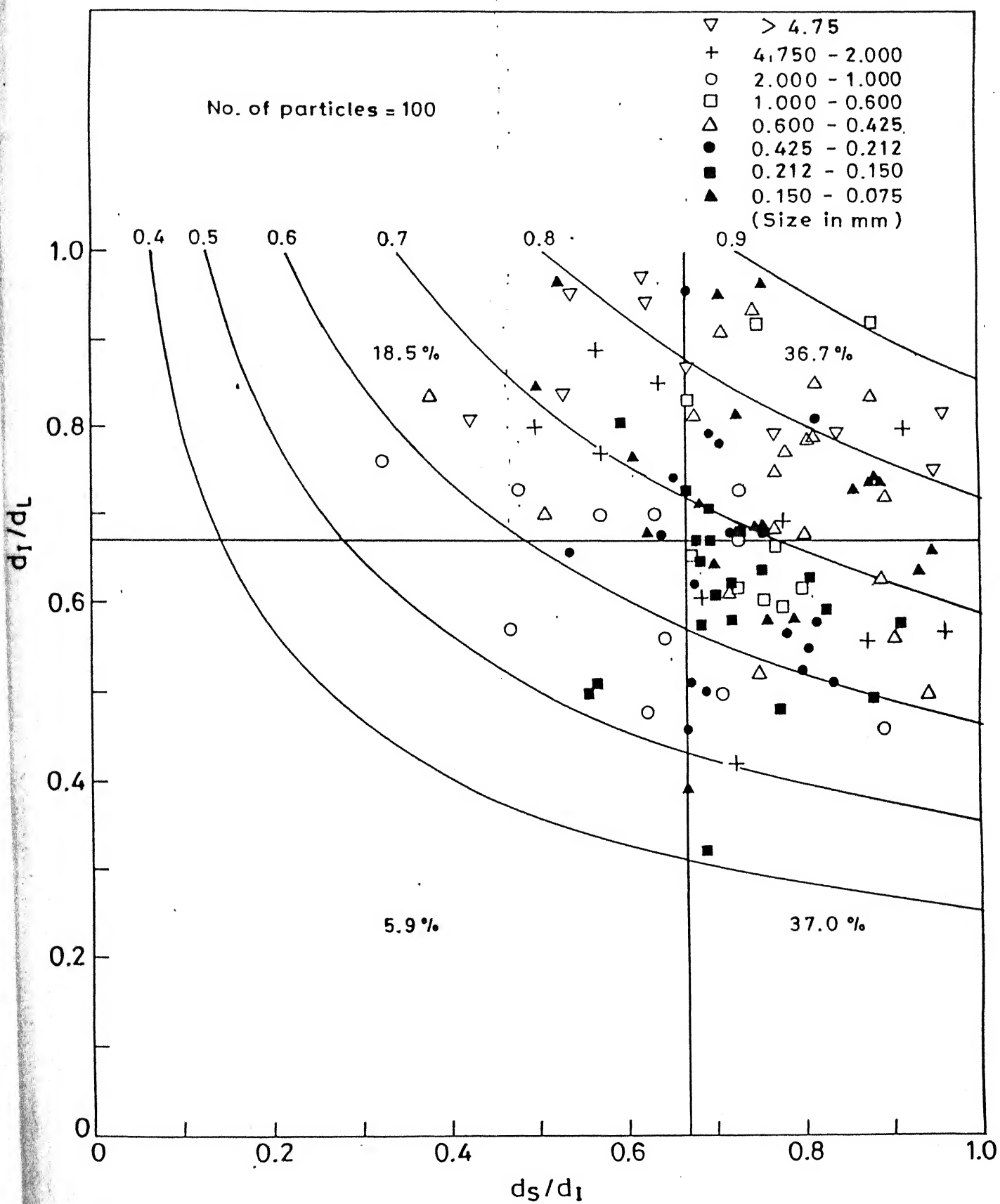


Fig. 4.27 Shape classification using Zingg diagram for artificial calcareous.

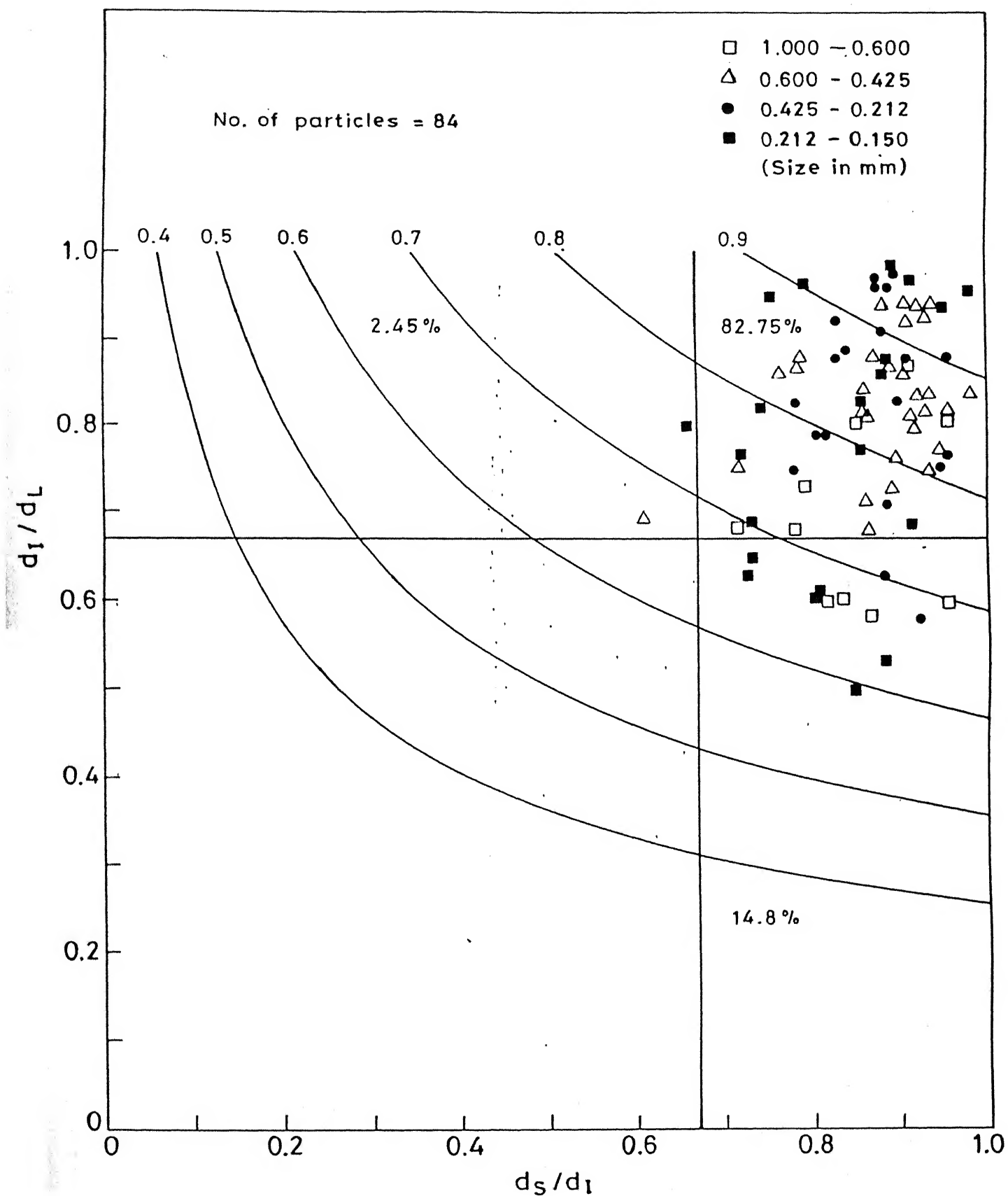


Fig. 4.28 Shape classification using Zingg diagram for standard sand.

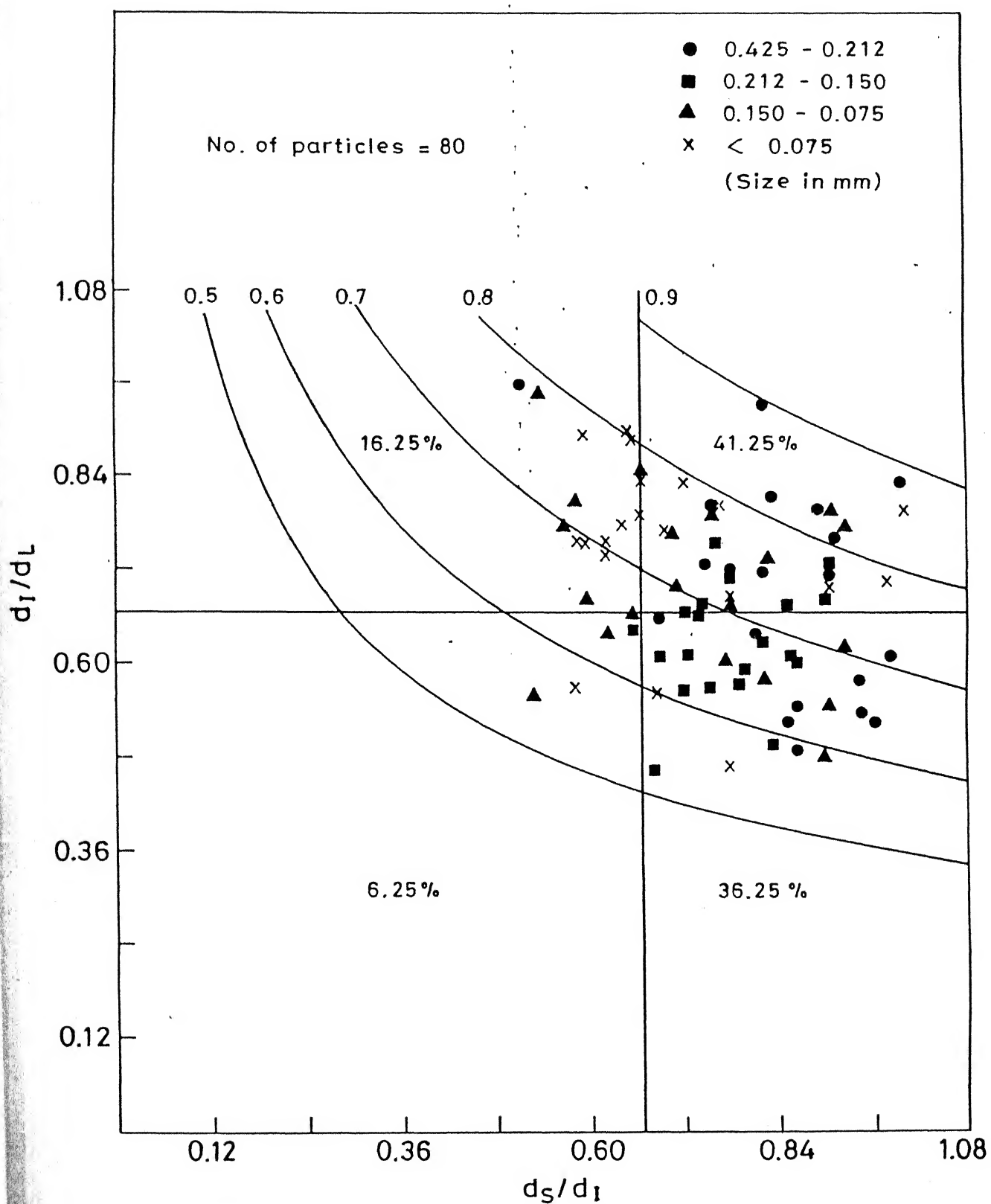


Fig. 4.29 Shape classification using Zingg diagram for Ottawa sand.

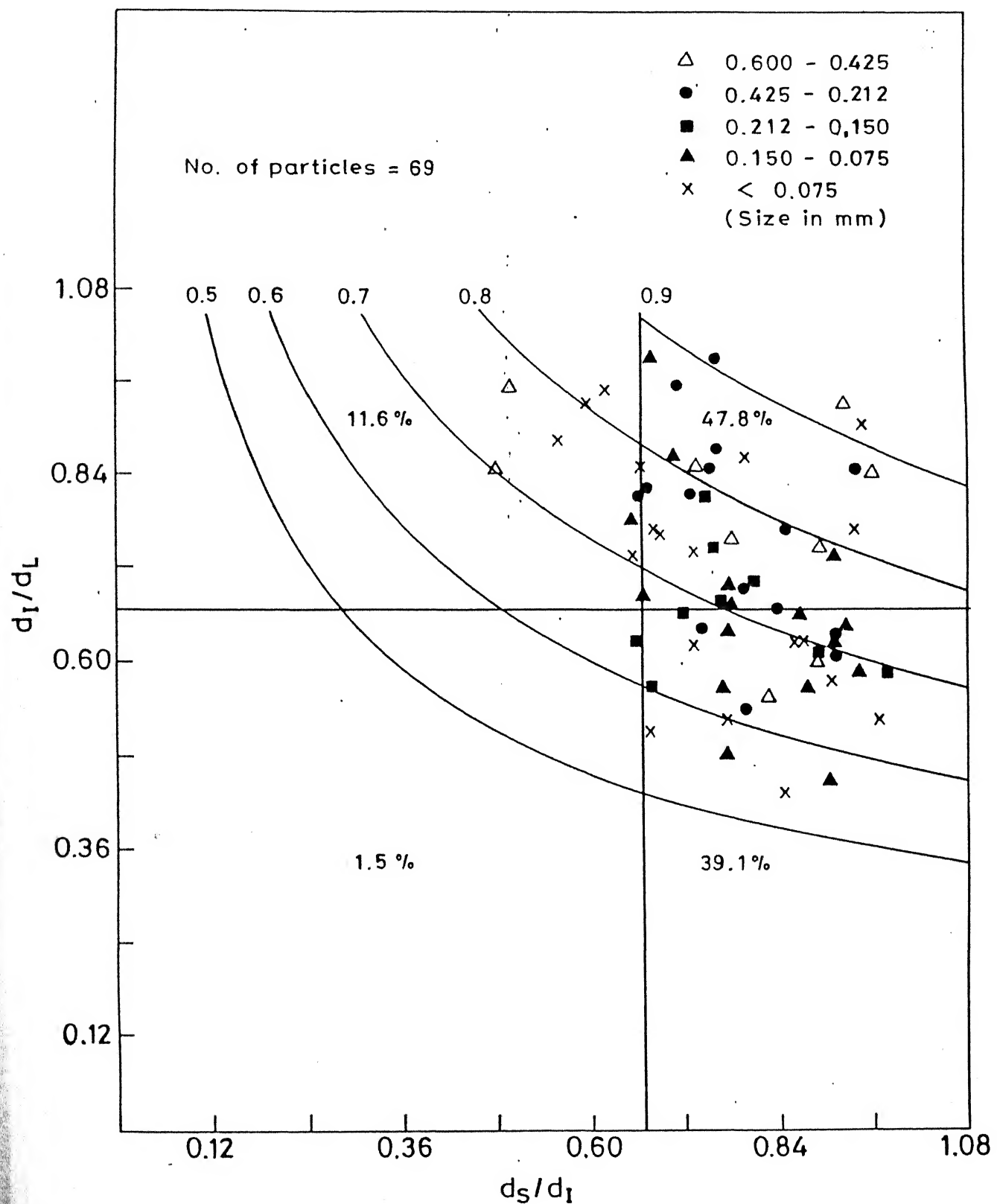


Fig. 4.30 Shape classification using Zingg diagram for San Fernando #5 sand.

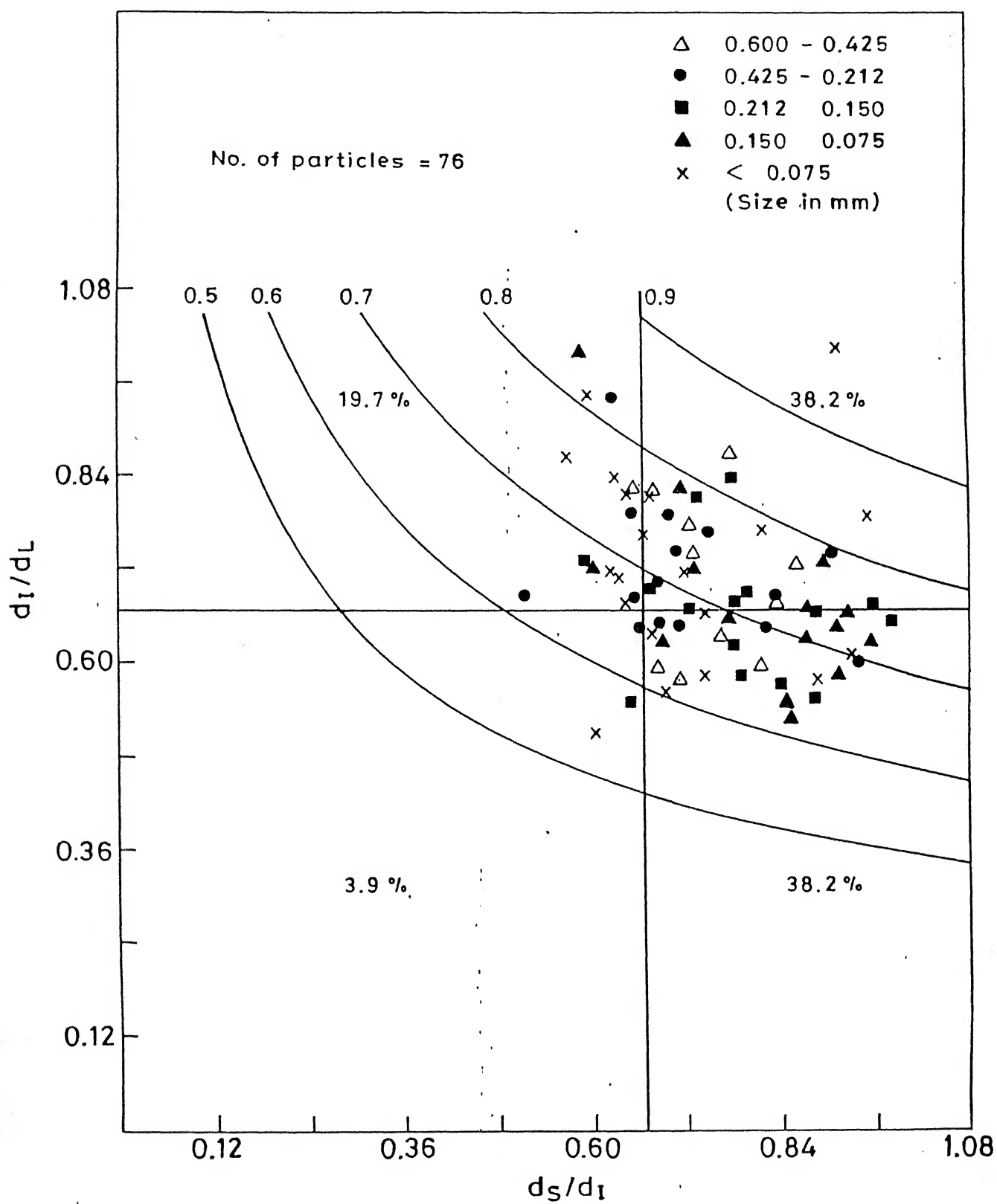


Fig. 4.31 Shape classification using Zingg diagram for San Fernando #6 sand.

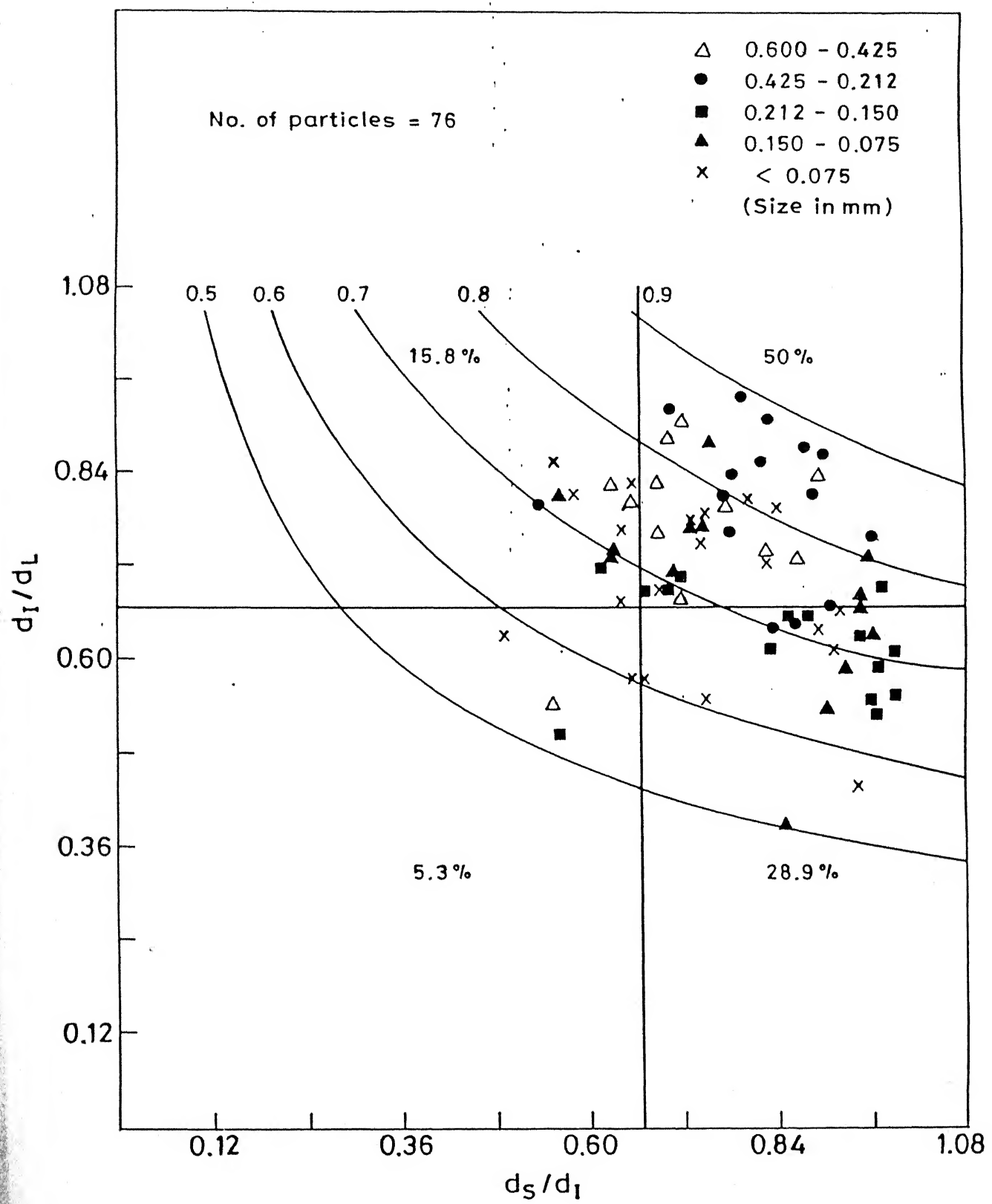


Fig. 4.32 Shape classification using Zingg diagram for San Fernando #7 sand.

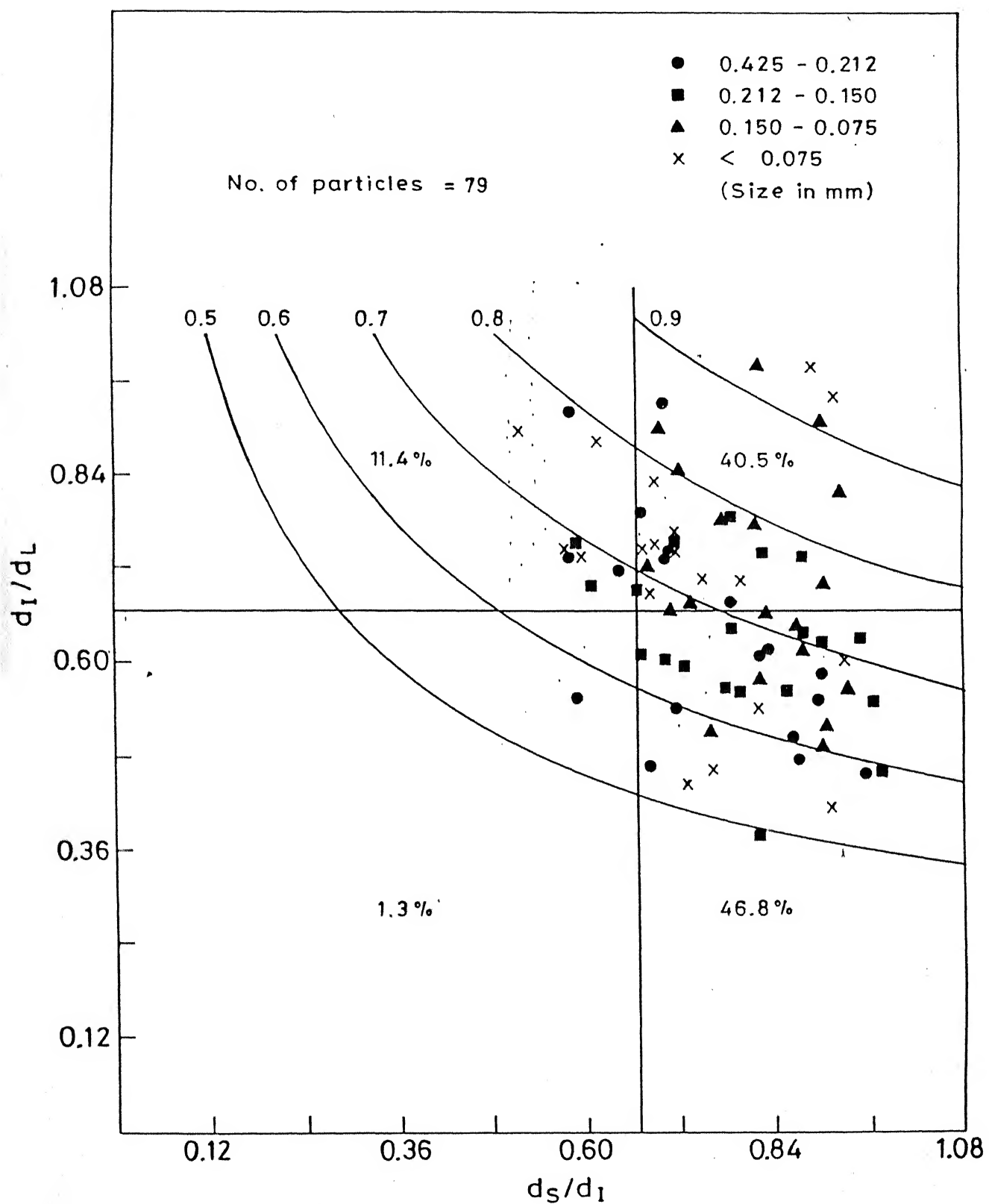


Fig. 4.33 Shape classification using Zingg diagram for Leighton Buzzard sand.

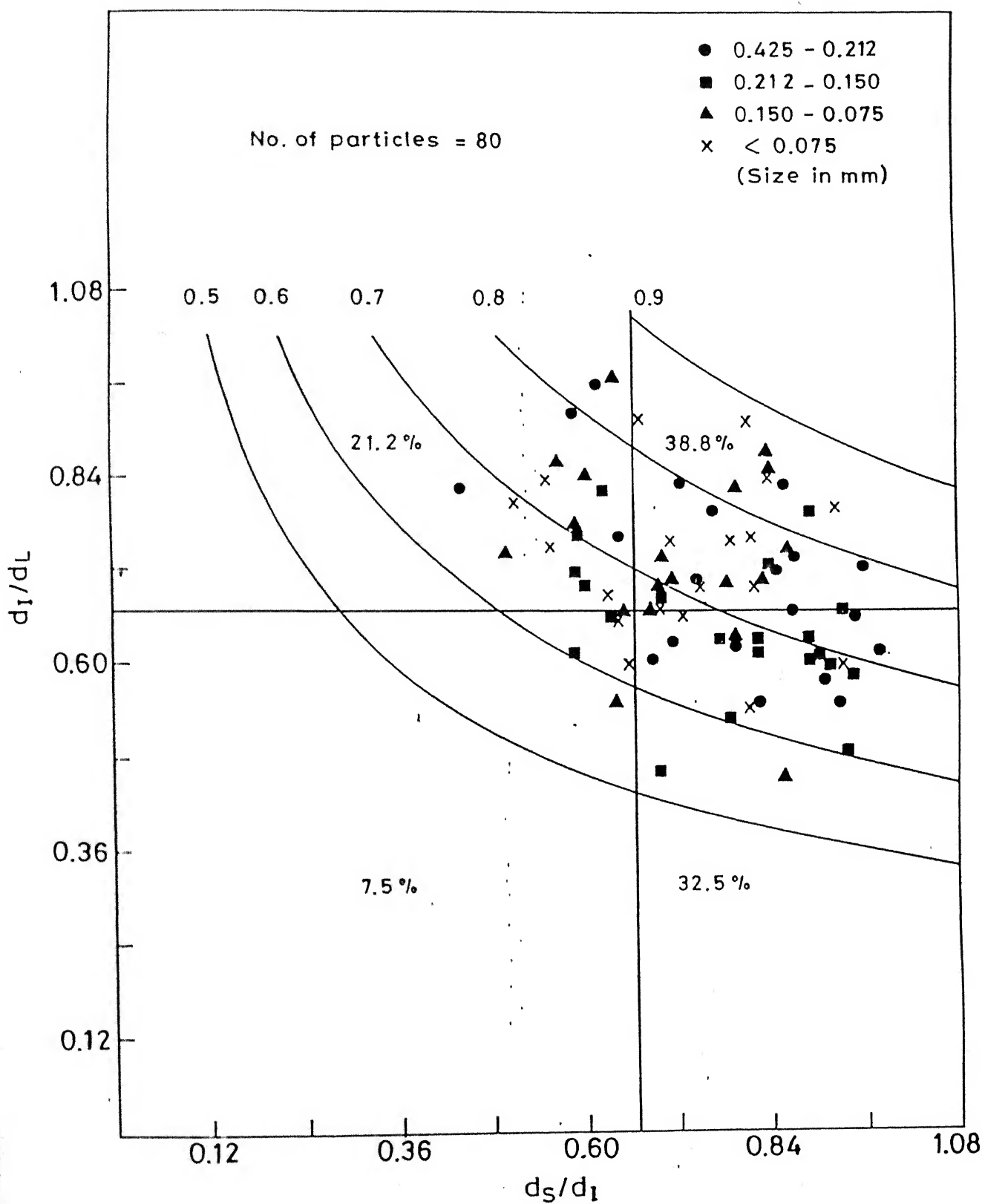


Fig. 4.34 Shape classification using Zingg diagram for Lagunillas (94A-M19) sand.

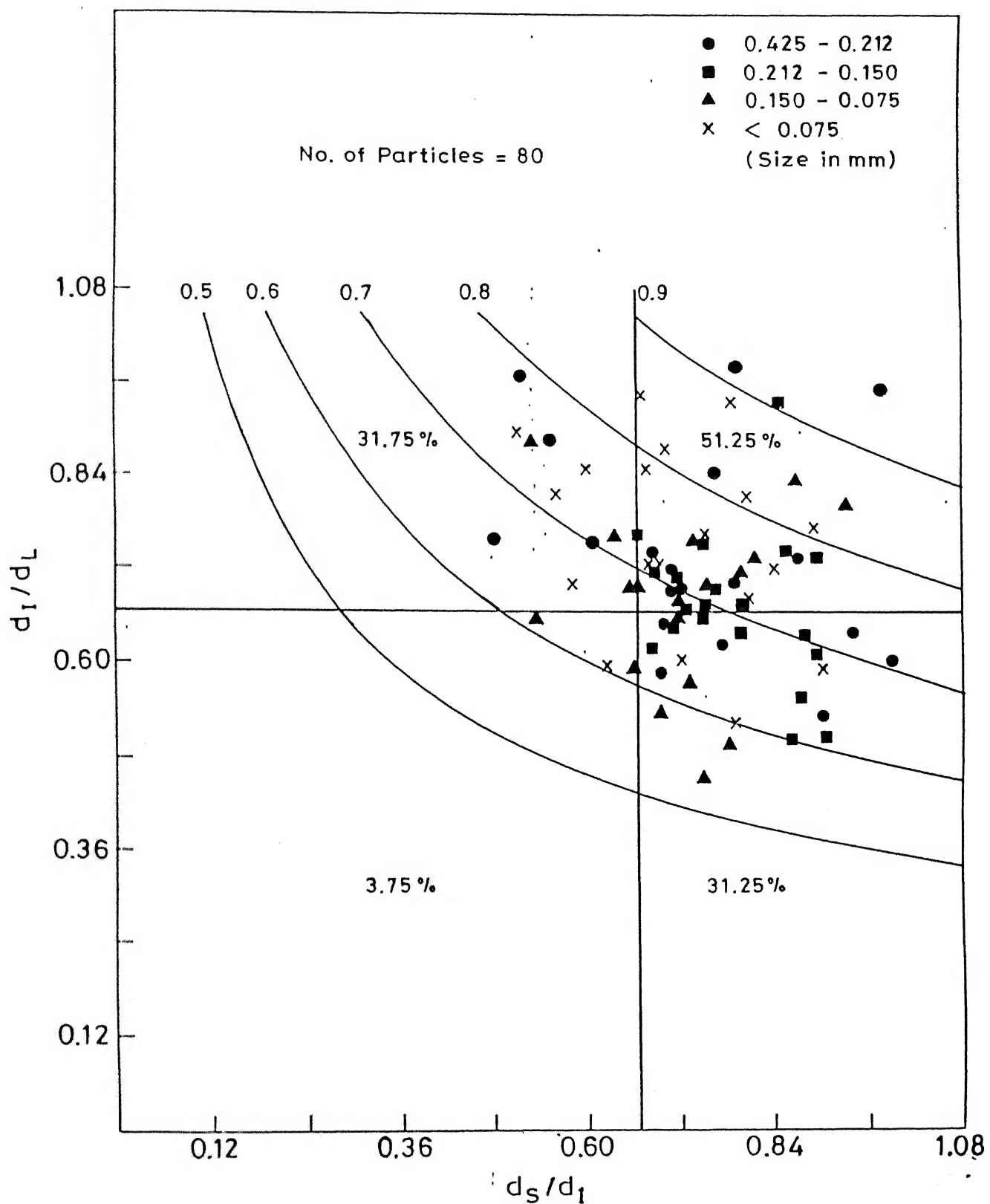


Fig. 4.35 Shape classification using Zingg diagram for Lagunillas (94A + 94B) sand.

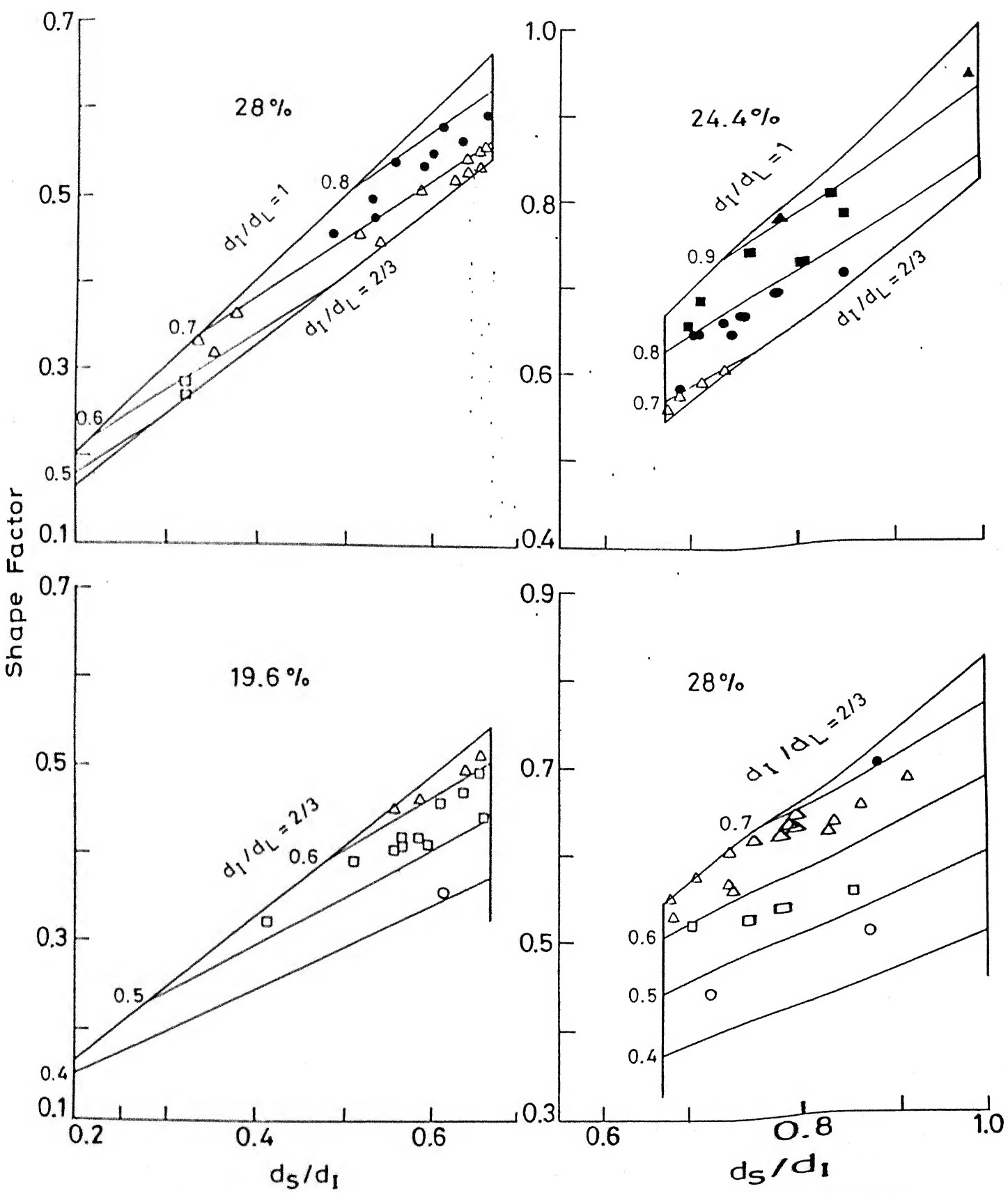


Fig. 4.36 Range of shape factors for Ganga sand.

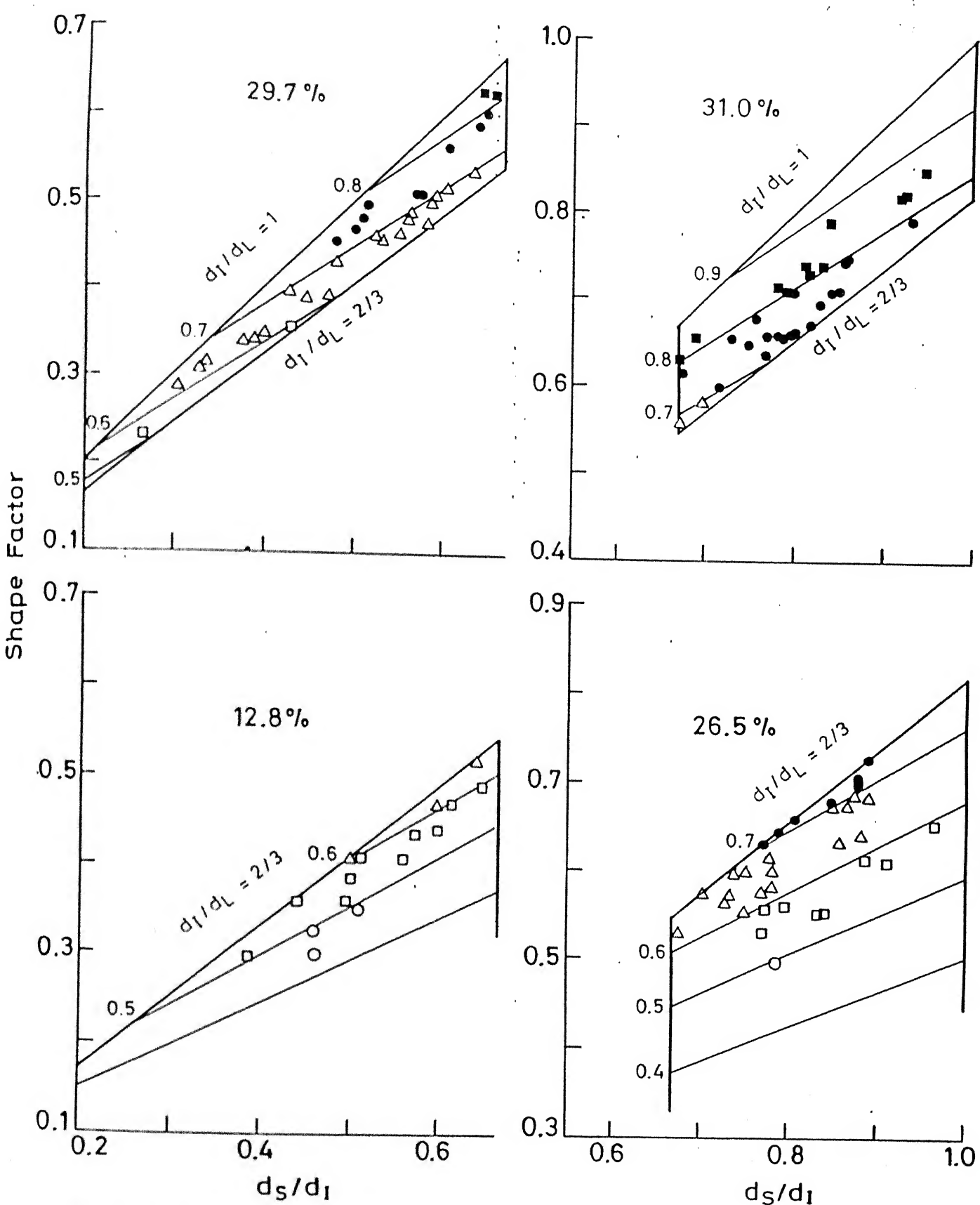


Fig. 4.37 Range of shape factors for Ganga sand subjected to 22.04 kg/cm^2 .

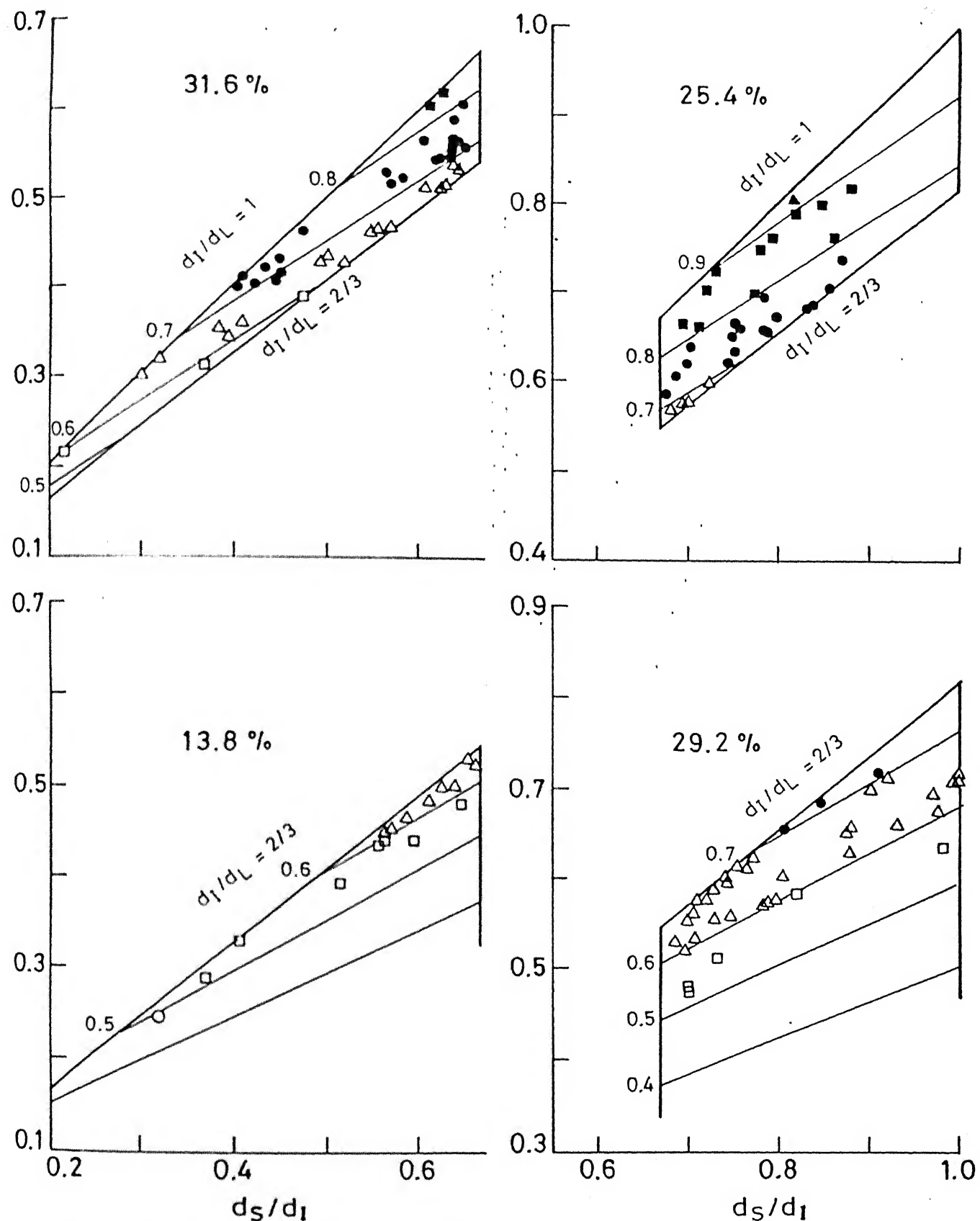


Fig. 4.38 Range of shape factors for Ganga sand subjected to 176.32 kg/cm².

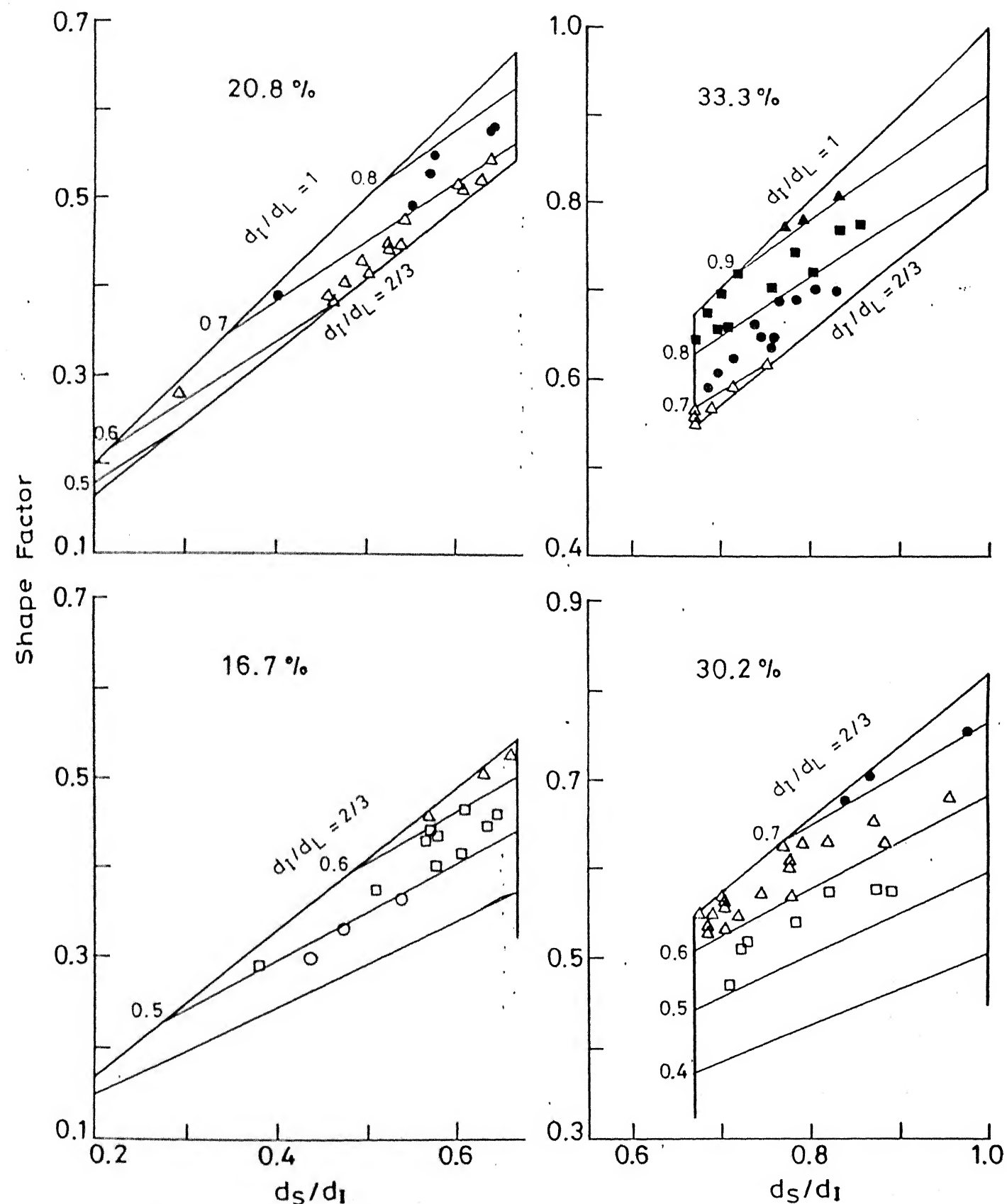


Fig. 4.39 Range of shape factors for coarse Ganga sand .

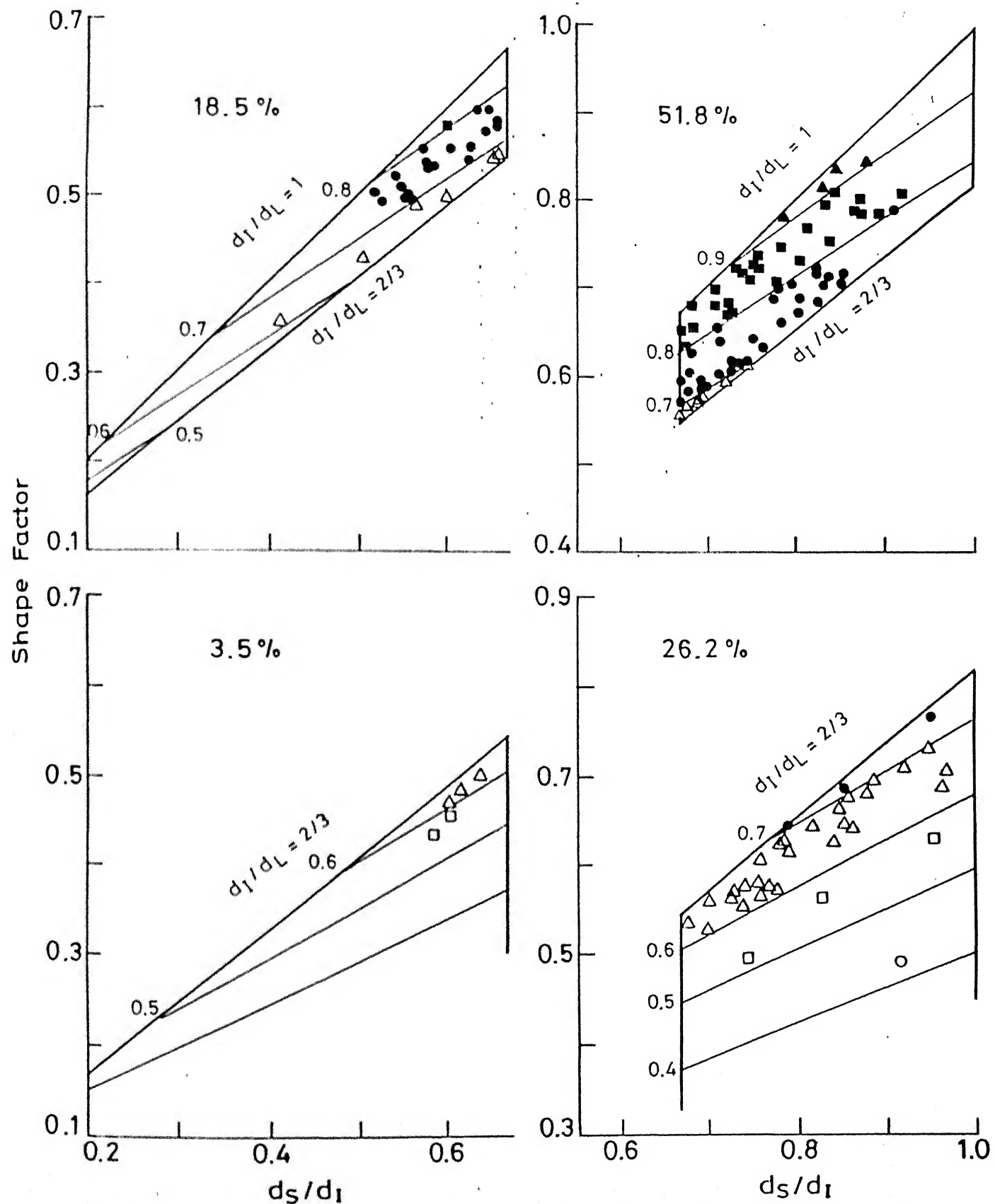


Fig. 4.41 Range of shape factors for Kalpi sand subjected to 22.04 kg/cm².

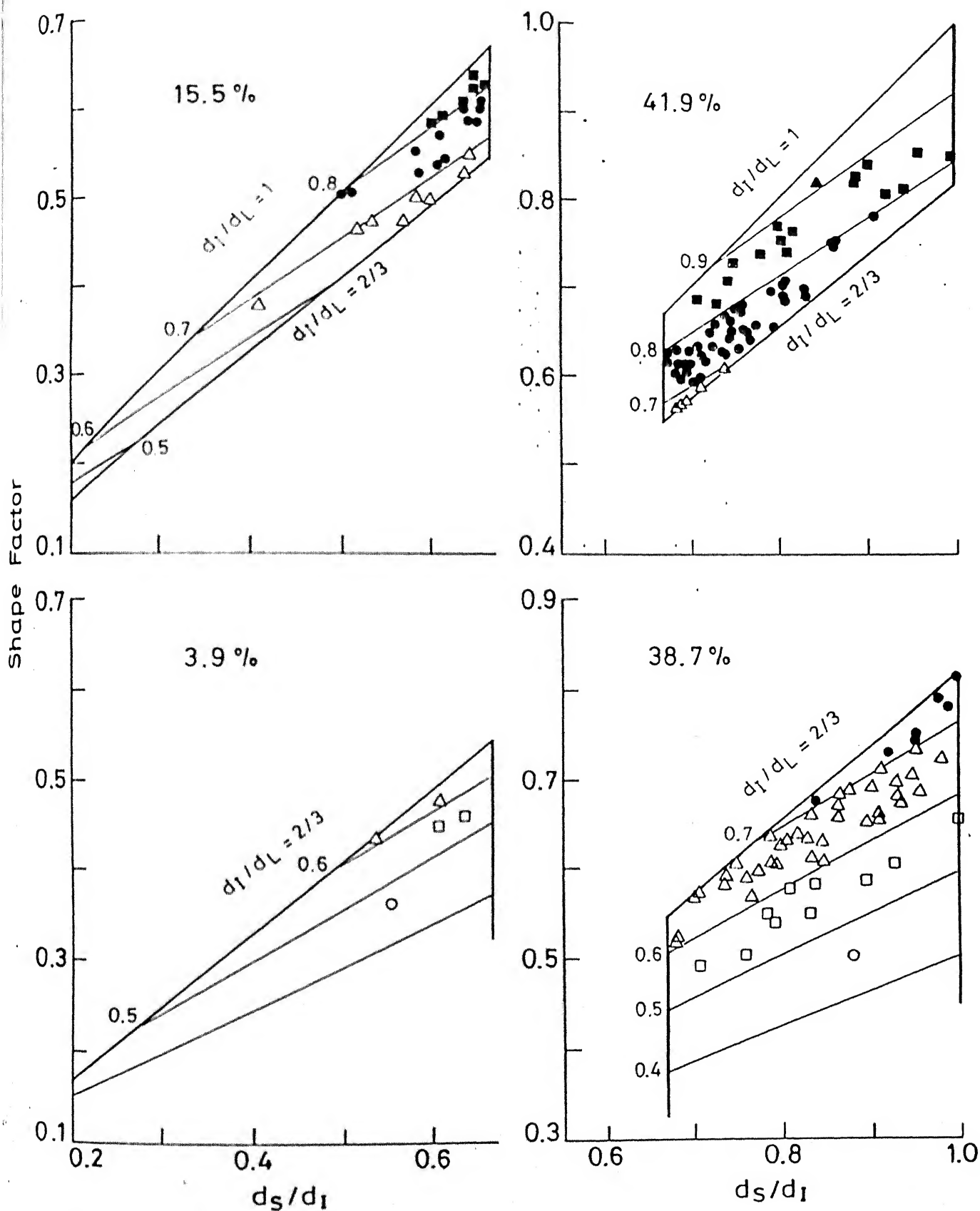


Fig. 4.42 Range of shape factors for Kalpi sand subjected to 176.32 kg/cm².

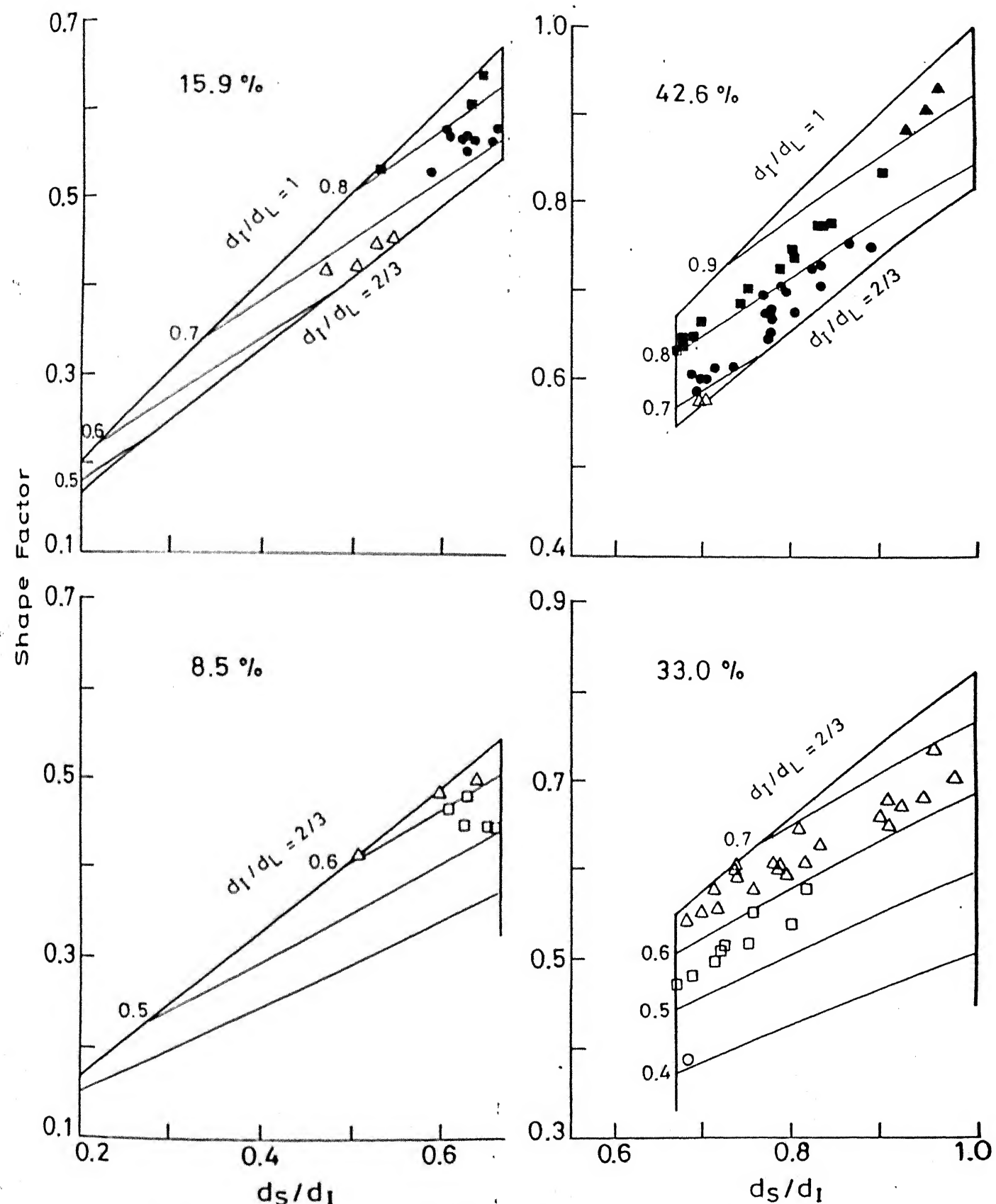


Fig. 4.43 Range of shape factors for Kalpi 1.

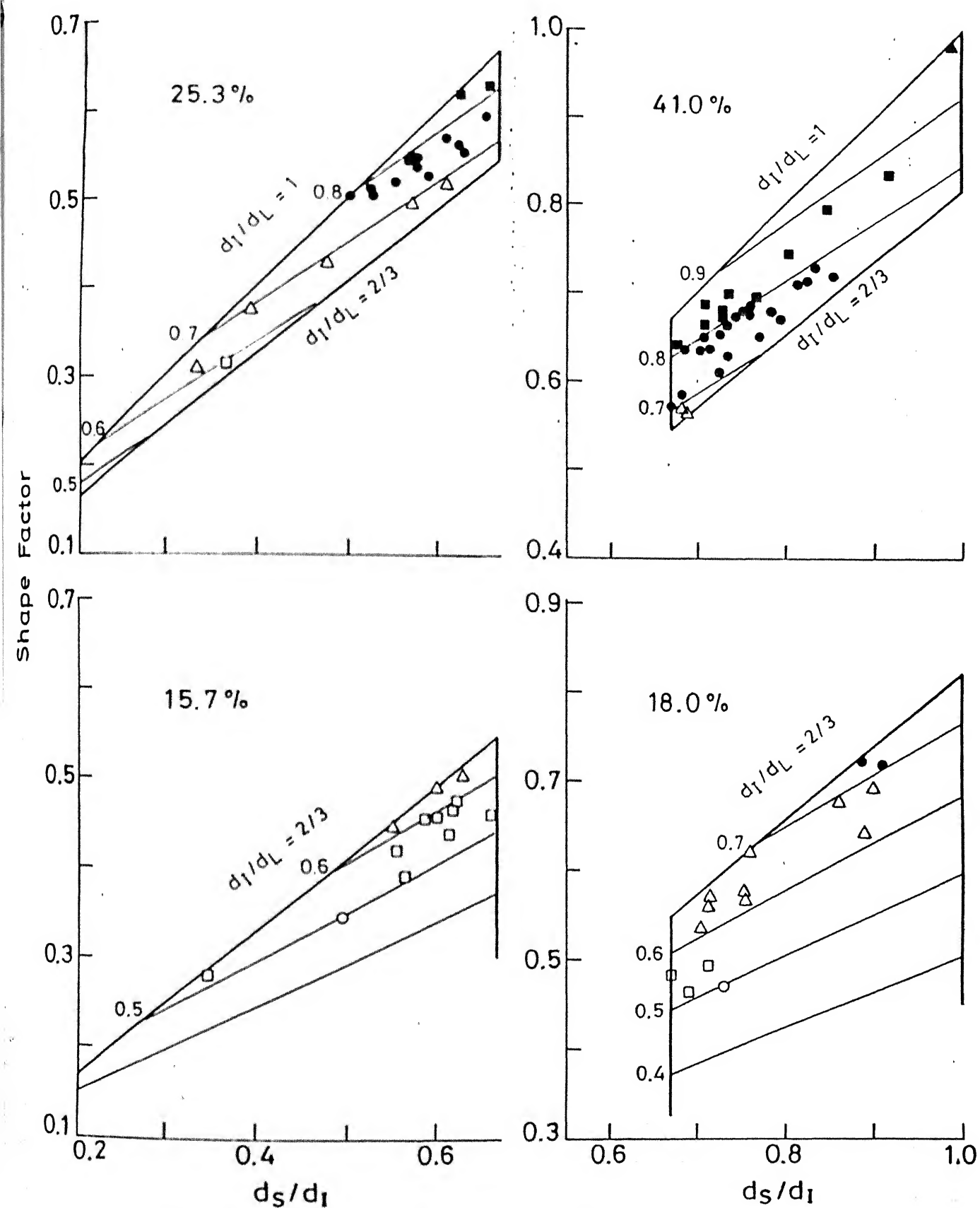


Fig. 4.44 Range of shape factors for Kalpi 2.

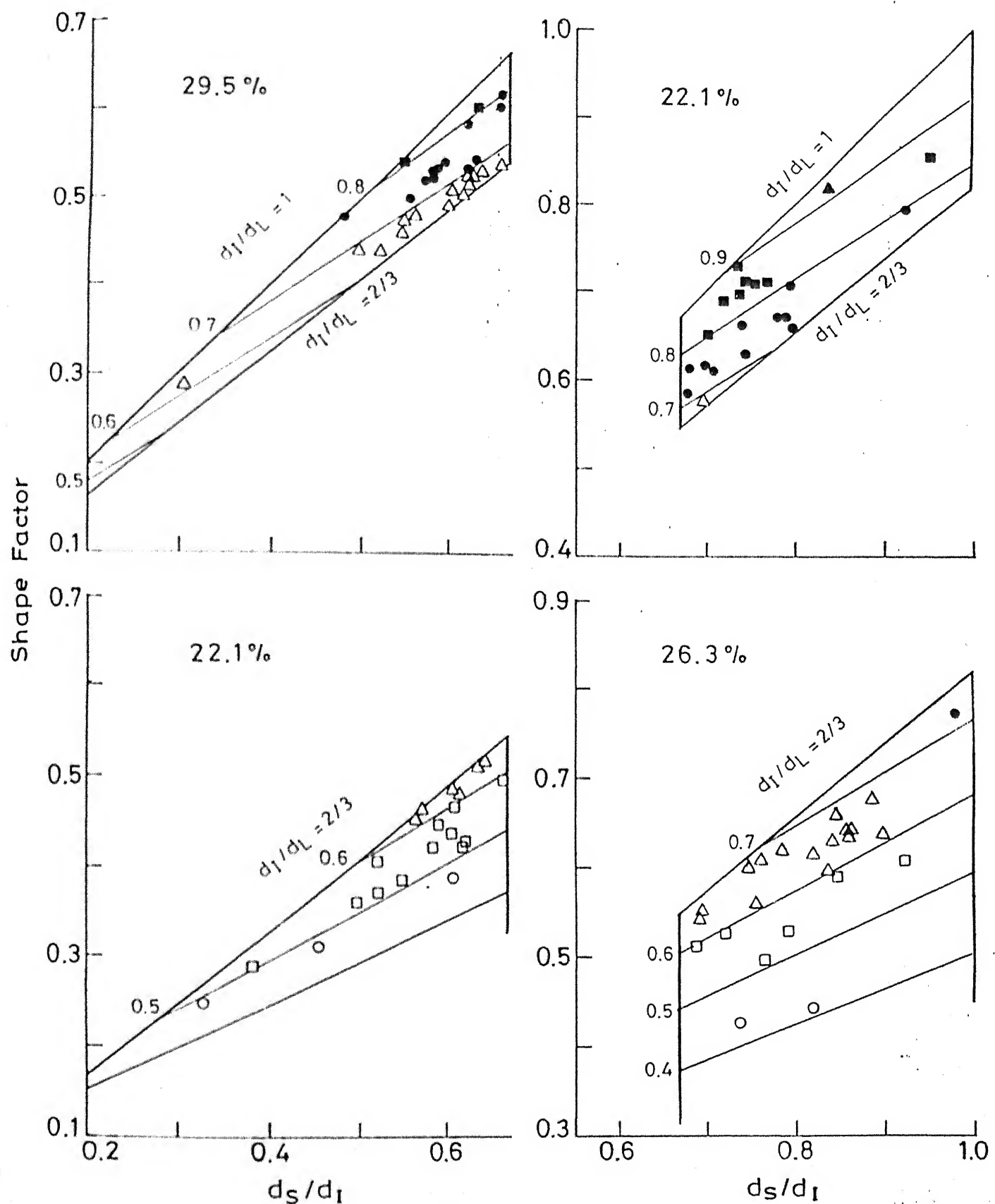


Fig. 4.45 Range of shape factors for calcareous sand.

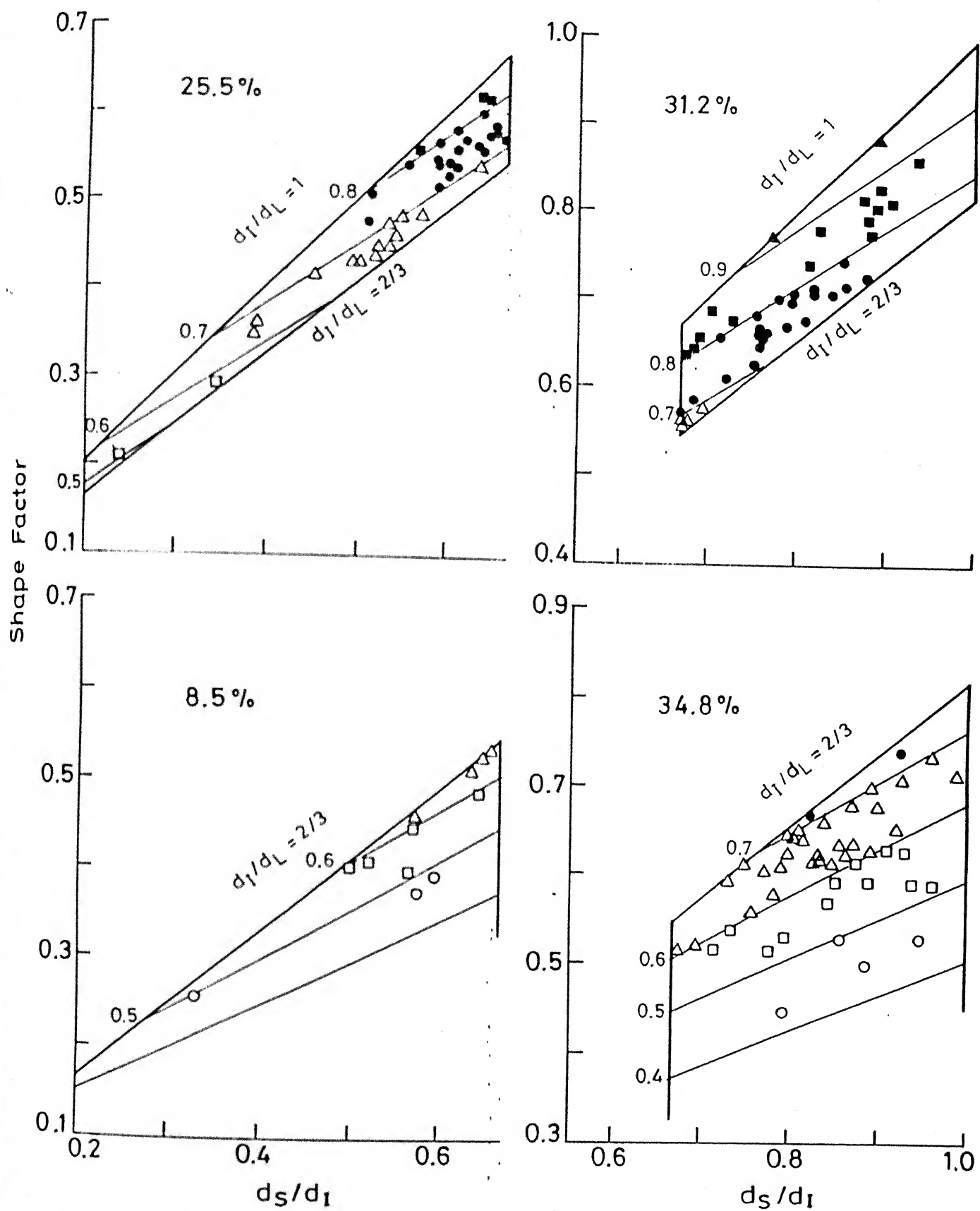


Fig. 4.46 Range of shape factors for calcareous subjected to 22.04 kg/cm^2 .

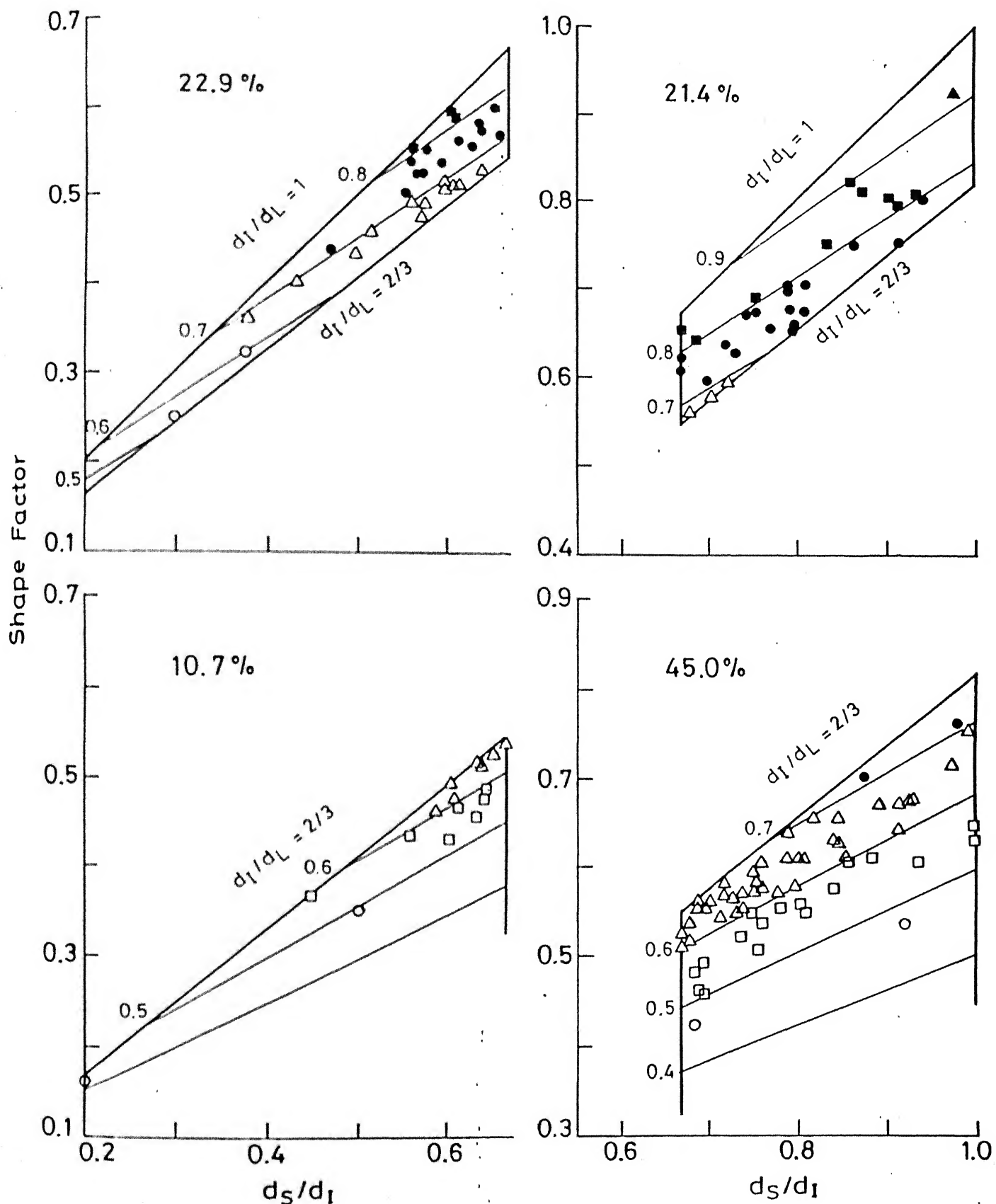


Fig. 4.47 Range of shape factors for calcareous subjected to 176.32 kg/cm².

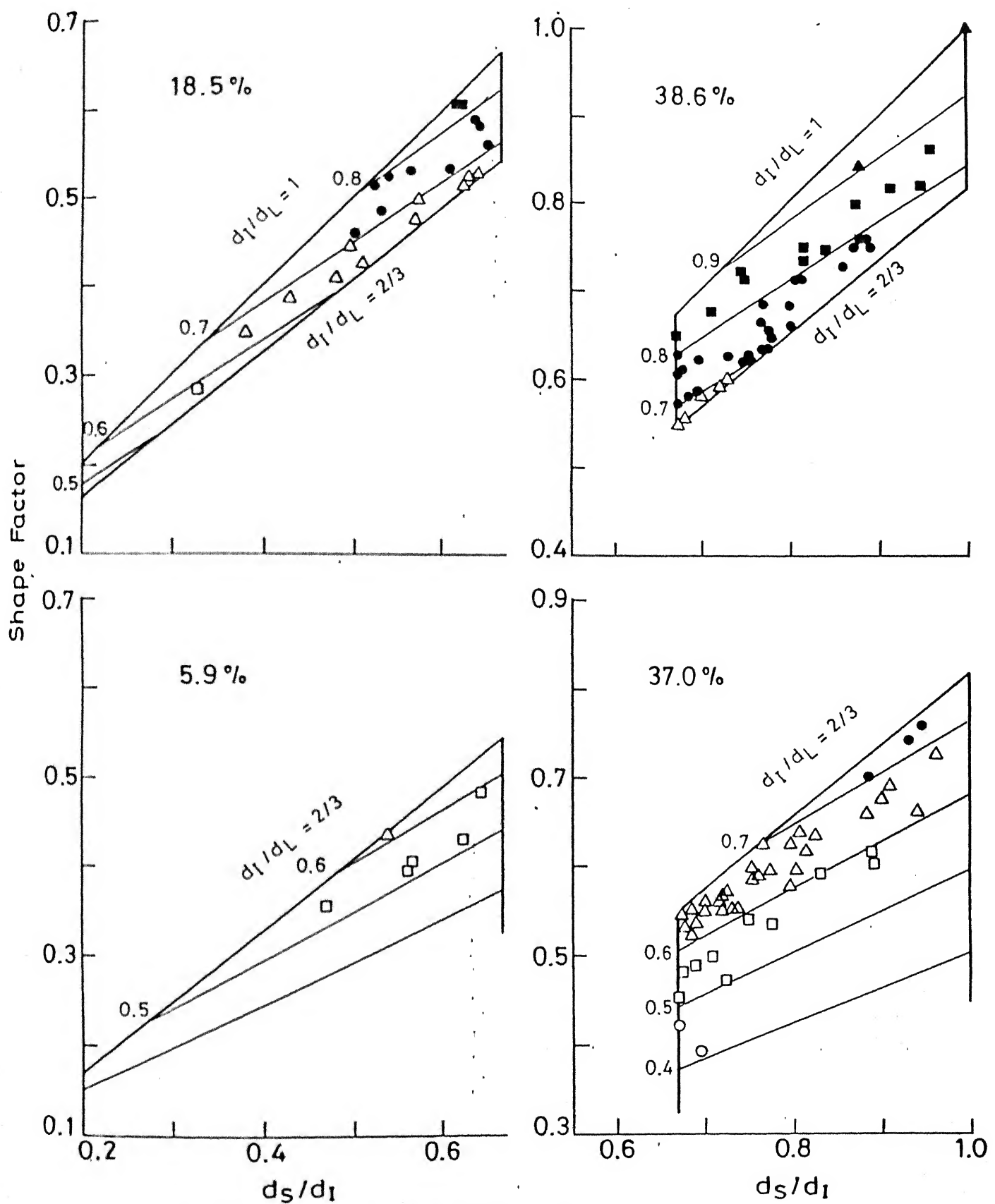


Fig. 4.48 Range of shape factors for artificial calcareous sand.

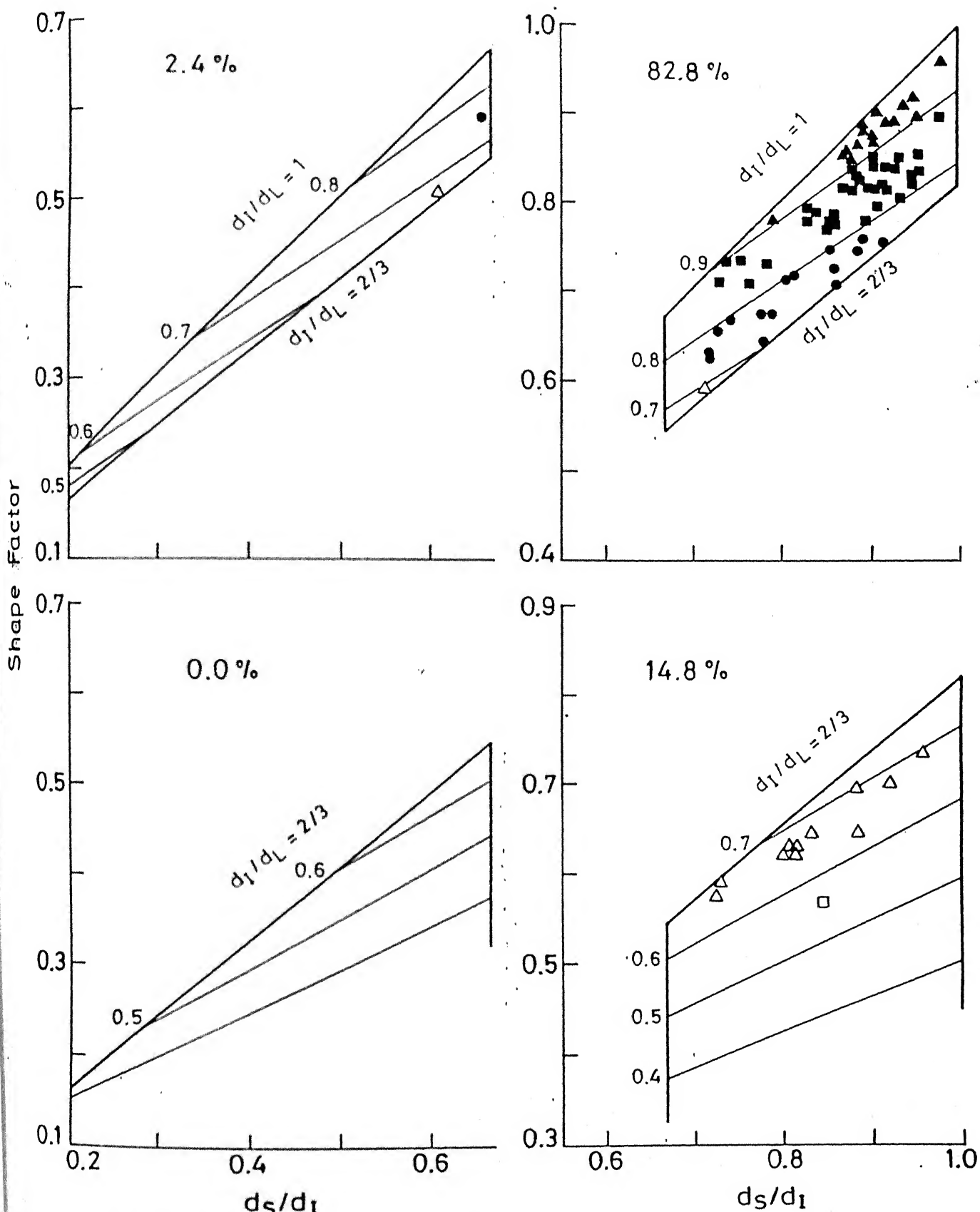


Fig. 4.49 Range of shape factors for standard sand.

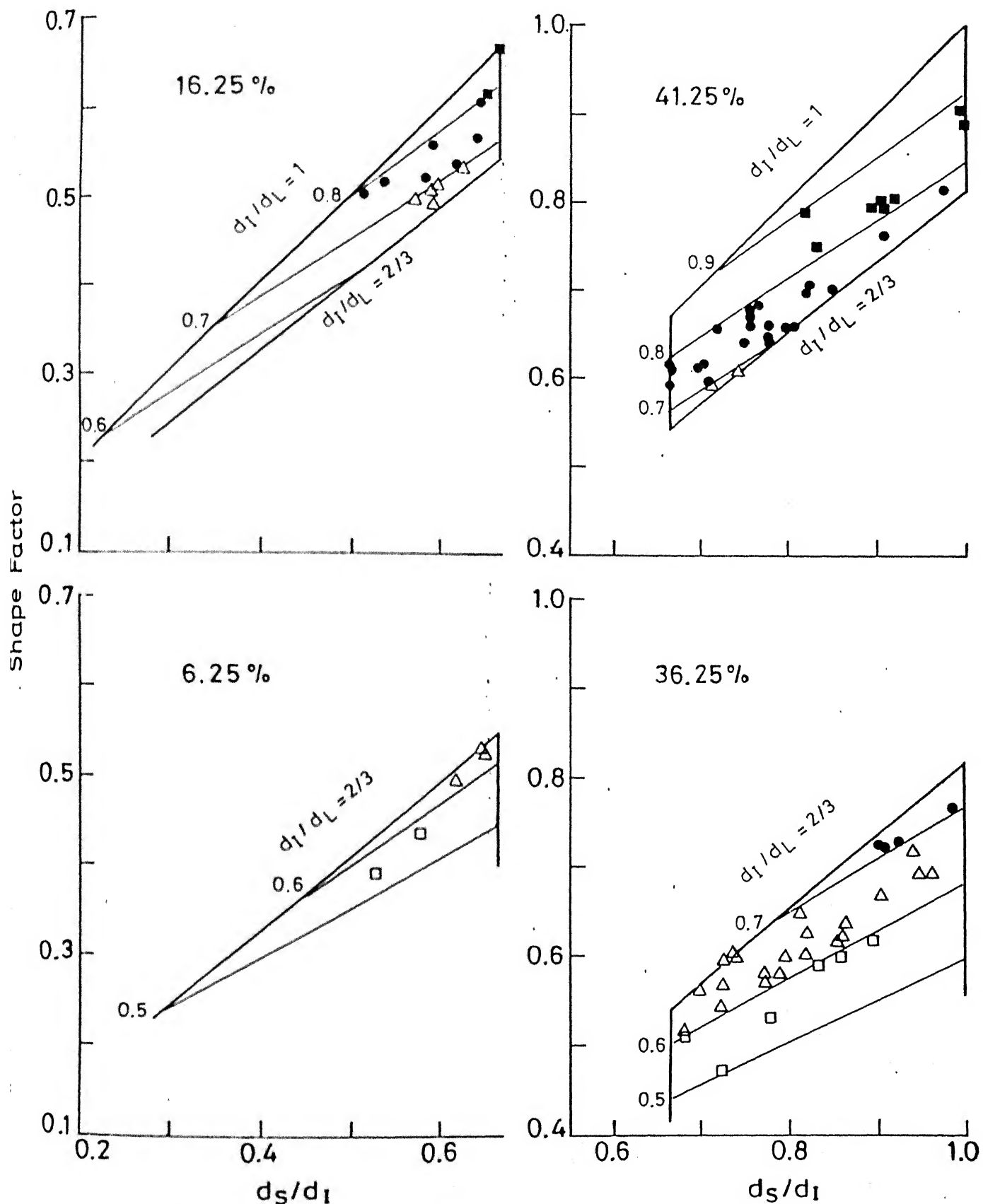


Fig. 4.50 Range of shape factors for Ottawa sand.

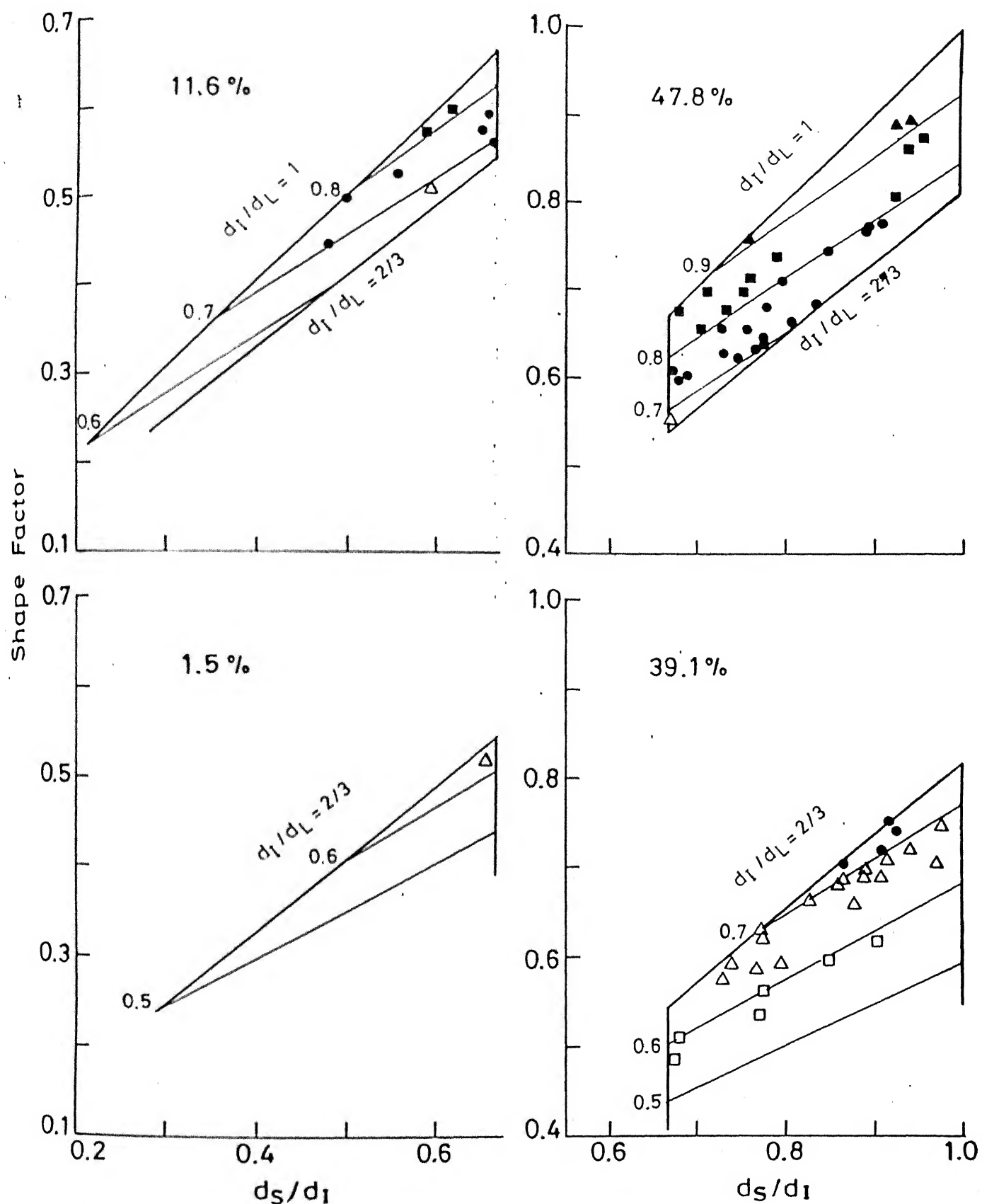


Fig. 4.51 Range of shape factors for San Fernando (#5) sand.

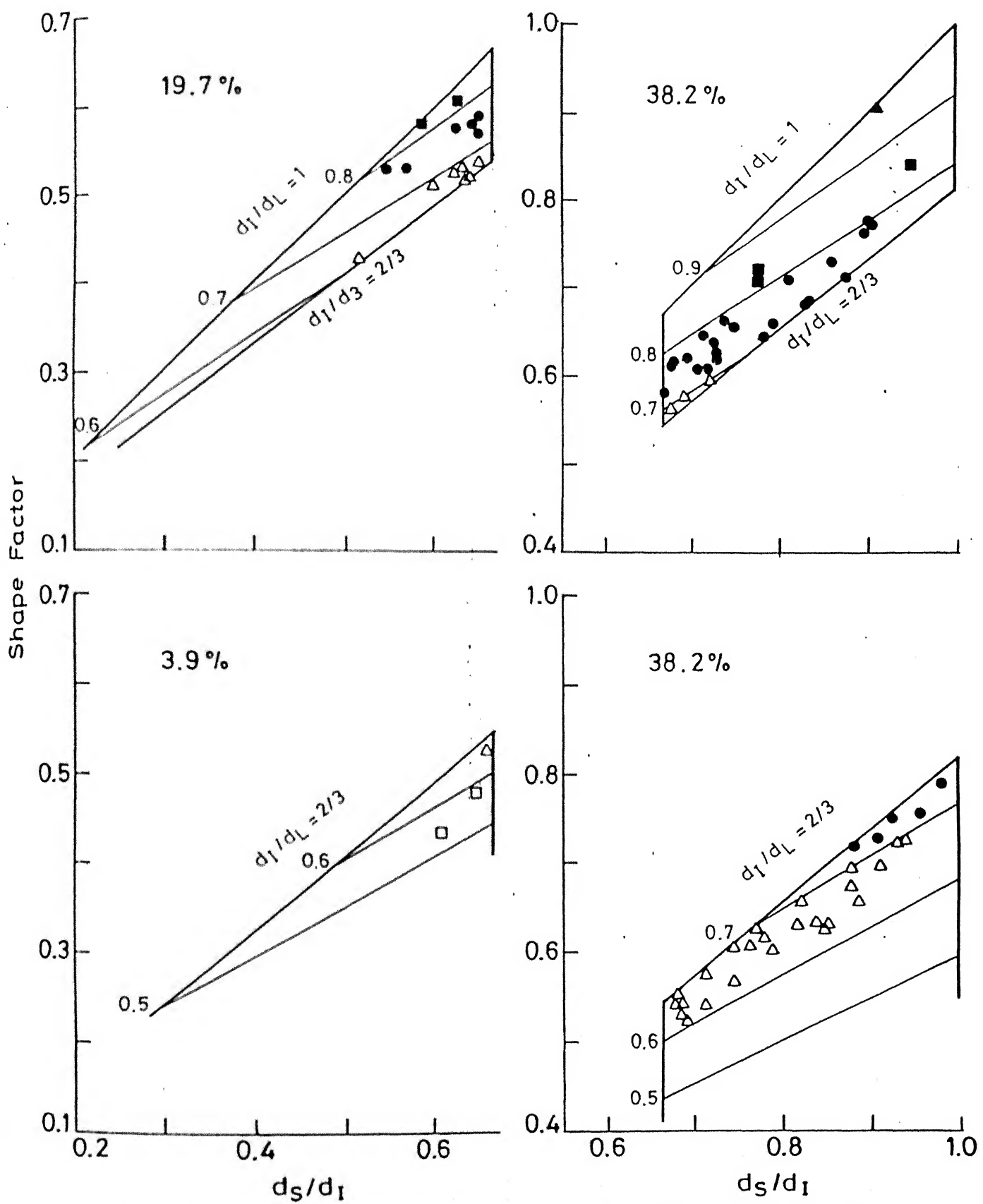


Fig. 4.52 Range of shape factors for San Fernando (#6) sand.

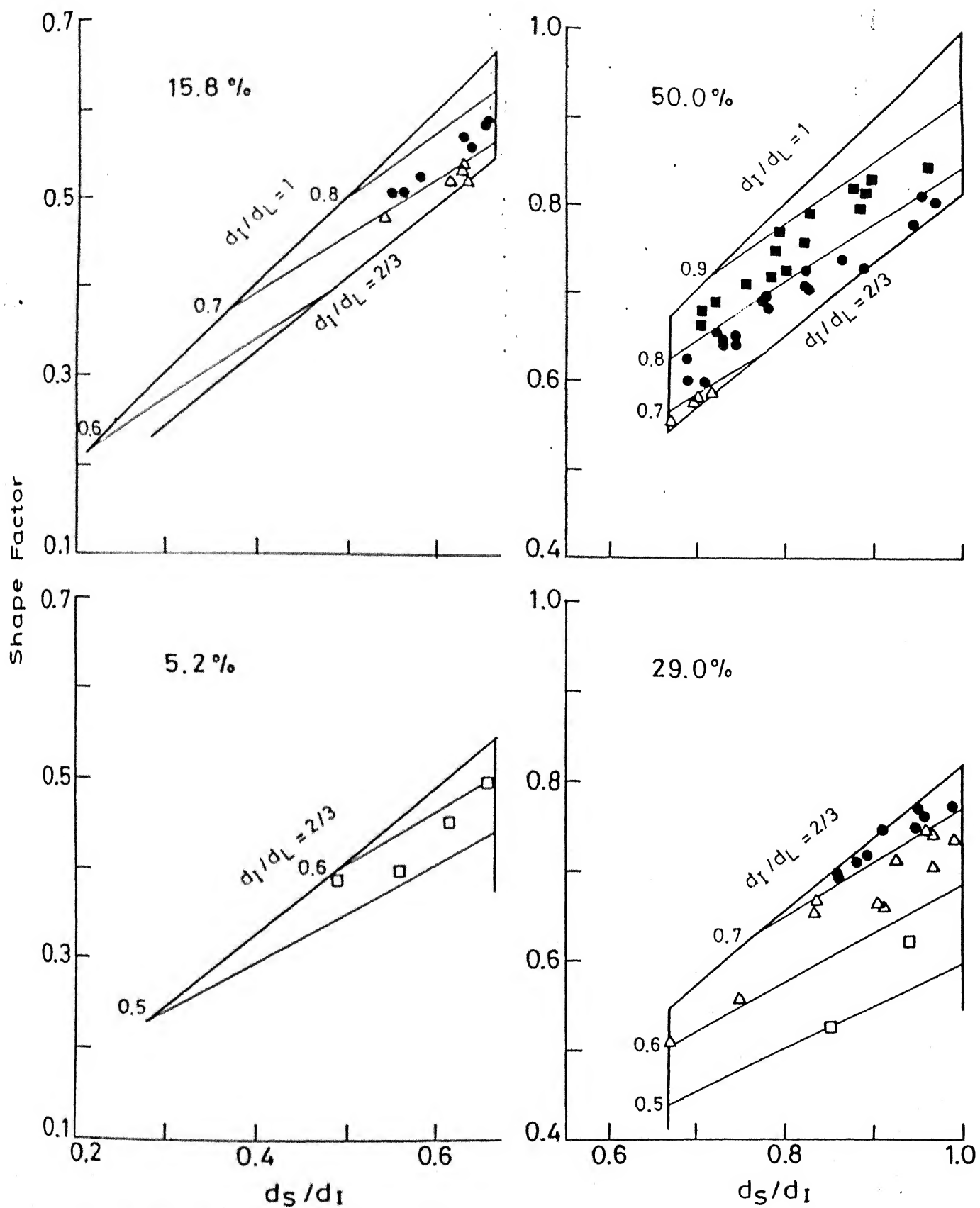


Fig. 4.53 Range of shape factors for San Fernando (#7) sand.

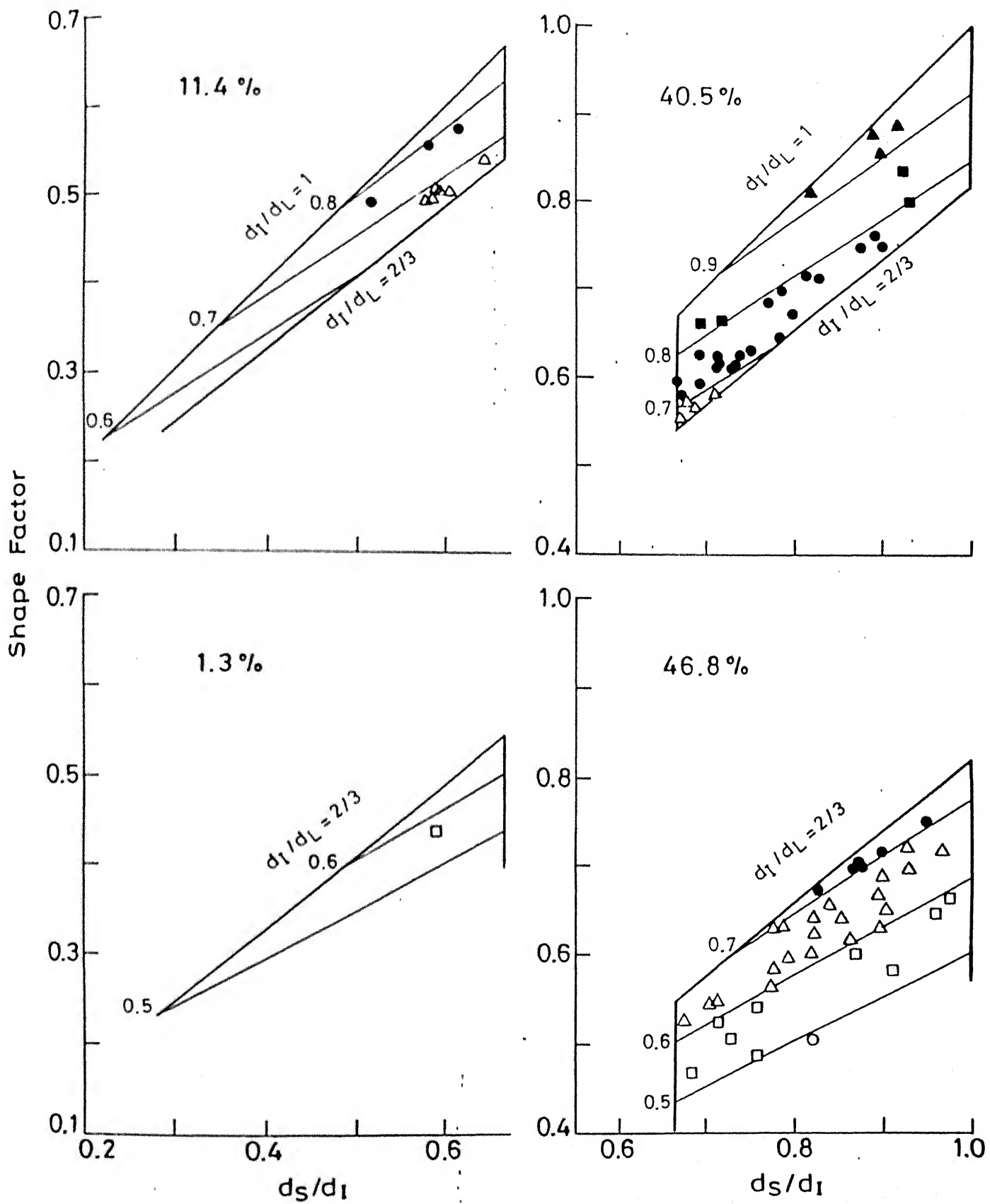


Fig. 4.54 Range of shape factors for Leighton Buzzard sand.

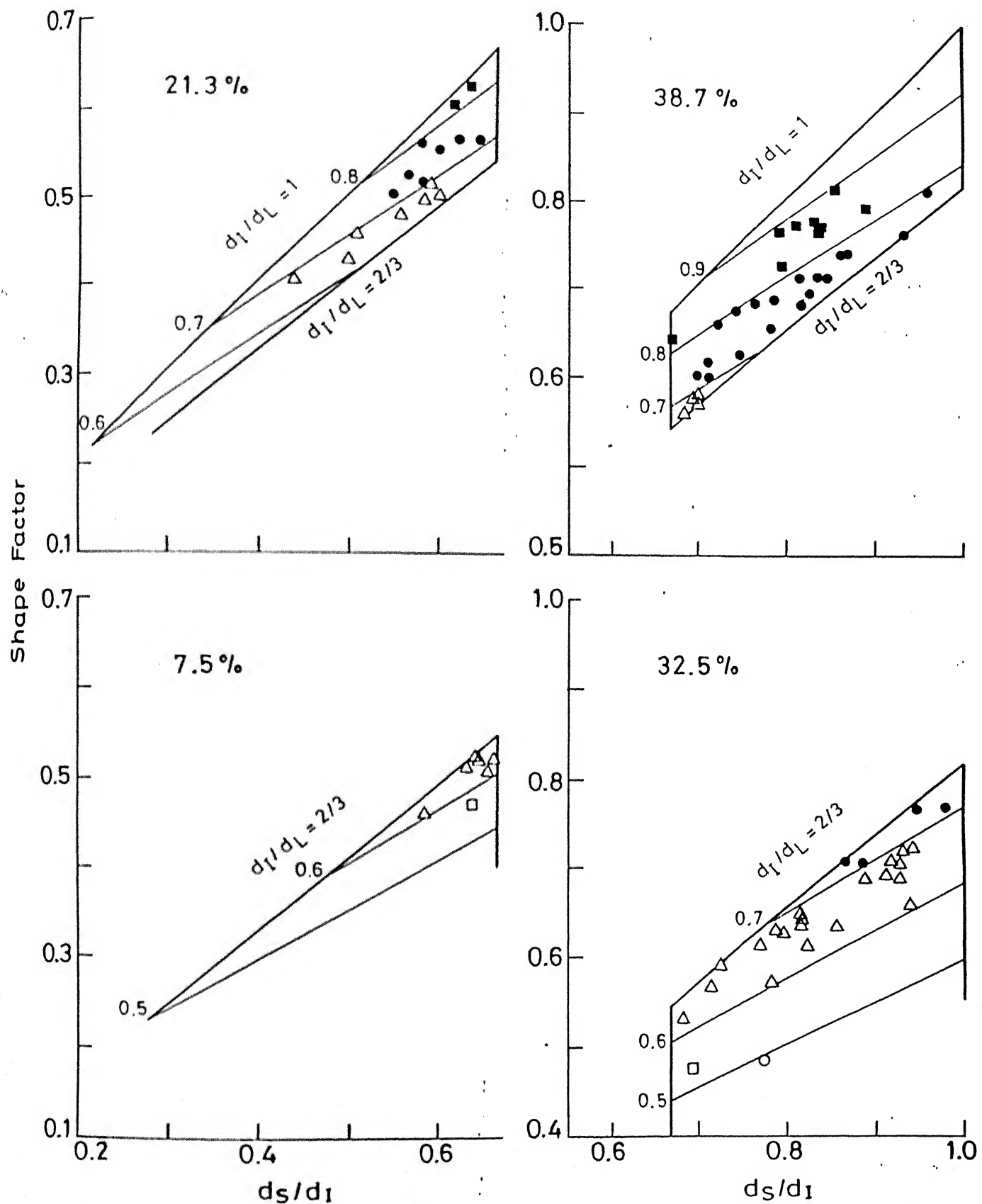


Fig. 4.55 Range of shape factors for Lagunillas (94A-M19) sand.

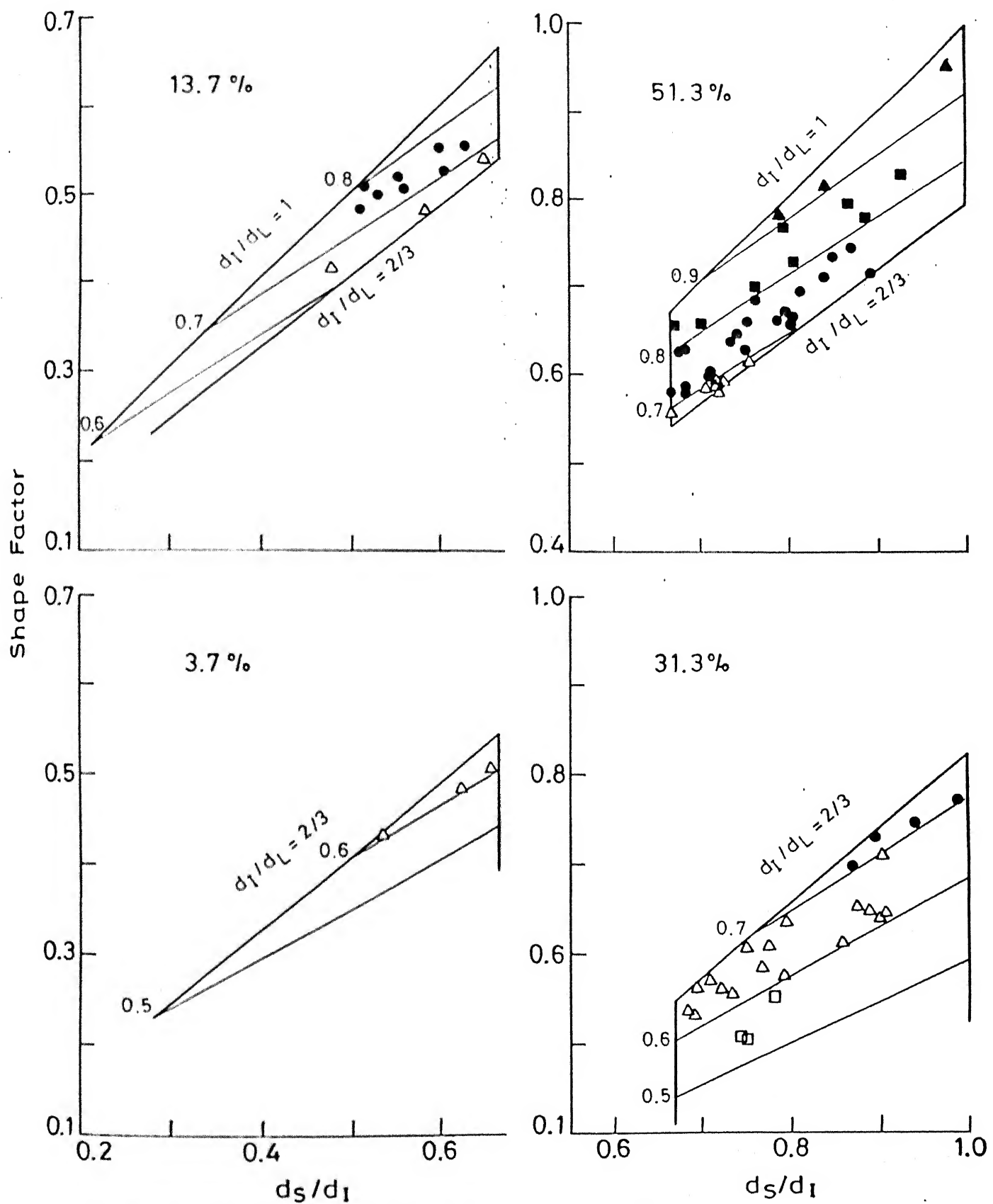


Fig. 4.56 Range of shape factors for Lagunillas (94A + 94B) sand.

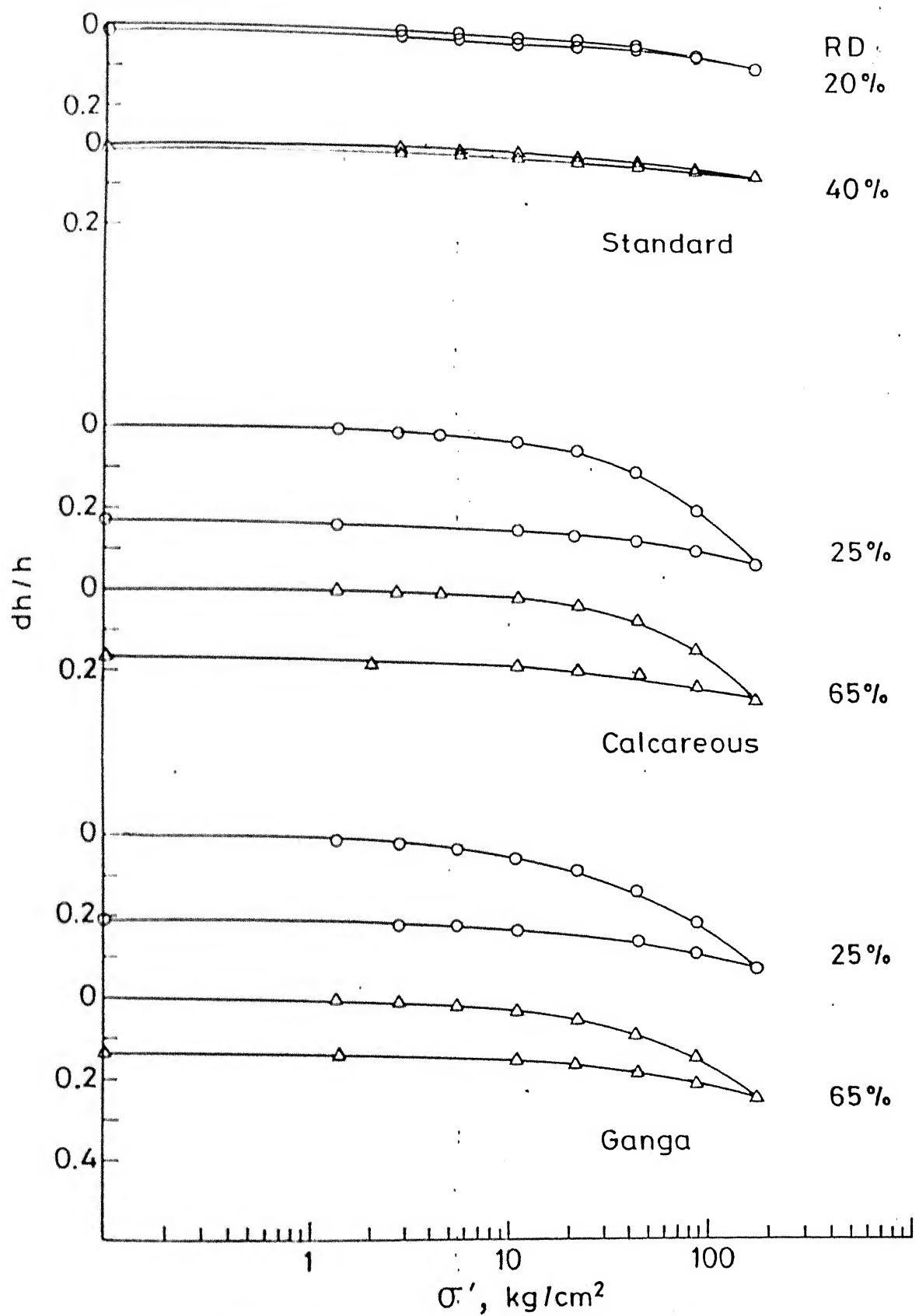


Fig. 4.57 One dimensional compression behaviour of sands.

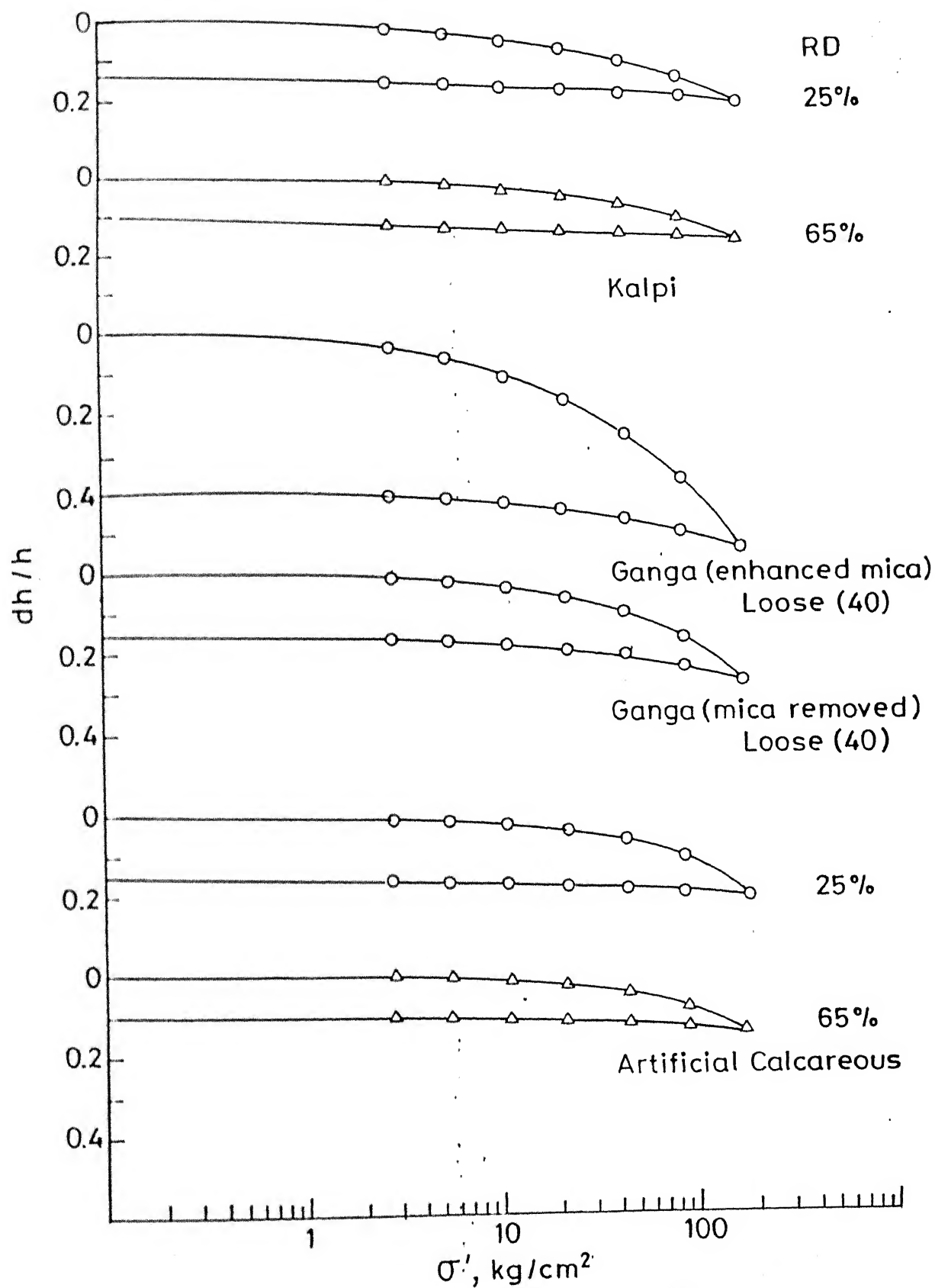


Fig. 4.58 One dimensional compression behaviour of sands.

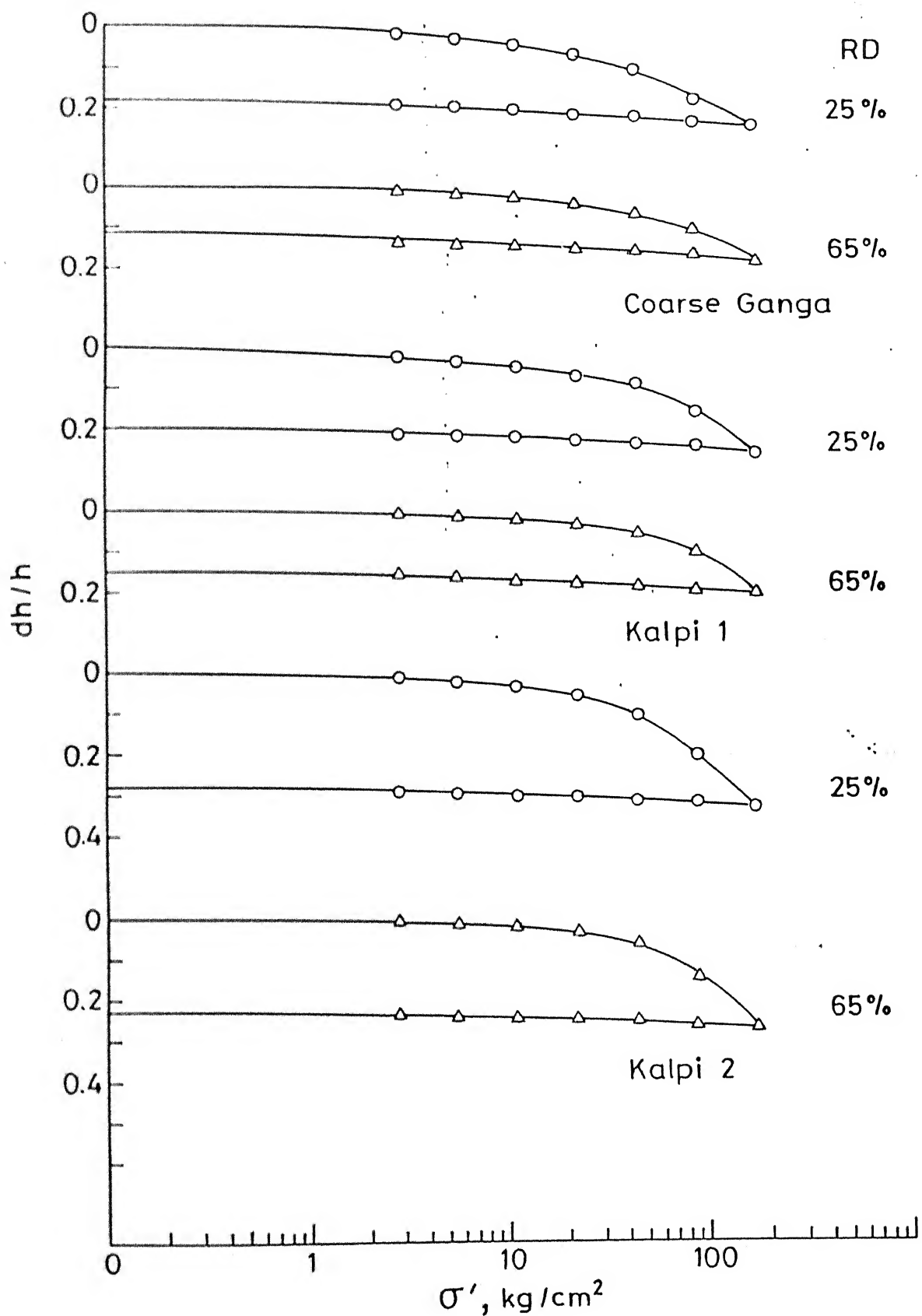


Fig. 4.59 One dimensional compression behaviour of sands

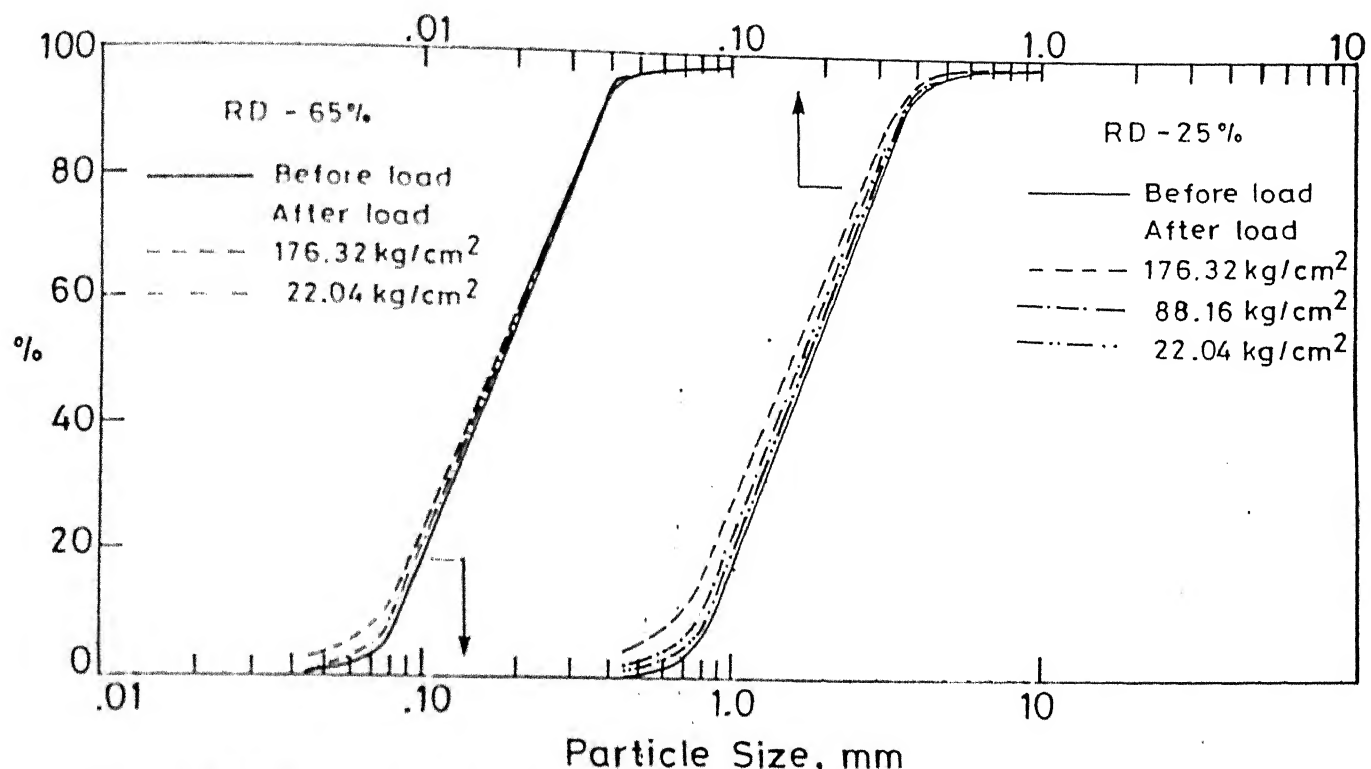


Fig. 4.60 Particle size gradation before and after loading for Ganga sand.

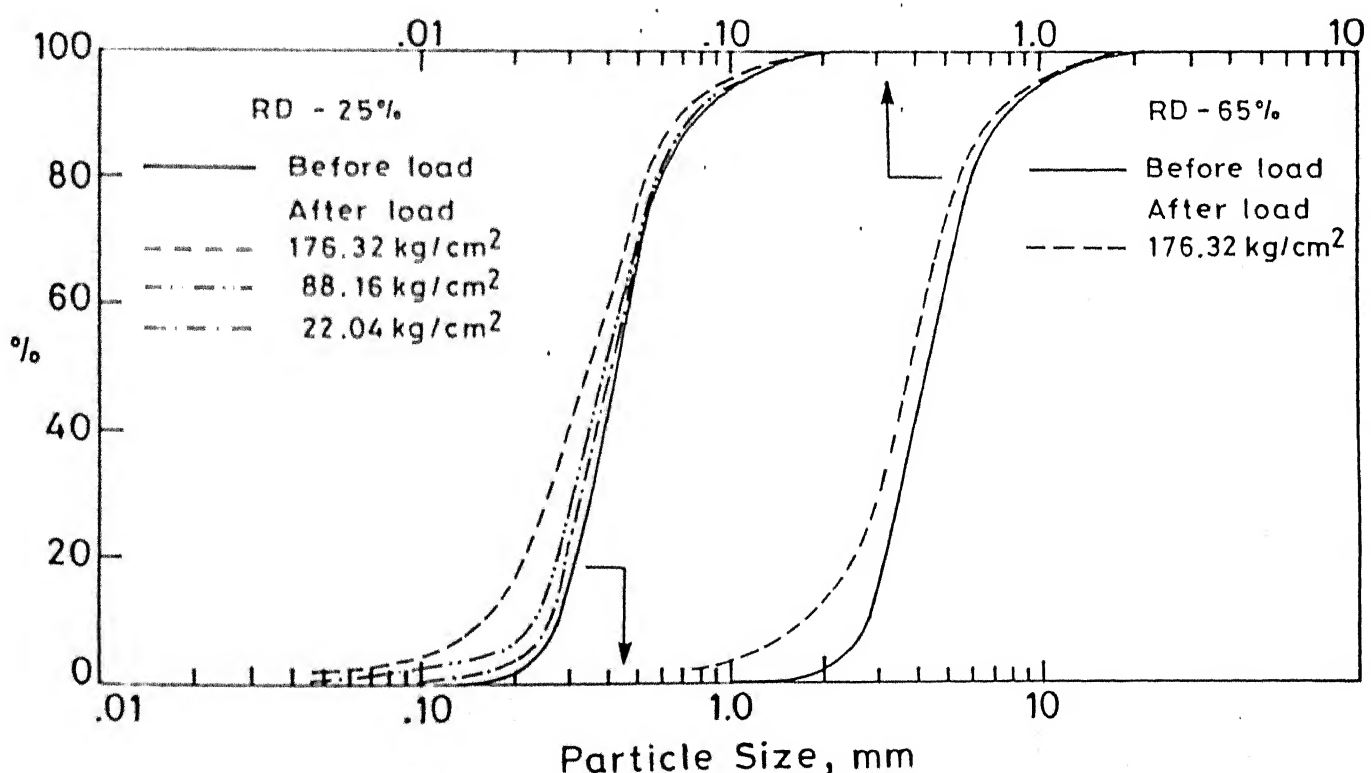


Fig. 4.61 Particle size gradation before and after loading for Calcareous sand

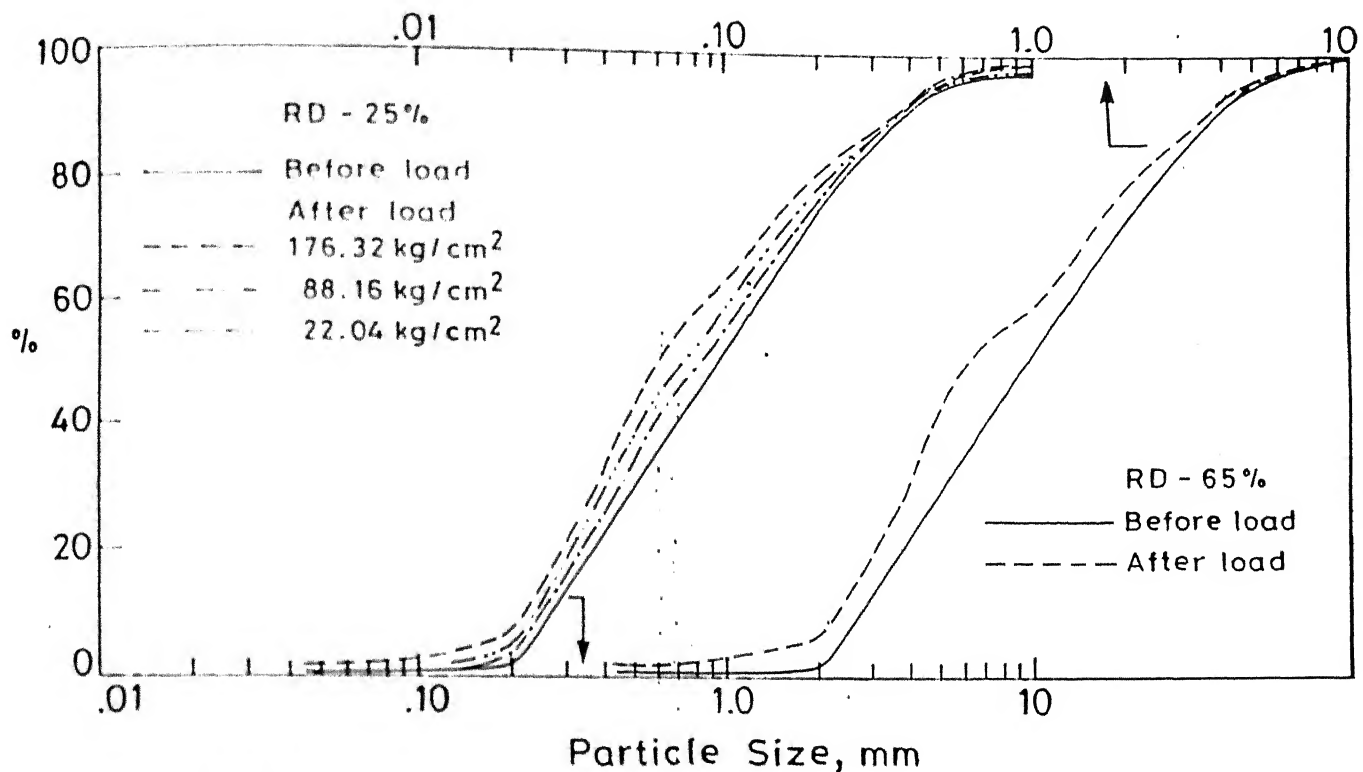


Fig. 4.62 Particle size gradation before and after loading for Kalpi sand.

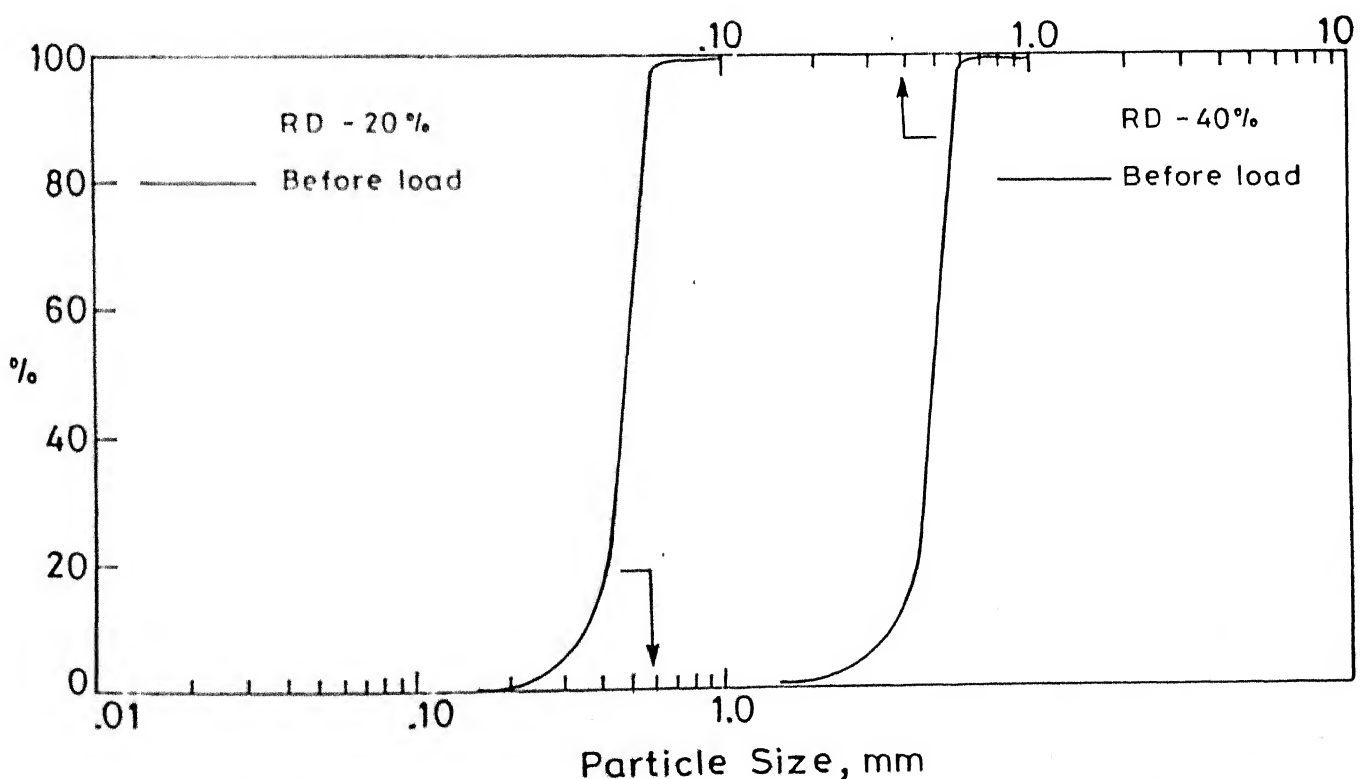


Fig. 4.63 Particle size gradation before and after loading for Standard sand.

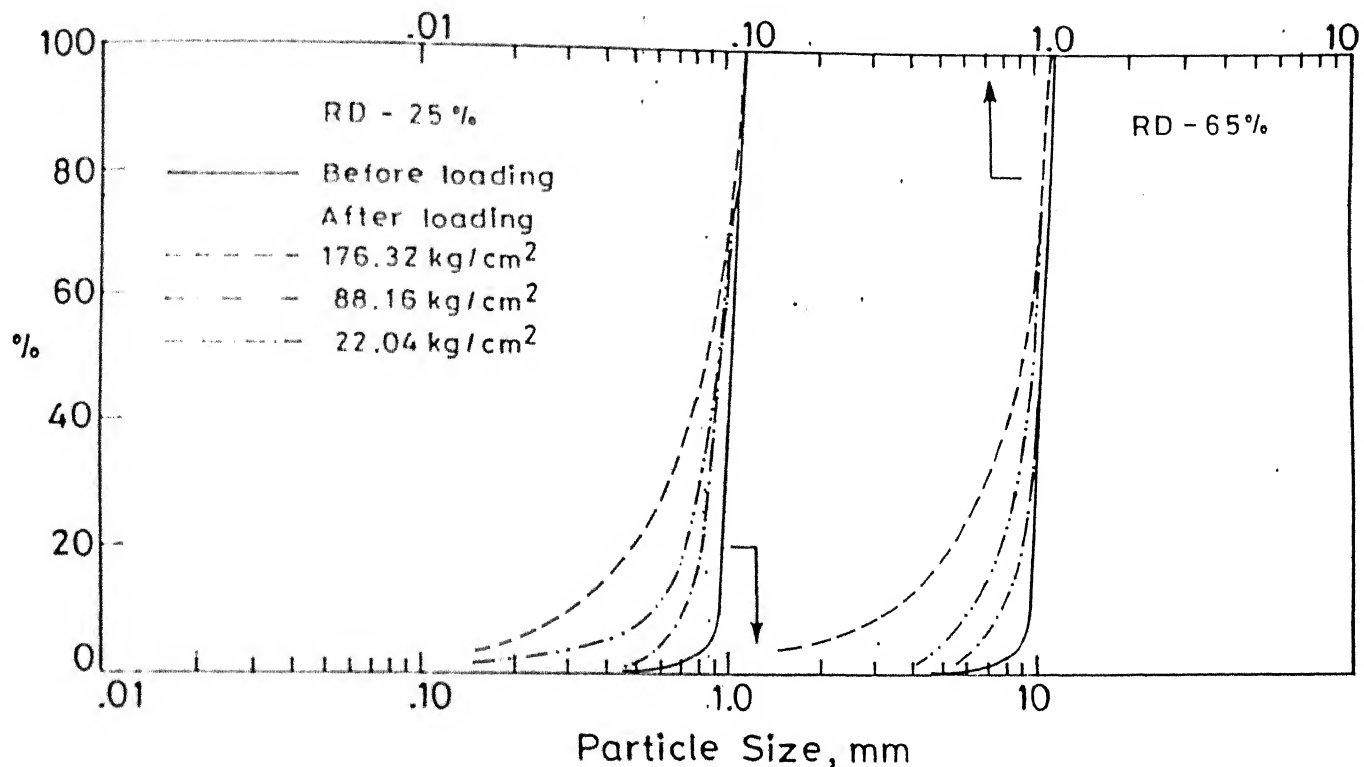


Fig. 4.64 Particle size gradation before and after loading for Kalpi 1 sand.

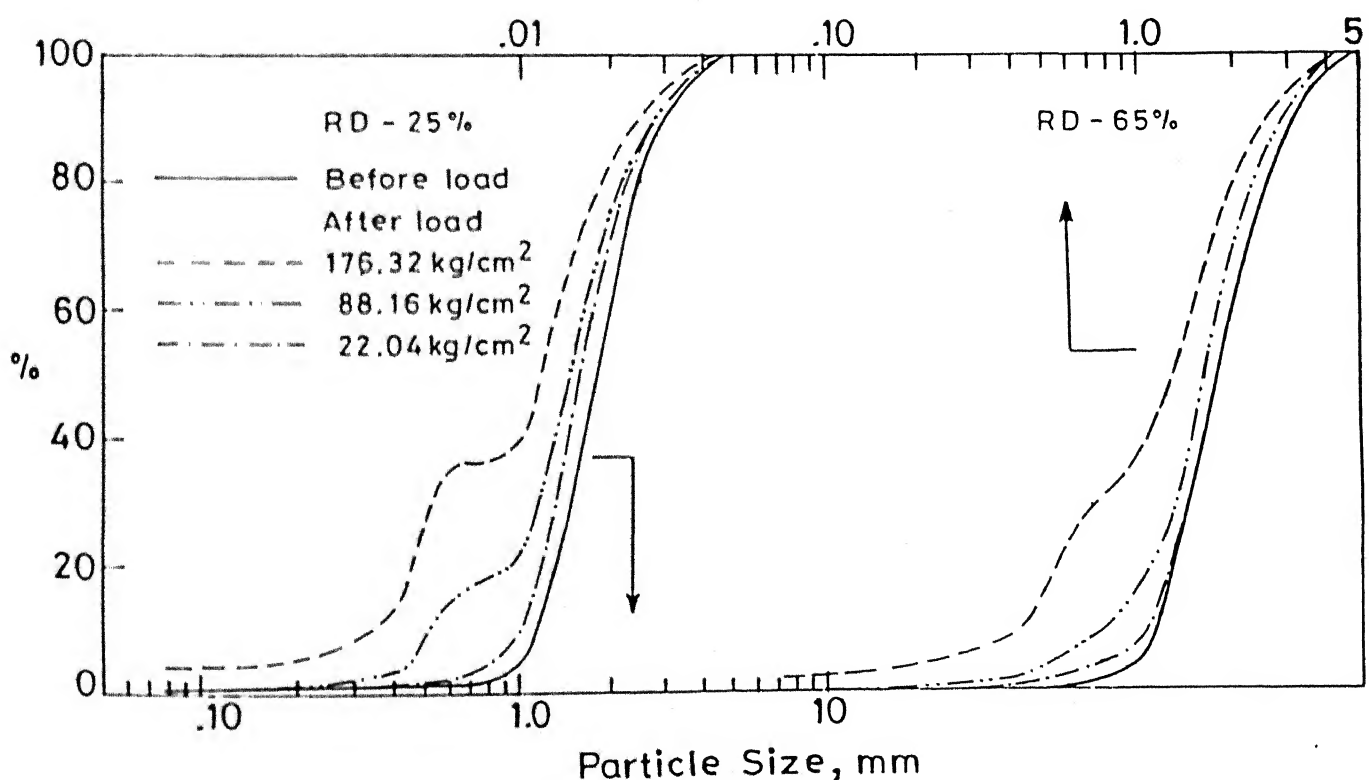


Fig. 4.65 Particle size gradation before and after loading for Kalpi 2 sand.

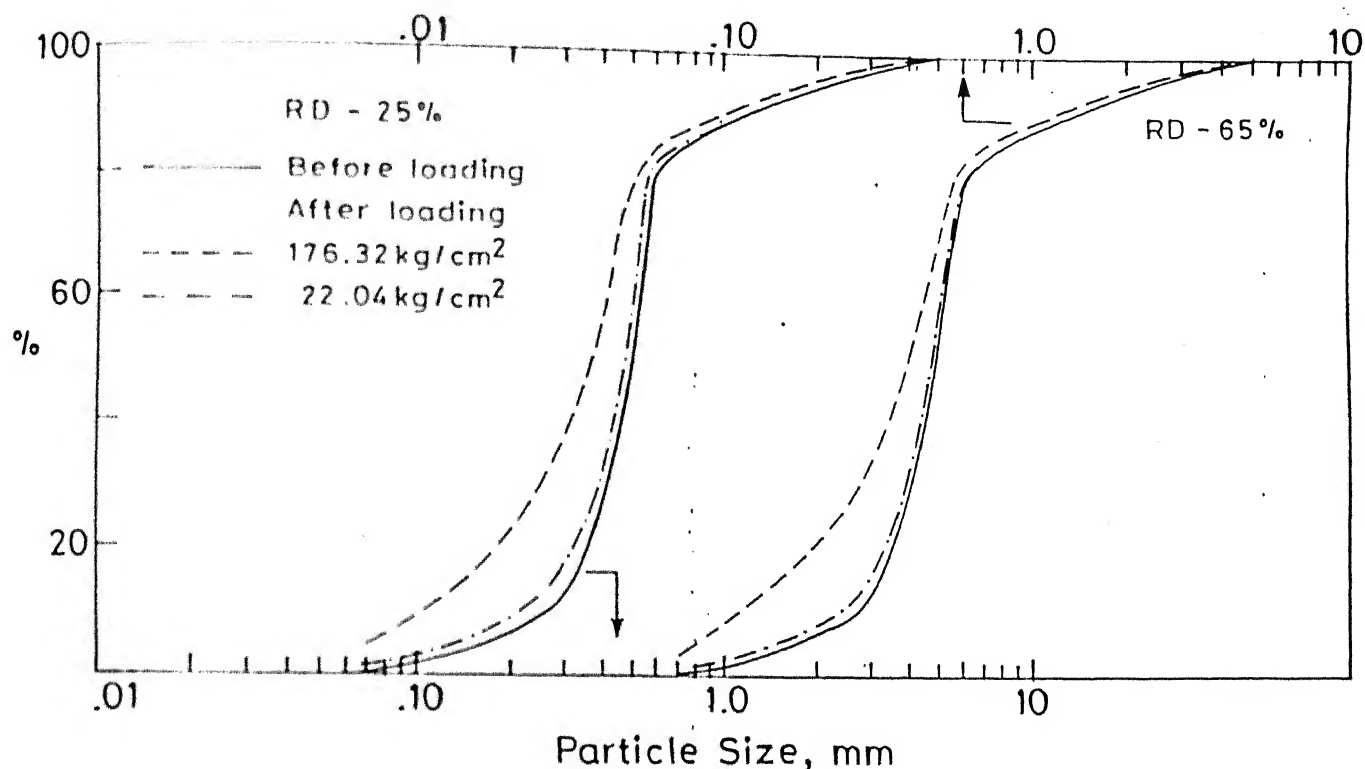


Fig. 4.66 Particle size gradation before and after loading for Artificial Calcareous sand.

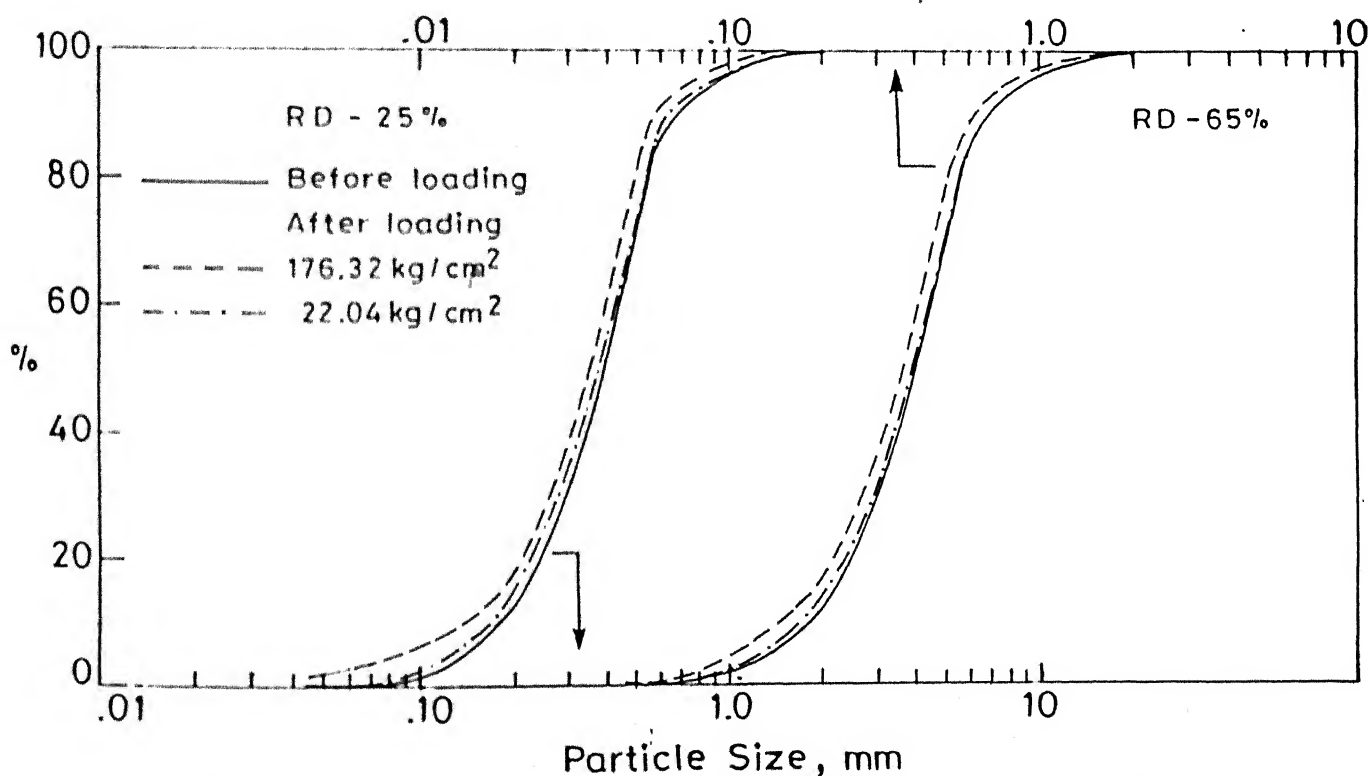


Fig. 4.67 Particle size gradation before and after loading for Coarse Ganga sand.

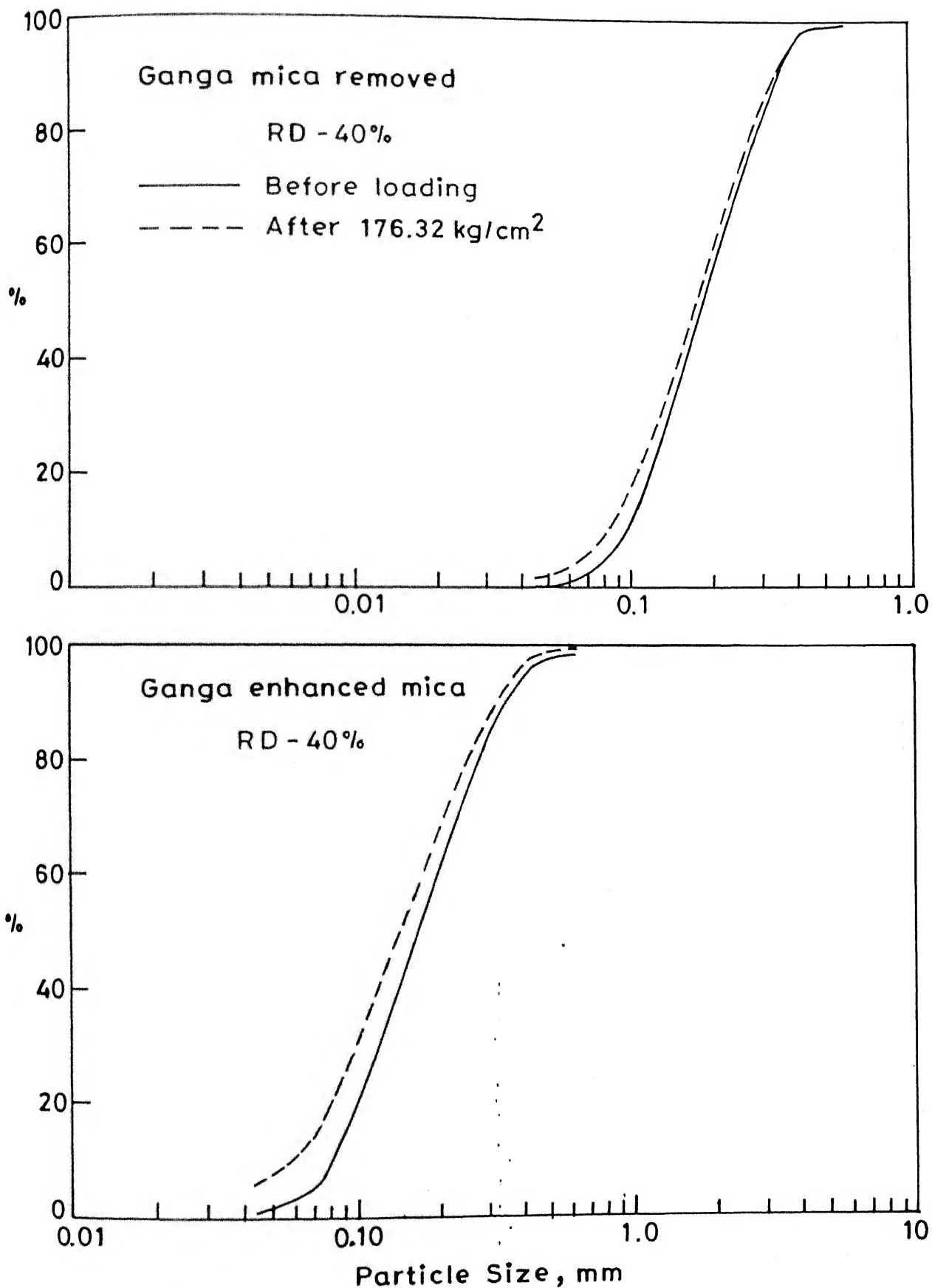


Fig. 4.68 Particle size gradation before and after loading for Ganga mica removed and Ganga enhanced mica.

CHAPTER V

INTERPRETATION AND DISCUSSION OF TEST DATA

The engineering behaviour of a sand is controlled by its grain morphology and mineral composition. While sporadic attempts have been made to characterize sand in terms of its size and shape attributes, there is need for a quantitative classification of the same in terms of size, angularity (roundness), sphericity and shape factor. Such a characterization is essential for continuously tracking the grain modification at different stress levels. The mineralogy of the sand system plays an important role in the grain modification. As detailed in the previous chapter, series of experiments have been conducted to accomplish not only the quantification of the grain morphology but also to gain an understanding of various parameters operative during the sand compressibility and interrelationship between the same. In the present chapter, the test data obtained are interpreted in the light of various operating parameters and the details are presented on morphological classification, role of grain modification and crushing on compressibility and constrained modulus. The role of mineralogical composition in the behaviour of the sands under stress has also been brought out.

5.1 GRAIN MORPHOLOGY

In this section results of studies related to particle sphericity, shape factor and angularity are discussed on the basis of which the particle morphology of a variety of

natural and artificial sands was characterized. Interrelationship between various parameters used for description of surface characteristics is established. Typical distributions of surface characteristics for different systems from rounded to highly angular nature of particles are presented.

5.1.1 Sphericity and Shape Factor

Particle shape can be designated as oblate, equant (spherical), prolate (roller, or rod like) and bladed (flaky) depending the location of the data plots in quadrants I, II, III, IV respectively on the zingg diagram (Fig. 2.1). The data pertaining to sphericity and shape factor for each of the size fractions of the sand used in the present study have been characterized for the particle shape using the Zingg diagram (Fig. 4.11 - 4.56). In case of four sands studied in detail, about 83% of particles for Standard sand lie within quadrant II, indicating spherical nature of the grains and about 15% of the particles lie along the boundary of quadrants II and III. In sharp contrast to the Standard sand, Calcareous and Ganga Sands have only 22 to 25% particles in quadrant II and roughly 50% of the particles for these sands lie in quadrants I and IV, depicting the plate like and flaky nature of the grains. In case of Kalpi sand about 37% of the grains lie within quadrant II with an equal percentage of grains located in quadrant III indicating elongated nature of the grains.

Most of the other natural sands examined (Table 5.1) show roughly 40-50% grains in quadrant II and 30-40% in quadrant III indicating abundance of bulky spherical and elongated grains. Only 10-20% of the grains are oblate and 5% are flaky. In addition to Zingg diagram with superposed sphericity values, the shape factor (SF) for all the sands was also calculated (Figs. 4.36 - 4.56). Shape factor data gives much better separation of different grain shapes belonging to various quadrants in Zingg diagram. For example, in case of Standard and San Fernando sands, Zingg diagrams (Figs. 4.28 and 4.30) would appear to suggest as if they have similar distribution of grain shapes. However, plots on the shape factor diagrams (Figs. 4.49 and 4.51) clearly bring out the abundance of plate and rod like particles in San Fernando sand as compared to Standard sand. Hence for a complete characterization of the shape of sand grains, shape factor diagrams are essential in addition to the Zingg diagram. The percentage of particles in each quadrant for different sands is presented in Table 5.1.

5.1.2 Particle Angularity

In addition to the study of particle sphericity and shape factor, to estimate particle angularity data were also obtained for each sieve fraction in terms of number of tangents which reflect the surface characteristics of the edges of the particles. As explained earlier, the image analyzer was used to examine the two dimensional projection

Table 5.1 : Percentage of Particles in Each Quadrant

Sands	Percentage in different quadrants				Remarks
	I	II	III	IV	
Standard	2.47	82.72	14.81	0.00	Mainly spherical grains
Kalpi	17.31	37.50	35.58	9.61	Rod like and bulky grains
Calcareous	29.79	22.34	25.53	22.24	Oblate and Flakey grains
Ganga	28.05	25.61	26.83	19.51	
Kalpi 1	15.96	42.55	32.98	8.51	
Kalpi 2	25.31	40.26	18.07	15.66	Bulky and rod like grain
Artificial Calcareous	18.49	38.16	36.97	5.88	
Coarse Ganga	20.88	32.29	30.21	16.67	Oblate and Flakey
Lagunillas 94A - 94B	14.10	51.28	30.77	3.85	Rod like and bulky grains
Lagunillas 94A - M19	20.00	40.00	32.50	7.50	" "
Leighton Buzzard	11.39	40.50	46.84	1.27	" "
SanFernando No.-5	13.04	46.39	39.13	1.44	Bulky and rod like grains
SanFernando No.-6	18.42	38.16	38.16	5.26	" "
SanFernando No.-7	15.79	50.00	28.95	5.26	" "
Ottawa	16.25	41.25	36.25	6.25	Spherical bulky grains

of the particles. Along with the tangent count, particle roundness index (R) (Powers, 1953; Youd, 1973), was also evaluated for each fraction and weighted average of both these measurements for a sand sample was calculated. On the basis of projected surface area data for particles obtained from the image analyzer, the circumference of an equivalent spherical grain was calculated, and the wave length (λ) of surface protrusions (depicted by the number of tangents) was evaluated. The amplitude (h) of the protrusion was estimated on the basis of the measured dimension d_L and the diameter, d_p of the inscribed equivalent circle. The values of λ and h were taken as

$$\lambda = \frac{\text{Circumference of the inscribed circle}}{(\text{No. of Tangents} - 1)} \quad (5.1)$$

$$h = (d_L - d_p)/2 \quad (5.2)$$

The ratio h/λ was taken as the measure of angularity.

Since the average number of tangents representing a given sand fraction would vary with the particle size, it is necessary to normalize the tangent counts with the possible average circumference of particles for a meaningful comparison between the different sand fractions. However for comparison between different sands, average value of the number of tangents for each sand (results averaged over all the sizes and their proportions) is a good indicator of particle angularity. Thus the particle angularity (PA) can also be expressed in terms of average number of tangents (T)

in a given sieve fraction and the average mean circumference of an equivalent circle (having the same surface area as that of the particle) as

$$PA = \frac{T}{\pi d_p} \quad (5.3)$$

where

d_p is the equivalent average mean diameter of the circle having the same surface area as that of the particle.

Results of particle angularity (PA) calculated on the above basis when plotted against the respective particle sizes (Fig. 5.1a) revealed an inverse relationship. This is in agreement with the observation by Twenhofel (1950). However, the exact nature of such a relationship for any sand would depend on its grain morphology and the distance of sediment transport. The weighted average values of particle sphericity (ψ), shape factor (SF), number of tangents and h/λ for the sands investigated are presented in Table 5.2.

5.1.3 Shape Factor Versus Sphericity

On the basis of available data a relationship between shape factor (SF) and sphericity (ψ) is indicated (Fig. 5.1b). Sands containing flaky grains show sphericity value of less than 0.68 and SF is 0.54, as compared to sands (most alluvial sands) with bulky spherical grains having $\psi > 0.74$ and SF of about .65. For sands containing elongated to bulky grains, sphericity value varies between 0.68 to 0.74. This

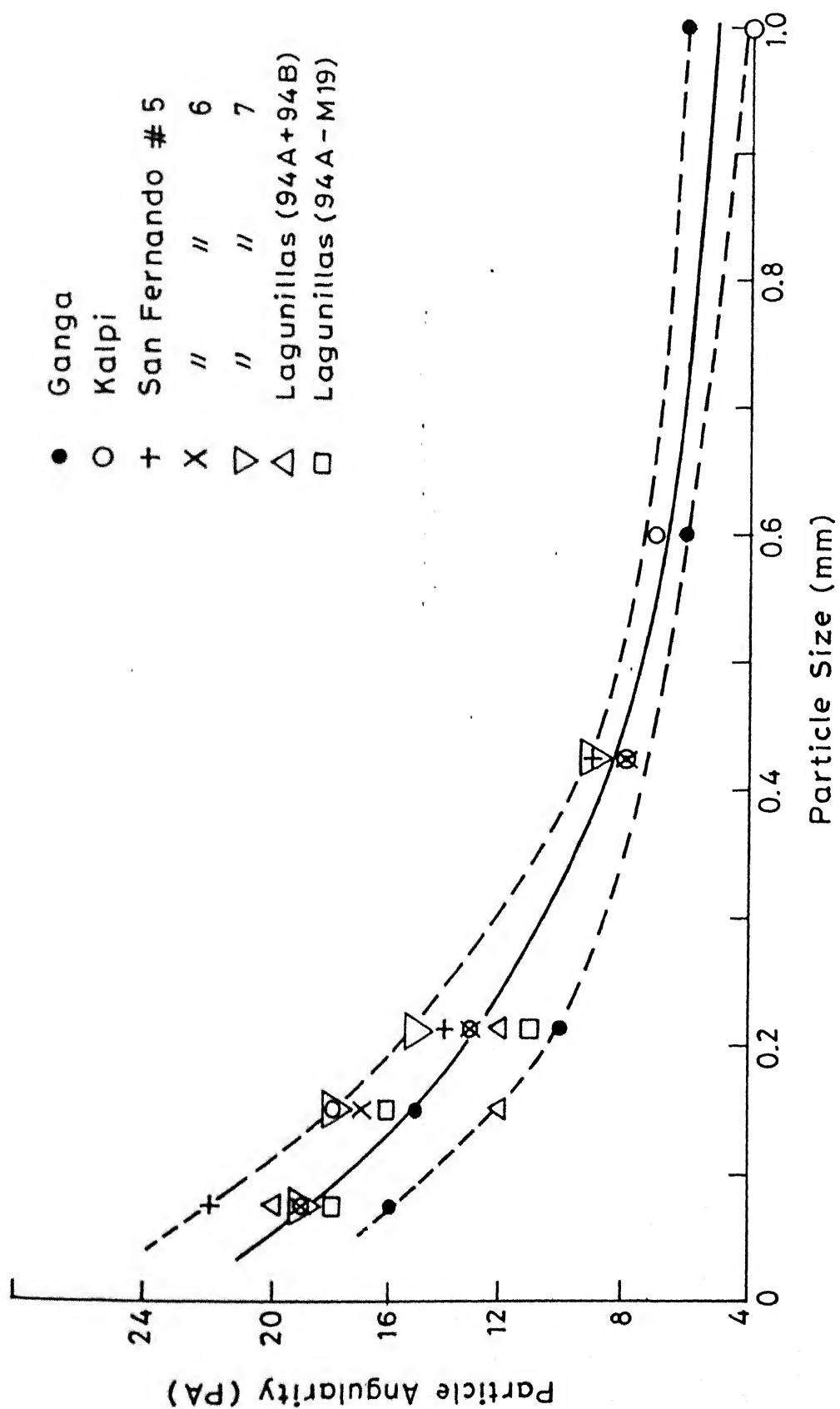
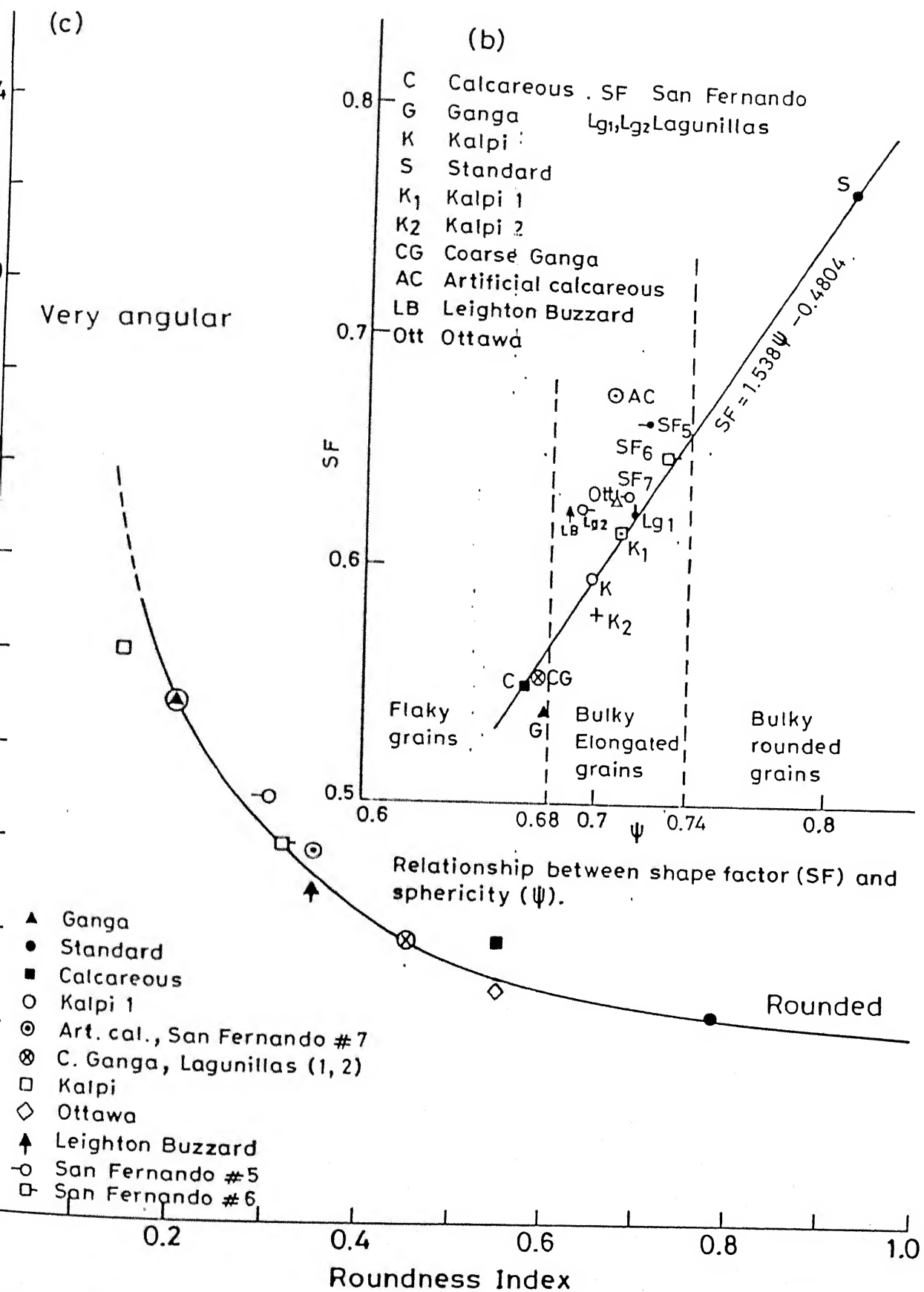


Fig. 5.1(a) Relationship between particle angularity (PA) and particle size.



9.5.1 Relationship between tangent count and roundness index.

Table 5.2 Weighted Average of Shape Factor, Sphericity, Number of Tangent, h/λ and Roundness Index

Sands	Average Shape Factor	Average Sphericity	Average Tangent	Average h/λ	Average Roundness
Standard	0.766	0.810	4	0.0465	0.78 -0.80
Kalpi	0.596	0.698	12	0.2511	0.10 -0.20
Calcareous	0.550	0.670	6	0.1218	0.50 -0.60
Ganga	0.539	0.678	11	0.2740	0.15 -0.25
Kalpi 1	0.616	0.710	10	0.3010	0.10 -0.20
Kalpi 2	0.578	0.708	13	0.3770	0.10 -0.20
Coarse Ganga	0.553	0.674	6	0.1673	0.40 -0.50
Artificial Calcareous	0.676	0.706	8	0.2281	0.30 -0.40
Lagunillas 94A - M19	0.625	0.693	6	0.1410	0.40 -0.50
Lagunillas 94A - 94B	0.624	0.715	6	0.1418	0.40 -0.50
Leighton Buzzard	0.623	0.689	7	0.1788	0.30 -0.40
San Fernando No.-5	0.663	0.722	9	0.2374	0.26 -0.35
San Fernando No.-6	0.632	0.712	9	0.2112	0.28 -0.38
San Fernando No.-7	0.648	0.731	8	0.2190	0.30 -0.40
Ottawa	0.630	0.709	5	0.0820	0.50 -0.60

data, a reliable method is developed to compute the Powers' roundness index which can be used to classify the sand according to their angularity (Table 2.2).

5.1.5 Distribution of Tangents

Distribution of tangents representing protrusions on the grain surface was studied in great detail. Data were obtained for different sieve sizes and a weighted average distribution curve was evaluated for each sand. Figures 5.2 to 5.5 show the results for Standard, Calcareous, Ganga and Kalpi sand respectively.

In case of Standard sand (Fig. 5.2), more than 70% of the grains indicate 4 tangents (which is taken as a measure of perfect roundness in this study). This in conjunction with the earlier observation that more than 80% of grains are spherical (Table 5.1) would suggest that Standard sand consists of smooth, rounded and spherical particles. In case of Calcareous sand, 47% of grains have smooth surface with 4 and 5 tangents (Fig. 5.3). This finding along with the earlier observation (Table 5.1) would suggest that this sand consists of subrounded, smooth, flaky and oblate particles, which is a good description of the shells comprising this materials. In case of Ganga sand only around 12% of the particles are having smooth surfaces (Fig. 5.4), the remaining having number of tangents varying from 6 to 17; some particles have as high as 24 to 33 tangents. These results along with the findings related to sphericity and

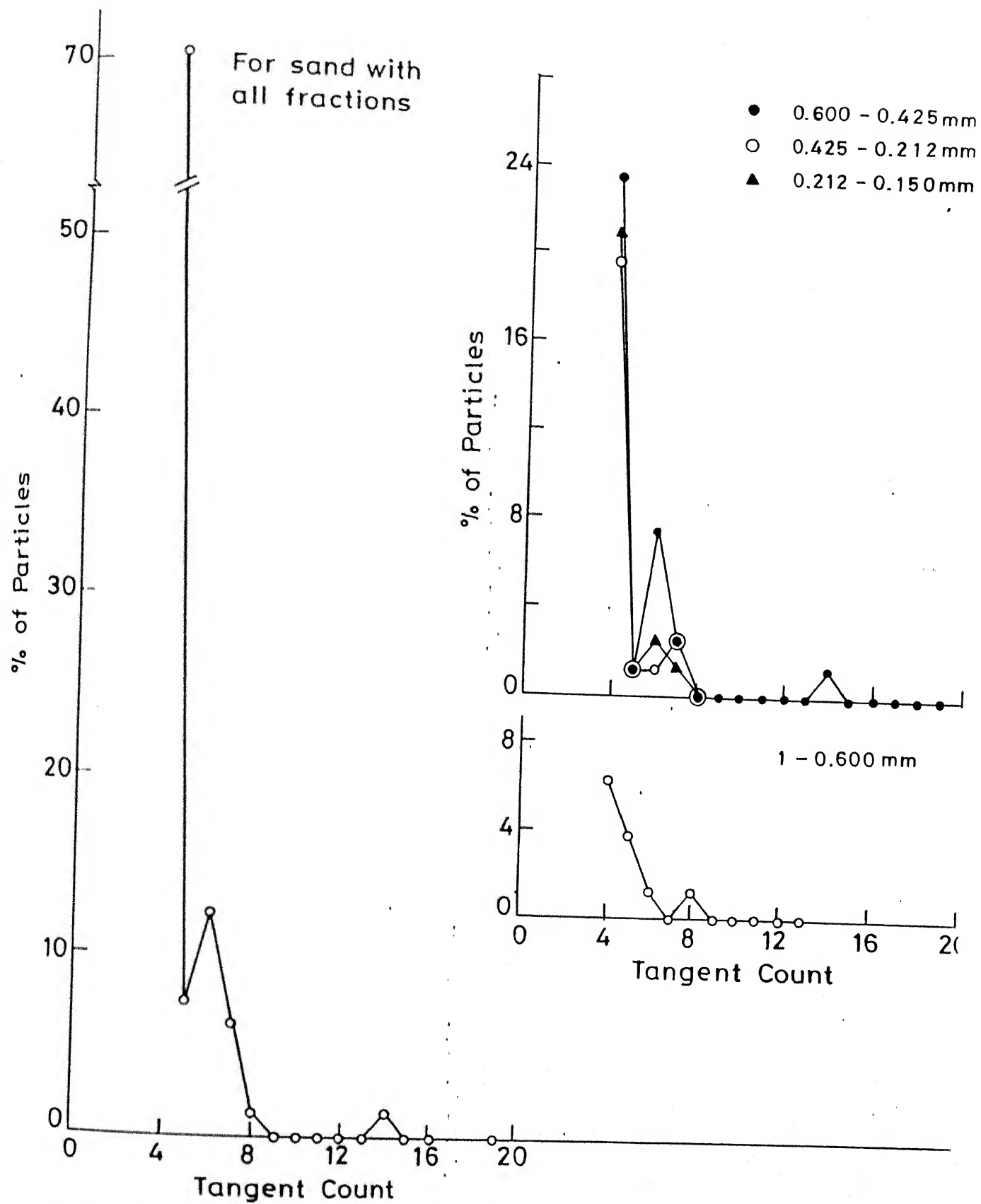


Fig. 5.2 Tangent count distribution for Standard sand.

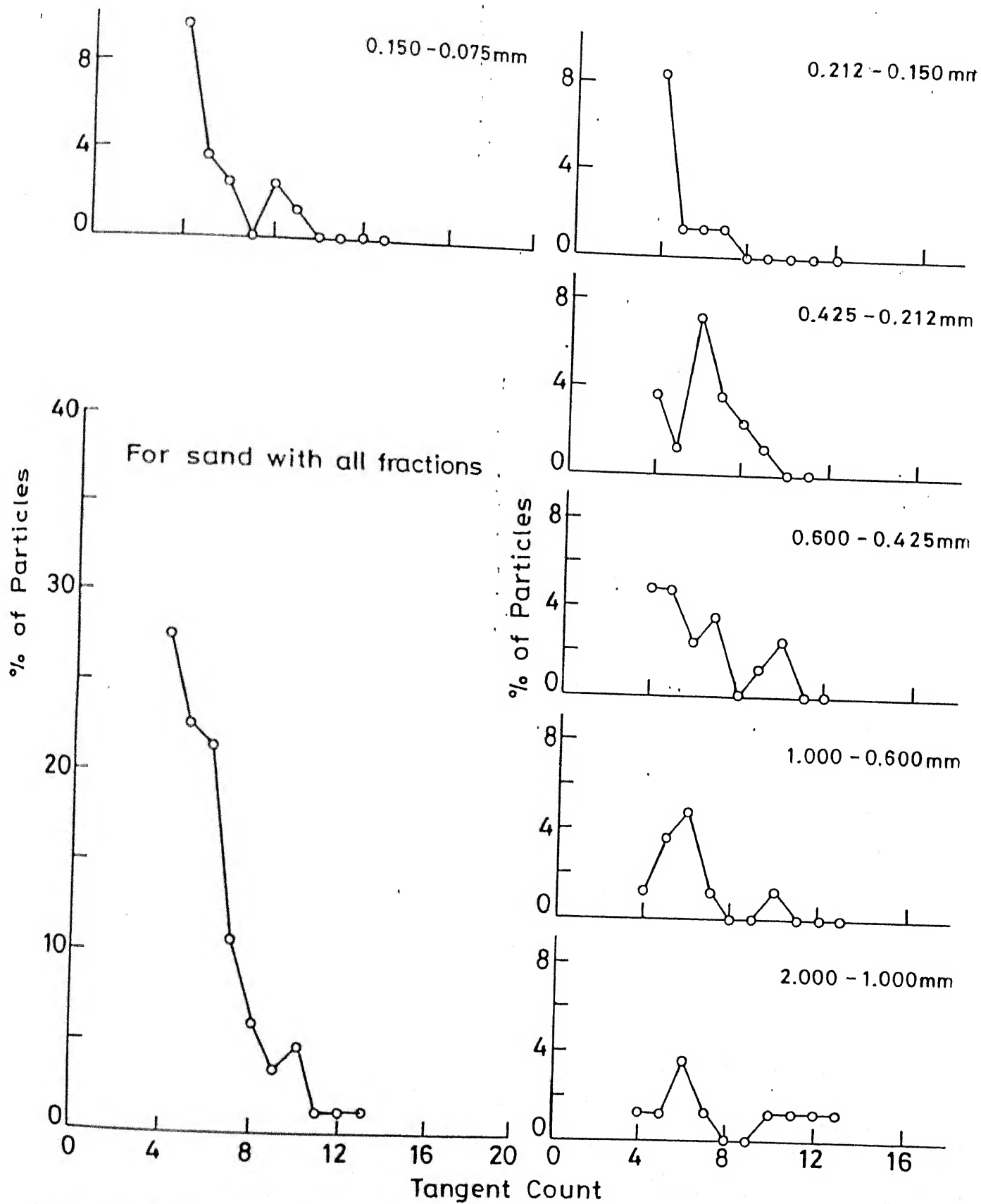


Fig. 5.3 Tangent count distribution for calcareous sand.

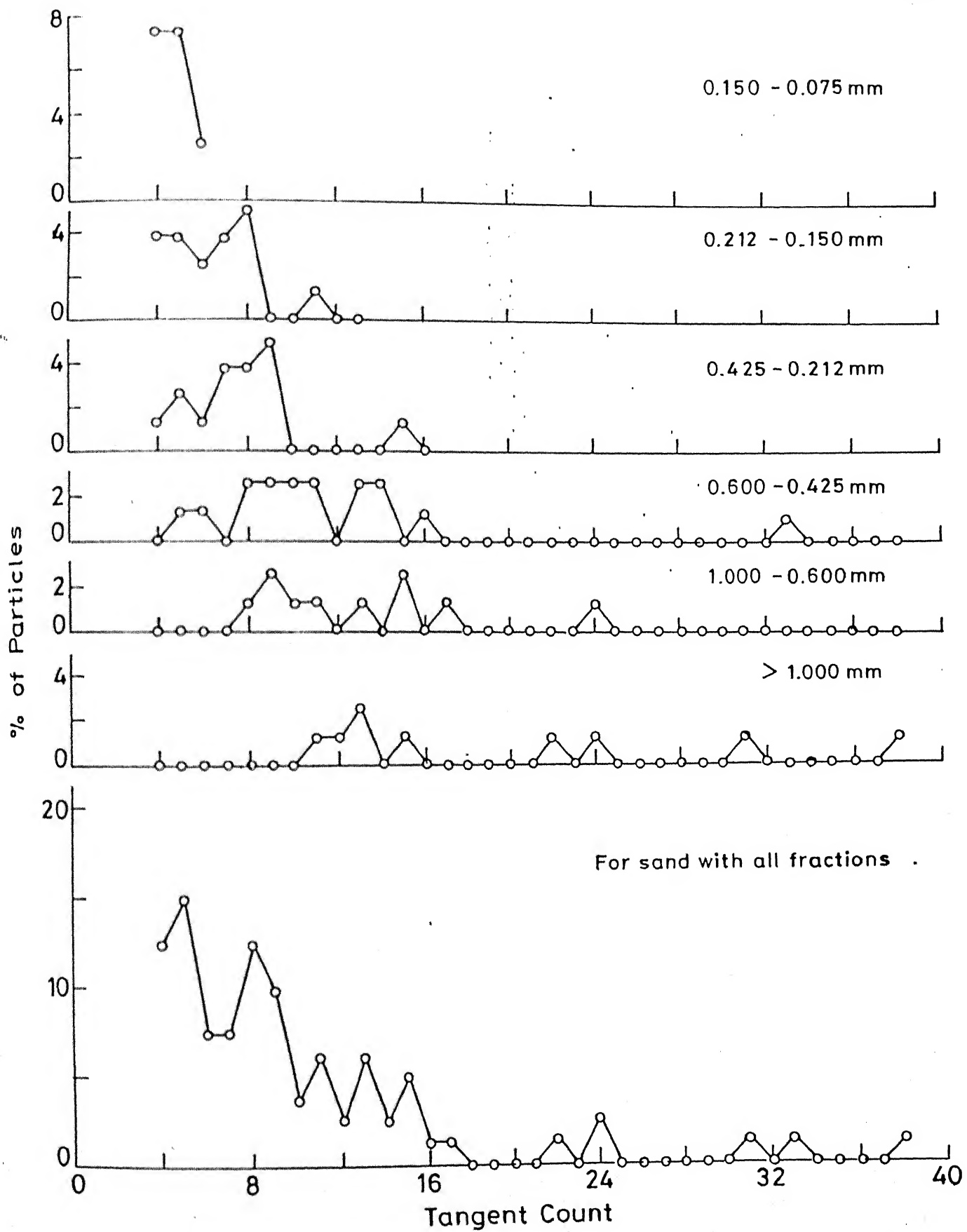


Fig. 5.4 Tangent count distribution for Ganga sand.

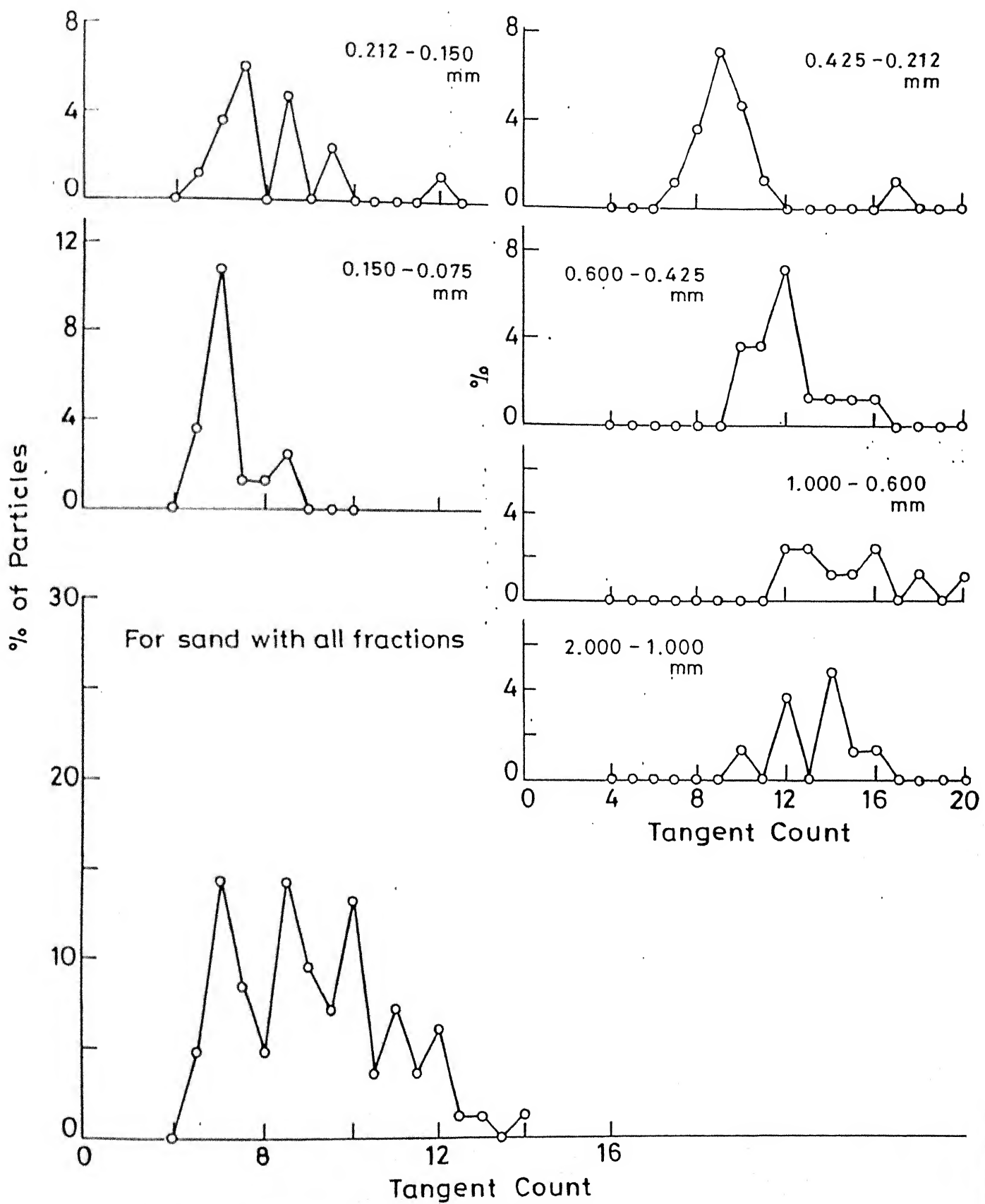


Fig. 5.5 Tangent count distribution for Kalpi sand.

shape factor would suggest that Ganga sand has angular, oblate and flaky grains.

Kalpi sand as indicated in Chapter 3, is distinctly different from others in more than one way in respect of short distance of sediment transport from the source and also the formation of carbonate on the sand grains by the circulating ground water. This sand shows quite an unique distribution of tangents with a total absence of any grains with four tangents (absence of smooth grains). Around 45 % grains show 6 to 12 tangents and 10% of grains reflect as high as 12 to 16 tangents (Fig. 5.5). Two fractions of this sand, called Kalpi 1 and Kalpi 2, were also investigated for angularity characteristics. The results presented in Figs. 5.6 and 5.7 indicate that roughly 50% of the grains show 14 to 18 tangents for Kalpi 2 sand.

These angularity characteristics along with the earlier results on sphericity and shape factor would indicate that Kalpi sand grains are highly angular, bulky and elongated in nature.

Results for two artificially prepared sands, viz. coarse Ganga and artificial Calcareous are shown in Figs. 5.8 and 5.9. In case of coarse Ganga the major component is Calcareous, and the tangent distribution shown in Fig. 5.8 agrees with the pattern shown for Calcareous sand (Fig. 5.3). Similarly, the tangent count distribution for artificial calcareous sand is influenced by the patterns of its components, viz., Standard, Kalpi and Ganga sands.

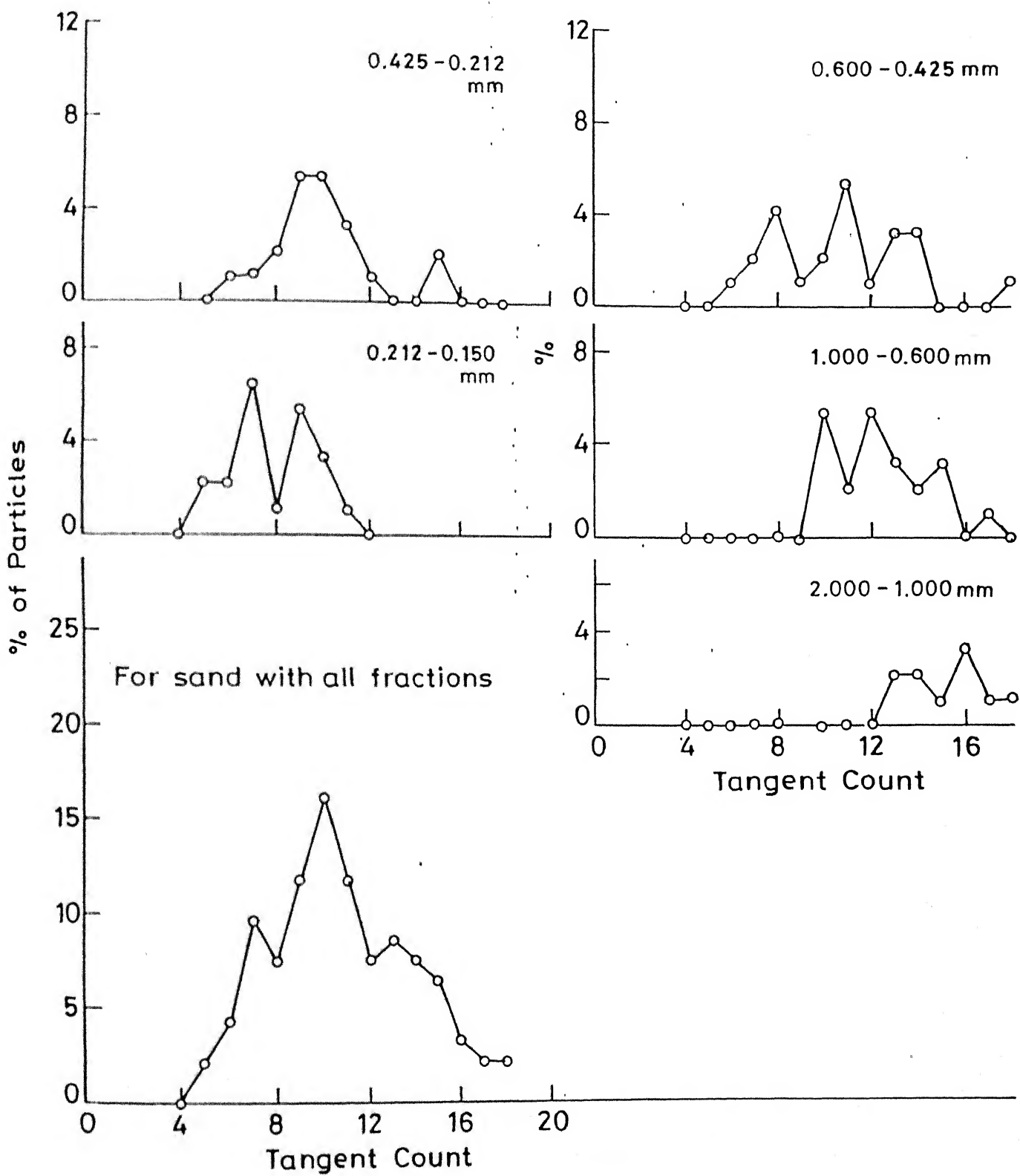


Fig. 5.6 Tangent count distribution for Kalpi 1 sand.

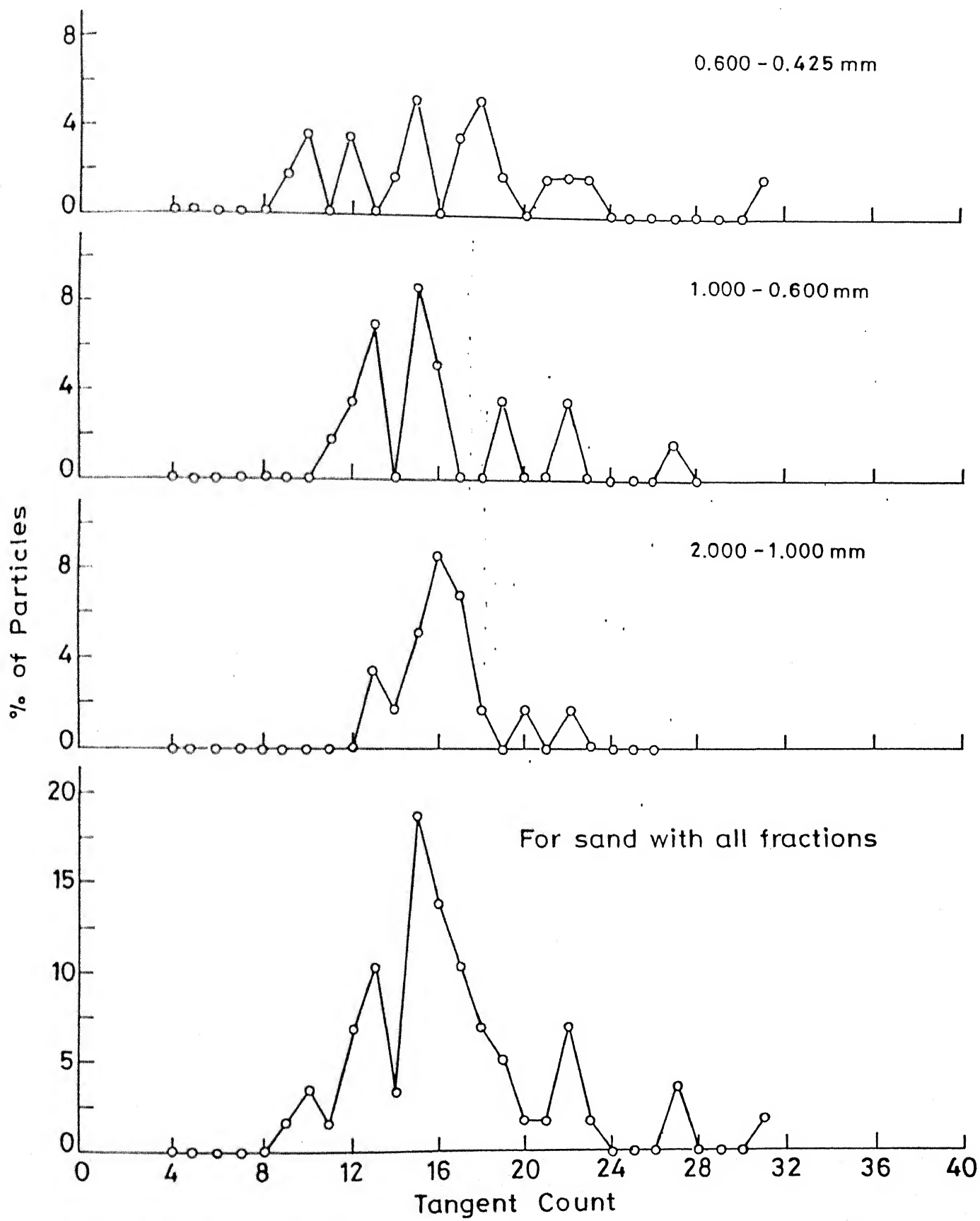


Fig. 5.7 Tangent count distribution for Kalpi 2 sand.

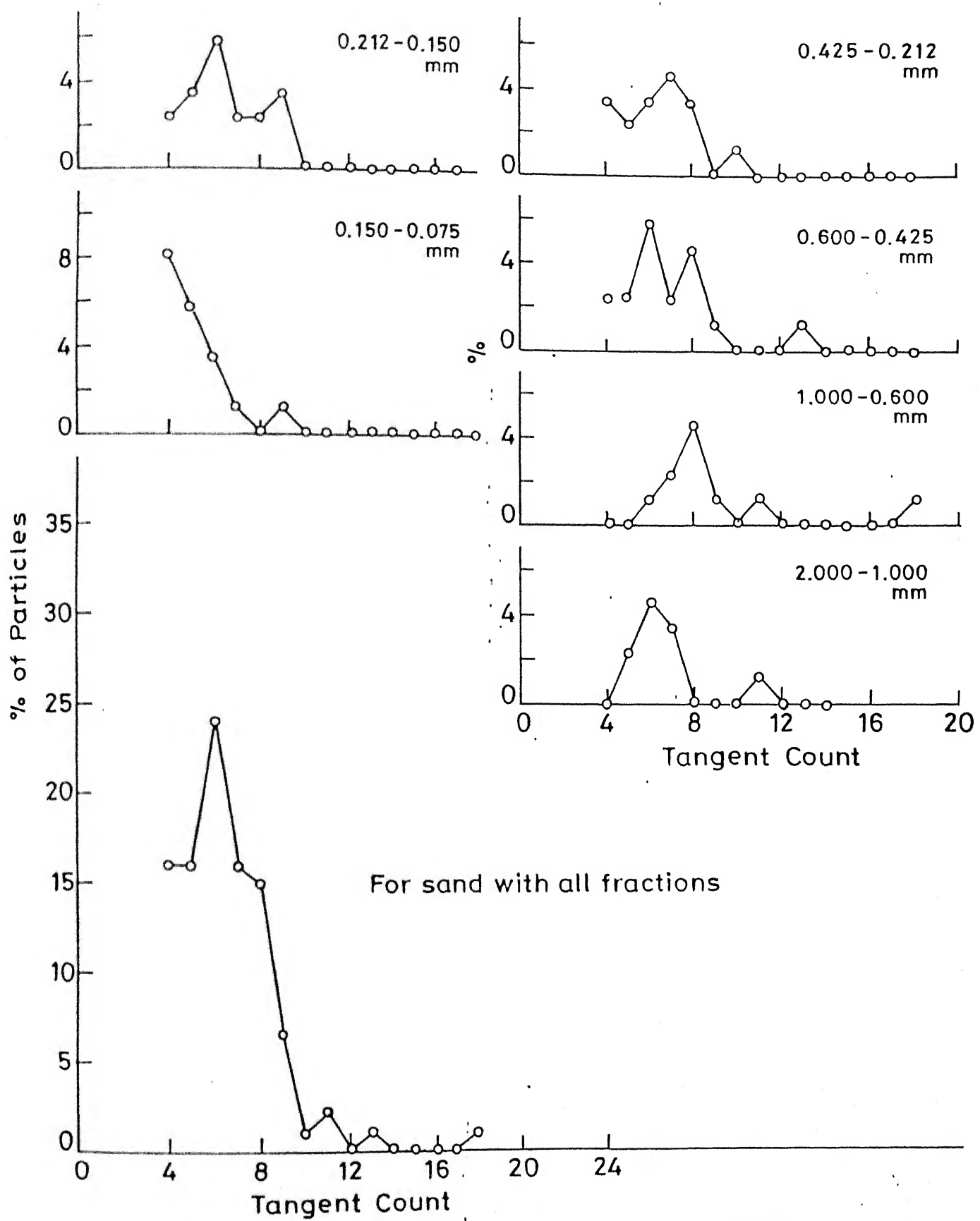


Fig. 5.8 Tangent count distribution for Coarse Ganga sand.

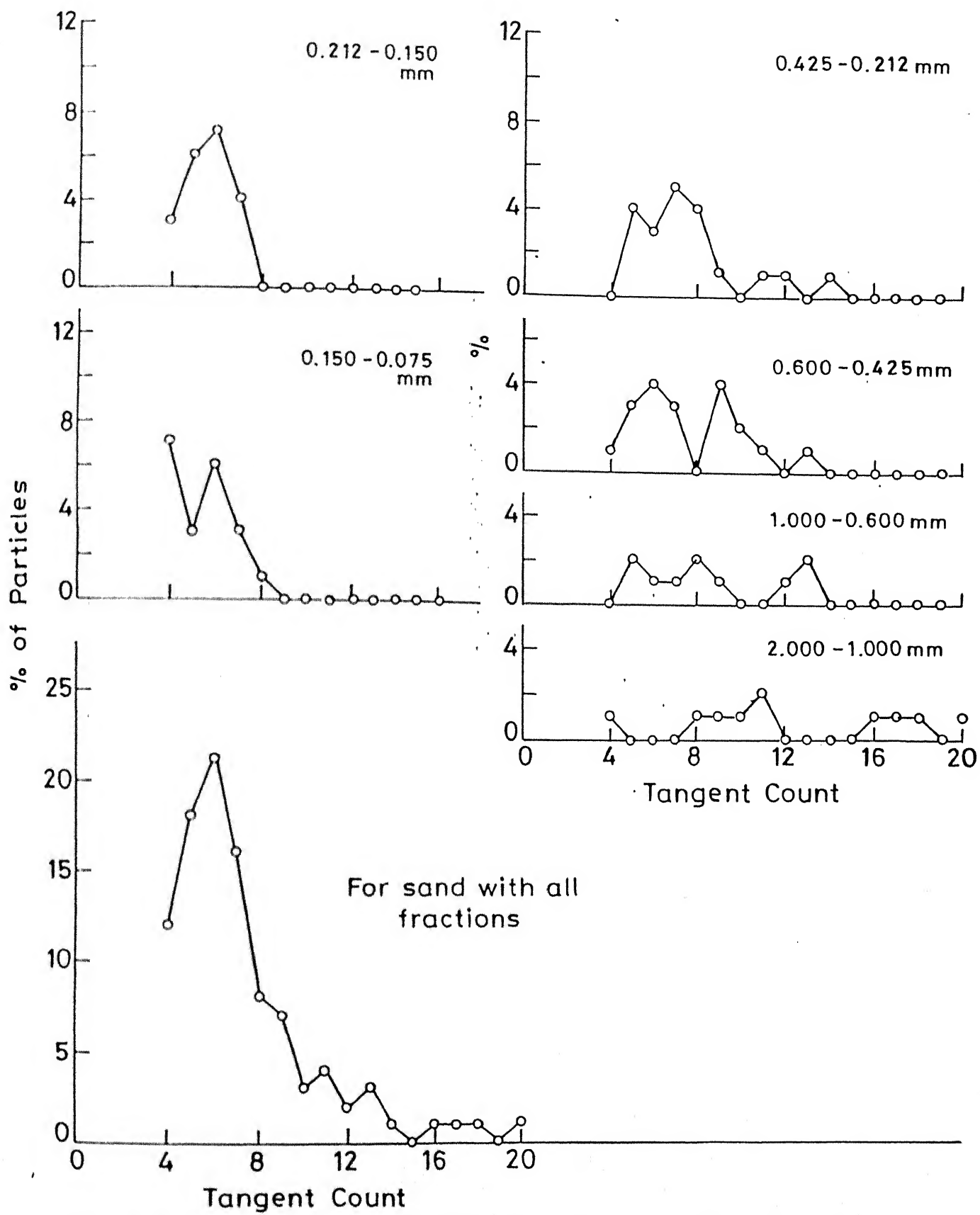


Fig. 5.9 Tangent count distribution for Artificial calcareous sand.

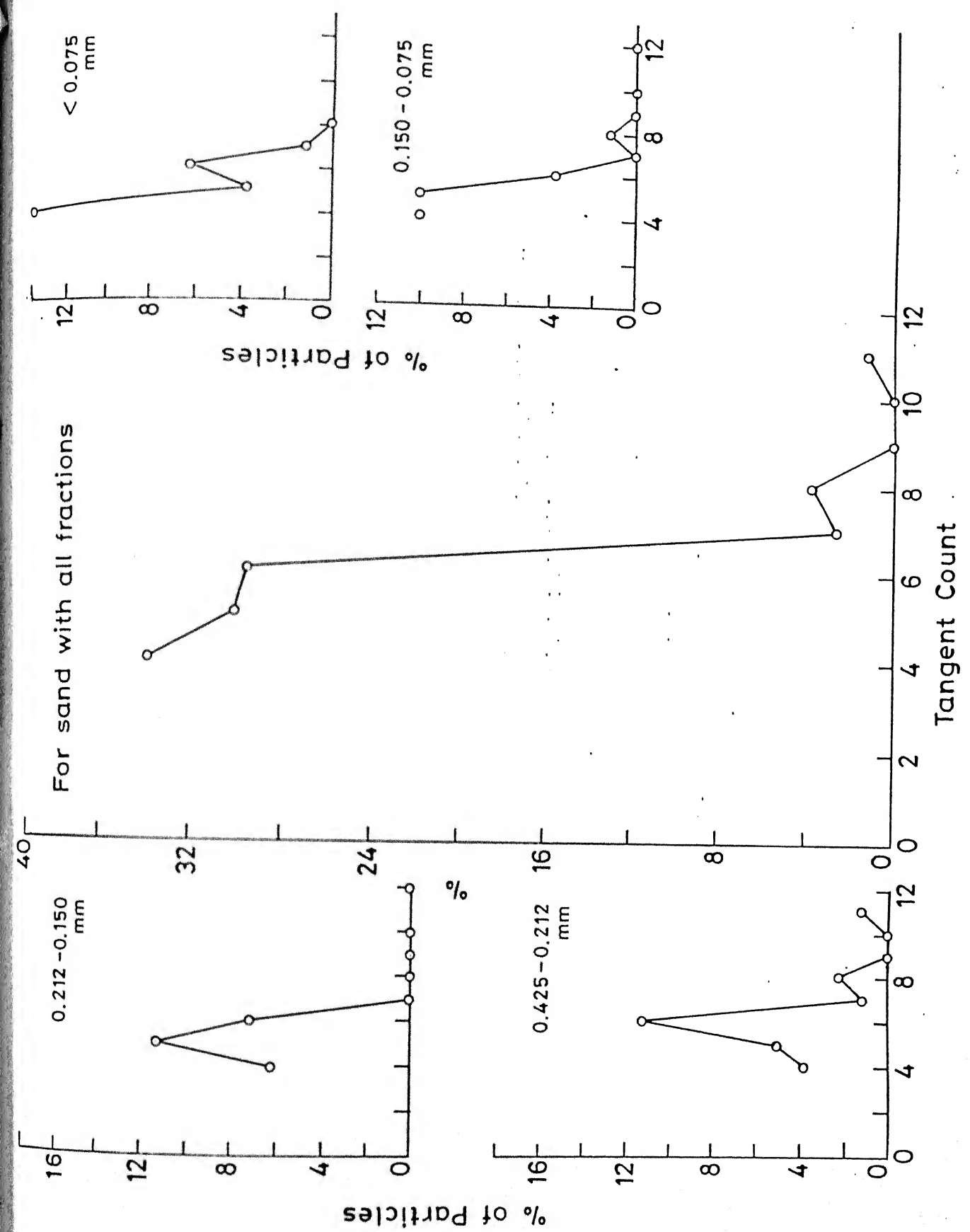


Fig. 5.10 Tangent count distribution for Ottawa sand.

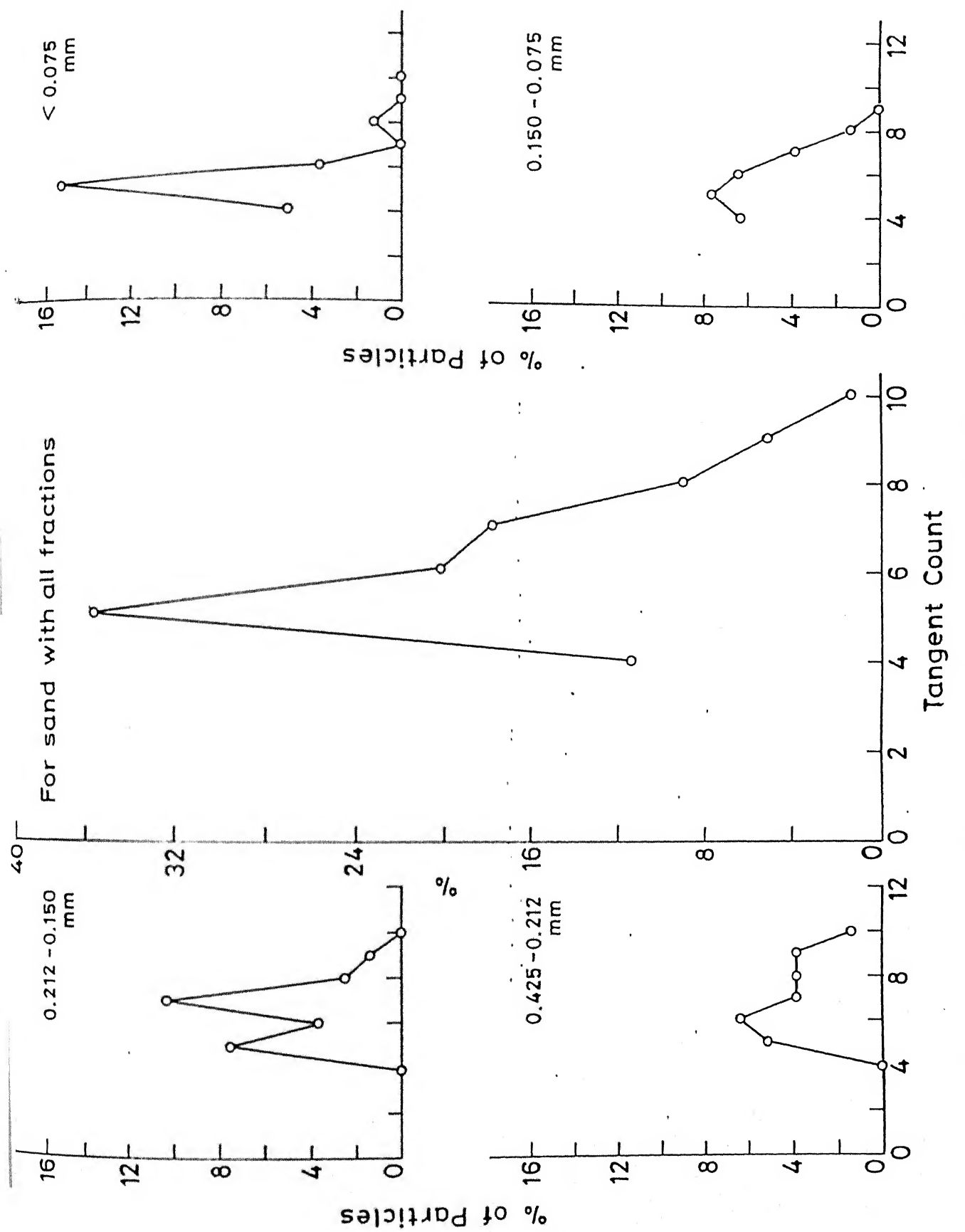


Fig. 5.11 Tangent count distribution for Leighton Buzzard sand.

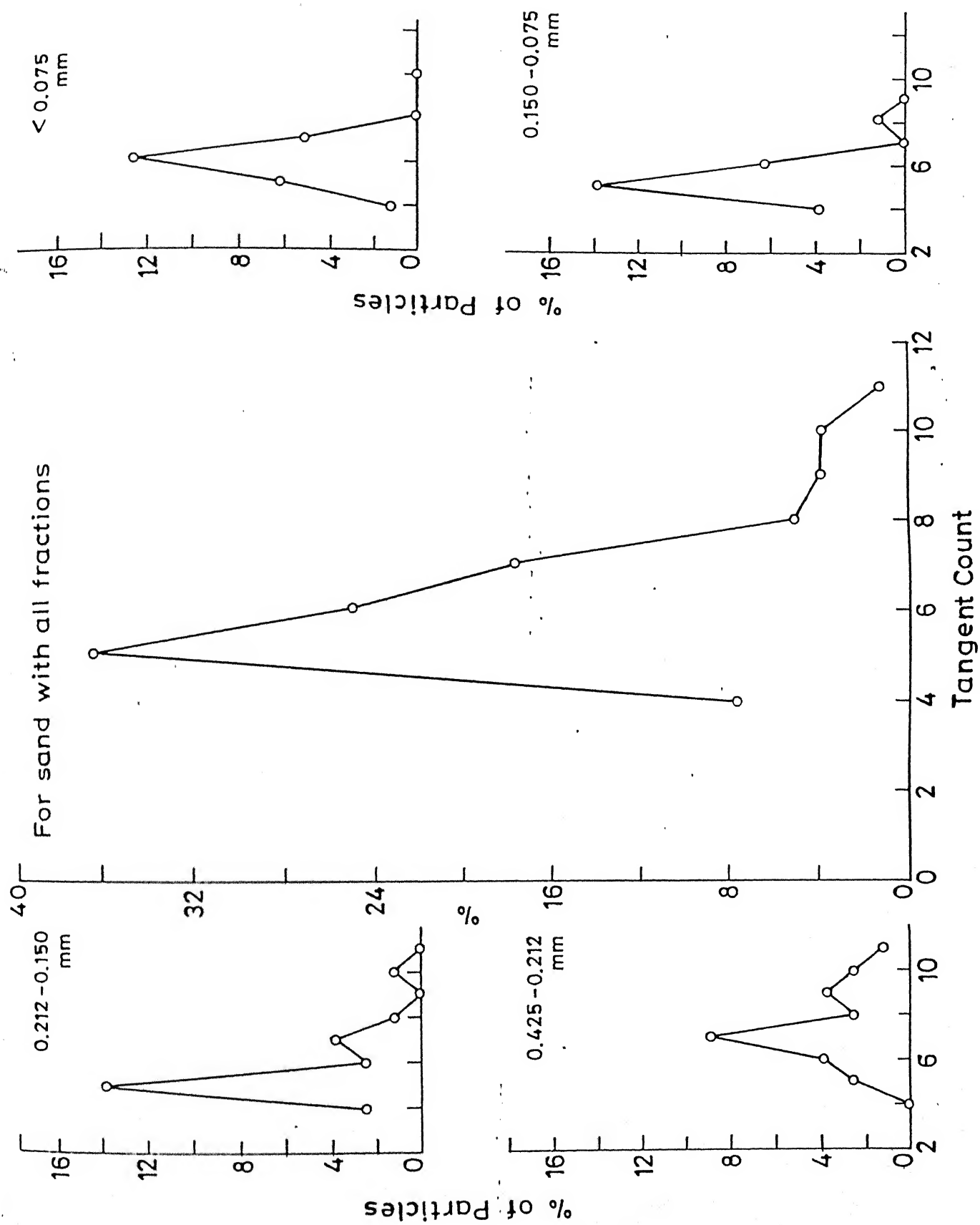


Fig. 5.12 Tangent count distribution for Lagunillas (94A-M18) sand.

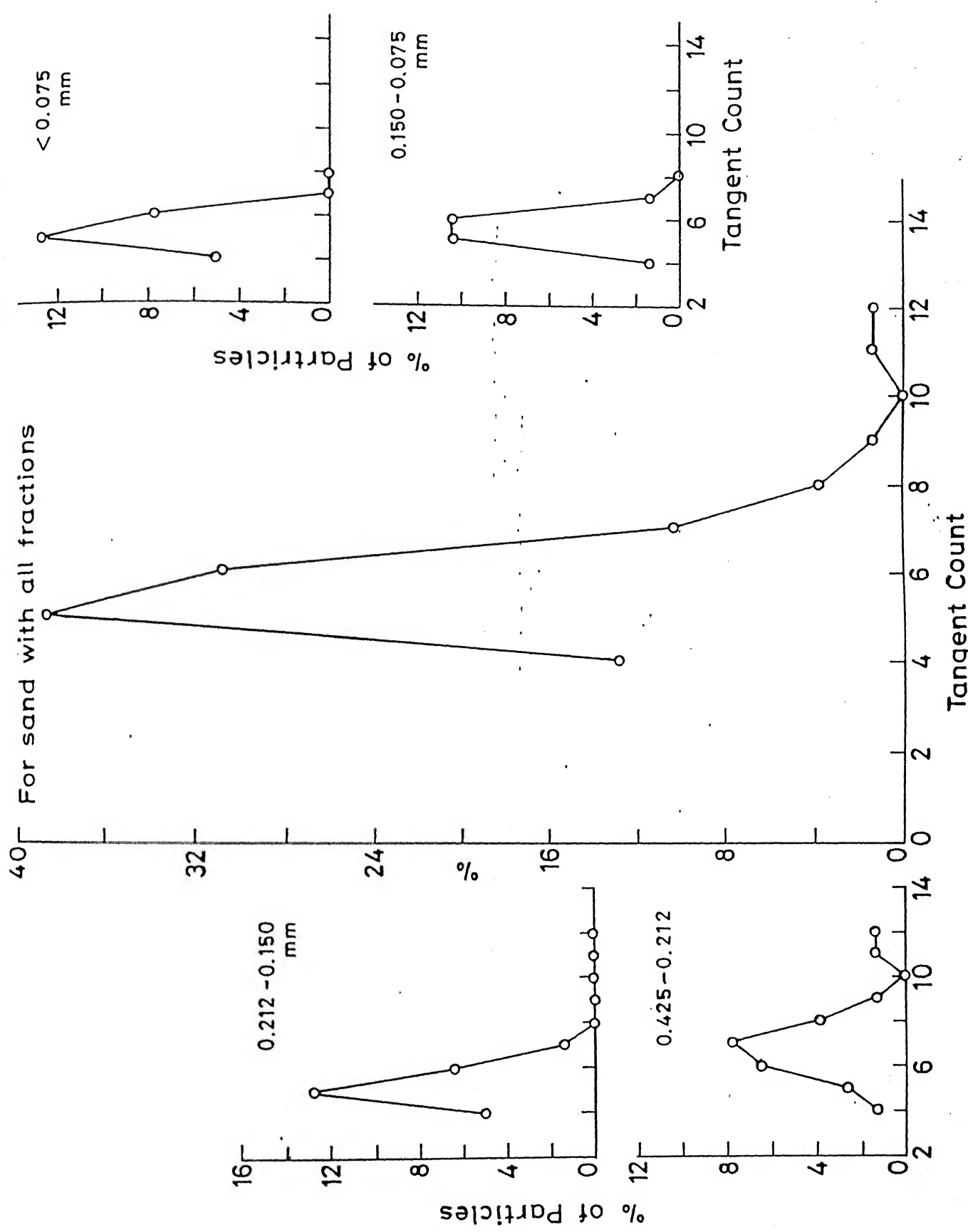


Fig. 5.13 Tangent count distribution for Lagunillas (94A + 94B).

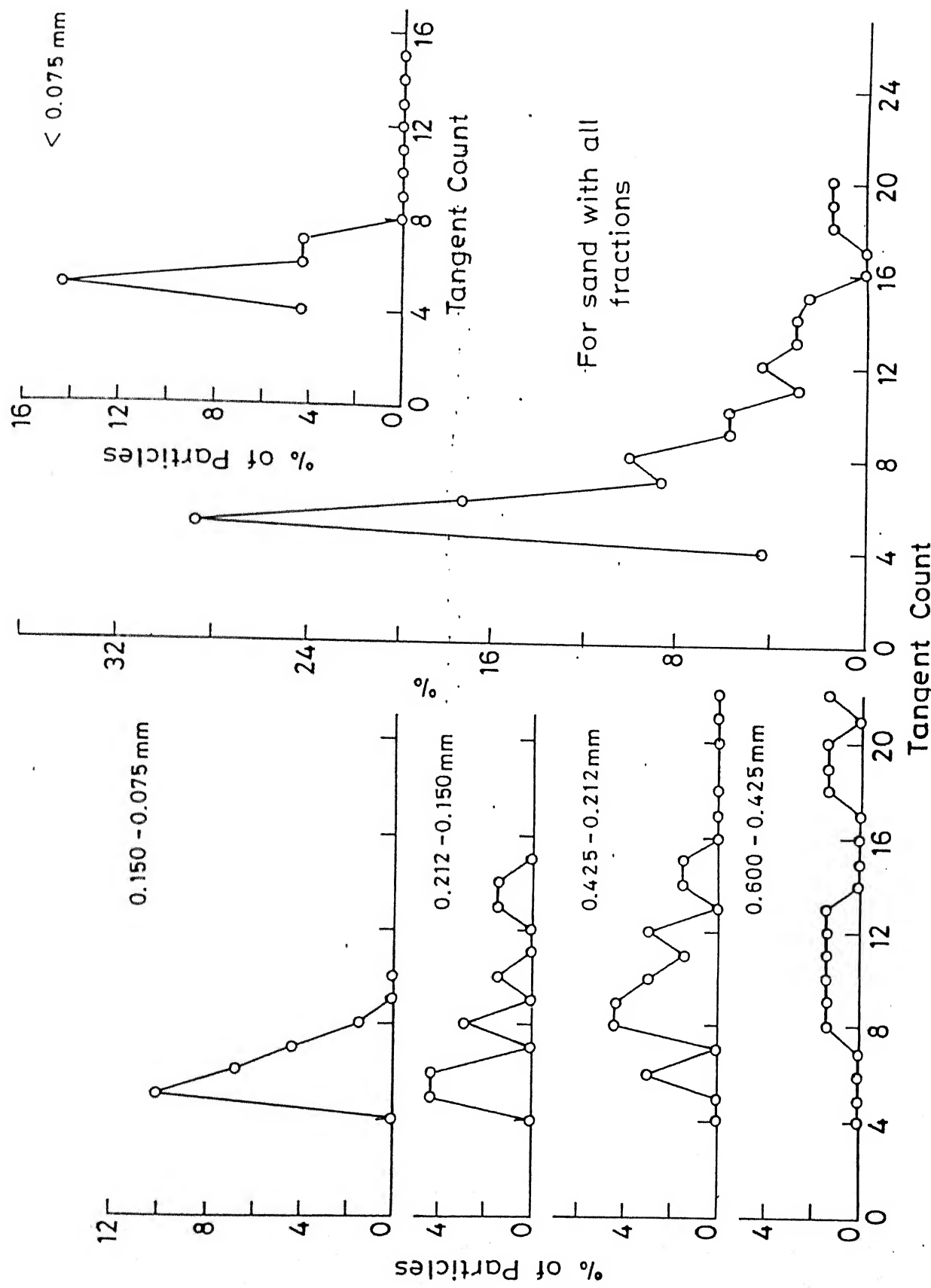


Fig. 5.14 Tangent count distribution for San Fernando mix # 5 sand.

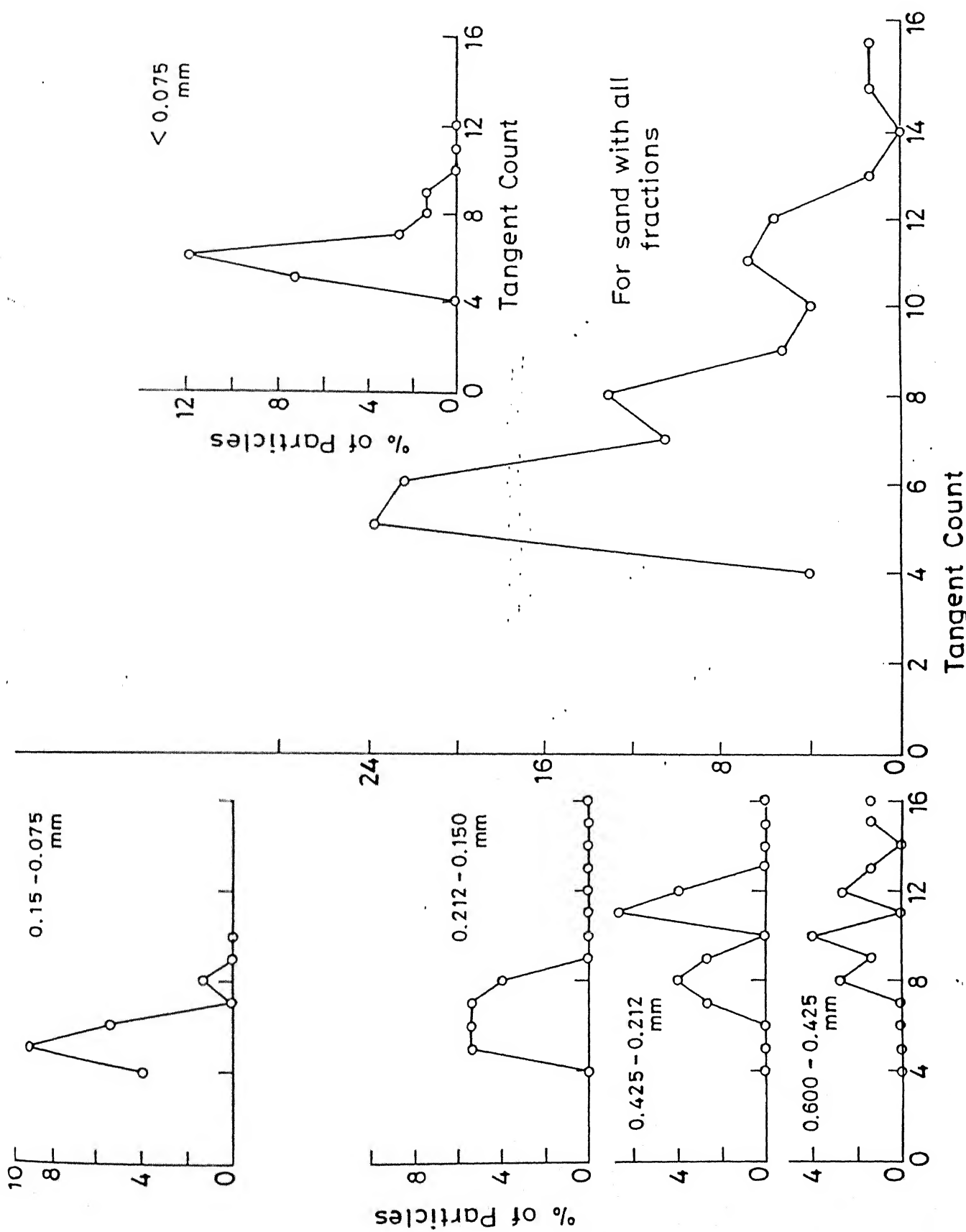


Fig. 5.15 Tangent count distribution for San Fernando mix #6 sand.

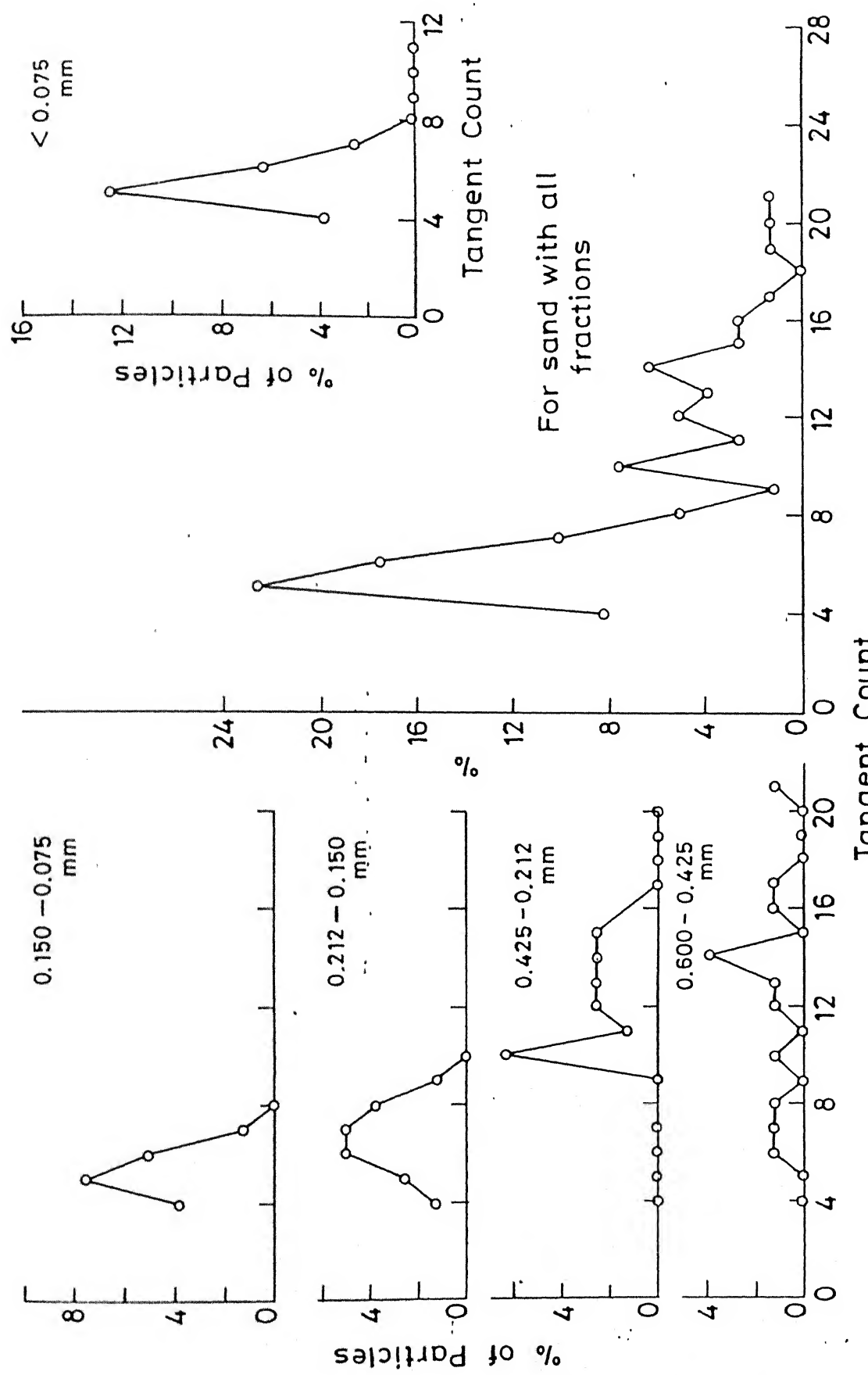


Fig. 5.16 Tangent count distribution for San Fernando mix #7 sand.

1. Subrounded to rounded grains (Fig.5.17a)
2. Subrounded to subangular (Fig.5.17b)
3. Subangular to angular (Fig.5.18a)
4. Very angular (Fig.5.18b)

These distributions are suggested as typical examples of sands with varying degrees of angularity. It is further suggested that the nature of tangent count distribution pattern may be used for the purpose of classification of sands on the basis of shape characteristics. Since the tangent count is inversely related to the roundness index (R) (Fig. 5.1c), it is also possible to construct similar distribution patterns for different sands, in terms of roundness index (R).

5.1.7 Main Observations

Study on particle morphology reported here leads to the following observations:

On the basis of Zingg diagram and the shape factor versus sphericity relationship, sands can be classified with respect to the grain shape.

The tangent count technique using the image analyzer provides an accurate and highly reliable method to quantify the particle shape characteristics. Typical tangent distributions for subrounded to rounded, subangular, angular and very angular grains have been developed and are recommended as a useful tool for classification of sands in respect of grain angularity.

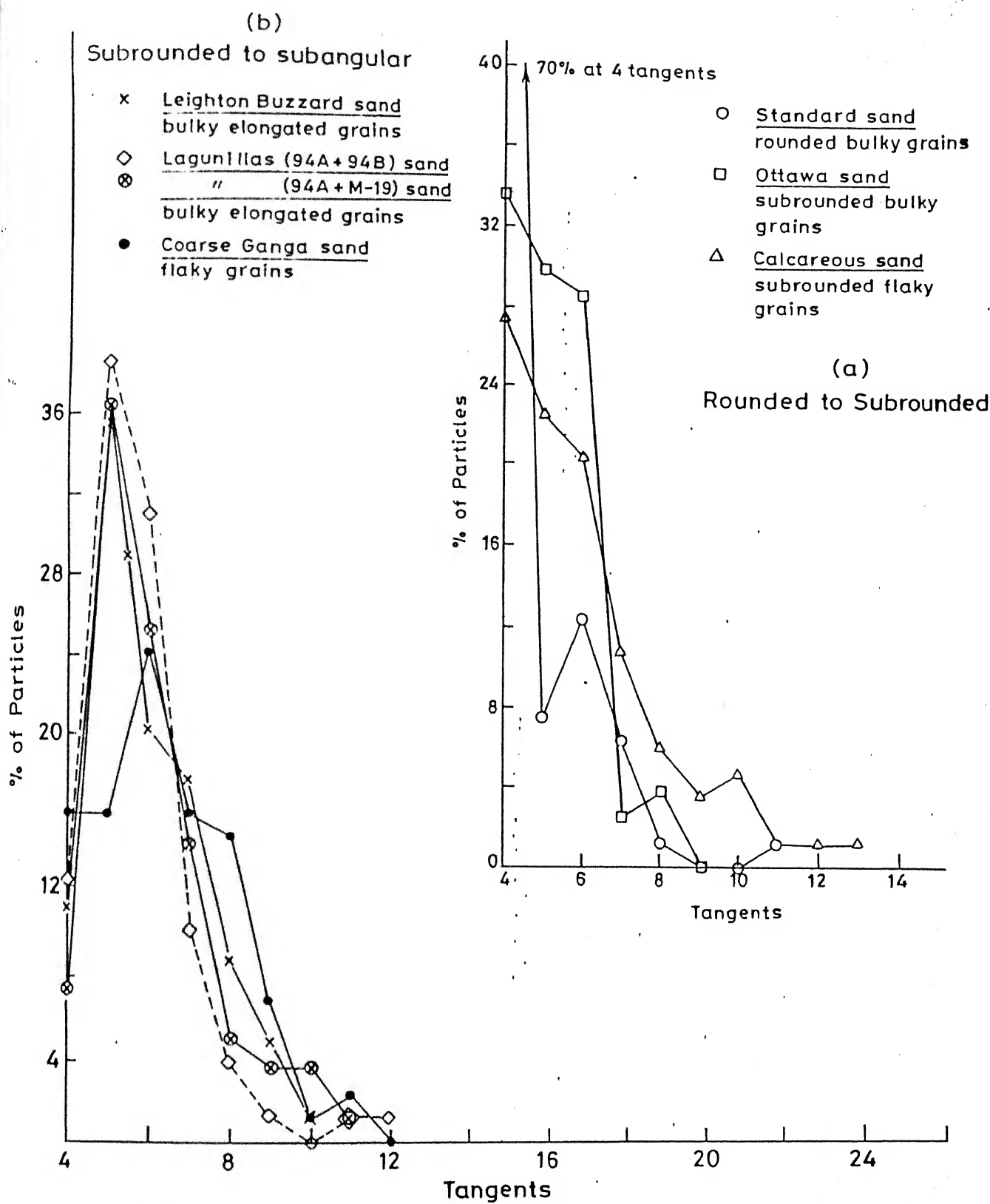


Fig. 5.17 Typical distribution of surface characteristics for subrounded to rounded and subangular to subrounded sands.

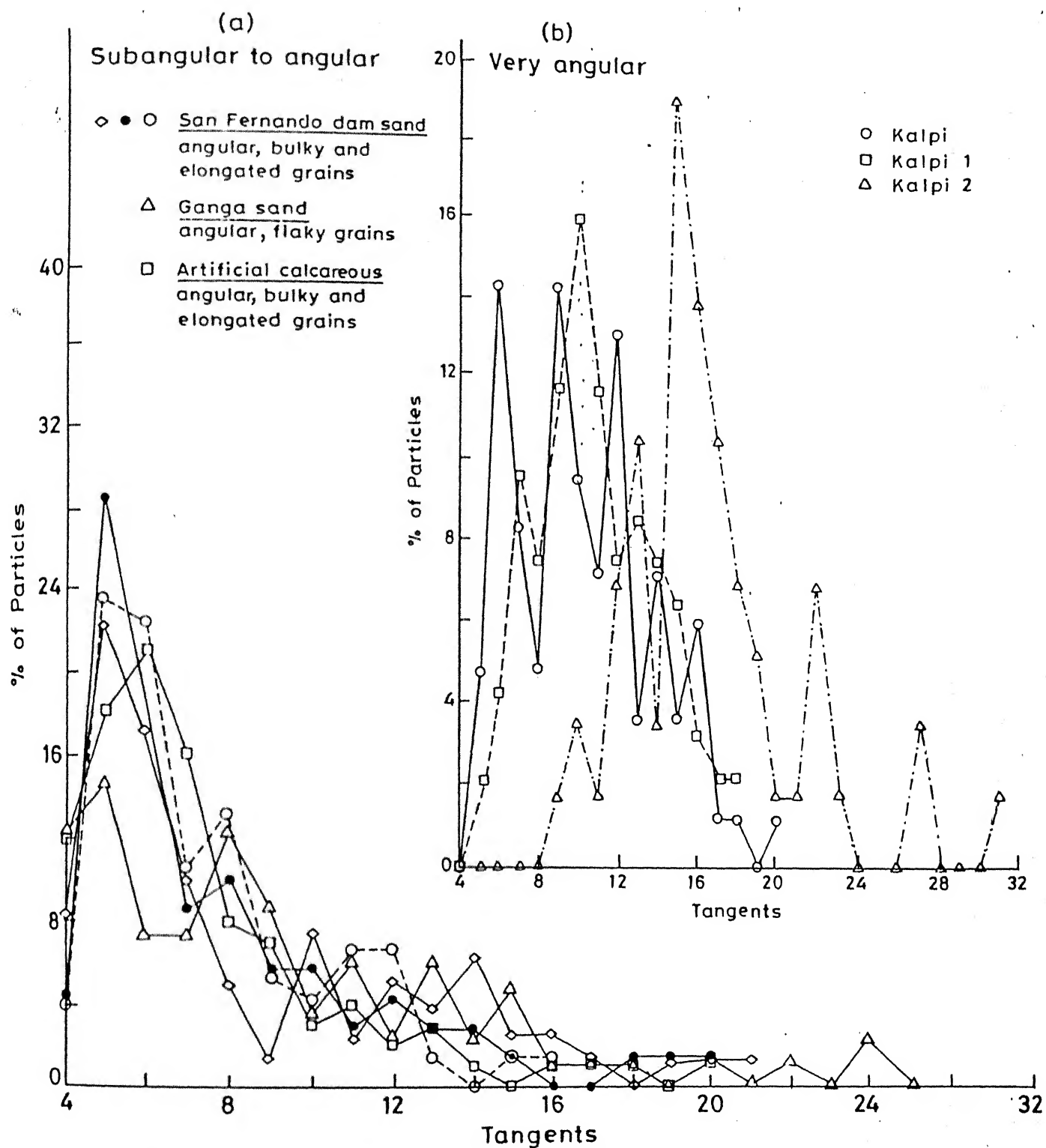


Fig. 5.18 Typical distribution of surface characteristics for angular and very angular sands.

The tangent count has been employed to provide a systematic method for evaluation of Powers' roundness index. An inverse relationship between average tangent count and roundness index (R) has been established.

It has also been shown that while average tangent count is useful for comparing sands having grains of different angularity, the particle angularity

average number of tangents in a sieve fraction
($PA = \frac{\text{average number of tangents in a sieve fraction}}{\text{average circumference of the particles in that fraction}}$)
is a good measure of variation of angularity with particle size for a given sand. Particle angularity for alluvial sands is shown to decrease with increase in grain size.

On the basis of these observations it is recommended that in addition to the usual classification tests for sands, the shape and angularity characteristics of sand grains should also be evaluated using the techniques and methodology as detailed in the present study.

5.2 PARTICLE MODIFICATION AND CRUSHING DURING COMPRESSION

5.2.1 General

Sands unlike clays undergo changes in grain shape and size during compression. The degree of alteration of the grains depends upon the mineralogy, size, gradation, angularity and stress level applied. While sufficient data on particle crushing under high stresses are available in literature (Hardin, 1985), very limited information is

reported on the degree of particle modification. In the present study, experiments were planned to attain a better understanding of the factors controlling particle modification during compression. A wide range of sands with different mineralogical composition, particle shape, size and gradation were studied. In this study, the overall sand particle breakage under stress has been separated into two components, viz. grain modification and grain crushing (changes in grain shape and size). Grain modification envisages breakage of angular surface protrusions at stress levels far less than that required for grain crushing. Such a modification would result in smoothening of particle boundaries (reducing the number of tangents) whereas subsequent grain crushing at higher stresses would again produce angular grain (increasing the number of tangents).

5.2.2 Modifications of Size and Shape of Grains

The potential for the grain modifications in terms of size and shape alterations including the crushing is best demonstrated through the study of changes in grain size distribution curves of a sand before and after testing. Hardin (1985) proposed the calculation of breakage potential (designated as B_p) for particle degradation on the basis of the area of grain size gradation curve for sizes greater than 0.074 mm, (Fig. 5.19 a). This parameter reflects the total potential for change of grain shape and size under stress for a given sand and includes both the potential modification and

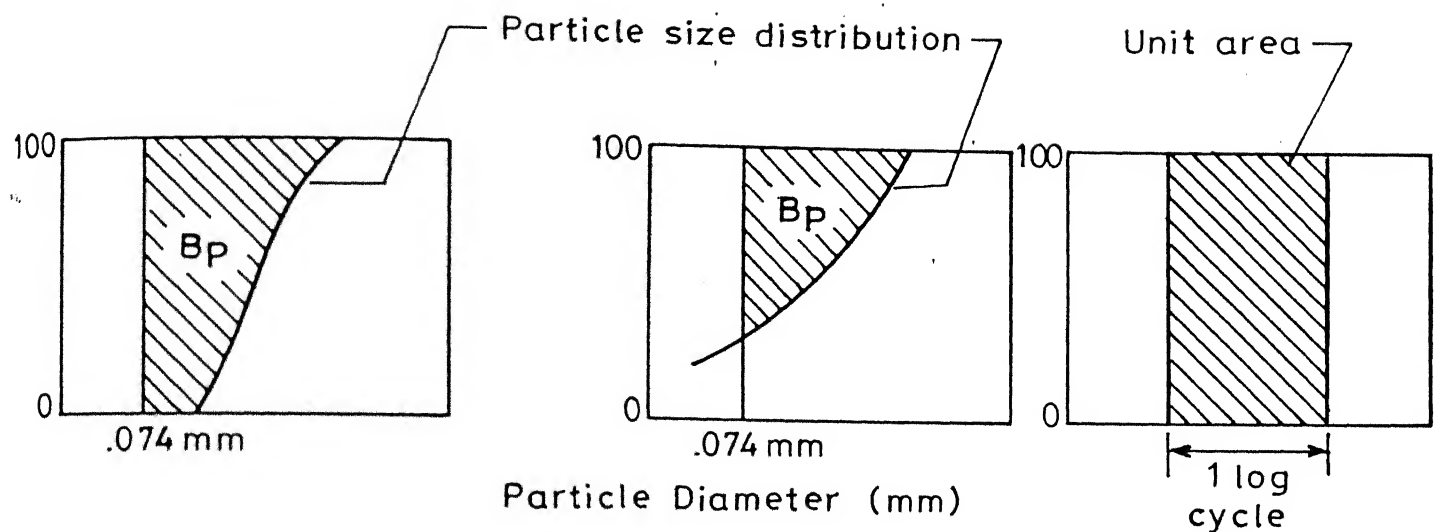


Fig. 5.19(a) Definition of breakage potential.

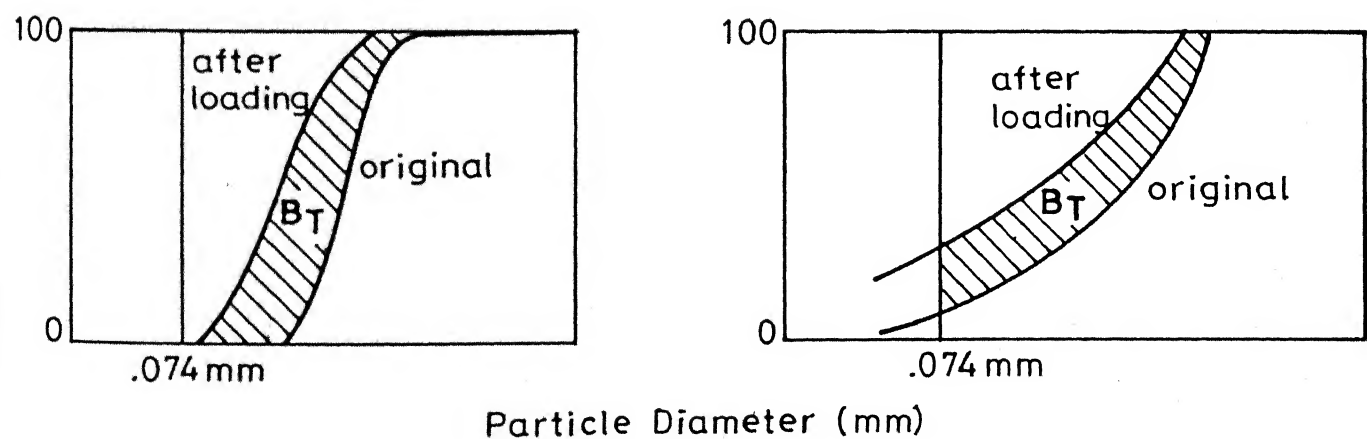


Fig. 5.19(b) Definition of total breakage.

crushing. The grain size curves for the sands studied (Fig. 5.20) and those reported in literature (Fig. 5.21) have been used to estimate B_p . The values of B_p along with the average particle size and coefficient of uniformity values of the respective sands are listed in Table 5.3. The relationship between B_p and the average grain size d_{50} has been developed (Fig. 5.22) on the basis of these estimations. Data from literature have been used to extend the range of d_{50} values, to test the validity of the proposed relationship. The relationship, tested for sands with a wide range of gradation curves, indicates that B_p is uniquely related to the average particle size (d_{50}). It may be indicated here that this relationship has not been tested for gap graded sands. In practice, for most of the sands, the value of B_p may therefore be estimated on the basis of d_{50} (in mm) as obtained from the sieve analysis by using the expression:

$$B_p = 1.02 \log (d_{50}) + 1.15 \quad (5.5)$$

The above simplified expression enables an estimation of B_p as a preliminary measure without undertaking the detailed area estimates of the grain size curves.

5.2.3 Particle Breakage

Hardin (1985) used a term B_T to define the difference in area under the gradation curves before and after loading (Fig. 5.19b) as a measure of total particle breakage comprising of changes in grain shape and/or shape and size,

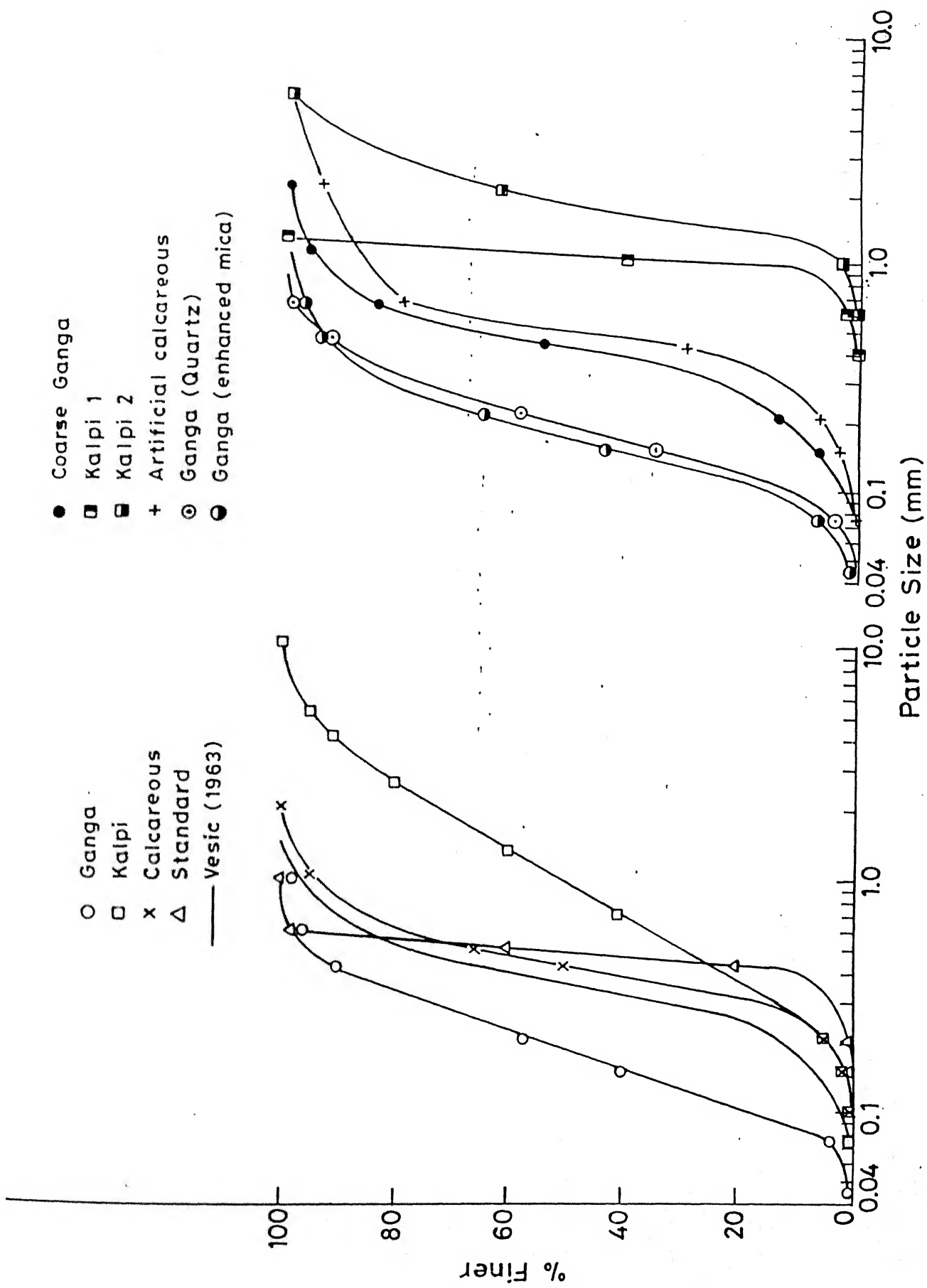


Fig. 5.20 Grain size distribution of different sands used for calculating total potential crushing (B_p)

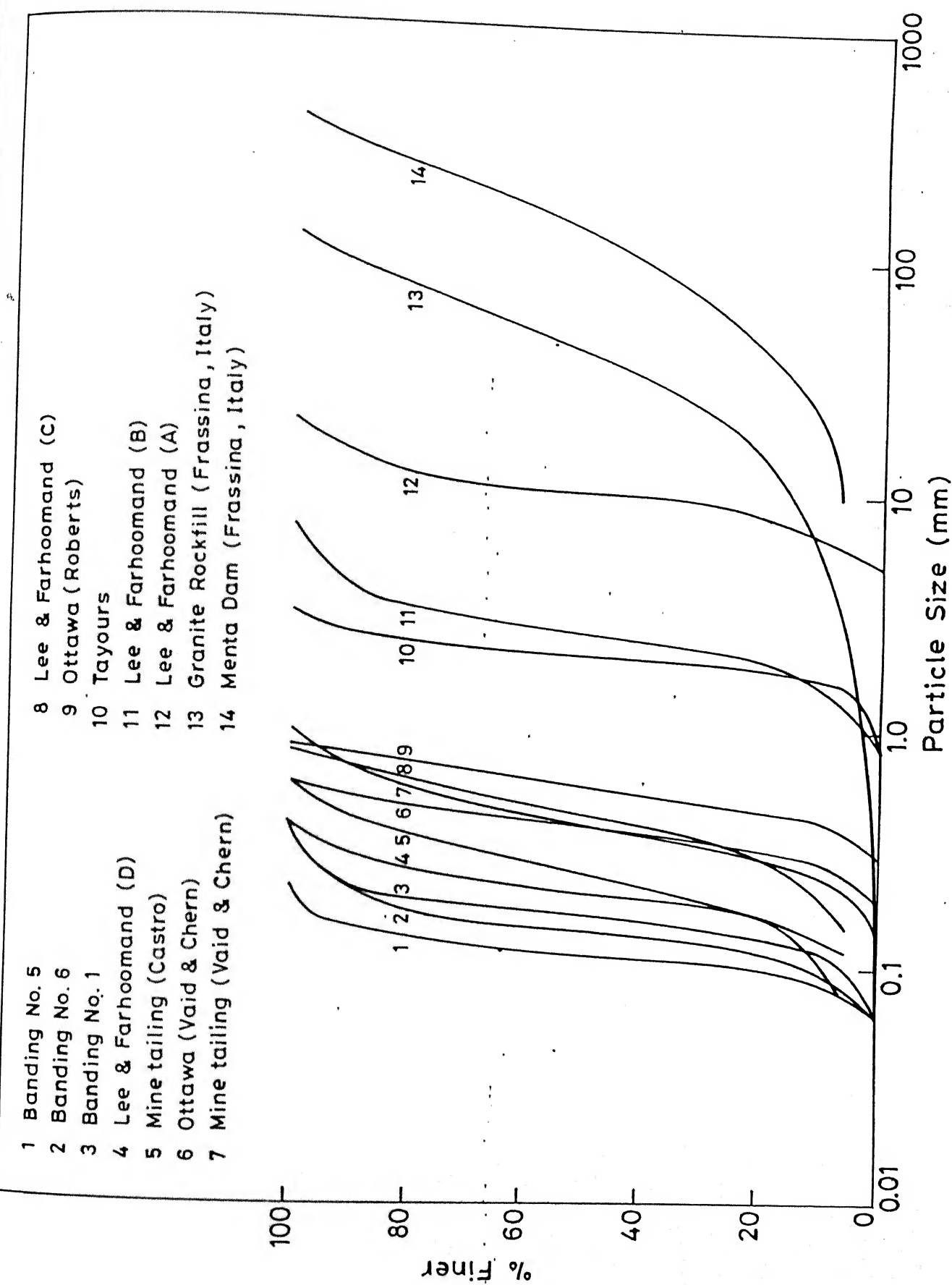


Fig. 5.21 Grain size distribution of variety of sands used for calculating total potential crushing (B_p).

Table 5.3 : Gradation, Size, Mineralogy and Grain Breakage Parameters for a Variety of Sands

Sands	C_u	d_{50}	DR	B_p	B_T	Br	Minerals (%)			
							Quartz	Feldspar	Mica	Carbonate
Kalpi	4.814	1.00	0.25	1.11	0.13	0.115	40	40	2	18
Kalpi 1	1.073	1.02	0.25	1.14	0.18	0.158	45	30	-	25
Kalpi 2	1.613	1.70	0.25	1.41	0.31	0.220	50	15-20	1-2	30
Ganga	2.565	0.18	0.25	0.39	0.065	0.166	62-65	20-25	8-10	2-5
Ganga (enhanced mica)	2.500	0.20	0.40	0.36	0.082	0.228	30-40	6	50-60	4
Ganga (mica removed)	2.180	0.18	0.40	0.39	0.022	0.056	65	30	5	5
Coarse Ganga	2.565	0.40	0.25	0.68	0.075	0.120	26-27	26-27	2-3	71
Chatta-hoochee	2.360	0.38	0.00	0.717	0.179	0.251	quartz	-	rich in mica	-
Calcareous	1.778	0.43	0.25	0.770	0.131	0.170	5	-	-	95
Artificial Calcareous	1.780	0.43	0.25	0.832	0.164	0.197	50	20	5	25
Standard	1.389	0.48	0.20	0.800	0.000	0.000	98-100	2-0	--	--
Tayoura (200 Kg/cm ²)	1.500	0.20	0.24	0.378	0.058	0.135	70	22	8 (chest)	--
Ottawa	1.500	0.60	--	0.907	0.012	0.014	100	--	--	--
Graded Ottawa	2.750	0.48	--	0.762	0.142	0.186	100	--	--	--
Banding No. 1	0.000	0.18	--	0.341	--	--	--	--	--	--
Banding No. 5	--	0.11	--	0.189	--	--	--	--	--	--
Banding No. 6	--	0.16	--	0.292	--	--	--	--	--	--
Tailing No. 10	--	0.60	--	0.506	--	--	--	--	--	--
Ottawa	--	0.40	--	0.739	--	--	--	--	--	--
Mol(DeBeer)	1.440	0.20	0.74	0.426	0.203	0.478	100	--	--	--
Crushed Granite	1.540	10.00	--	2.160	0.184	0.080	--	--	--	--
Napa Basalt	--	--	--	1.520	0.804	0.200	--	--	--	--
Napa Basalt	--	--	--	2.16	0.414	0.192	--	--	--	--

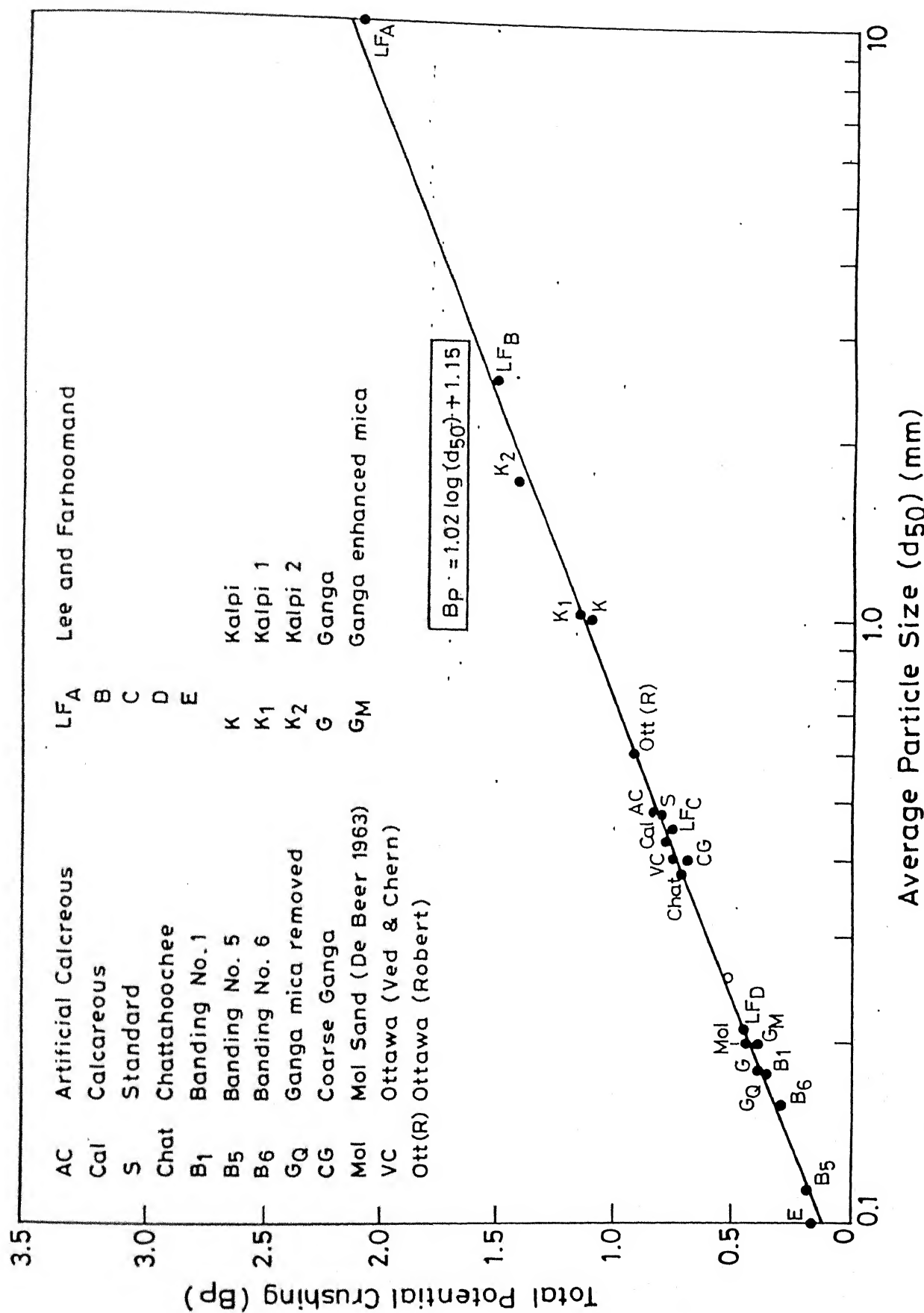


Fig. 5.22 Relationship between total potential crushing and average particle size.

depending on the stress level. Variations of values of B_T with stress level for a variety of sands tested in this study and for those reported by other workers are indicated in Fig. 5.23. The gradation curves before and after loading for the sands investigated have already been presented earlier (Figs. 4.59 - 4.67). The gradation curves for Tayoura sand (Miura and Yamanouchi, 1973), Ottawa sand (Robert and De Souza, 1958), Chattahoochee river sand (Vesic, 1968) and Mol sand (De Beer, 1963) before and after loading are given in Figs. 5.24 and 5.25.

5.2.4 Variation of B_T with Stress

Plots of B_T versus stress (Fig. 5.23) for different sands have revealed the following interesting trends:

1. Standard sand and Mol sand (De Beer 1963) composed of well-rounded quartz grains do not undergo any breakage ($B_T=0$) at stress of 176 Kg/cm^2 in sharp contrast to Kalpi 2 sand (composed of highly angular, elongated grains coated with carbonate) which attains a value of B_T around 0.31 for the same stress level. Thus the effect of particle angularity, mineralogy, size and relative density on total breakage is clearly evidenced from the data presented in Fig. 5.23.
2. Sands consisting entirely of quartz, with either perfectly rounded, subrounded or subangular grains, exhibit a typical variation of B_T with confining stress. For example, at stress level of 984 Kg/cm^2 , the poorly

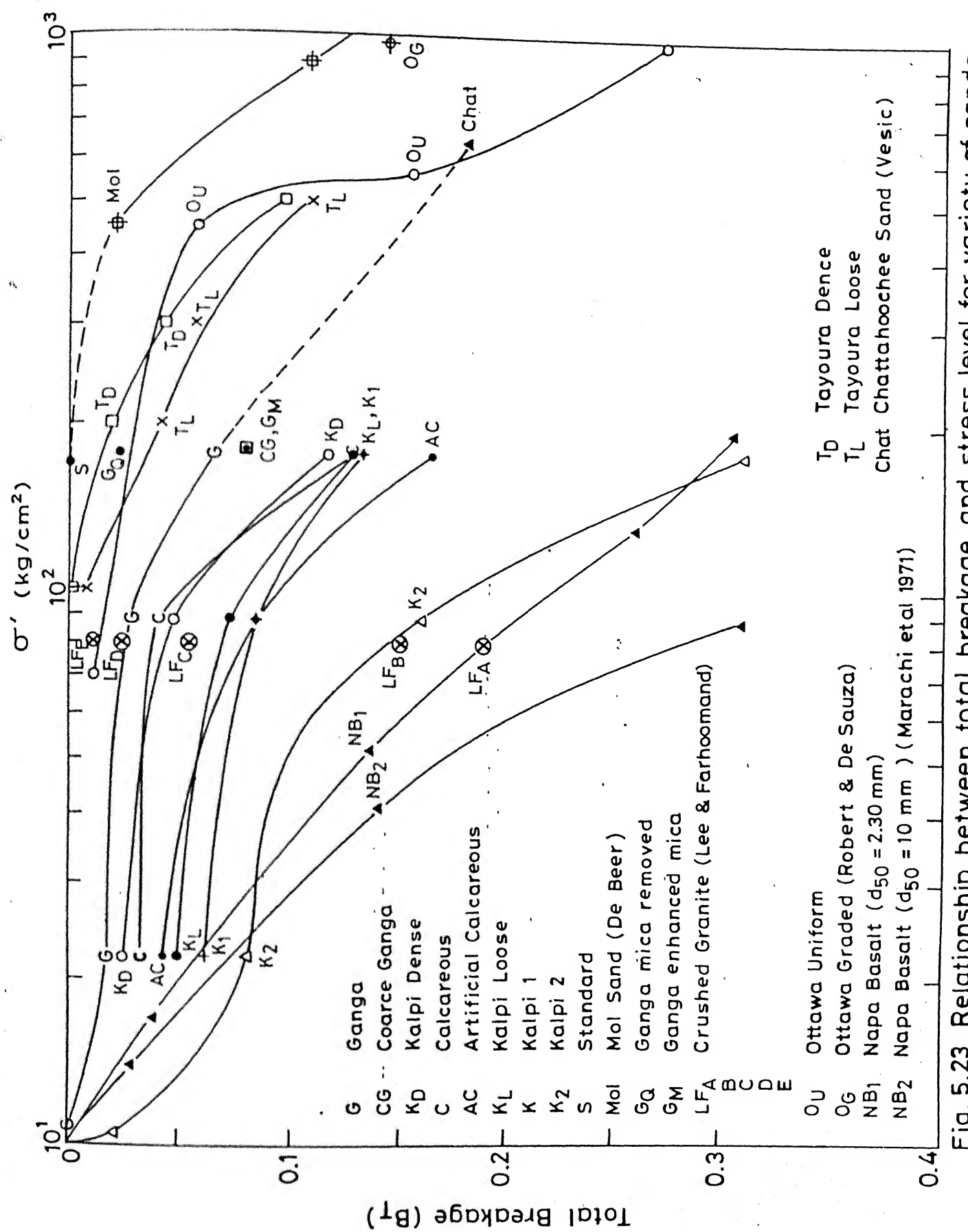


Fig. 5.23 Relationship between total breakage and stress level for variety of sands.

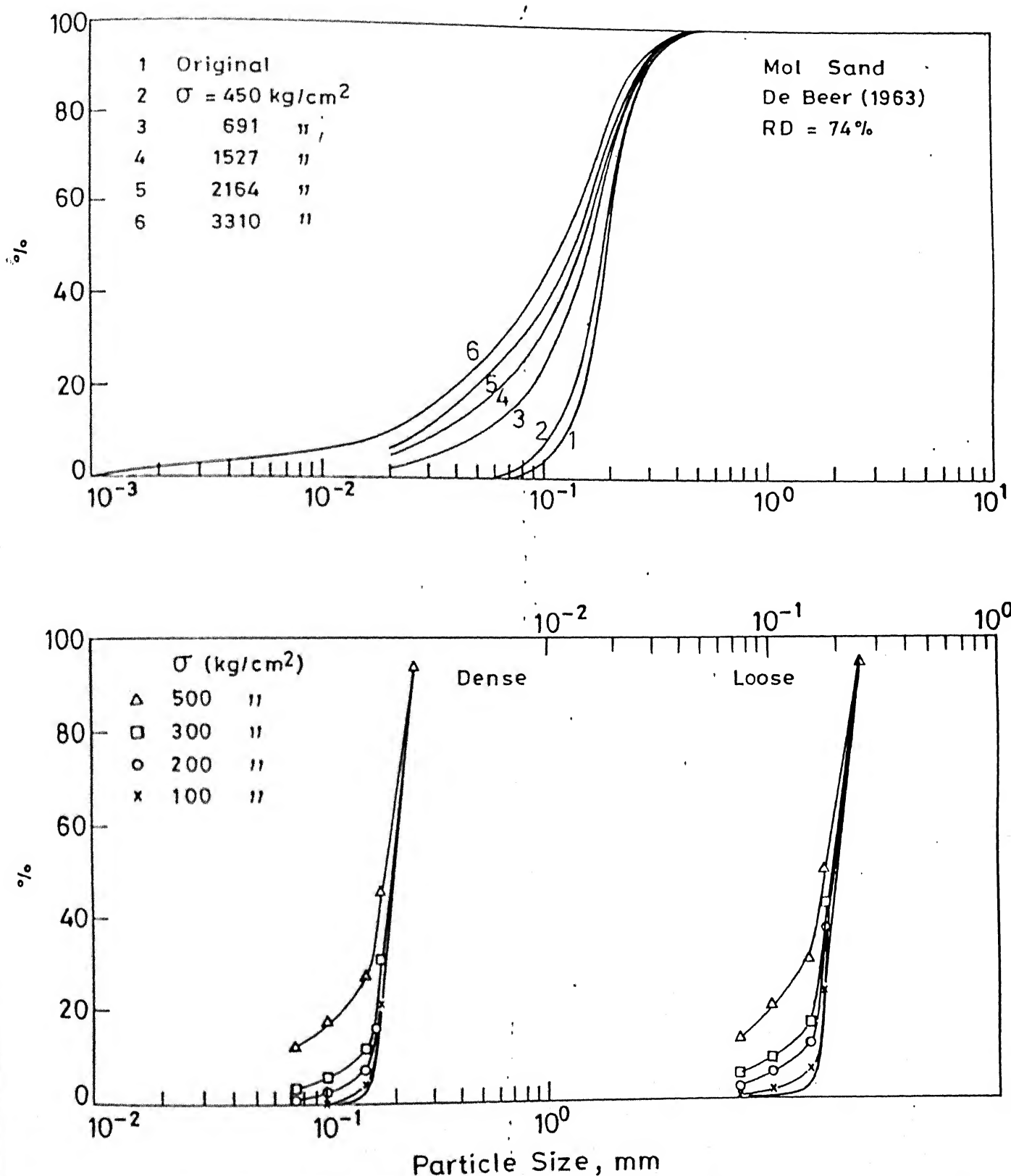


Fig. 5.24 Particle size distribution before and after load for Mol sand De Beer (1963) & Tayoura sand Miura et al.(1973).

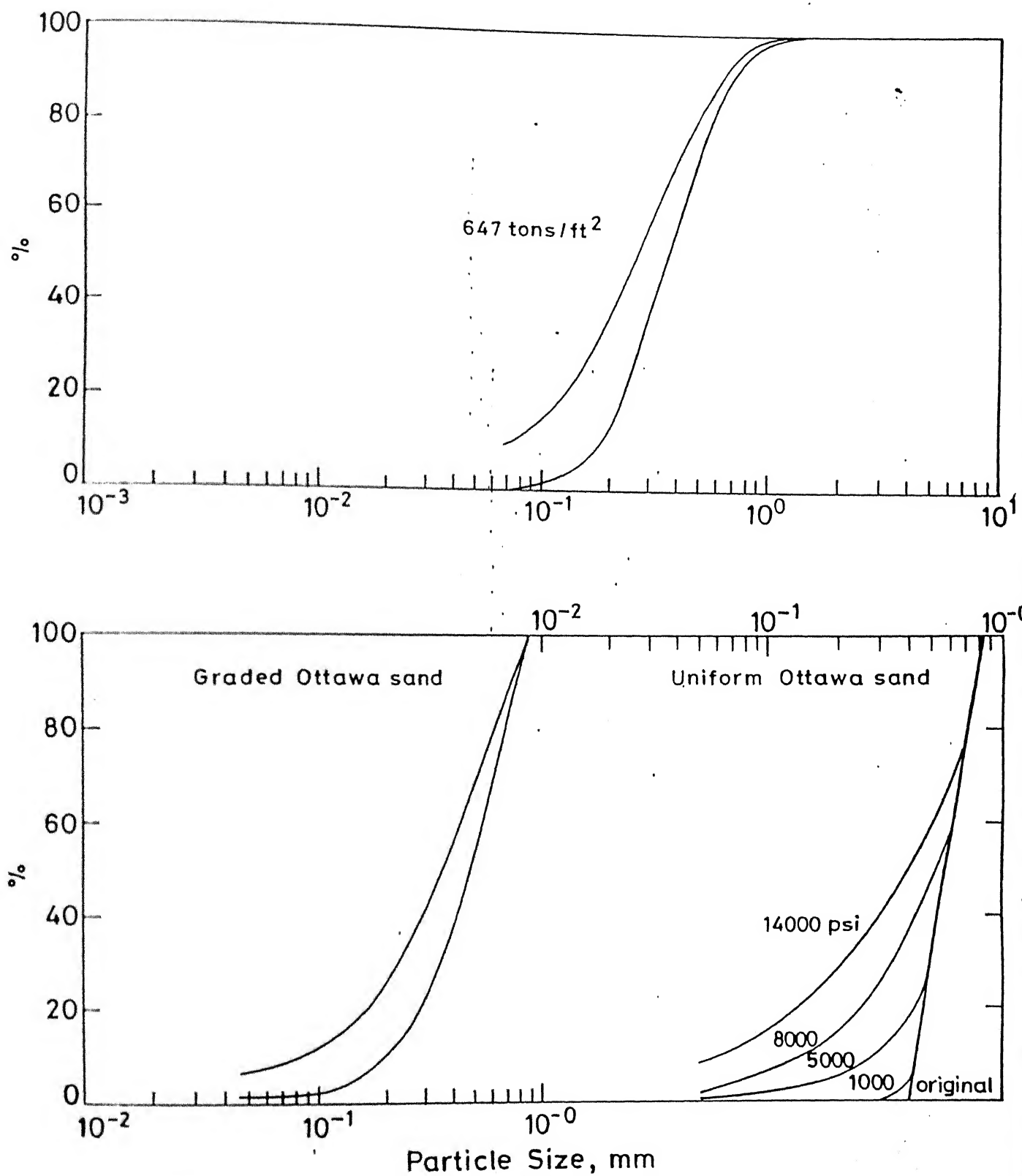


Fig. 5.25 Particle size distribution before and after load for Chattahoochi river sand (Vesic, 1968) and Ottawa sand (Robert & De Souza, 1958).

graded Ottawa sand ($Cu = 1.5$, $d_{50} = 0.6$ mm) indicated relatively higher B_T ($= 0.274$) as compared to the value of B_T ($= .14$) for a graded Ottawa sand sample ($Cu = 2.75$, $d_{50} = .475$ mm).

Values of B_T are also dependent on the grain size of sand. For example, at the same stress level of 984 Kg/cm^2 , Mol sand gives $B_T = 0.124$ compared to $B_T = 0.274$ for uniform Ottawa sand. While Cu values for both uniform Ottawa (1.44) and Mol (1.5) sands are practically same, the Ottawa sand is medium to coarse ($d_{50} = 0.6$ mm) and Mol sand is fine ($d_{50} = .195$).

The Tayoura sand has subrounded to subangular quartz grains and shows $B_T = 0.035$ for relative density of 0.24 compared to $B_T = 0.14$ at relative density of 0.90 for the same stress level of 176 Kg/cm^2 . The Ganga sample with mica removed (composed mainly of quartz and feldspars) shows behaviour similar to the Tayoura sand, e.g. at stress level of 176 Kg/cm^2 , the B_T value of Ganga with mica removed (at relative density of .40) fits very well in between the B_T values for Tayoura sand at relative density of 0.24 and 0.90. These two sands have approximately the same d_{50} ($\approx .2$ mm). The effect of initial relative density on B_T is clearly exhibited by the loose and dense samples of Tayoura sand.

3. For the same mineralogy and degree of particle angularity (in case of crushed granite as used by Lee and

Farhoomand, 1967), the value of B_T increases with d_{50} for the same confining stress (points A, B, C, D and E in Fig. 5.23). Results for Napa basalt (Marachi et al., 1969) also depict similar behaviour. Identical behaviour is also illustrated by the data for Kalpi, Kalpi 1 and Kalpi 2 samples with d_{50} values of 1.0, 1.02 and 1.7 mm respectively. However, the disproportionately higher response observed in the case of Kalpi 2 sand can be attributed to the uniform and coarse nature of the grains as well as the abundant carbonate coating on the same. Influence of d_{50} on B_T is further illustrated by the B_T versus stress behaviour of micaceous Ganga sand having the same degree of particle angularity as exhibited by Kalpi sand with 20% carbonate coating. The smaller values of B_T at the same stress level in case of Ganga sand can only be attributed to the fact that d_{50} (around 0.18 mm) of Ganga sand is less than that for Kalpi sand ($d_{50} = 1.0$ mm).

4. For the same d_{50} (0.2 mm) and comparable relative density, Ganga sand having 8 - 10% mica has indicated higher B_T (0.0625) as compared to Tayoura sand and Ganga sand (with mica removed) at the same stress level of 176 Kg/Cm^2 .
5. In case of Ganga sand, at the same stress level (176.32 kg/cm^2) the value of B_T increases with the increase in mica content (points G_Q , G and G_M in Fig. 5.23).

Incidentally all three samples have same d_{50} and similar gradation curves.

6. Calcareous sand, composed of 95% of carbonate material, with subrounded to subangular grains exhibited variations of B_T with stress corresponding to those between micaceous angular Ganga sand and highly angular Kalpi sand with 20% carbonate coating. It may be recalled that the B_p values for Ganga, Calcareous and Kalpi sands show a similar trend (0.39, 0.77 and 1.11 respectively). Particle breakage response of different sands can be best expressed in terms of relative breakage $B_r = (B_T/B_p)$, the details of which are presented in the subsequent pages.

It can thus be concluded that for the same mineralogy and particle angularity, B_T increases with d_{50} and decreases with C_u . Further for the same d_{50} , increase in mica and carbonate contents results in the increase of B_T .

Except for Ganga sand, B_T for all the sands tested in this study increases with grain angularity (h/λ) at low stress levels. Data at 22.04 Kg/cm^2 is shown in Fig. 5.26a. The Ganga sand behaviour is perhaps due to the fact that the grain size ($d_{50} = 0.18 \text{ mm}$) is very fine, whereas for all other sands, the d_{50} values vary from 0.4 to 1.7 mm (Fig. 5.26a). Had Ganga grain size been coarser ($\approx 1.0 \text{ mm}$) its plot would have followed the trend depicted by other sands. Variation of B_T with average number of tangent for these sands would give a similar trend.

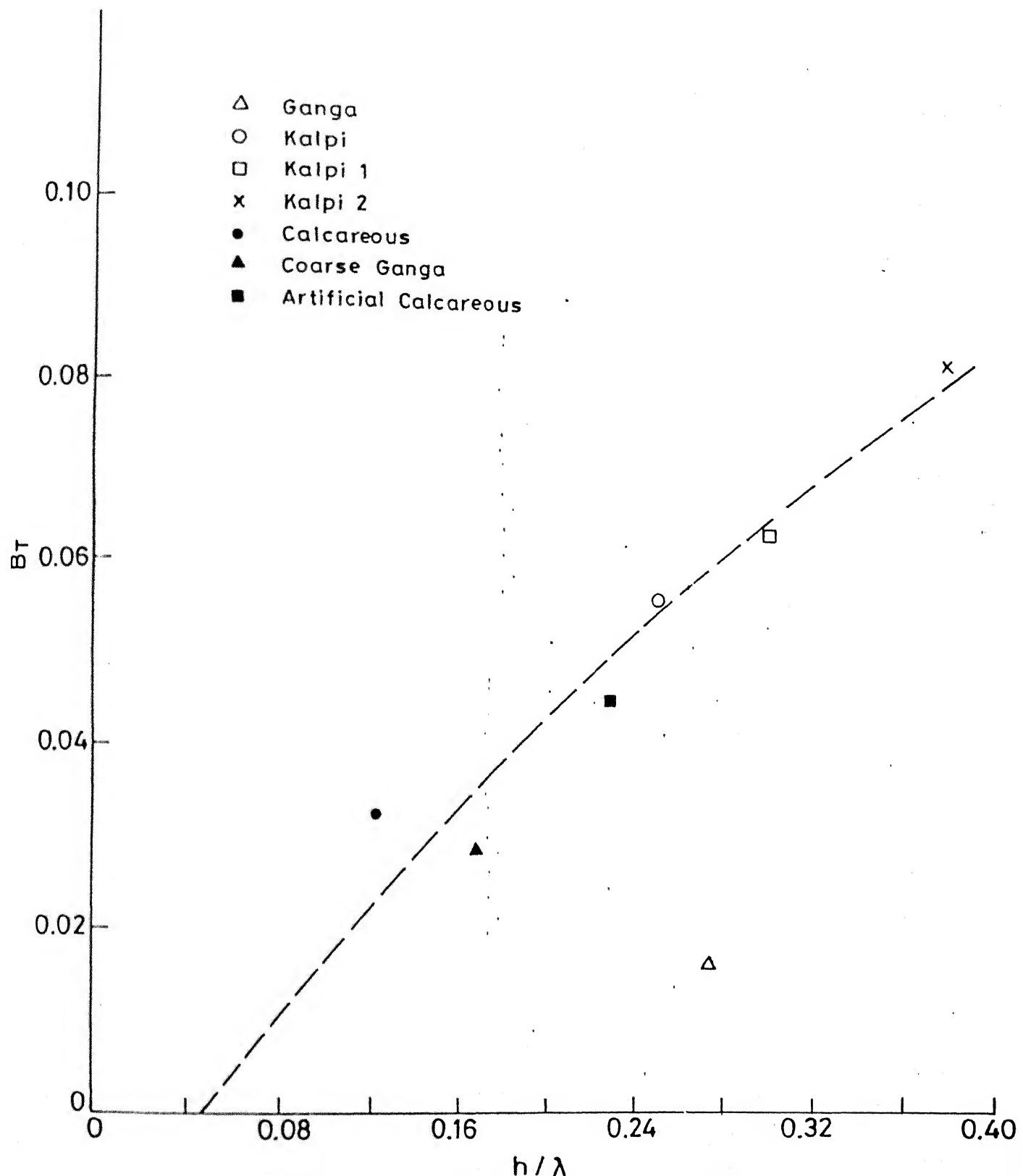


Fig. 5.26(a) Relationship between B_T and grain angularity (h/λ) for different sands at RD of 0.25 and stress 22.04 kg/cm^2 .

5.2.5 Variation of B_T with d_{50}

Dependence of B_T on d_{50} for different sands is illustrated in Fig. 5.26b. Here the effect of particle angularity, mineralogy and stress level are brought out. At the same stress level, samples with same C_u , grain mineralogy, and angularity (in case of particles for crushed granite) show consistent increase in B_T with d_{50} . Similar trends are shown by well-rounded quartz sands (Ottawa and Mol sands). Angular Kalpi and Napa basalt samples also exhibit an increase in B_T with d_{50} but the rate of increase is greater compared to the rounded and subrounded to subangular grains. For loose samples of micaceous Ganga sand and Tayoura sand with similar values of d_{50} , the value of B_T for Ganga sand at 176 Kg/cm^2 is about 1.9 times greater than that of Tayoura sand at the same stress. The effect of initial relative density on B_T in case of Tayoura sand (loose = 0.24, dense = 0.9) is less than 20%. However, the effect of stress level for the same particle angularity and relative density is much more pronounced. B_T for loose Tayoura sand sample increases from 0.035 at 176 Kg/cm^2 to 0.095 at 450 Kg/cm^2 . It may be noted that as the stress increases by a factor of about 2.6, the corresponding increase in B_T is of the same order (2.7 times). From Fig. 5.26b, it may be concluded that as in case of Tayoura sand, for the same mineralogy, particle size (d_{50}), and grain angularity, stress level controls the magnitude of particle breakage. Also for the same d_{50} and at comparable relative density, sands of

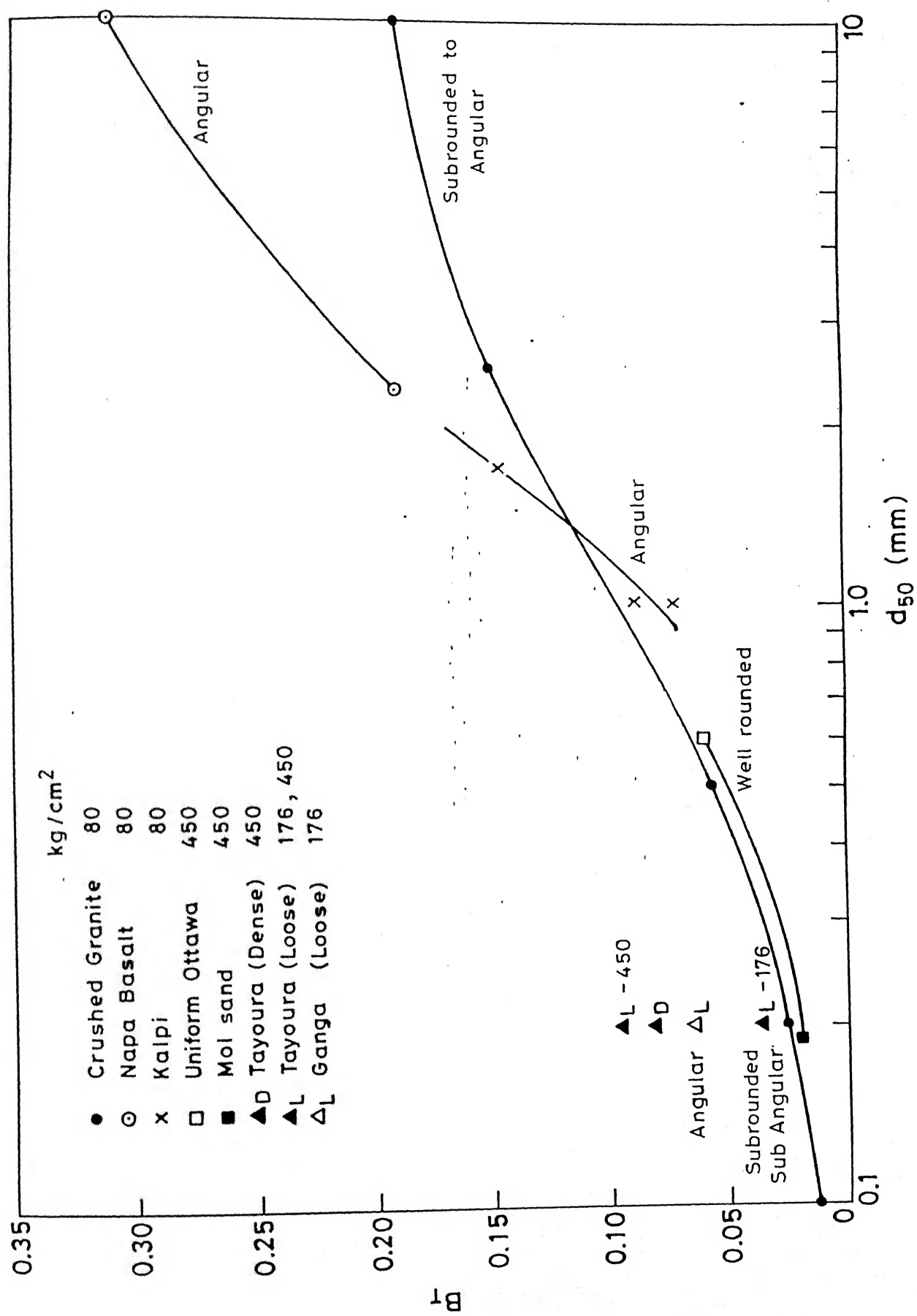


Fig. 5.26(b) Relationship between average particle size (d_{50}) and total breakage (B_T)

similar mineralogy show increase in B_T with particle angularity when Mol and Tayoura sands in dense state are compared.

5.2.6 Particle Modification

The earlier discussion on particle breakage in terms of B_T did not distinguish between two different phenomena leading to particle degradation. They are:

1. Grain modification at low stress levels, when the grain boundary protrusions are knocked off without any grain splitting. This leads to reduction in particle angularity.
2. Grain splitting at high stresses which would again produce angular grains.

There is hardly any data available on grain modification.

The basic questions to be answered are:

1. At what stress level does the grain modification start for different sands.
2. Upto what stress level does grain modification continue?

Standard Ganga, Kalpi and Calcareous sands were investigated for grain modification. Since loose samples would experience more grain degradation, samples of these sands at relative density of 0.25 were subjected to compression under stress levels of 11.02, 22.04, 88.16 and 176.32 Kg/cm^2 . At the end of each stress level the samples were taken out and were screened for grain size distribution. Except for the samples tested at 11.02 Kg/cm^2 studies for

surface modification were undertaken for all others using image analyzer.

5.2.6.1 Changes in Grain Shape

Based on flatness (d_S/d_I) and elongation (d_I/d_L) ratios the changes in grain shape due to particle degradation under stress are best illustrated by the Zingg diagram with sphericity and shape factor superimposed. The results of experiments for Standard sand, Ganga Sand, Calcareous Sand and Kalpi Sand are presented in Fig. 5.27 (a, b, c and d). In the case of Standard sand where no particle breakage was observed even upto stress level of 176.32 kg/cm^2 , sieve analysis at all stress levels indicates no changes in grain size distribution. The measurement of particle dimensions (d_S , d_I and d_L) revealed no alteration in either flatness or elongation ratios. The initially rounded grains remained so even after loading upto 176.32 Kg/cm^2 . However, in the case of Ganga Sand (Fig. 5.27b), the initial average point 1, representing the original particle shape changes to position 2 after loading to 22.04 Kg/cm^2 . Point 2 in quadrant II indicates an increase in particle shape factor and sphericity. This is due to the modification of the grain surface protrusion which reduces the particle angularity. Further loading to 176.32 Kg/cm^2 leads to particle rupture for this sand resulting again in the production of grains with increased surface protrusions as indicated by point 3 located in quadrant I once again. Position of points marked

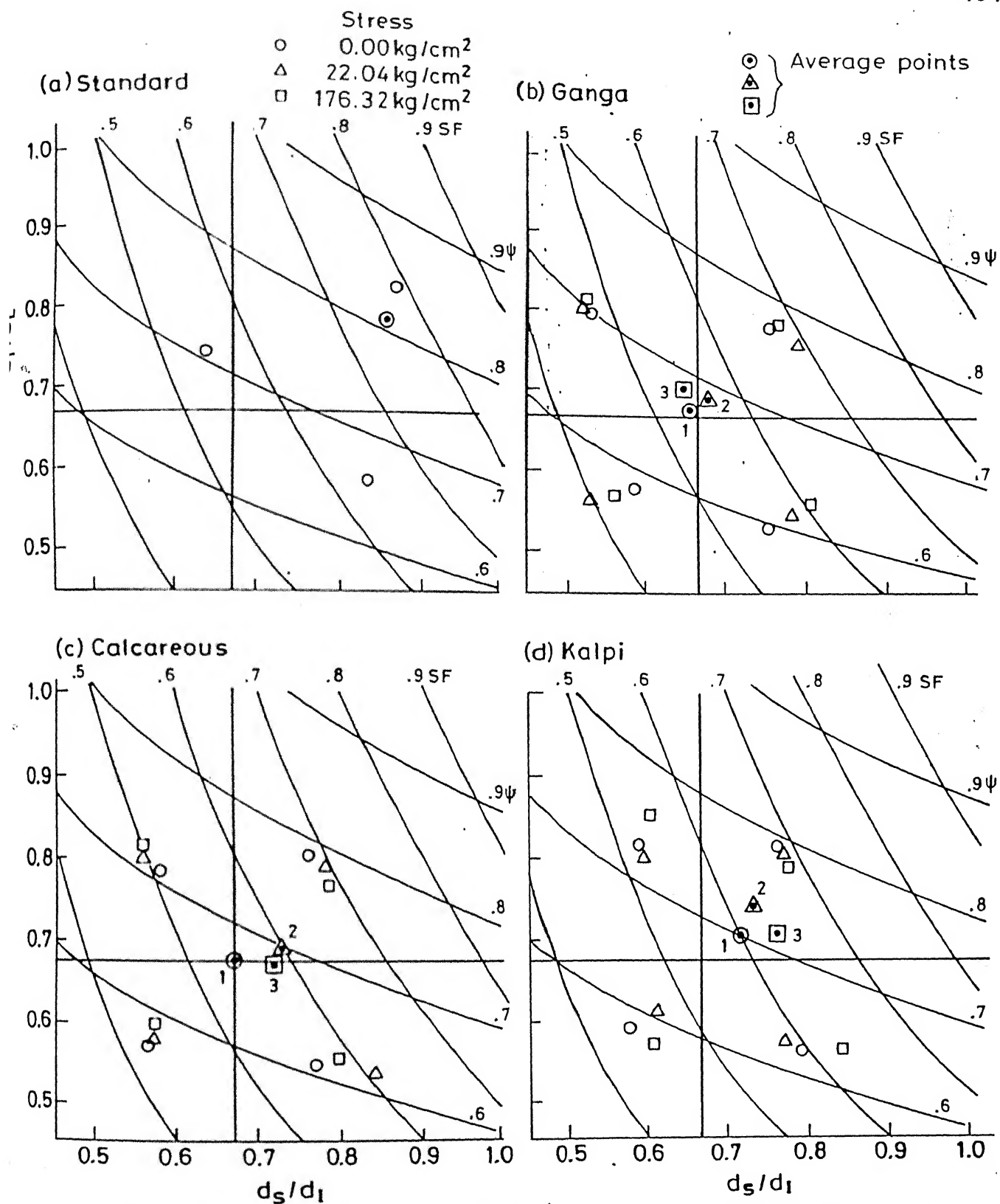


Fig. 5.27 Relationship between flatness and elongation ratios showing the particle degradation under stress for Standard, Ganga, Calcareous and Kalpi sands.

1,2,3 for Calcareous and Kalpi sands illustrate similar changes in particle shape for stress levels of 22.04 and 176.32 Kg/cm² respectively. While in case of Ganga sand the final point 3 moves towards quadrant I, the final grain shape in case of Calcareous and Kalpi tends towards elongated grains represented by quadrant III.

5.2.6.2 Changes in Grain Angularity

Based on tangent count, the distribution of tangents at stress levels of 22.04 and 176.32 Kg/cm² as well as original samples for Ganga, Calcareous and Kalpi sands are presented in Figs. 5.28, 5.29 and 5.30 respectively. Here again at stress levels of 22.04 Kg/cm², the number of tangents decreases as the surface protrusions are modified and the grains experience reduction in surface angularity. Further loading to 176.32 Kg/cm² leads to grain splitting which in turn leads to increased surface protrusions and increased tangent count. This evidence also supports the fact that at a stress level of 22.04 Kg/cm², the grains had experienced surface modifications (as evidence from the lesser number of tangent counts) which resulted in lower particle angularity and at stress level of 176.32 Kg/cm² crushing of the grains once again resulted in the increase in their angularity as observed from the increase in tangent counts. The Standard sand shows no change in tangent distributions. The tangent count data were also used to interpret the changes in percentage of particles having edges with one tangent count only. All tangent counts were carried out on the four projected edges of the grain. All grain edges (1 to 4) with

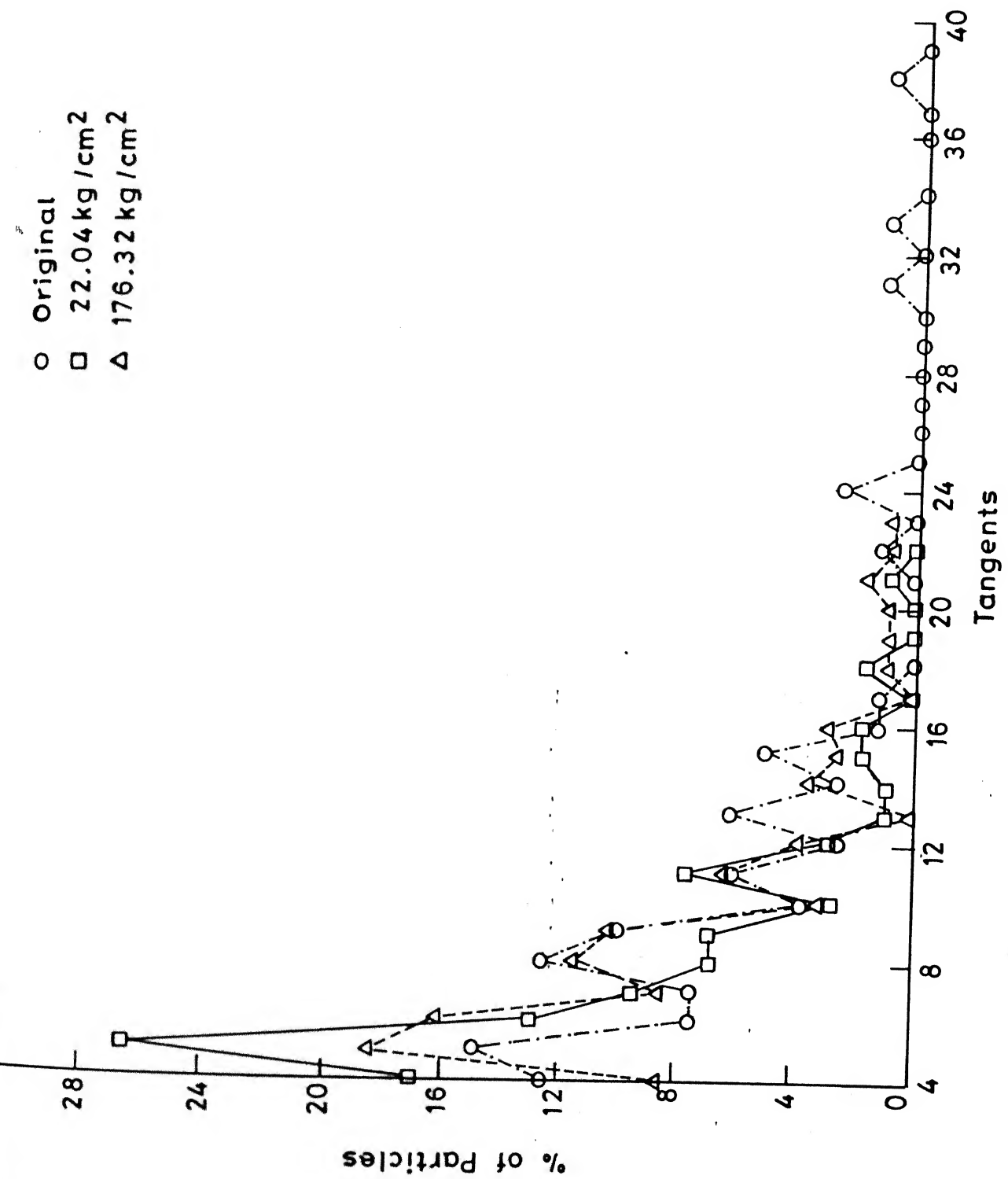


Fig. 5.28 Distribution of tangents at $\sigma' = 0.0$, 22.04 and 176.32 kg/cm^2 for Ganga sand.

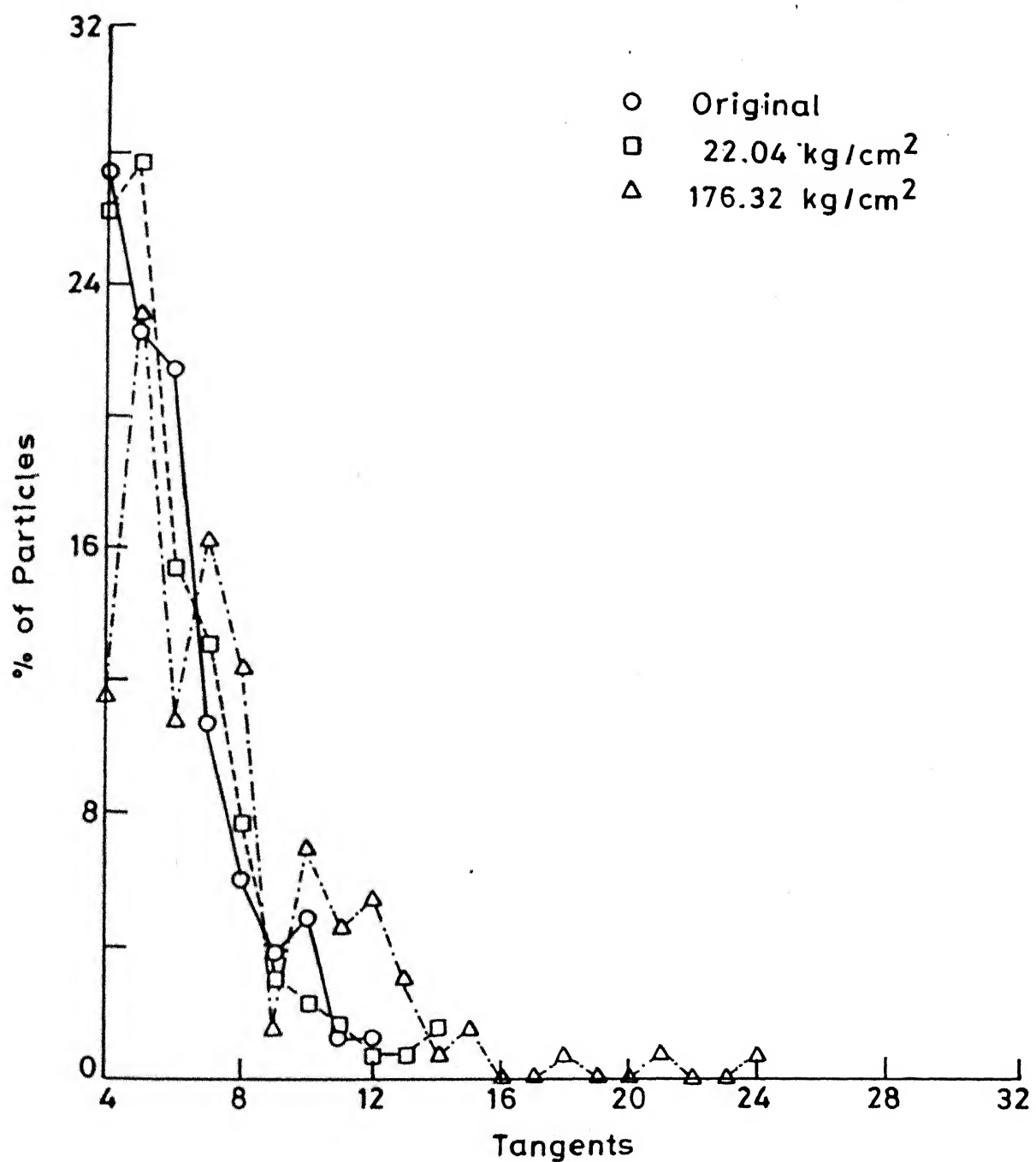


Fig. 5.29 Distribution of tangents at $\sigma' = 0.0$, 22.04 and 176.32 kg/cm² for Calcareous sand.

one tangent only are designated as smooth in Figs. 5.31 to 5.33. The data for smooth edges for original samples and after subjected to stress levels of 0.0, 22.04 and 176.32 Kg/cm^2 for total sample and also for the different sieve fractions in case of Ganga, Calcareous and Kalpi are presented in Figs. 5.31, 5.32 and 5.33 respectively. Here again at 22.04 Kg/cm^2 , the number of particles with smooth edges increases (angularity decreases) and when grains are fractured at 176.32 Kg/cm^2 , the number of particles with smooth edges is once again reduced. These observations are complimentary to the data on tangent distribution count (Figs. 5.28, 5.29 and 5.30).

Since h/λ is a direct measure of grain angularity, values of average tangent have been plotted against h/λ (Fig. 5.34). The data for Ganga, Calcareous and Kalpi sands at stress levels of 22.04 and 176.32 Kg/cm^2 are also shown in Fig. 5.34. For a variety of original sand samples, a very good correlation exists between the number of tangents and h/λ . However, at a stress level of 22.04 Kg/cm^2 as the number of tangents decreases, the grain angularity represented by h/λ also decreases and on grain crushing at 176.32 Kg/cm^2 the data point tends towards higher initial tangent count and h/λ . For example 1,2,3 represent loading stages for Ganga under stress level of 0.0, 22.04 and 176.32 Kg/cm^2 respectively. For three sands, viz., Ganga, Calcareous and Kalpi, the h/λ versus tangents relationship shifts from curve A to B and to C (close to A) as stress level increases

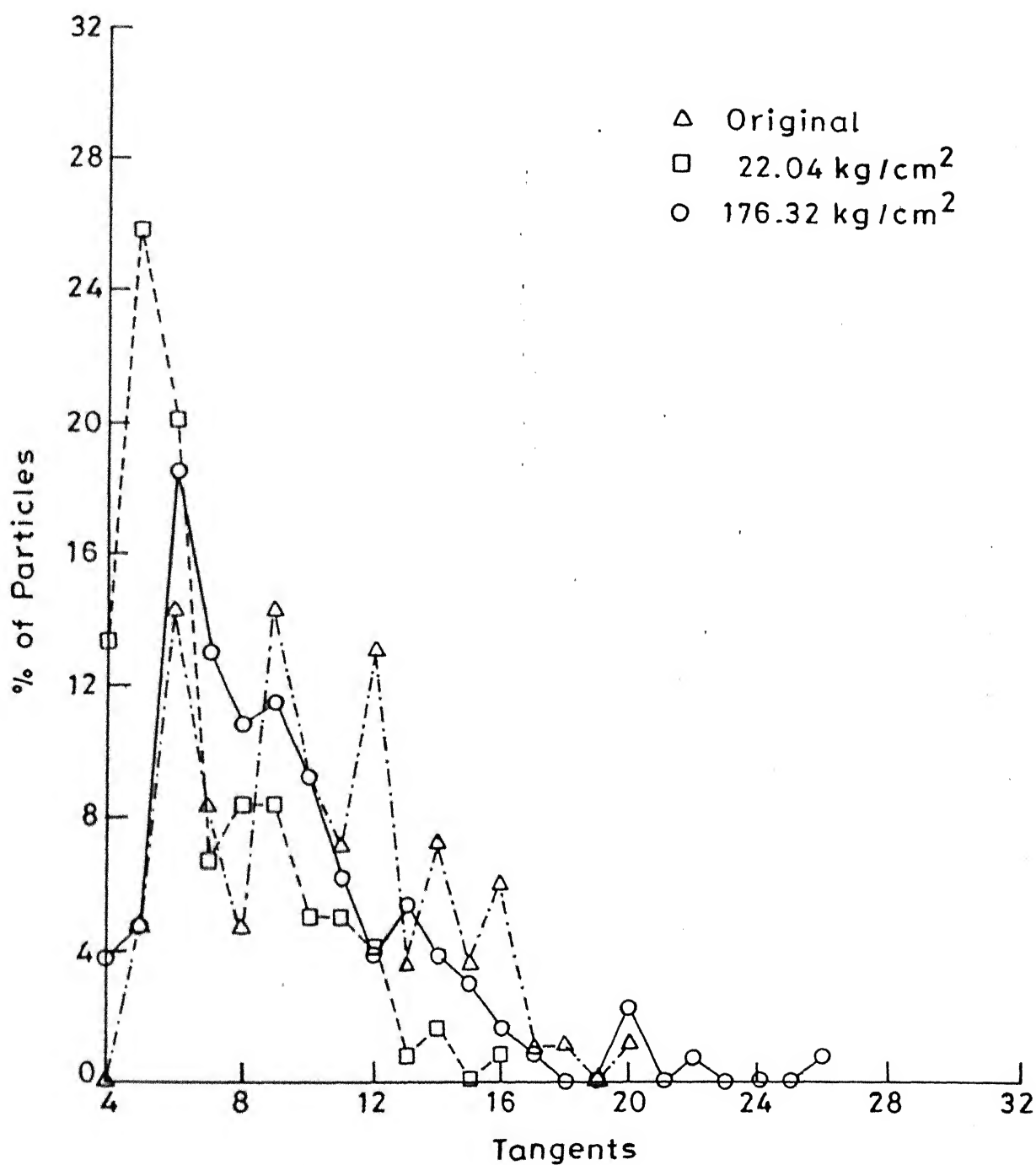


Fig. 5.30 Distribution of tangents at $\sigma' = 0.00$, 22.04 and 176.32 kg/cm² for Kalpi sand.

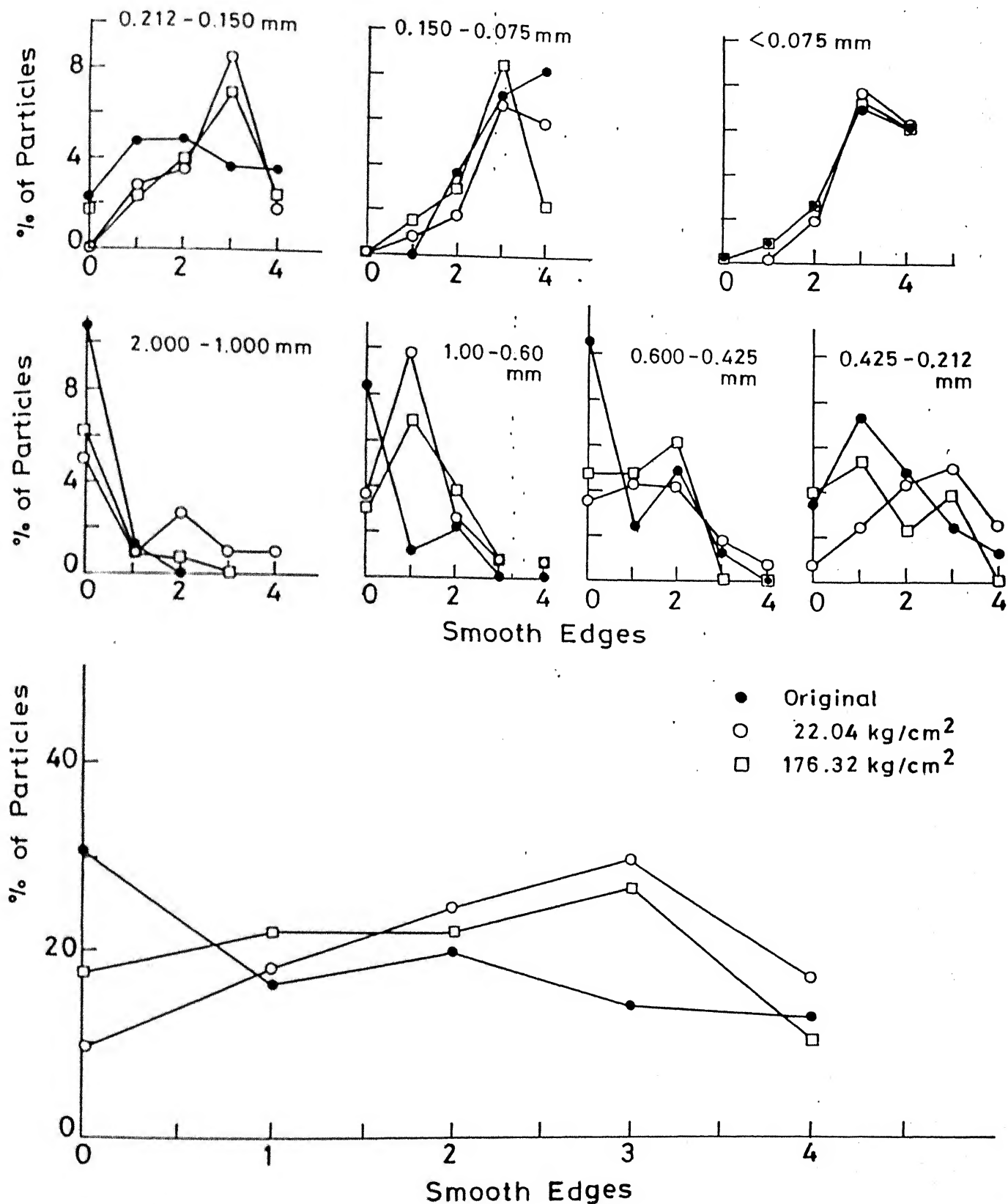


Fig. 5.31 The smooth edge distribution at $\sigma' = 0.0, 22.04$ and 176.32 kg/cm^2 for Ganga sand.

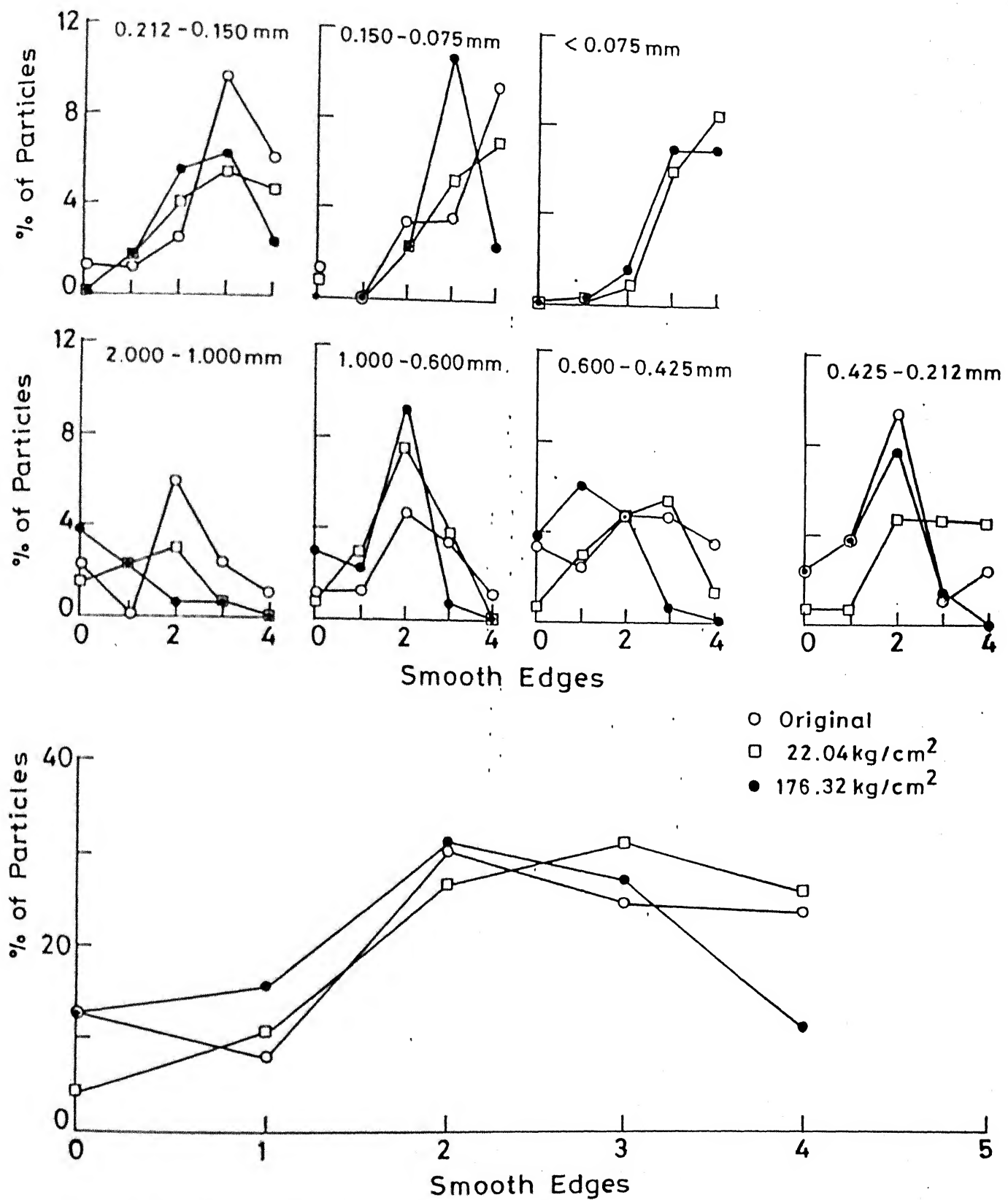


Fig. 5.32 Smooth edge distribution at $\sigma' = 0.0, 22.04$ and 176.32 kg/cm^2 for calcareous sand.

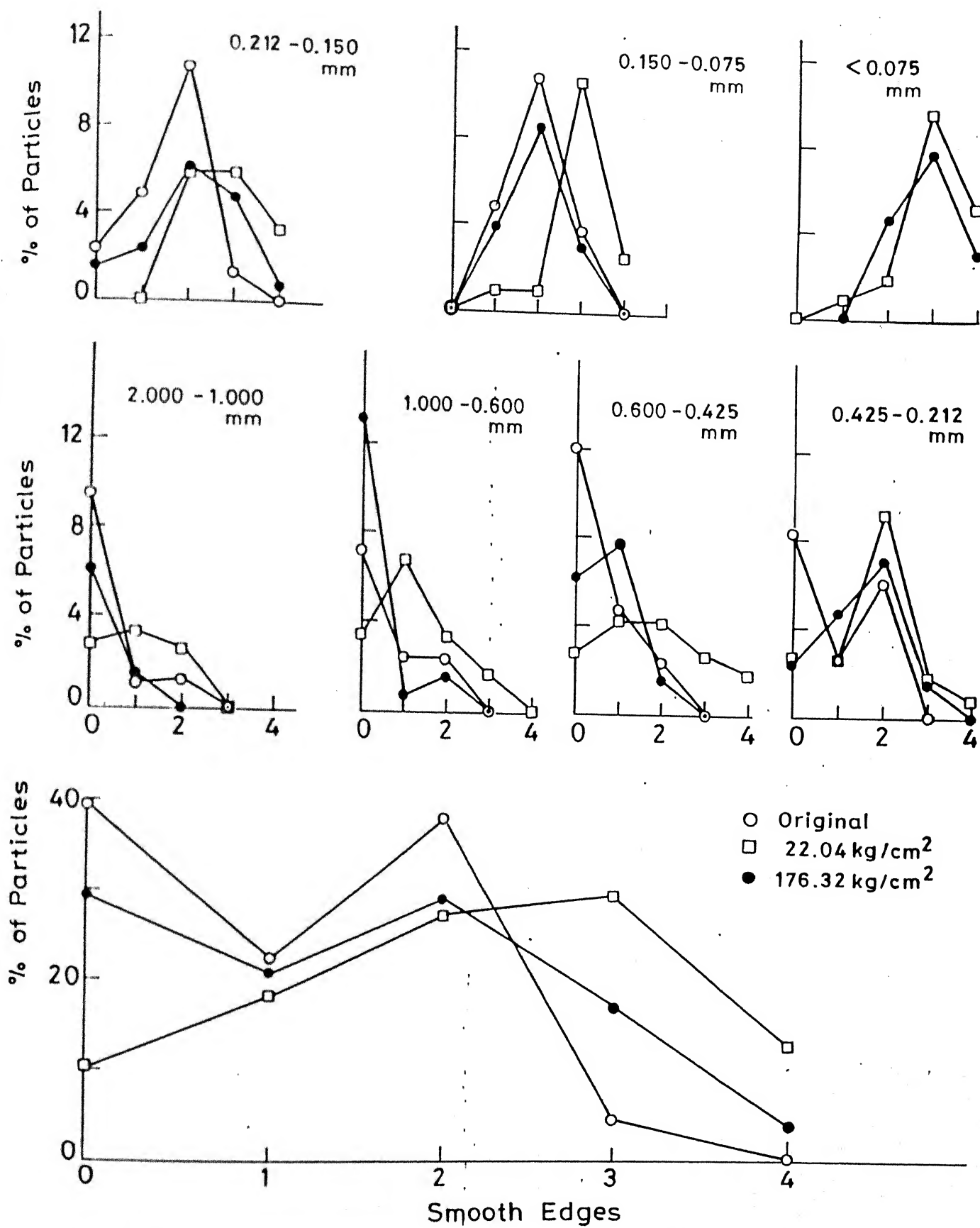


Fig. 5.33 Smooth edge distribution at $\sigma' = 0.0, 22.04$ and 176.32 kg/cm^2 for Kalpi Sand.

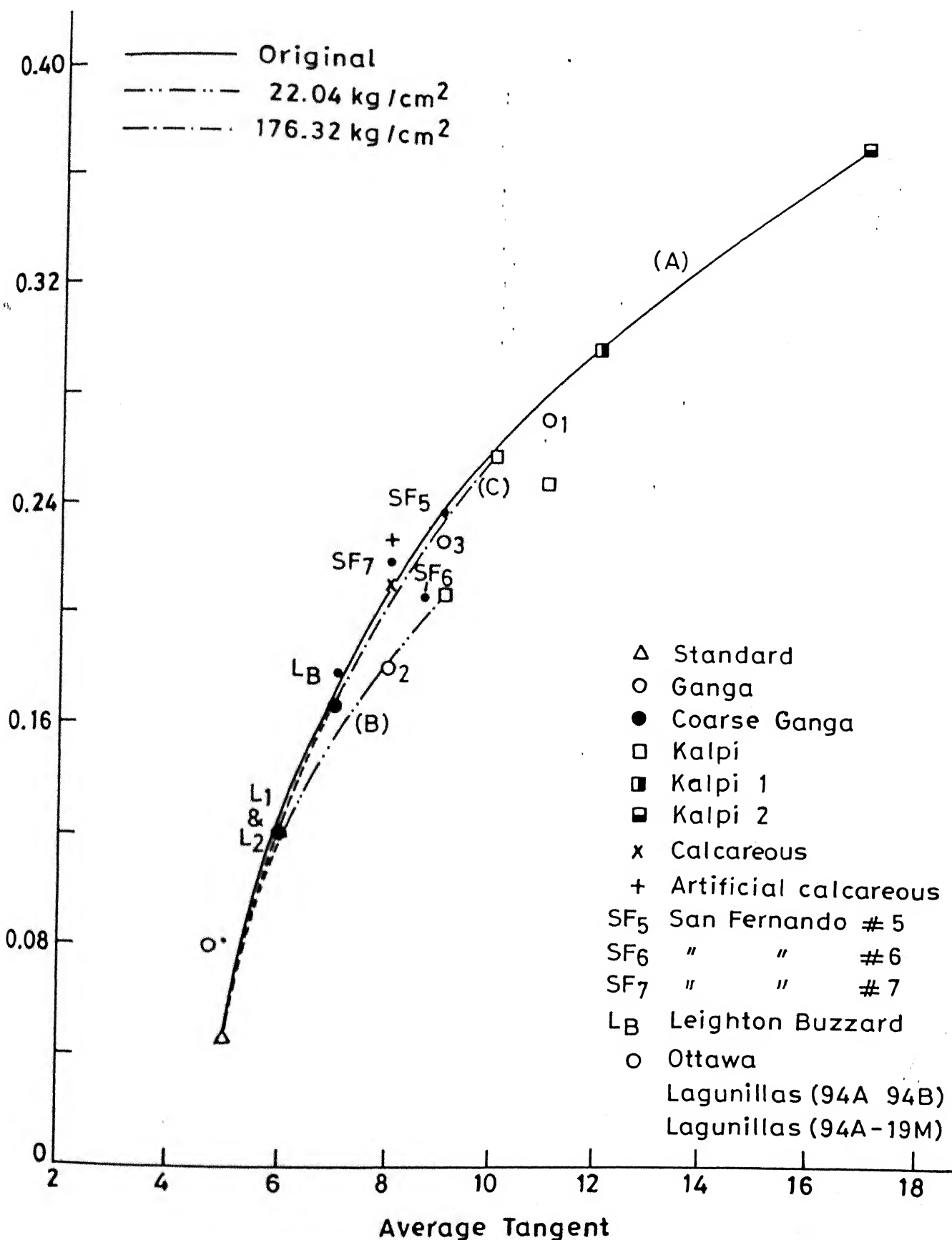


Fig. 5.34 Relationship between average h/λ and average tangent count at $\sigma' = 0.0, 22.04$ and 176.32 kg/cm^2 for variety of sands.

from 0.0 to 22.04 and 176.32 Kg/cm^2 .

Thus the present investigations on the grain shape and angularity have clearly brought out the fact that prior to the grain crushing at very high stresses, there exists a stress level (<<crushing stress) at which the grains undergo surface modifications. These surface modifications, as detailed in succeeding pages, exert a significant influence on the variation of constrained modulus with confining stress. Grain modification at a certain stress level (<<crushing stress) under cyclic triaxial undrained loading leading to change from dilatant to compressive response of the sands has also been reported by Vaid and Chem (1985) who have suggested the dependence of this stress level on the initial relative density for angular mine tailing sand.

Recognizing the grain modification at lower stresses, a detailed study was undertaken for all the sands tested under stress levels of 11.02, 22.04 and 88.16 Kg/cm^2 for establishing the threshold critical stress at which the grain modification begins. Since grain degradation is expected to be maximum under loose packing, all the tests were carried out on samples with initial relative density of 0.25 except for Standard sand for which the relative density used was 0.20. The results of this investigation are presented in Fig. 5.35 where the relative particle breakage B_r (calculated as a ratio of B_T and B_p) is plotted against the measure of particle angularity h/λ for data at 11.02 Kg/cm^2 , 22.04 Kg/cm^2 and 88.16 Kg/cm^2 stress levels. At 11.02 Kg/cm^2 , significant changes were evidenced in Calcareous and Kalpi 2

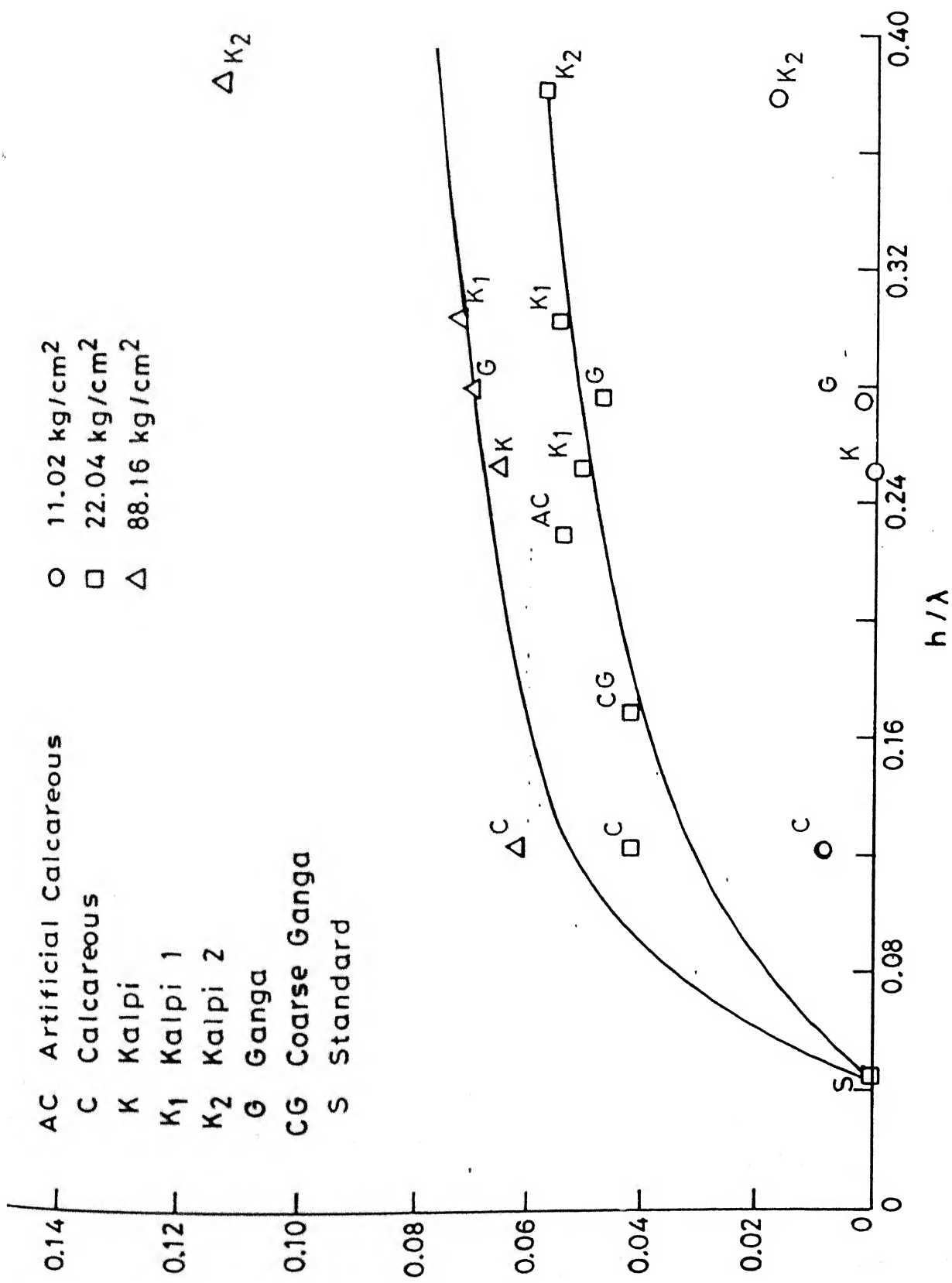


Fig. 5.35 Relationship between the relative breakage and h/λ for variety of sands.

sands while Kalpi sand showed no grain modification. Major increase in B_r takes place under stress level of 22.04 Kg/cm^2 . For stress increase from 22.04 to 88.16 Kg/cm^2 , most sands except Kalpi 2 show minimal increase in B_r . The behaviour of Kalpi 2 at 88.16 Kg/cm^2 may be due to the early onset of grain crushing since this sand, as indicated earlier, has uniform grading, coarser grains and higher carbonate content.

These results thus indicate that significant grain modification can occur even at a stress level less than 22.04 Kg/cm^2 . As described in a subsequent section, the variation of modulus with stress has been used in the present study to determine the critical stress level at which the behaviour of the sand changes. This stress level is related to the stage at which grain modification also commences. A tentative relationship has also been proposed between this critical stress causing grain modification and relative density (Section 5.3.2).

5.2.7 Particle Crushing

As indicated by Marsal (1967), the phenomenon of particle fragmentation under stress, both during compression and shear, a very significant influence on the shear strength and compressibility of granular materials. Hardin (1985) has proposed a parameter called relative breakage (B_r), to quantify the degree of particle fragmentation or crushing, defined (Fig. 5.19) as the ratio of total particle breakage (B_T) and total particle potential breakage (B_p). In the

present study, all compression tests were one-dimensional. Data from literature used for comparison also pertained to the compression stage only.

In the previous section, various aspects related to particle modification at low-stress levels were discussed. The overall variation of B_r with stress is discussed in the following sections in some detail.

5.2.7.1 Variation of B_r with Stress

In Fig. 5.36, experimental data for the sands investigated in this study as well as for Tayoura sand (Miura and Yamanouchi, 1973), Ottawa Sand (Robert and De Souza, 1958), Chattahoochee river sand (Vesic 1978), Mol sand (De Beer, 1963) and Crushed Granite (Lee and Farhoomand, 1967), are presented. The same data alongwith Napa Basalts (Marachi et al., 1969) has been shown on a semi-log graph (Fig. 5.37) in order to better illustrate the trends over a wide range of stresses. In the following discussions, the rounded to subrounded quartz sands of low to very low compressibility will be broadly referred to as strong sands. The angular to very angular, compressible to very compressible sands containing mica and carbonate will be called as weak sands. Angular rockfill falls in between these two categories. This categorization is more for the purpose of simplified presentation rather than a strict classification. From Figs. 5.36, 5.37, 5.38 and 5.39 the following observation can be made:

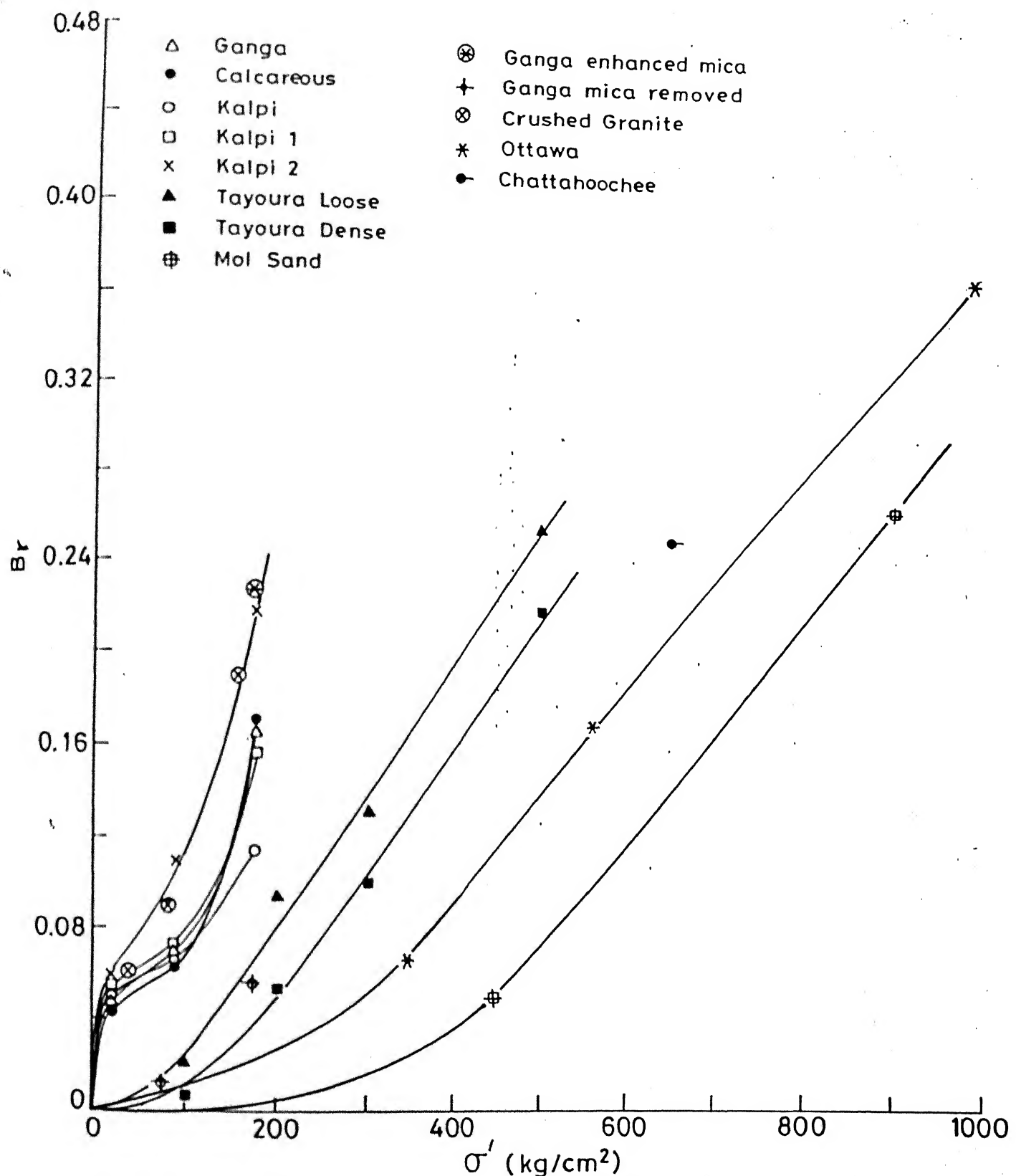


Fig. 5.36 Relationship between relative breakage and vertical effective stress.

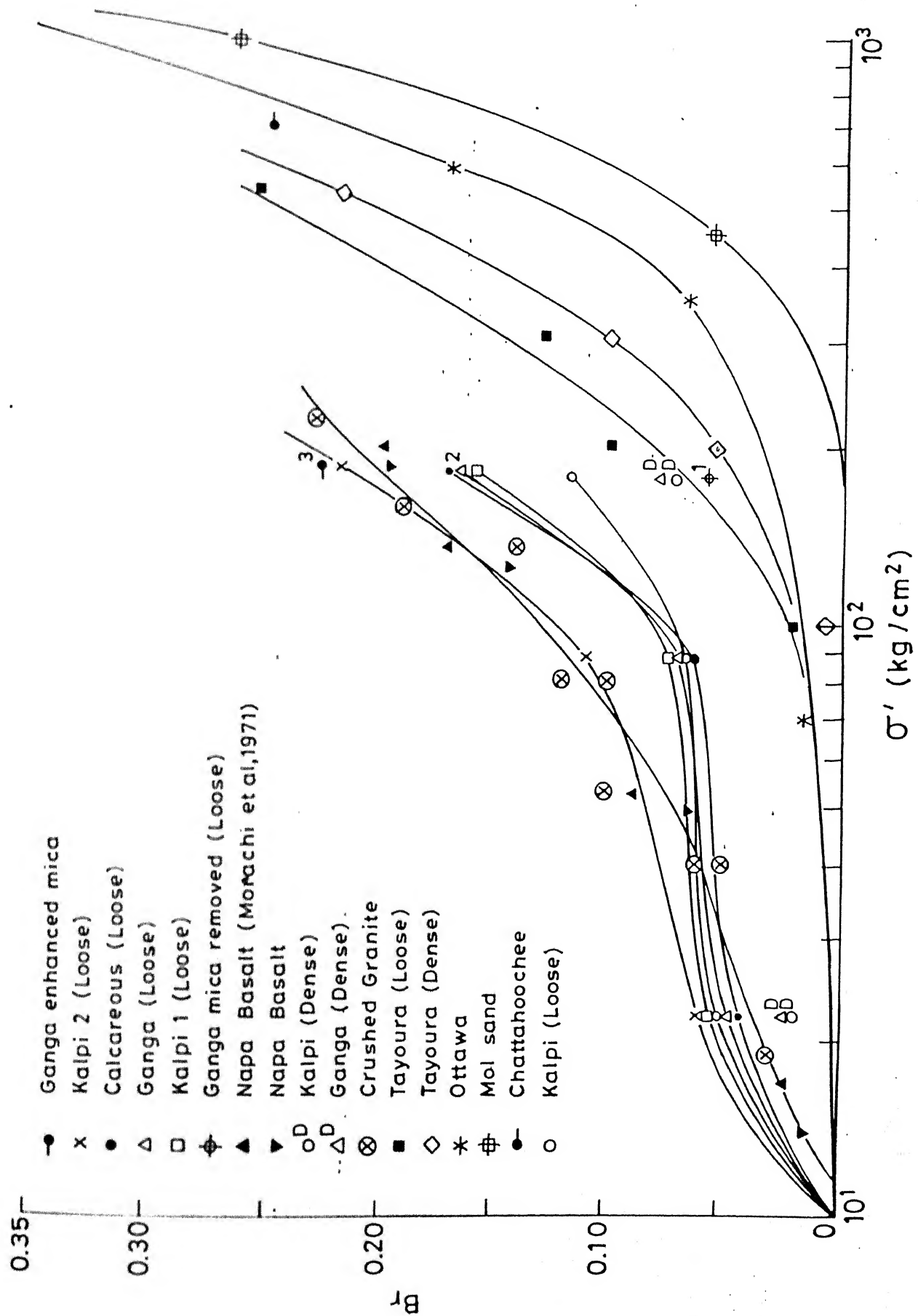


Fig. 5.37 Relationship between relative breakage and vertical effective stress.

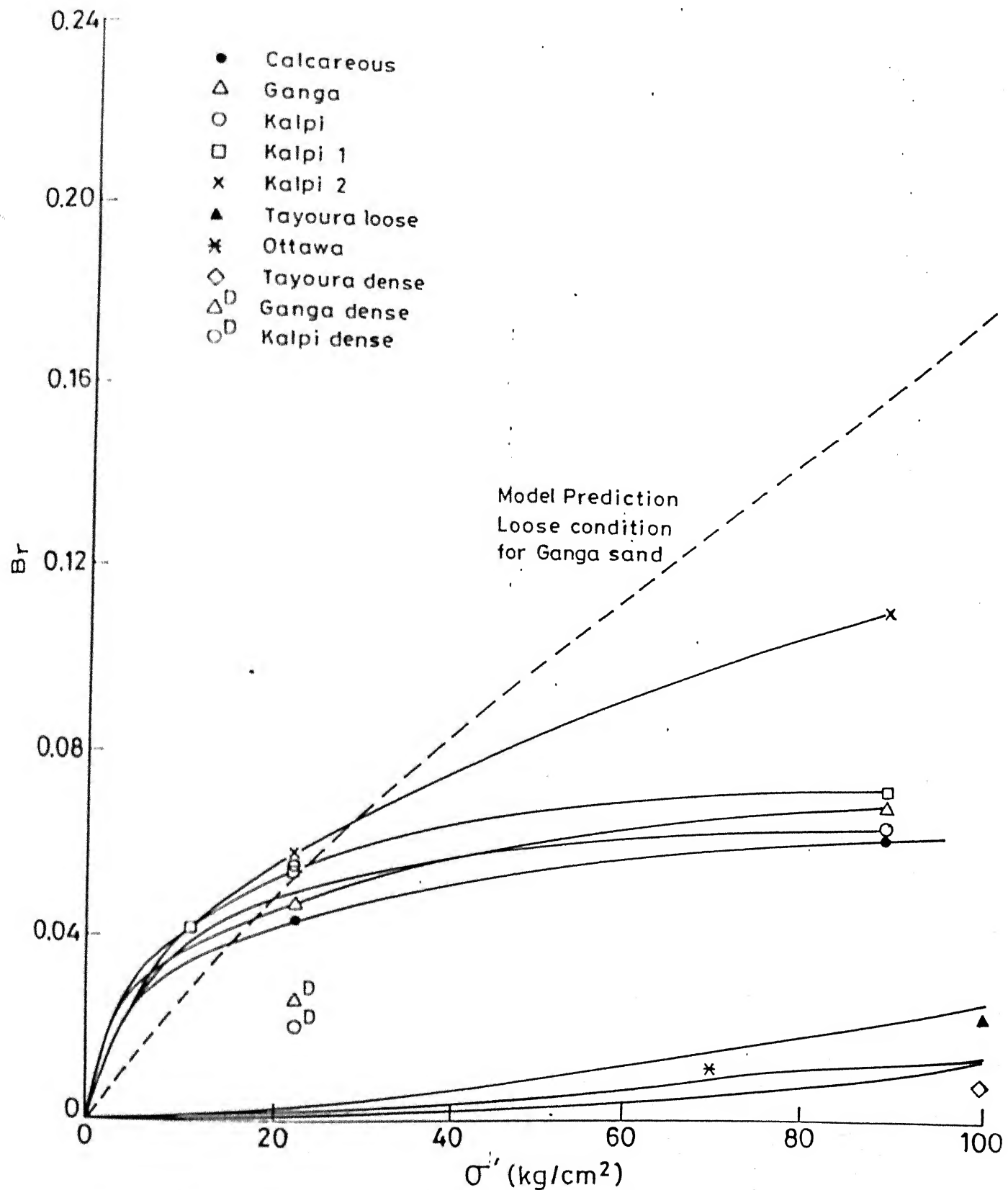


Fig. 5.38 Variation of relative breakage at low stress and model prediction.

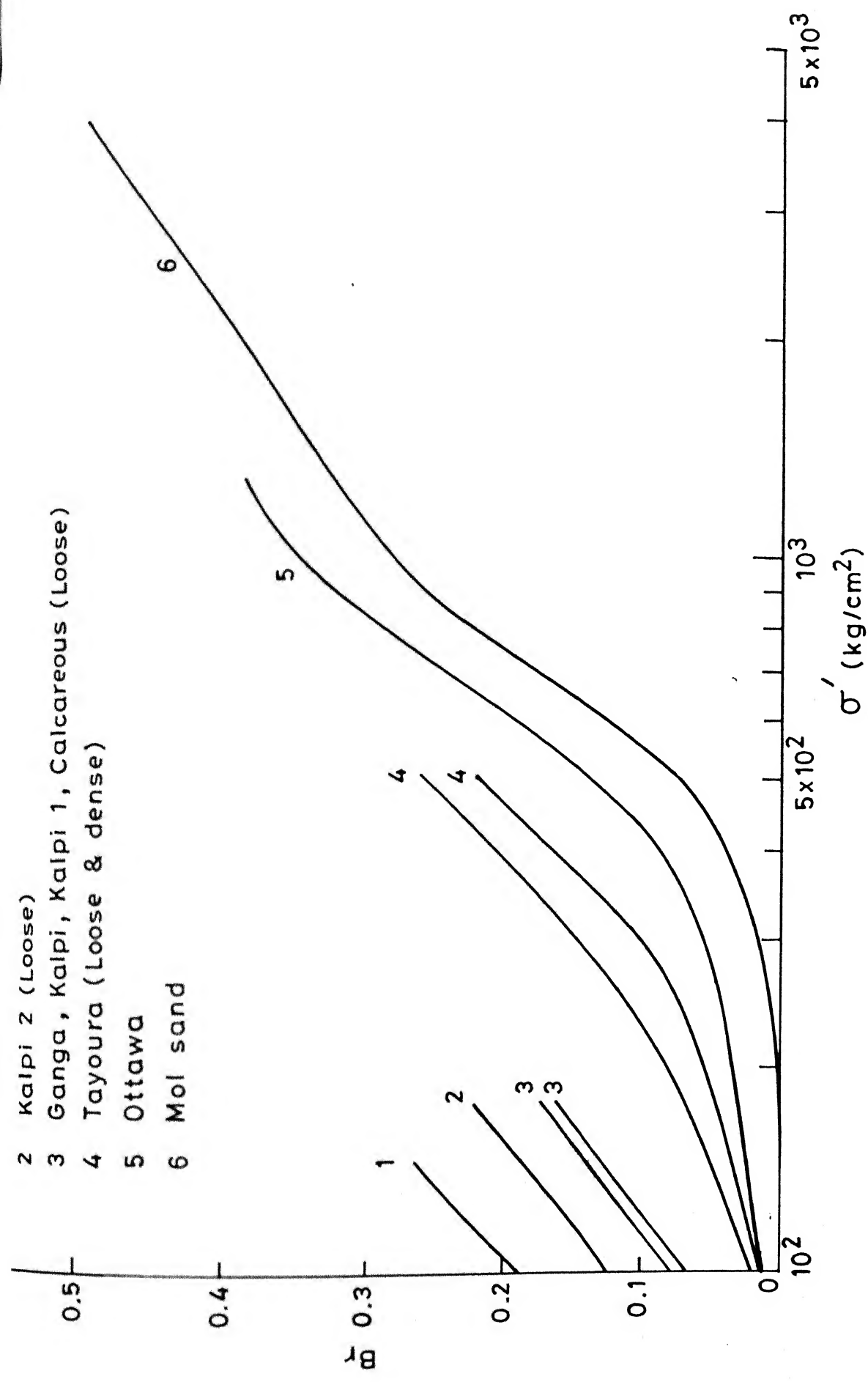


Fig. 5.39 Variation of relative breakage at high stresses.

1. In case of well rounded strong sands (e.g. Mol sand and standard sand) upto a stress level of 176.32 to 200 Kg/cm^2 , practically no grain degradation takes place (Figs. 5.36, 5.37), Ottawa sand (Robert and De Sourza, 1958) which is less rounded than Mol and Standard sands shows $B_r = 0.01$ at 100 Kg/cm^2 and 0.03 at 200 Kg/cm^2 . The value of B_r at stress level of 500 Kg/cm^2 is comparable with of weak sand at 100 Kg/cm^2 . At stress levels greater than 500 Kg/cm^2 , B_r increases at faster rate (0.0005 Kg/cm^2). The increased rate of change of B_r for strong sands is about 1/2 of that for weak sands.
2. For weak sands (such as Ganga and Kalpi), values of B_r between 0.07 and 0.12 are obtained at a stress level of 100 Kg/cm^2 and roughly 2/3 of the grain modification has already taken place at a stress level of 20 Kg/cm^2 . This fact was used earlier to confirm the grain modification phenomenon at low stresses. At a stress level greater than 100 Kg/cm^2 , the values of B_r increases at a faster rate (0.0012 Kg/cm^2).
3. The trends of the subangular to subrounded sands (Tayoura sand) are intermediate between the same for weak and strong sands.
4. Angular rockfill behaves almost similar to the weak sands at low stress levels (see Napa Basalt Fig. 5.37). At 20 Kg/cm^2 the slightly lower value of B_r is due to the fact that this rock fill is stronger than the micaceous Ganga sand and weakly cemented Kalpi sand. At stresses greater

than 50 kg/cm^2 , high angularity of rockfill gives greater value of B_r as compared to weak sands. Napa basalt (Marachi et al, 1971), has d_{50} ranging from 2-10 mm and this would explain higher B_r at higher stresses. It may be interesting to observe (Table 5.4) that at the same stress both B_p and B_T increase with increasing particle size (d_{50}), whereas the relative breakage B_r , remains practically same for a given material. In case of Kalpi sand, B_r value for Kalpi 2 is higher than that of Kalpi. This is because of two factors:

1. Kalpi is well-graded ($Cu=4.8$) compared to Kalpi 2 ($Cu = 1.6$).
2. Kalpi 2 consists of coarser fraction where the small grains have been cemented together to form the larger aggregate grains.

From this limited information it may be possible to suggest that, except for the case where aggregated grains are involved, both B_p and B_T for a material of similar gradation, angularity and mineralogy, increase with particle size whereas B_r at a given stress remains essentially the same. These observations are clearly supported by the trends shown in Figs 5.23 and 5.37. In Fig. 5.23, the B_T versus stress relationships are distinctive for each d_{50} in case of Kalpi, Napa basalt and crushed granite whereas the same data when normalized with respect to B_p shows almost identical behaviour for both particle sizes (Fig. 5.37). From Fig. 5.37 it can also be seen that loose materials give higher B_r for the same stress as compared to dense materials (Ganga, Kalpi

Table 5.4 : Values of d_{50} , B_p , B_T and B_r for Different Sand
at Effective Stress of 80 Kg/cm^2

Sands	Particle shape	d_{50} mm	B_p	B_T	B_r	Stress level
Napa-Basalt 1	Angular	10.0	2.16	0.27	0.125	80 Kg/cm^2
Napa-Basalt 2	Angular	2.3	1.52	0.19	0.125	" "
Crushed Granite 1	Subrounded to Angular	10.0	2.16	0.18	0.083	" "
Crushed Granite 2	Subrounded to Angular	2.0	1.50	0.14	0.093	" "
Kalpi 2	Very Angular	1.7	1.40	0.14	0.100	" "
Kalpi	Very Angular	1.0	1.10	0.07	0.064	" "

and Tayoura sands). The effect of particle gradation on B_r has already been pointed out in case of Kalpi and Kalpi 2 sands i.e. for sands of same mineralogy and angularity, a poorly-graded sand gives higher B_r compared to a well-graded sand. The effect of mica content on B_r at same stress level is well brought out by Ganga sand with mica removed, Ganga sand and Ganga sand with enhanced mica shown as 1, 2, 3 respectively in Fig. 5.37. Incidentally all the three samples of Ganga sand had identical gradation, d_{50} and comparable relative density. The value of B_r increases as mica content increases (Fig. 5.40a). Test data point for mica-rich Chattahoochee river sand (Vesic, 1968) is also shown in Fig. 5.40a. The higher value of B_r for Chattahoochee sand is due to the fact that it was tested at 647 Kg/cm^2 compared to 176.32 Kg/cm^2 in case of Ganga sand. Also the d_{50} of Chattahoochee river sand is 0.38 mm compared to 0.18 for Ganga sand.

The effect of mineralogy on the value of B_r at 176.32 Kg/cm^2 has also be examined in terms of quartz or quartz plus feldspar content of sands. These relationships are indicated in Fig. 5.40 b for a variety of sands. An inverse linear relationship (which may be fortuitous) is evidenced between B_r and quartz content. Of course, a relationship of this nature is expected. The relationship between B_r and quartz plus feldspar is shown in Fig. 5.40 b. It may be noted that the Ganga Sand data point (Fig. 5.40b) lies closer to the B_r versus quartz plus feldspar content curve than the B_r versus

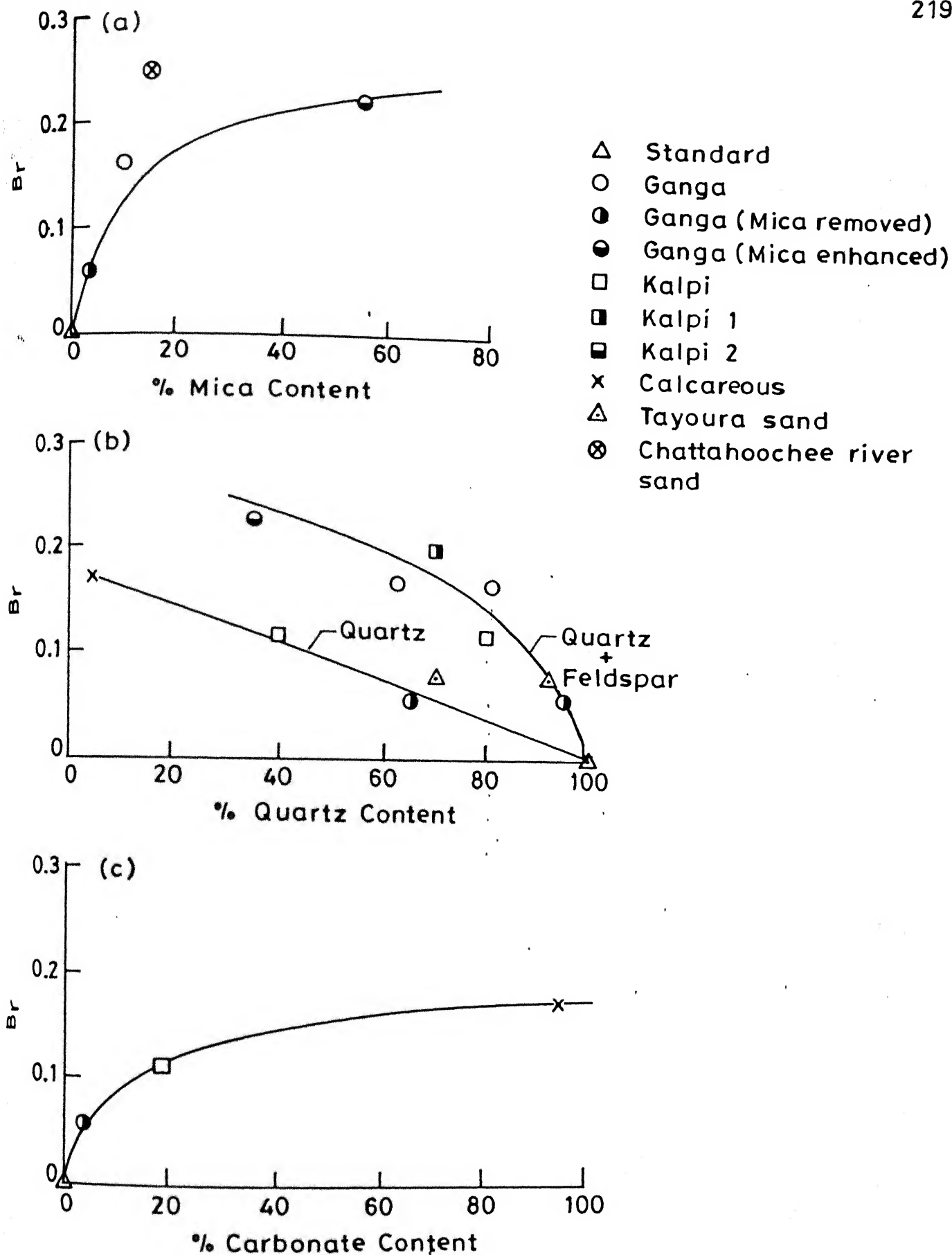


Fig. 5.40 Variation of B_r with mineral content of sands.

quartz content relationship. It may thus be noted that the B_r versus quartz content relationship is for non micaceous sands only.

Based on the data for Calcareous and Kalpi sands, the effect of carbonate material on particle crushing has been evaluated (Fig. 5.40 c). Ganga sand (with mica removed) has 4-5% carbonate content and the data fits well with Kalpi sand Calcareous. A distinct increase of B_r with increasing percentage of carbonate content is evidenced.

These results clearly reflect the markedly different particle crushing behaviour of weak sands, as compared to strong quartz sand. The effect of mineralogy, gradation and particle size has been brought out and tentative relationships, based on available data, have been suggested (Fig. 5.40a,b,c). The variation of particle crushing with stress is in general shown to follow the pattern suggested by Terzaghi and Peck (1943) and De Beer (1963). However, the weak sands exhibit a distinctly different relationship as compared to strong quartz sands for stress levels less than 100 Kg/cm^2 .

In case of strong quartz sands (Fig. 5.39) (well-rounded Standard and Mol sand), the variation of B_r with stress occurs in four phases:

- I. For stresses upto 200 Kg/cm^2 , there is no degradation of particles and B_r is almost negligible (close to the zero value).

- III. For stresses between 200 to 400 Kg/cm^2 , B_r increases relatively faster than that in phase I. In this phase grain crushing has started.
- III. A rapid rate of increase of B_r occurs for stresses between 400 to 1000 Kg/cm^2 .
- IV. For stress greater than a limiting stress of 1000 Kg/cm^2 , rate of increase of B_r is relatively less than that in Phase III.

For weak sands (Ganga, Kalpi, Calcareous and also crushed Granite and Napa basalt), the change of B_r with stress (Fig. 5.37) may also be described as:

- i) For stresses less than 20 Kg/cm^2 , the increase of B_r is considerable and particles undergo modification.
- ii) For stresses between 20 to 100 Kg/cm^2 , the modification continues but B_r increases at a lower rate compared to the rate in phase (i).
- iii) For stresses greater than 100 Kg/cm^2 , significant particle crushing begins and a significant enhancement in the rate of B_r is evidenced upto a limiting stress which is likely to be smaller than 1000 Kg/cm^2 .
- iv) For stresses greater than the limiting value, increase of B_r would be at a lower rate than that in phase (iii). A measure of the magnitude of limiting stress upto which B_r increases at higher rate and also the decrease in the rate of B_r at

stresses higher than the limiting stress, are best illustrated by the data for Napa basalt as indicated in Fig. 5.41. Here instead of σ'_1 , a stress function σ'_b , called the breakage effective stress (Hardin, 1985), has been used.

$$\sigma'_b = \sigma'_0 [1 + 9(\tau'_0 / \sigma'_0)^3] \quad (5.6)$$

where $\sigma'_0 = \frac{\sigma'_1 + 2\sigma'_3}{3}$

$$\tau'_0 = \frac{\sigma'_1 - \sigma'_3}{2}$$

It will be seen that in case of Marachi's data, the enhanced rate of increase of B_r is upto a limiting stress (σ'_b) of 250 Kg/cm^2 as compared to $\sigma'_b = 1150 \text{ Kg/cm}^2$ for strong Mol sand. Further the increase of B_r at a much smaller rate after the limiting stress are clearly noticed from the data of Marachi (1975) and Leslie (1975).

The behaviour of subangular to subrounded sands conformed to the range intermediate between that of weak and strong sands described above.

5.2.8 Hardin's Model for Particle Crushing

The hyperbolic relationship (Hardin, 1985) between relative crushing ratio (B_r) and stress ratio of breakage effective stress σ'_b and breakage reference effective stress, $\sigma'_{r'}$ is expressed as

$$B_r = \frac{(\sigma'_b / \sigma'_{r'})^{n_b}}{1 + (\sigma'_b / \sigma'_{r'})^{n_b}} \quad (5.7)$$

where n_b is called the breakage number.

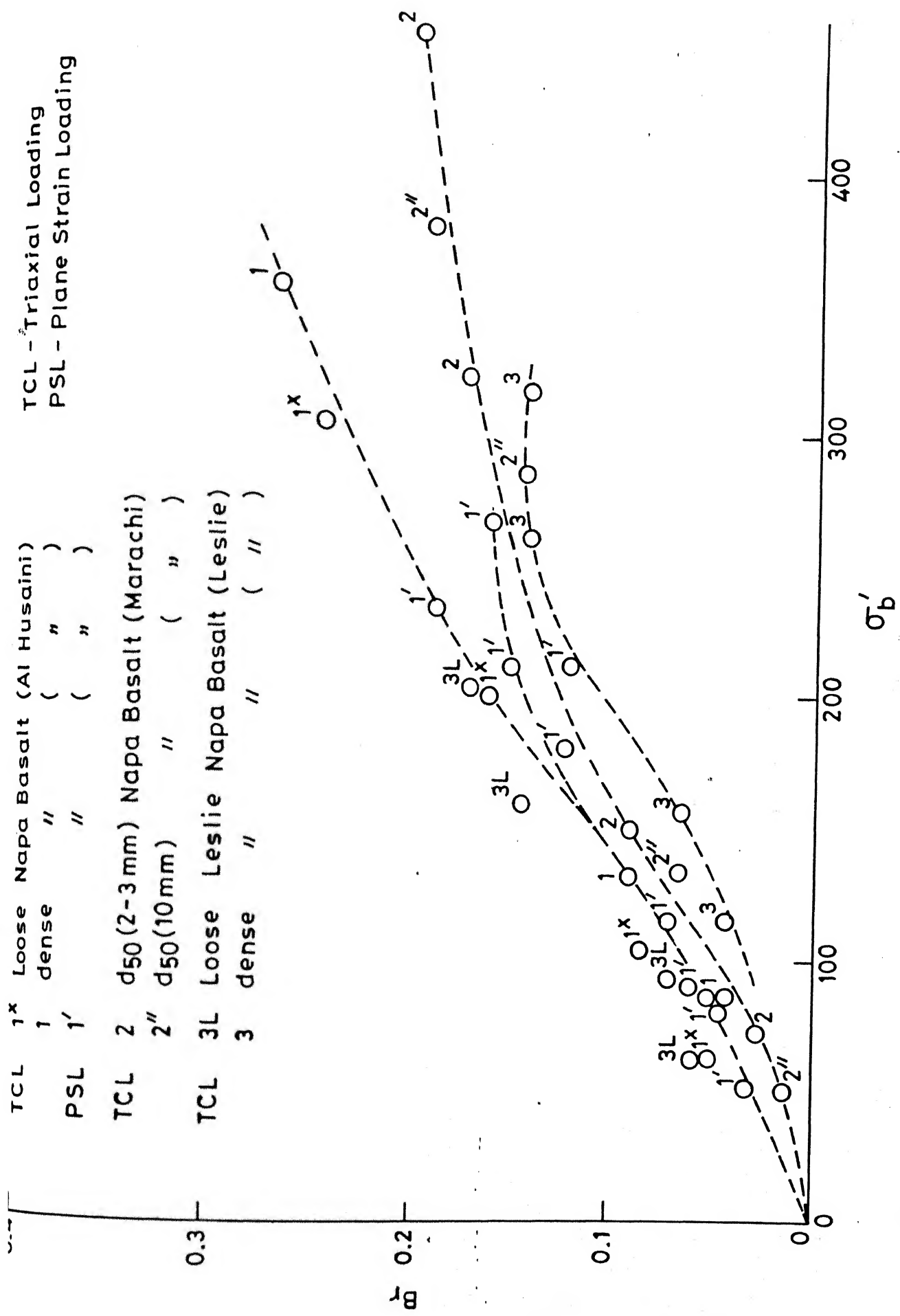


Fig. 5.41 Relationship between relative particle breakage and breakage effective stress.

Based on the analysis of available data on crushing for variety of sands, Hardin proposed a relationship between σ'_r and n_b as

$$\sigma'_r = 800 P_a (n_b - 0.3) \quad (5.8)$$

σ'_r has been shown to be related to particle shape number (n_s), crushing hardness (h), and initial void ratio (e_i). Using the values of σ'_r at different e_i , Hardin proposed that

$$\frac{(1+e_i)}{800 P_a} = H \text{ (constant)} \quad (5.9)$$

From the values of H , and the definition of particle shape number (n_s) the particle crushing hardness (h) is estimated using the expression

$$H = \frac{h^2}{n_s} \quad (5.10)$$

The computed value of h is approximately equal to the scratch hardness (Moh's Scale). The value of h and n_s for a variety of sands are reported by Hardin. In order to establish a stress path independent relationship between B_r and effective stress, the breakage effective stress, σ'_b , was defined by Hardin as

$$\sigma'_b = \sigma'_o (1 + 9(\tau'_o / \sigma'_o)^3) \quad (5.6)$$

where

σ'_b is a first stress invariant,

$$\sigma'_o = \frac{\sigma'_1 + 2\sigma'_3}{3} \quad \text{and}$$

$$\tau'_o = \frac{\sigma'_1 - \sigma'_3}{2}$$

According to Hardin, σ'_b normalized the relative breakage data from tests with varying values of $\sigma'_1/\sigma'_3 = R$ and to illustrate the above relationship crushed granite data of Lee and Farhoomand (1967) was used. The relationship of B_r with σ'_b and σ'_1 for crushed granite and Napa basalt are indicated in Figs. 5.42(a, b) and 5.43(a, b). The data of crushed granite show that scatter of data point for different $R(\sigma'_1/\sigma'_3)$ values is of the same order in Fig. 5.42(a) and 5.42(b). All the data points for Napa basalt (Hardin 1985) have been plotted in terms of B_r versus σ'_b/P_a (Fig. 5.43a) and B_r versus σ'_1/P_a (Fig. 5.43b). Hence again there is no unique normalization with respect to R in either plot (spot R values indicated). These comparisons tend to suggest that both σ'_1 and σ'_b produce more or less identical normalization of test data with varying values of $R = \sigma'_1/\sigma'_3$. It is thus evident that Hardin's particle crushing law (equation 5.7) could as well be stated in terms of σ'_1 instead of σ'_b . The advantages of such a formulation are obvious.

Incidentally, it is interesting to examine the σ'_b/σ'_1 ratio for a wide range of $R = \sigma'_1/\sigma'_3$ or $K = \sigma'_3/\sigma'_1$

$$\sigma'_b = \sigma'_1 \left(\frac{1+2K}{3} \right) \left[1 + 9 \left(\frac{3/2}{1+2K} \right)^3 \right]^{1-K}$$

$$= \sigma'_1 \left(\frac{1+2K}{3} \right) \left(1 + 30.4 \left(\frac{1}{1+2K} \right)^3 \right)^{1-K}$$

or

$$\frac{\sigma'_b}{\sigma'_1} = \frac{1+2K}{3} \left(1 + 30.4 \left(\frac{1}{1+2K} \right)^3 \right)^{1-K} \quad (5.11)$$

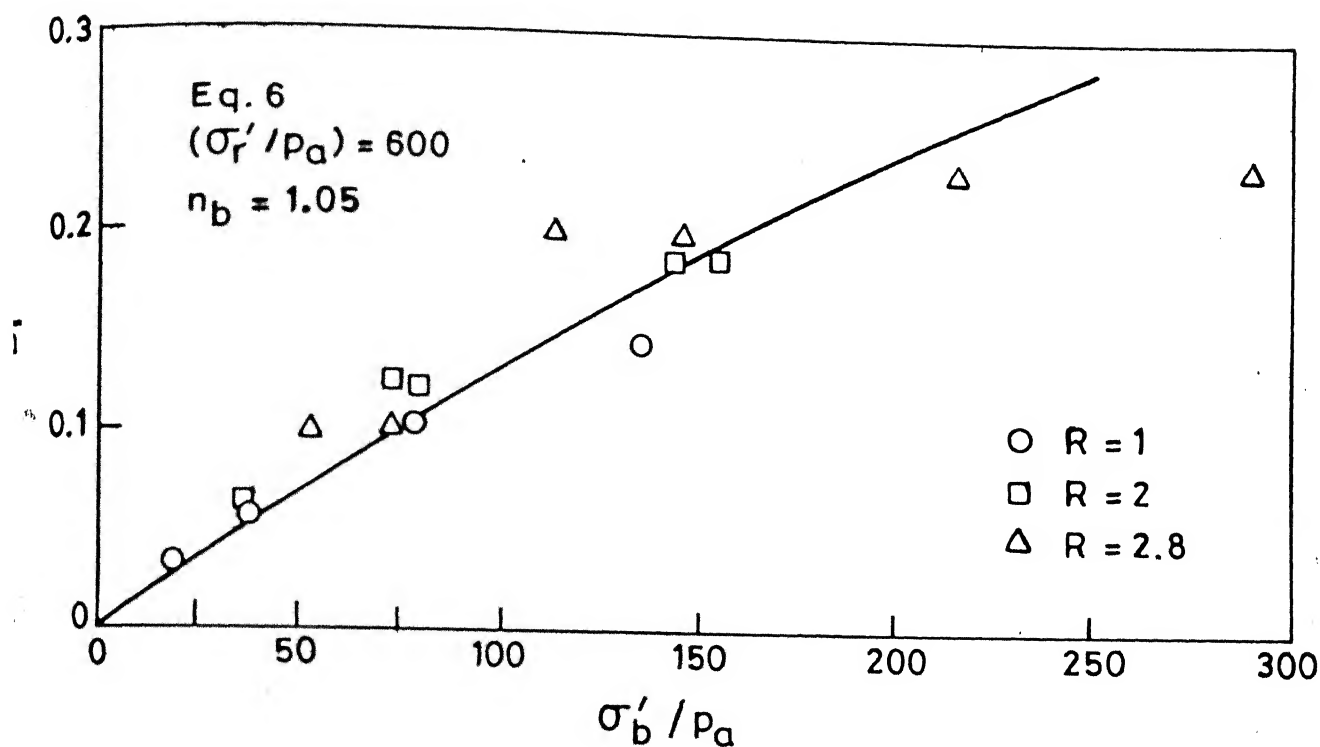


Fig. 5.42(a) Relationship between relative breakage and breakage effective stress; tests by Lee and Farhoomand

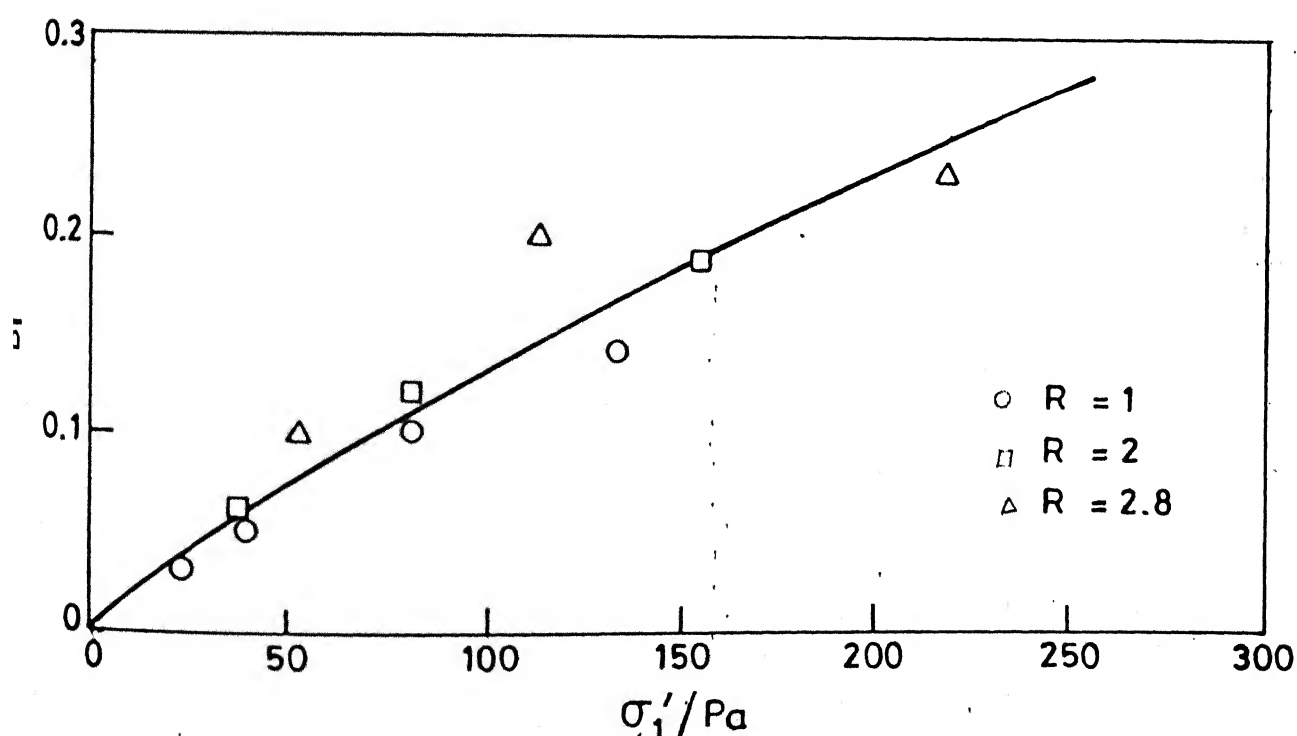


Fig. 5.42(b) Relationship between Br and σ_1' / P_a for crushed Granite (Based on the data from Lee and Farhoomand 1967)

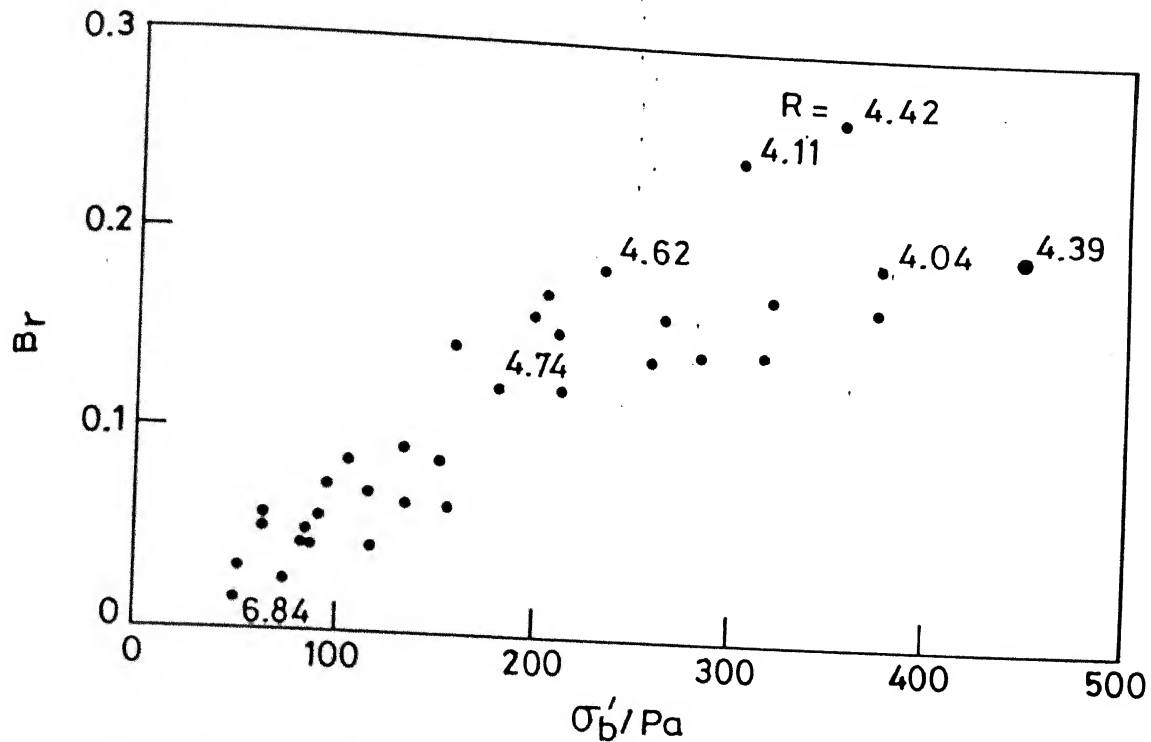


Fig. 5.43(a) Relationship between σ_b' / σ_y' and relative breakage (Based on data from Hardin, 1985)

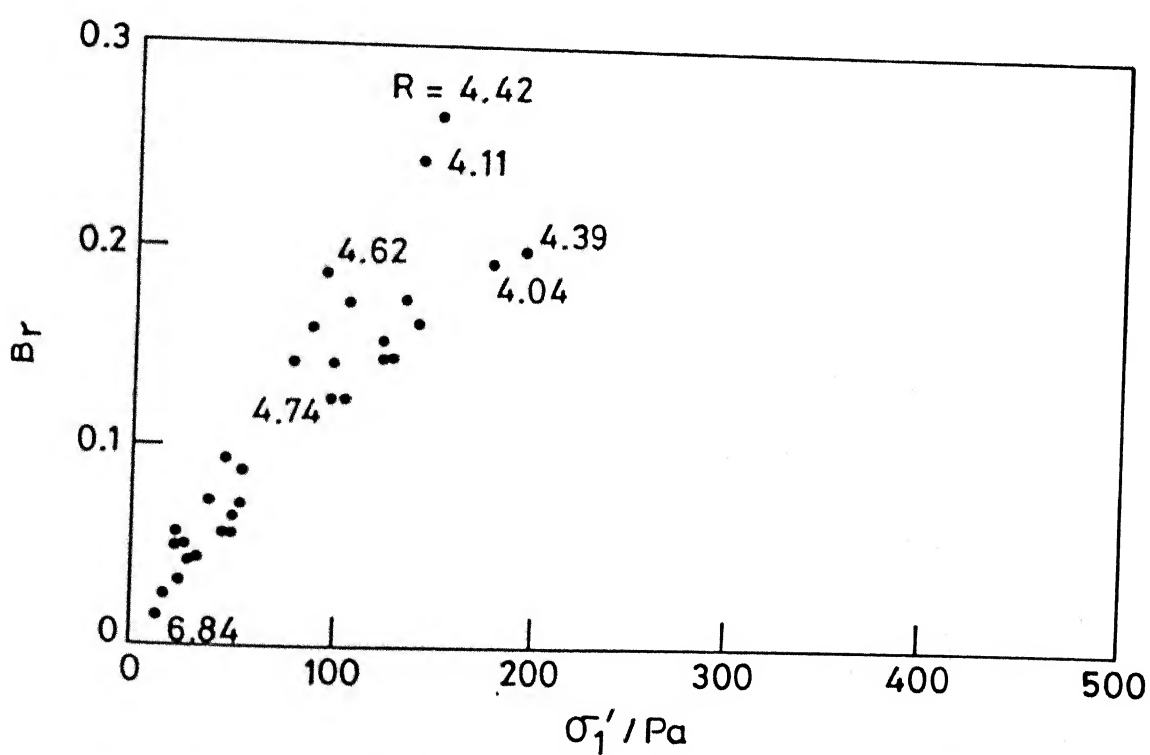


Fig. 5.43(b) Relationship between σ_1' / σ_y' and relative breakage (Based on data from Hardin, 1985)

For values of K ranging from 0.1 ($R=10$) to 1.0 ($R=1.0$), σ'_b/σ'_1 values are plotted (Fig. 5.44). The relationship suggests $\sigma'_b/\sigma'_1 = 5.5$ for $K=0.1$ ($R=10$) and $\sigma'_b/\sigma'_1 = 1.0$ for $K=0.485$ ($R=2.06$) and $K=1.0$ ($R=10$).

In case of Napa basalt, K_o under one-dimensional compression is 0.34 and the average value of K_o under plane strain is between 0.22 to 0.26. From Fig. 5.44, it can be seen that for compression under K_o and plane strain condition, the values of σ'_b/σ'_1 are 1.5 and 2.3 respectively. Under isotropic compression the value of σ'_b/σ'_1 is equal to one. Under condition of one-dimensional compression of sands, where K_o under normally consolidated state ranges between 0.33 to 0.55 (Mayne and Kulhawy, 1982), the values of σ'_b/σ'_1 would vary between 1.65 to 0.95 respectively. Therefore, as a first approximation, the value of σ'_b/σ'_1 could be taken as unity for estimating the crushing behaviour of sands under one-dimensional compression using the guidelines for h, n_s and σ'_r as proposed by Hardin (1985).

However, as shown in Figs. 5.42 and 5.43 the model parameters can as well be worked out in terms of σ'_1 rather than σ'_b in which case no approximations are necessary. The main difficulty in σ'_b parameter is the necessity of obtaining reliable values of K_o in one-dimensional and plane strain conditions of compression. In case of triaxial anisotropic compression σ'_b can be readily estimated.

Hardin's particle crushing law (equation 5.7) assumes a hyperbolic relationship between B_r and stress (σ'_b or σ'_1).

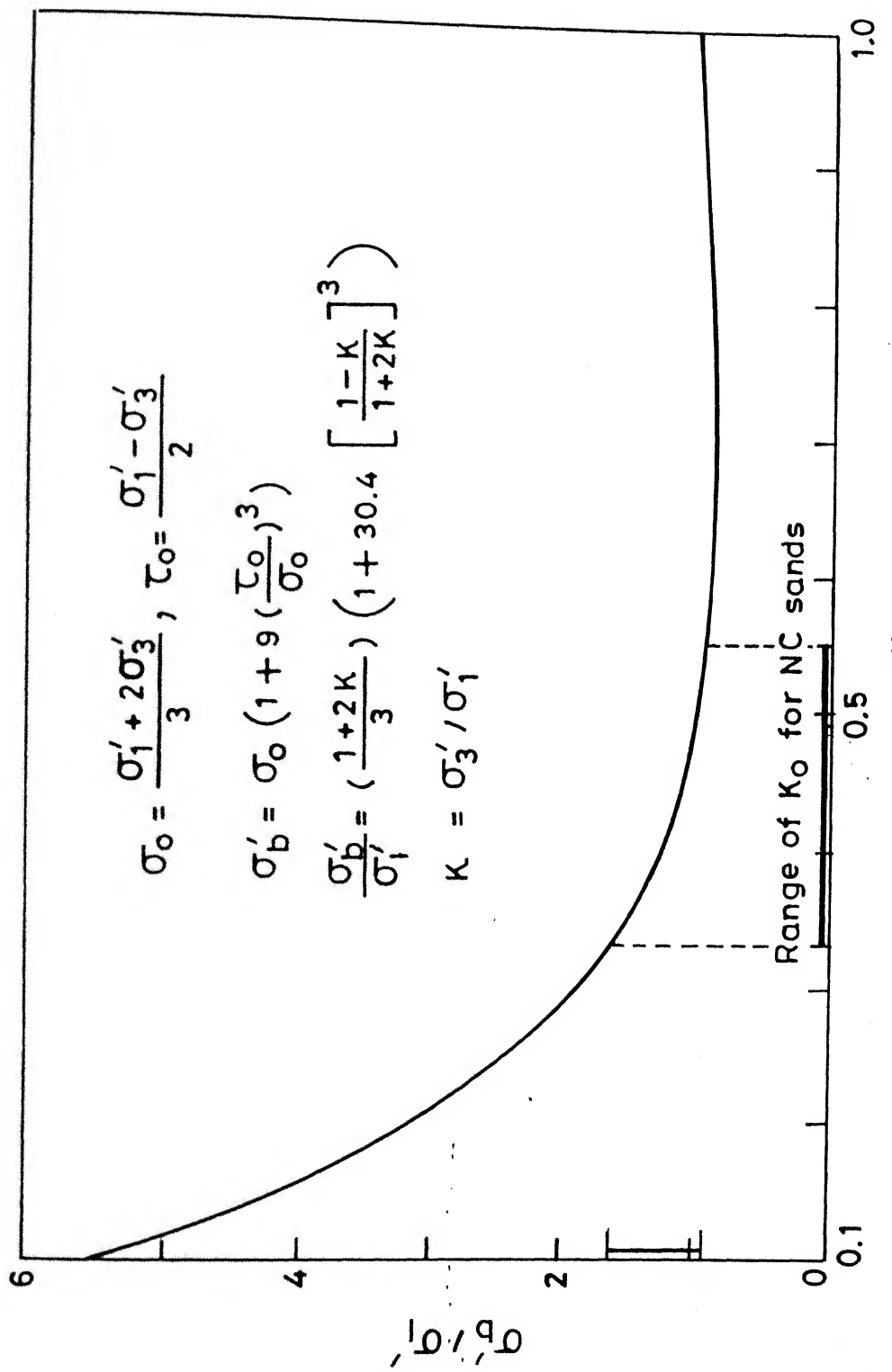


Fig. 5.44 Relationship between σ_b'/σ'_1 and K .

However, the proposed relationship has two material parameters (σ'_r and n_b) which, if varying over a wide range, may control the shape of the B_r versus stress relationship as evident from Fig 5.45. The values of σ'_r and n_b have been chosen for the extreme cases of weak and strong sands. It is clear that the form of B_r versus stress relationship varies with σ'_r and n_b values. The characteristic form as proposed by Hardin is valid for all sands having σ'_r between 300 to 1000 Kg/cm ($h=6.3$ to 6.5). In particular, this is true for angular weak sands. Available data for a variety of sands is also shown in Fig. 5.45.

Although at the onset, it appears tempting to conclude that within the scatter range the experimental data seems to fit the computed relationship based on equation 5.7, it would be instructive to observe the rate of change of B_r with stress for the weak as well as the strong sands and then compare these trends with the experimental observations made earlier.

In case of weak sands ($\sigma'_r = 300 - 1000 \text{ Kg/cm}^2$), the model indicates initial higher rate of change of B_r upto a limiting stress after which the rate decreases significantly. The limiting stress increases with increasing σ'_r . However, in case of strong sands, a low initial rate of change of B_r followed by an increased rate at high stresses is noticed. The experimental data for Napa basalt (Marachi et al 1969) and Mol sand (De Beer 1963) contradict this predicted trend.

(Fig. 5.45). For all materials plotted here, either σ'_b was available in literature (Napa basalt) or was computed on the basis of available information on τ'_o/σ'_o and σ'_o for Mol and Ottawa sands. The data for Tayoura sand is for isotropic consolidation and hence $\sigma'_1 = \sigma'_b$.

In case of Napa basalt, the data points plot well on the predicted curve upto 250 Kg/cm^2 after which the data transcends towards the predicted curve for a stronger sand. The comparison between data and the model prediction is illustrated in Fig. 5.46. The model would thus predict B_r well upto 250 Kg/cm^2 for Napa basalt data which was used to calibrate the model. At higher stresses, the model however, would considerably over predict B_r values. A similar trend is observed in case of Mol sand (Fig. 5.45). The experimental evidence reviewed in Figs. 5.36, 5.37, 5.38, 5.41 and 5.45 also suggest that a value of B_r of around 0.25 will be attained at a stress levels of the order 200 Kg/cm^2 and 900 Kg/cm^2 in case of weak sands and strong sands respectively. Therefore, it would seem that within 100 Kg/cm^2 maximum B_r values that could be attained for weak sands are of the order 0.15 and for strong sands $B_r=0$. As already indicated values of B_r between 0.25 to 0.3 may only be obtained at much higher stresses. In practice in the range of stresses encountered, the B_r value is thus likely to be less than 0.5. The model prediction would estimate $\sigma_b=500 - 1500 \text{ Kg/cm}^2$ (weak to strong) for $B_r=0.5$ and $\sigma'_b > 10,000 \text{ Kg/cm}^2$ for $B_r=1.0$ for all types of sands (Fig. 5.47). Clearly such high stresses needed to get values of $B_r > 0.5$

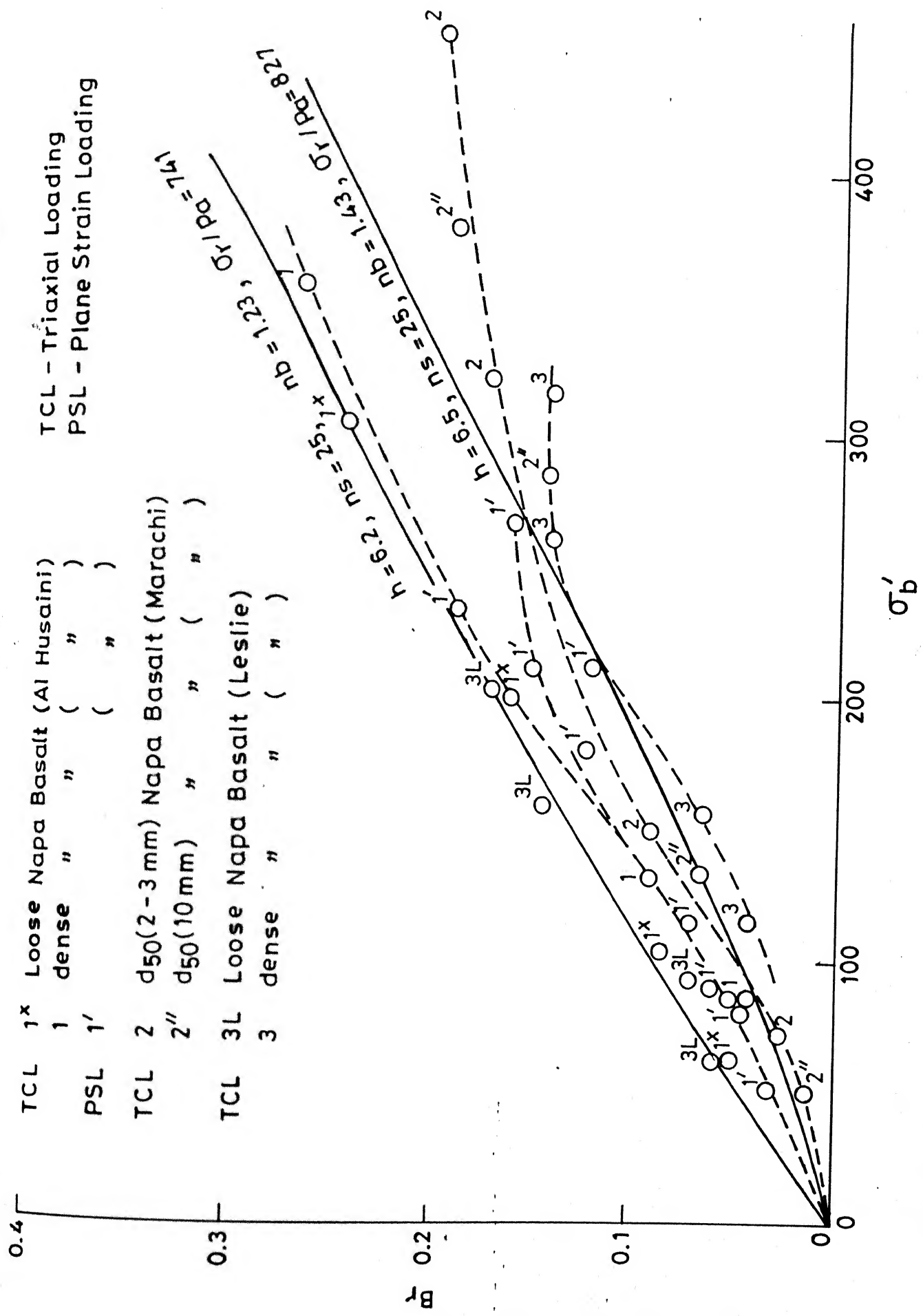


Fig. 5.46 Relationship between relative particle breakage and breakage effective stress.

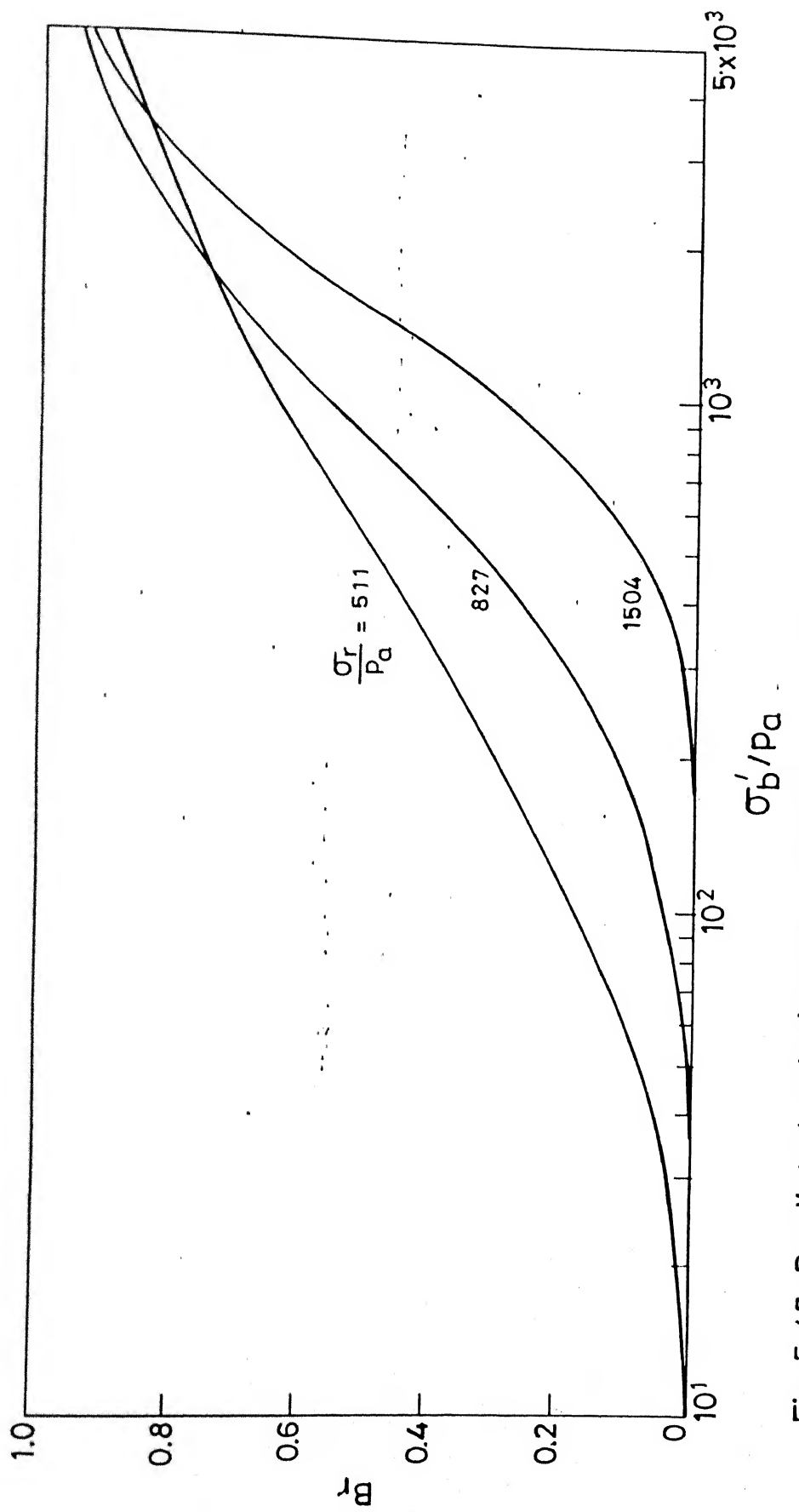


Fig. 5.47 Predicted relationship between relative breakage and breakage effective stress.

are not likely to be encountered in routine engineering practice.

It would also seem that in case of weak sands, grain crushing is of major concern in the study of strength and compressibility behaviour in the range of stresses encountered in case of deep foundation or during cone penetration testing. However, in case of strong sands, like Mol and standard, grain crushing becomes important for stresses greater than 300 Kg/cm^2 . For subrounded to subangular sands which fall in between weak and strong sands, there is likely to be significant grain crushing at stress level upto 300 Kg/cm^2 .

Based on these results and comparisons with prediction, the following comments on the Hardin's model are pertinent:

1. In case of prediction of relative breakage under stress based on the hyperbolic law, the shape of the predicted curve seems to be highly sensitive to the magnitude of reference breakage stress (G'_r) and n_b , both of which depend strongly on the nature of sand (Fig. 5.45).
2. The continuous increase of B_r upto unity with stress, following the hyperbolic law, is not reflected by the experimental data, for both weak and strong sands (Figs. 5.45, 5.46). The available trends suggest flattening of the B_r versus stress curves around B_r between 0.2 to 0.3, and thus the predicted rates of increase of B_r beyond the corresponding limiting stresses for weak and strong sands are much higher than the actual experimental values (e.g. Napa basalt and Mol sand).

3. For the data on crushed granite and Napa basalt used by Hardin to calibrate his model, it would appear that σ'_1 is as good a stress path normalizing function as σ'_b (Figs. 5.42 and 5.43). Thus it may be suggested that the model could be worked out in terms of σ'_1 which is much easier to obtain directly. With this modification, equation 5.7 may then be written in the form

$$B_r = \frac{(\sigma'_1 / \sigma'_r)^{n_b}}{1 + (\sigma'_1 / \sigma'_r)^{n_b}} \quad (5.7)$$

For the weak angular sands used in this study, the relevant values of σ'_r and n_b obtained from Hardin's guidelines are

$$\sigma'_r = 511 - 800$$

$$n_b = 0.939 - 1.230$$

For these sands $n_g = 25$ and h varies from 6.5 to 7.2.

It is interesting to compare the range of B_r values at stress level of 176 Kg/cm^2 for these sands using Eqn. 5.7 with different σ'_r and n_b values. The values of B_r works out to be around 0.27 and for $\sigma'_r = 511$ and $n_b = 0.939$ whereas it is around 0.13 for $\sigma'_r = 80000$ and $n_b = 1.230$. This range of B_r (0.13 to 0.27) compares very well (Fig. 5.37) with the experimental range of B_r (0.13 to 0.23). In this range of stresses, the modified Hardin's model clearly provides a reasonably good prediction of particle crushing for weak angular sands.

4. The relative breakage parameter (B_r), proposed by Hardin is a much superior index for overall crushing than some of

the indices reported by others. For example, one such index designated as the crushing coefficient (C_c) expressed as "the ratio of percentage of particles after being subjected to stress finer than D_{10} of the original sand, and percentage of particles of the original sand finer than D_{10} of the original sand" (Datta et al, 1980), developed for Calcareous sand takes into account only the D_{10} fraction. In contrast to this, B_r takes into consideration the changes in size for the entire range of grains. Also in its definition, the particle size is considered in terms of B_p (Fig. 5.22) and the total breakage, B_T takes into account particle size and gradation shape and mineralogy (Fig. 5.46a). Thus the index C_c in some cases may provide misleading results as it considers changes in one particular size only. Values of C_c for Kalpi 1, Kalpi 2, Ganga and Ganga with enhanced mica (Fig. 5.48) reveal that the C_c for Kalpi 1 is higher than Kalpi 2, whereas the B_r value for Kalpi 2 is roughly 1.5 times higher than that of Kalpi 1. Kalpi 2 has larger grains which are aggregates of small particles cemented together by carbonate and therefore at same stress a higher particle breakage B_T is expected which is in fact obtained. The value of B_T for Kalpi 2 is roughly 1.7 times higher than that of Kalpi 1. In case of Ganga sand samples similar trends can be observed. Again C_c for Ganga works out higher than for that same sand with enhanced mica content (65% mica as compared to 10% in original Ganga). The B_r value however follows the expected trend.

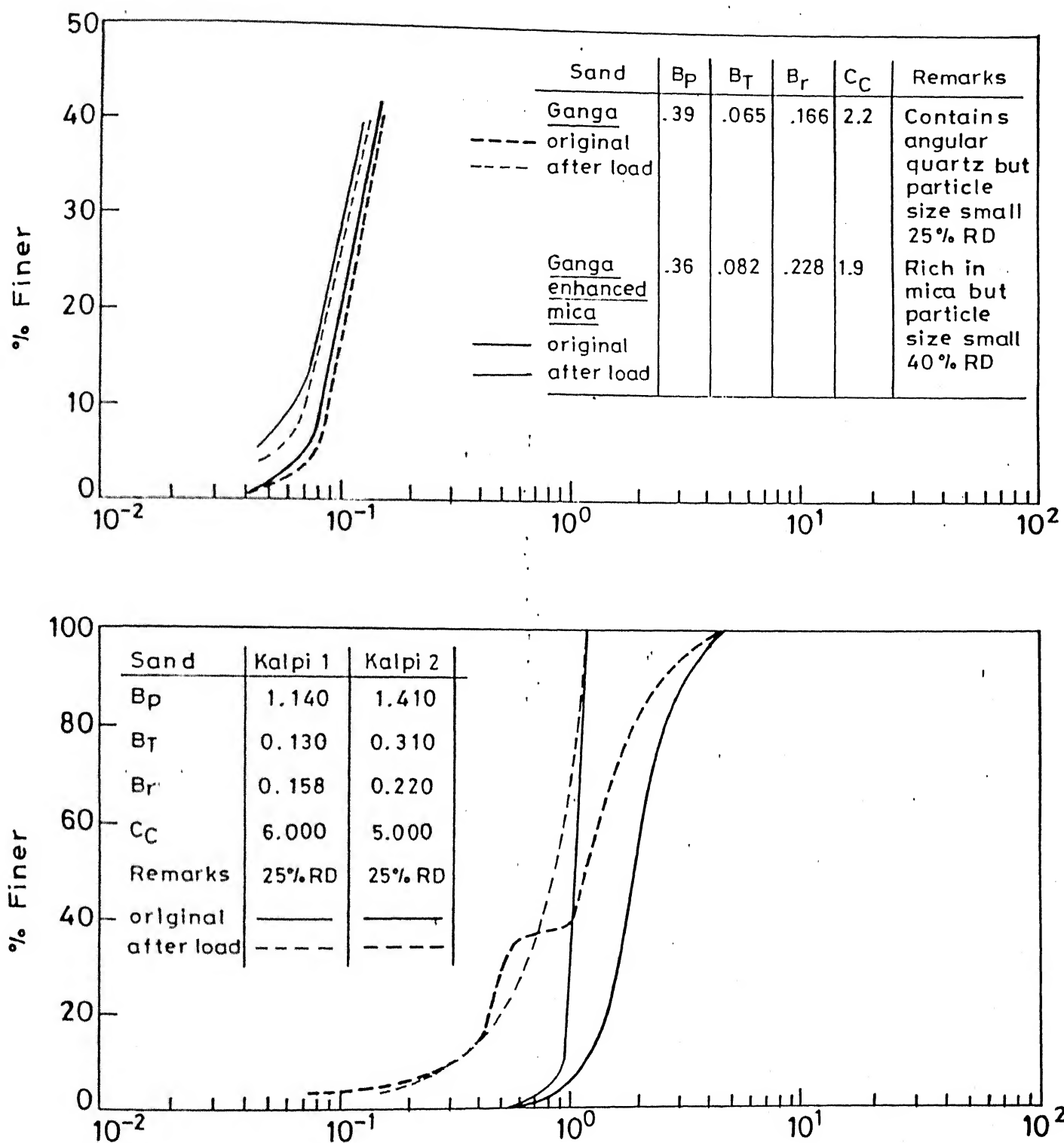


Fig. 5.48 Gradation curve before and after loading for Ganga, Ganga enhanced mica, Kalpi 1 and Kalpi 2.

Thus it can be inferred that the Hardin's B_r index is a superior indicator of crushing of grains and therefore should be preferred over all other indices that consider changes of one particular size only.

5. The shape number (n_s) used in the computations of reference breakage stress may be correlated with the Powers' roundness index (Fig. 5.49). This empirical correlation between n_s and roundness index would enable a better classification of grain shape which correlates with number of tangents on grain boundary as discussed earlier (Table 5.5). Thus the four parts shape description of Hardin can further be refined.

5.3 COMPRESSIBILITY AND CONSTRAINED MODULUS OF SANDS

5.3.1 Compressibility

5.3.1.1 General

Stress-strain behaviour of sands, as studied in the oedometer test (Hendron, 1963; Roberts, 1964) has been considered to be of three stages (Lambe and Whitman, 1969) as below:

- a) Locking behaviour during which sand gets "stiffer and stiffer as the level of stress increases" upto 150 Kg/cm^2 and "finally, a stage is reached in which already dense arrays (of particles) are being squeezed more tightly together as contact points crush, thus following a little more sliding".

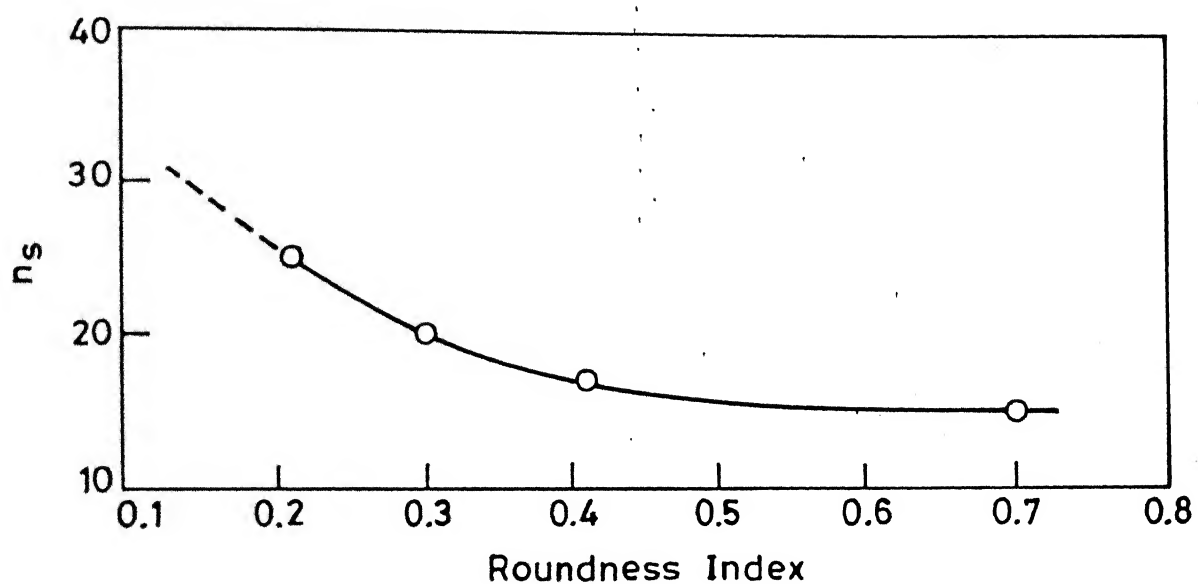


Fig. 5.49 Relationship between shape number and roundness.

Table 5.5 : Value of Shape Number(n_s), Roundness Index (R) and Tangent (T) for Different Particle Shapes

Particle Shape	Value of n_s	Value of roundness	Average tangent
Angular	25	0.21	11
Subangular	20	0.30	8
Subrounded	17	0.41	6
Rounded	15	0.84	4

- b) Yielding behaviour as a "result of fracturing of individual sand particles which permits large relative motions between particles" - at stresses equal to and greater than 150 Kg/cm^2 . Considerable particle degradation takes place during this stage.
- c) Fracturing and crushing, leading to tighter packing of particles and increase of number of particle contacts, thus the sand once again becomes stiffer and stiffer as the stress increases still further".

These distinct stages of compression were observed for Ottawa sand which is medium to coarse and well rounded quartz sand. However, actual stress level at which compression behaviour of sand changes from locking to yielding depends on many factors such as mineralogy, particle size, shape, roughness, gradation and relative density. The stress level at which crushing and fracturing of particle becomes significant is designated as the "critical stress". This stress is smallest when the particle size is large, the soil is loose and has uniform gradation, the particles are angular and the strength of the individual mineral particle is low (Lambe and Whitman, 1969). The compressibility of sands depends on a number of material-related and stress-related factors (Clayton et al, 1985). Relative density of sands alone is not sufficient to characterize the performance of different granular soils. For example, the compressibility of two sands having same mineral composition and relative density is significantly influenced by particle shape (Holubec and D'Appolonia, 1973; Kapoor, 1985). In general

the compressibility is high when the sand is loose, the grains are angular, the coefficient of uniformity (C_u) is low, the average particle size is small, inter-particle cementation is weak and the ageing effects are insignificant. Stress history, stress level and stress path have significant influence on compressibility of sands (Yudhbir and Rahim, 1987). This then portrays the broad picture of deformation behaviour of sands over a wide range of stresses. Much needs to be done to quantify the effect of these varied factors.

5.3.1.2 Test Results

The compression test data on oedometer for the sands investigated under both loose and dense states has already been presented in Chapter 4. In order to highlight the major factors influencing compressibility, test results of loose samples only will be considered here. The stress versus strain relationships upto a stress level of 176.32 Kg/cm^2 for rounded quartz Standard sand, angular Kalpi sand with carbonate coating, subrounded to subangular Calcareous sand and angular micaceous Ganga sand are presented in Fig. 5.50. Results for two fractions of Kalpi sand i.e. Kalpi 1 and Kalpi 2, and two variations of Ganga sand i.e. Ganga with enhanced mica and with mica removed, are also shown in this figure. The stress-strain behaviour of these sands, in the low stress ranges is illustrated in Figs. 5.51 and 5.52a. At a given stress level upto 10 Kg/cm^2 , the axial strain increases from low compressible well-rounded quartz Standard

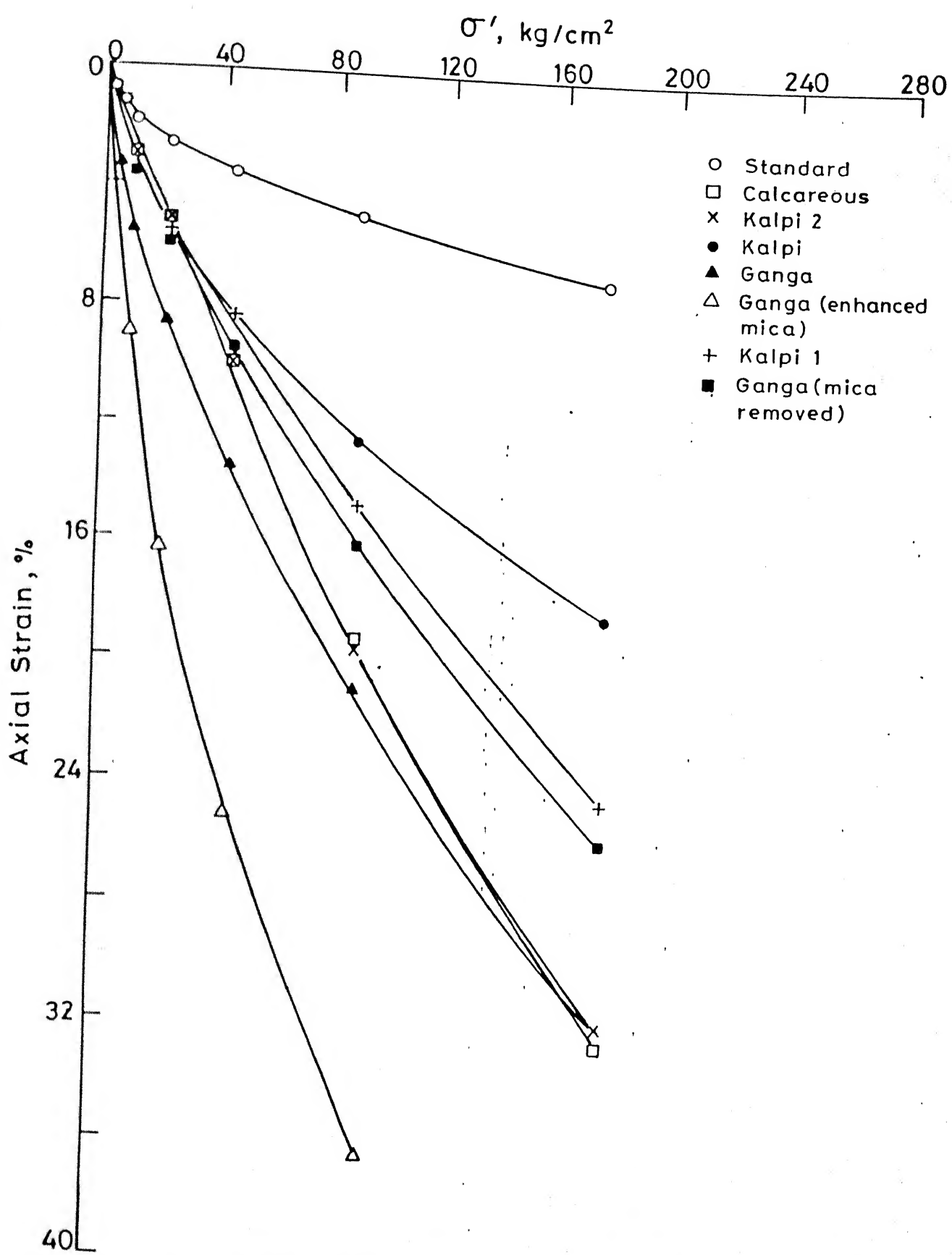


Fig. 5.50 Stress-strain relationship for the loose sands at high stress level.

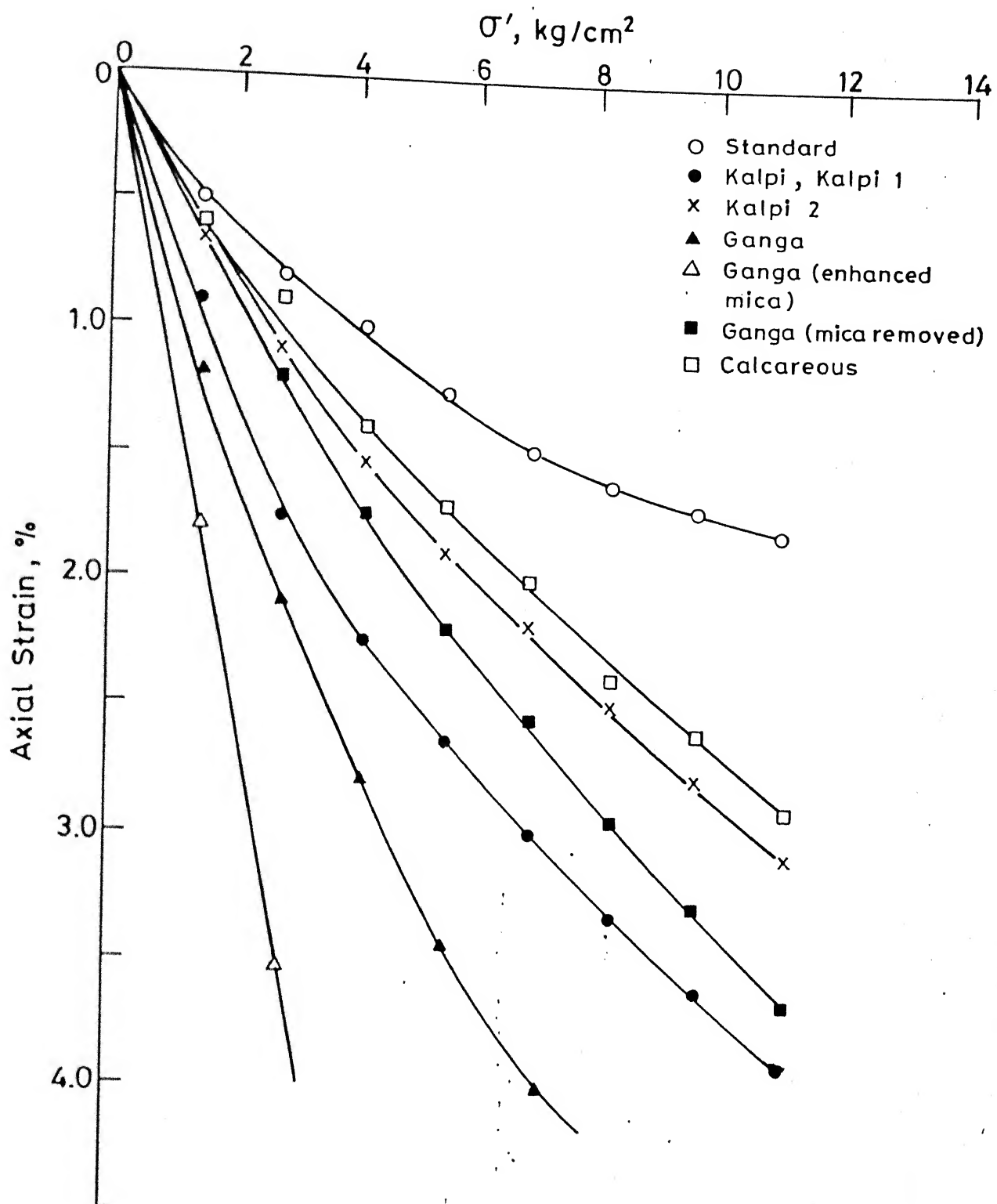


Fig. 5.51 Stress-strain relationships at low confining stress for loose sands

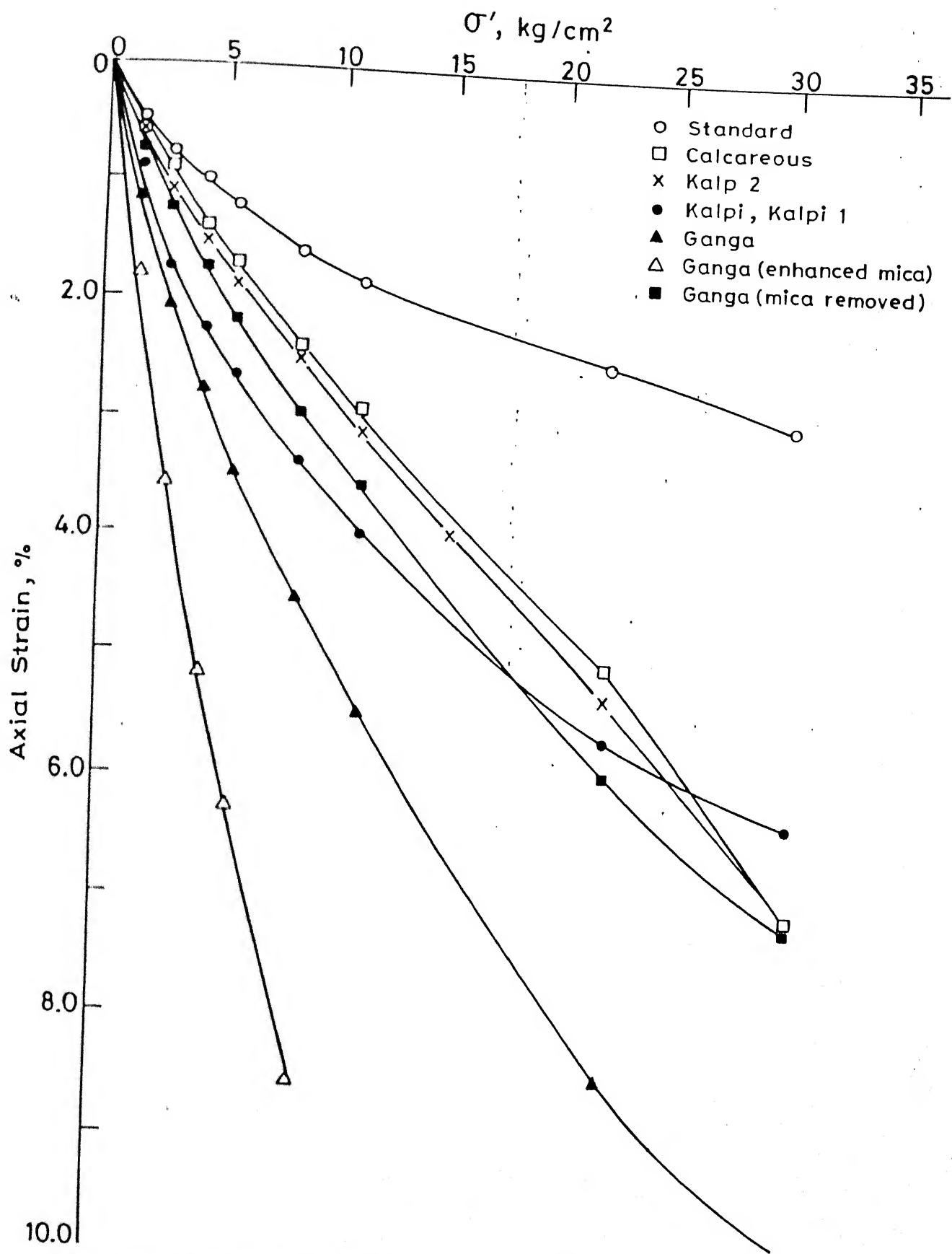


Fig.5.52(a) Stress - strain relationship at low confining stress for loose sands.

sand to very high compressible mica-enhanced fraction of Ganga sand ($\approx 60\%$ mica). Calcareous, Kalpi 2, Ganga with mica removed, Kalpi, Kalpi 1 and Ganga sands arranged in the order of increasing axial strain.

In case of Kalpi 1, Kalpi 2, and Calcareous sands (Fig. 5.52a), their compressibility undergoes a significant change under stress level greater than $25-30 \text{ Kg/cm}^2$. Kalpi sand and its fraction Kalpi 1 have identical behaviour upto a stress level of 40 Kg/cm^2 (Fig. 5.50) after which Kalpi 1 exhibits higher compressibility compared to the Kalpi sand. Kalpi 1 being coarse-grained and poorly graded ($C_u=1.07$) shows higher compression as compared to a well-graded ($C_u=4.81$) Kalpi sample at the same stress level. This marked difference in the stress-strain behaviour of Kalpi and Kalpi 1 is related to the higher degree of grain modification under stress as indicated earlier (Fig. 5.35). The Kalpi 2 fraction, consisting of large angular grains, shows a better interlocking upto 25 Kg/cm^2 after which due to very high degree of grain modification (Fig. 5.26), it experiences much greater strain than Kalpi and Kalpi 1 at the same stress level. The Calcareous sand exhibited even better interlocking behaviour than Kalpi 2 sand upto stress level of 25 Kg/cm^2 after which both these materials exhibited identical stress-strain response. The Ganga-fraction with mica removed has slender angular quartz and feldspar grains and upto a stress level of 18 Kg/cm^2 it has indicated lower strain than Kalpi sand. However, at higher stress levels this Ganga-fraction experiences much greater axial strain

and upto a stress level of 18 Kg/cm^2 it has indicated lower strain than Kalpi sand. However, at higher stress levels this Ganga-fraction experiences much greater axial strain than Kalpi, with identical stress-strain behaviour as that of Kalpi 1. Here again slender, angular quartz and feldspar grains of poorly graded sand have experienced much more grain modification than the well-graded Kalpi sand. The stress-strain behaviour depicted by Standard sand, Ganga sand and Ganga with mica enhanced has consistently shown the increasing strain with stress right upto stress level of 176.32 Kg/cm^2 . However, the rate of variation of strain with stress, progressively decreases as stress level increases throughout the loading in case of Standard sand. However, a progressive flattening of the slope of stress-strain curve has been noticed for Ganga sand at a stress level of 4 Kg/cm^2 and for the Ganga sands fraction with mica enhanced at a stress level of 10 Kg/cm^2 .

The distinct differences in the stress-strain response of sands under high stress conditions as brought out in the present study can be attributed to variations in grain shape, size, gradation and mineralogy. The effect of grain angularity and gradation on the behaviour of Standard, Calcareous, Kalpi and Ganga sand at comparable density under stress was independently brought out by Sahu (1988) in a series of well conducted plate load tests on these sands, the results for which are presented in Fig. 5.52b. These tests represent the behaviour of the sands at extremely low

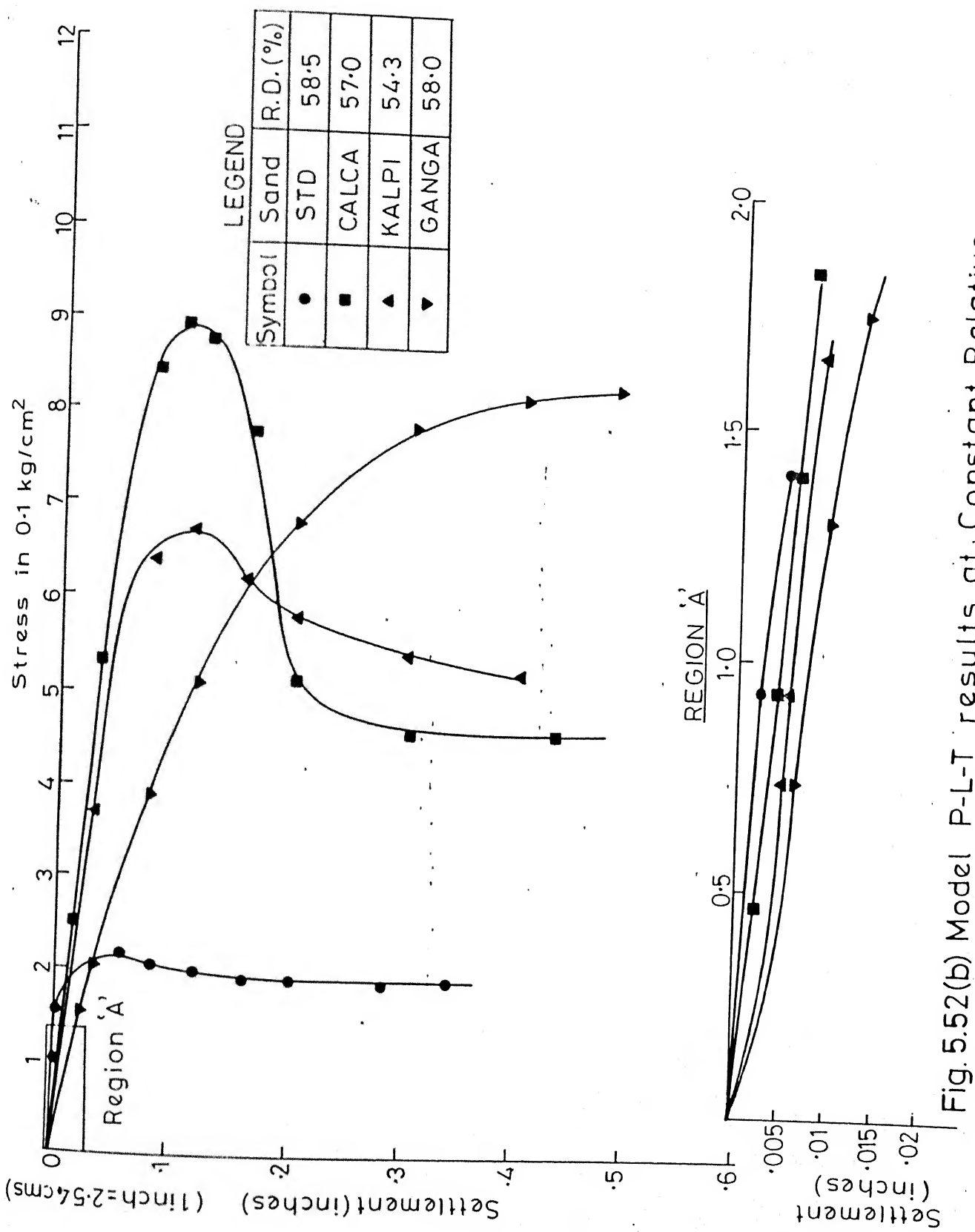


Fig. 5.52(b) Model P-L-T results at Constant Relative density for four sands (Sahu, 1988)

contrast to practically non-dilatant 'Standard sand' composed of nearly non-interlocking well-rounded quartz grains. Ganga sand being most compressible undergoes larger settlement for the same stress and does not exhibit general shear failure as exhibited by Kalpi and Calcareous sands. This is in conformity with the compressibility considerations reported by Vesic (1963). Inset of region A in Fig. 5.52b clearly shows that the slope of the stress settlement curves is in the order of compressibility of these sands (Fig. 5.51).

Yudhbir and Rahim (1987) in a review of the available information on sand compressibility have observed that the compressibility is high in general when the sand is loose, the grains are angular, C_u is low, the average particle size is small, the particle surface is rough, the grain mineral strength is small, interparticle cementation is weak and ageing effects are insignificant. Except for the effect of ageing, the results obtained in the present study (Figs. 5.50, 5.51 and 5.52) clearly highlight the effect of grain shape, size, roughness, gradation and mineralogy. However, stress-strain curve of sands having same mineral composition is the end result of a complex interaction of particle shape, size, angularity and gradation. This is well illustrated in case of Kalpi, Kalpi 1 and Kalpi 2 sands. Ganga sand and its variations (one with mica removed and other with enhanced mica) clearly bring out the effect of mica content on sand compressibility. Terzaghi (1925), Moore (1971) and Yudhbir (1978) have brought out the influence of mica content on the compressibility of sands. Mitchell (1976) has observed that

addition of mica significantly increases the compressibility of poorly graded sands only. The three Ganga samples have practically identical particle size and gradation. The Standard sand exhibits the characteristics of a sand made of smooth well-rounded quartz grains.

The stress-strain relationships for the sands investigated in this study are presented in Fig. 5.53 along with the results for a variety of sands reported by earlier workers. Mol sand, Standard sand, Ottawa sand, Sandy point sand, and Dune sand etc. depict stress-strain-behaviour of quartz sands of low compressibility having rounded to well-rounded grains. The Ottawa sand, Sandy point sand and Mol sand results are for dense-state whereas the data for Dune sand and Standard sand is for loose state. Results for angular ground quartz show clearly the effect of d_{50} , the higher compression recorded for ground quartz with 0.42-0.84 mm size (curves 6, Fig. 5.53) grains is no doubt due to higher grain crushing. Kalpi, Kalpi 1, and Ganga sand with mica removed are predominantly angular sands with dominant quartz and feldspar, with Kalpi samples having 18-24% carbonate (as coating on quartz and feldspar grains) and Ganga fraction having 2-5% mica. Fine-grained Ganga fraction gives higher compression than coarse-grained Kalpi, Kalpi 1 and Kalpi 2 sands. Ganga sand, and Calcareous sand, in the high stress range give more or less identical compression. Extremely high compression was observed for mica-enhanced Ganga sand fraction and crushed mica (Oberoi 1983).

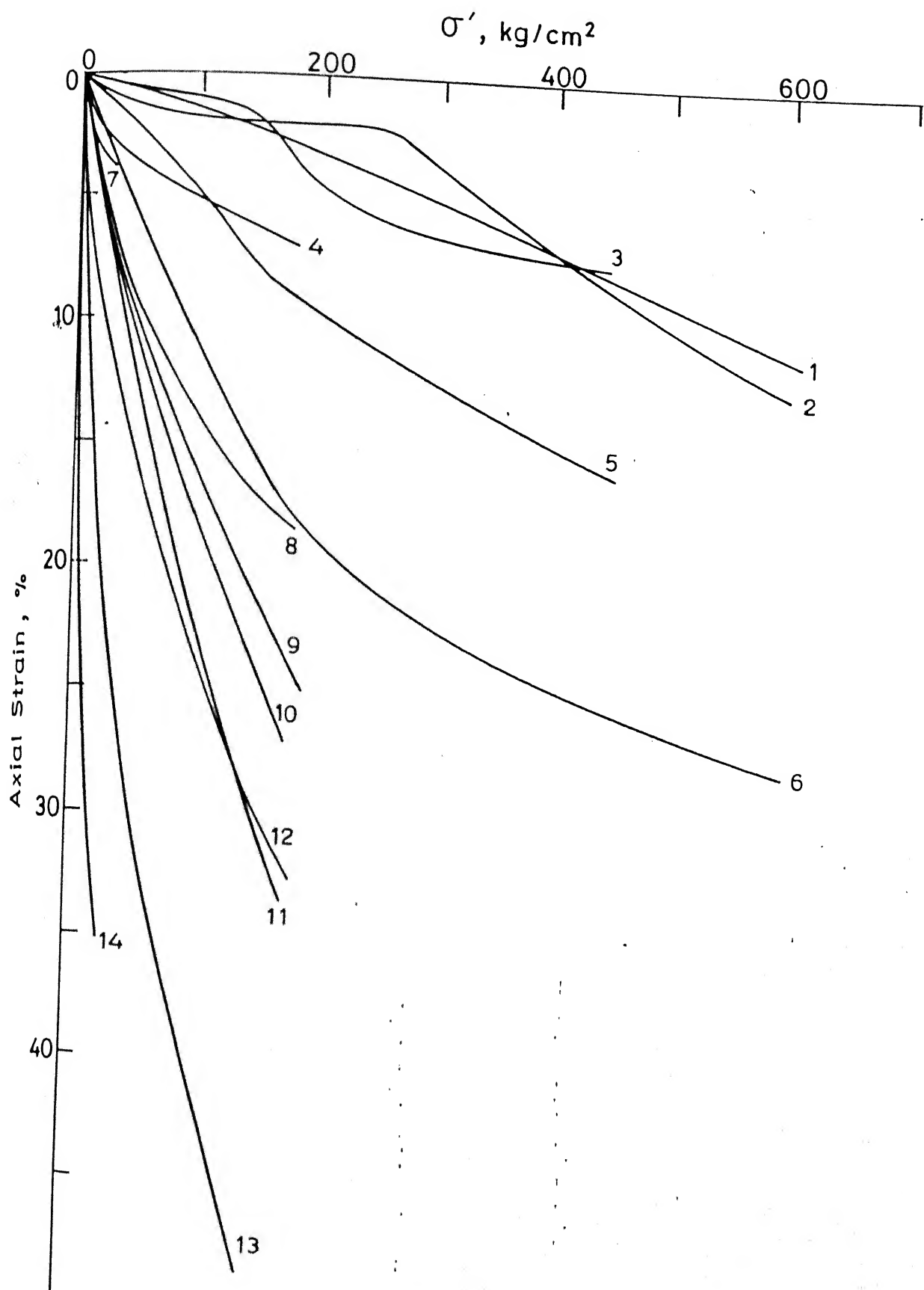


Fig. 5.53 Stress-strain relationships for variety of sands at high confining stress (Index for numbers as in Table 5.6)

On the basis of results shown in Fig. 5.53, it may be concluded that typical compression response for three categories of sands can be clearly characterized. Sands with well-rounded to subrounded quartz grains behave as materials of low compressibility. Angular quartz and feldspar-rich sands with or without carbonate cementation depict behaviour of moderately compressible materials while the micaceous (10-15%) and carbonate sands (\approx 95%) behave as highly compressible materials. The flaky mica sample gives the highest compression compared to all the sands shown in Fig. 5.53. The grouping of sands of low, moderate and high compressibility is indicated in Table 5.6. Even though factors such as grain size, shape, angularity, gradation, relative density and mineralogy seem to govern the compressibility of sands in a complex manner, the grain angularity and mineralogy (for the same relative density) appear to be the significant controlling factors.

5.3.2 Constrained Modulus

Janbu (1963, 1985) proposed a parabolic law governing variation of constrained tangent modulus, $M (= \frac{d\sigma'}{de})$ with vertical stress in the form

$$M = m_0 P_a (\sigma'/P_a)^{m_1} \quad (5.12)$$

where

P_a is atmospheric pressure,

m_0 is a modulus number, and

m_1 is the exponent indicating rate of "change of M with σ' , taken as 0.5 by Janbu.

Table 5.6 : Classification of Sands According to Their Compressibility

Sands Shown in Fig. 5.53	No. Assigned	Grain Size d_{10} d_{50} d_{60}	Shape	DR	Remarks
Mol Sand (De Beer 1963)	1	— 0.2 —	rounded	dense	
Ottawa (Robert 1964)	2	0.45 0.6 0.64	rounded	dense	
Sandy Point Sand (Lambe & Whitman 1969)	3	— — —	rounded	dense	low compressibility
Standard	4	0.36 0.48 0.50	well rounded	loose	
Dune Sand (Oberoi 1983)	7	0.15 0.3 0.30	rounded	loose	
Ground quartz (0.15 to .48 mm Lambe & Whitman)	5	— — —	either dense or rounded to subrounded or both		
Ground Quartz (.42 - 0.84)	6	— — —			
Kalpi	8	0.27 1.0 1.30	very angular	loose	Moderate compressibility
Kalpi 1	9	0.95 1.0 1.05	very angular	loose	
Ganga (mica removed)	10	0.10 0.48 0.22	angular	loose	
Ganga	11	0.09 0.18 0.22	angular	loose	High compressibility
Calcareous	12	0.27 0.43 0.48	sub rounded to subangular	loose	
Ganga (enhanced mica)	13	0.08 0.17 0.20	very angular	loose	Very high compressibility
Micaeous sand (Oberoi, 1983)	14	0.14 0.7 0.90	very angular	loose	

Yudhbir and Rahim (1987) have examined the stress range for which this law may be applicable for sands with varying relative density and particle angularity. Bellotti et al (1985), on the basis of a set of chamber test results for two sands, proposed that constrained modulus (M) is related to the relative density and applied stress as

$$M = m_0 P_a (\sigma'/P_a)^{m_1} \exp(m_2 \cdot D_R) \quad (5.13)$$

where

m_0 , P_a , and m_1 have the same meaning as

defined in eqn. 5.12 and

m_2 is an experimental coefficient indicating the rate of change of M with relative density (D_R).

Using Eqn. 5.12, the variations of modulus M with stress and relative density have been investigated for the sands chosen in this study. Evaluation of experimental coefficients m_0 , m_1 and m_2 is illustrated in Figs. 5.54 to 5.61. Coefficient m_0 is the value of M at $\sigma' = 1.0 \text{ Kg/cm}^2$ for $D_R = 0.0$, m_2 is obtained as natural logarithm of the ratio of the values of M at $\sigma' = 1.0 \text{ Kg/cm}^2$ for $D_R = 1.0$ and the value of m_0 . The coefficient m_1 is given by

$$m_1 = \frac{1}{2.303} \ln \frac{M}{m_0} \quad (5.14)$$

where

M is the modulus at stress level of 10 Kg/cm^2 for $D_R = 0.0$

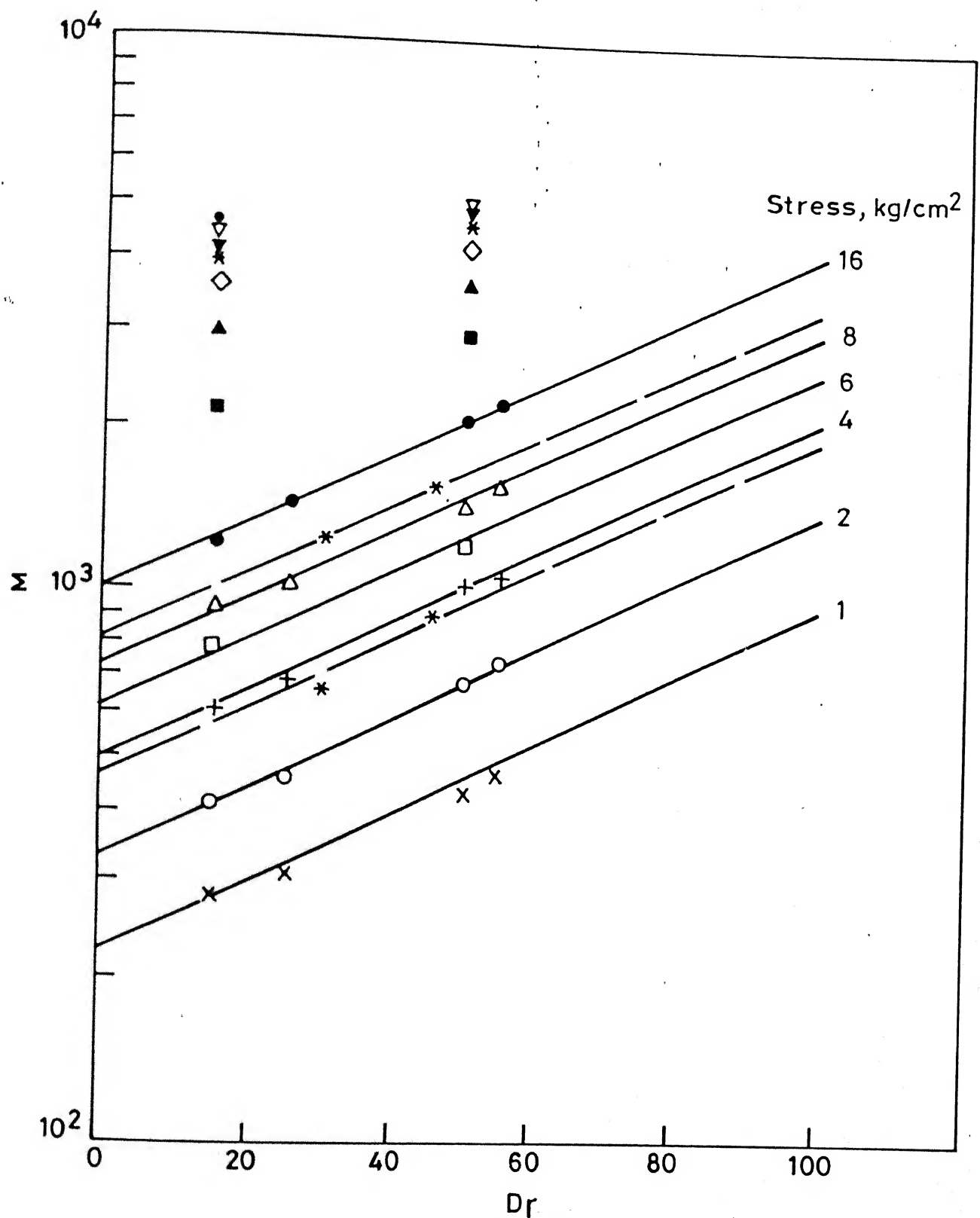


Fig. 5.54 Relationship between M and Dr at different stress levels for standard sand.

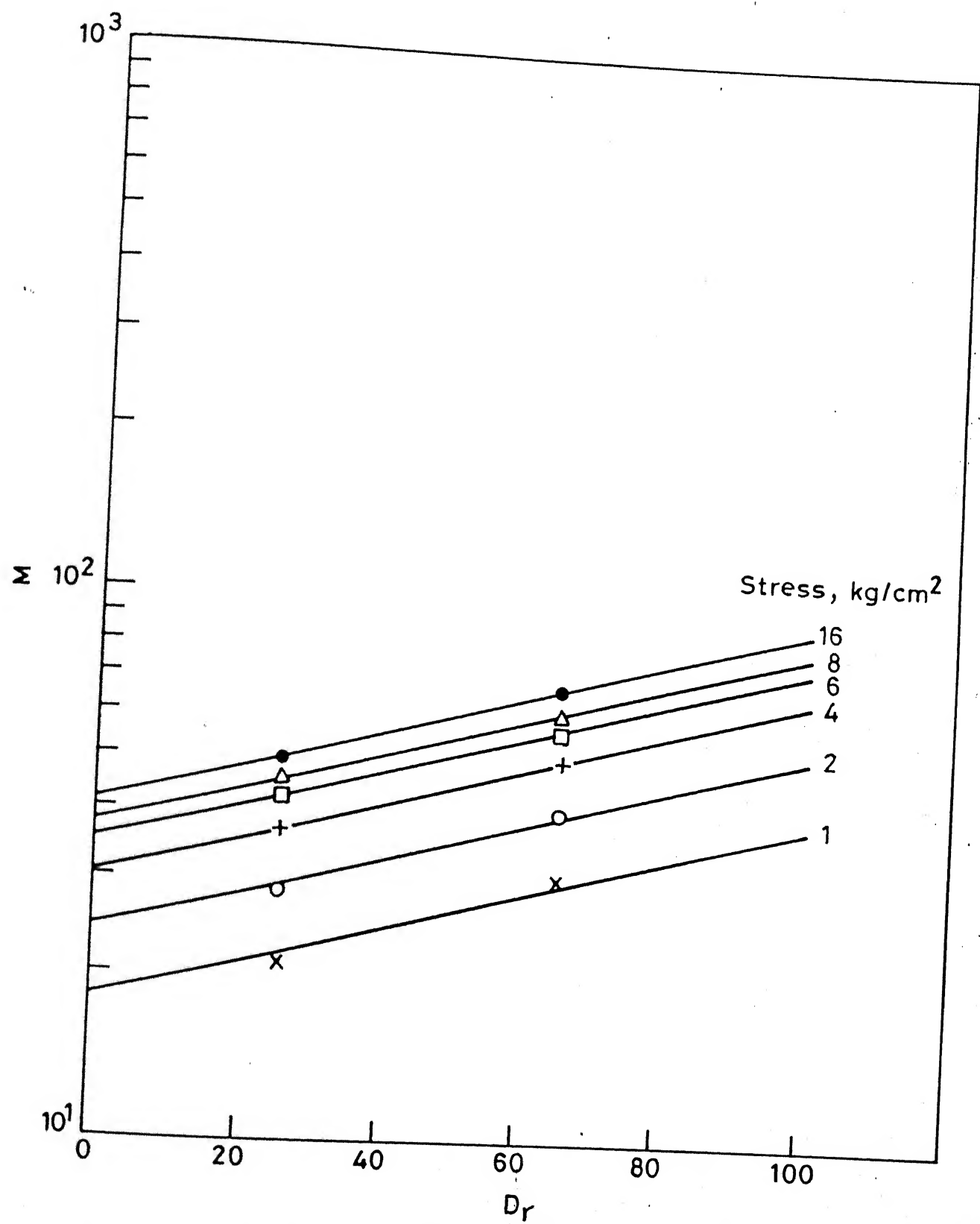


Fig. 5.55 Relationship between M and D_r at different stress levels for calcareous sand.

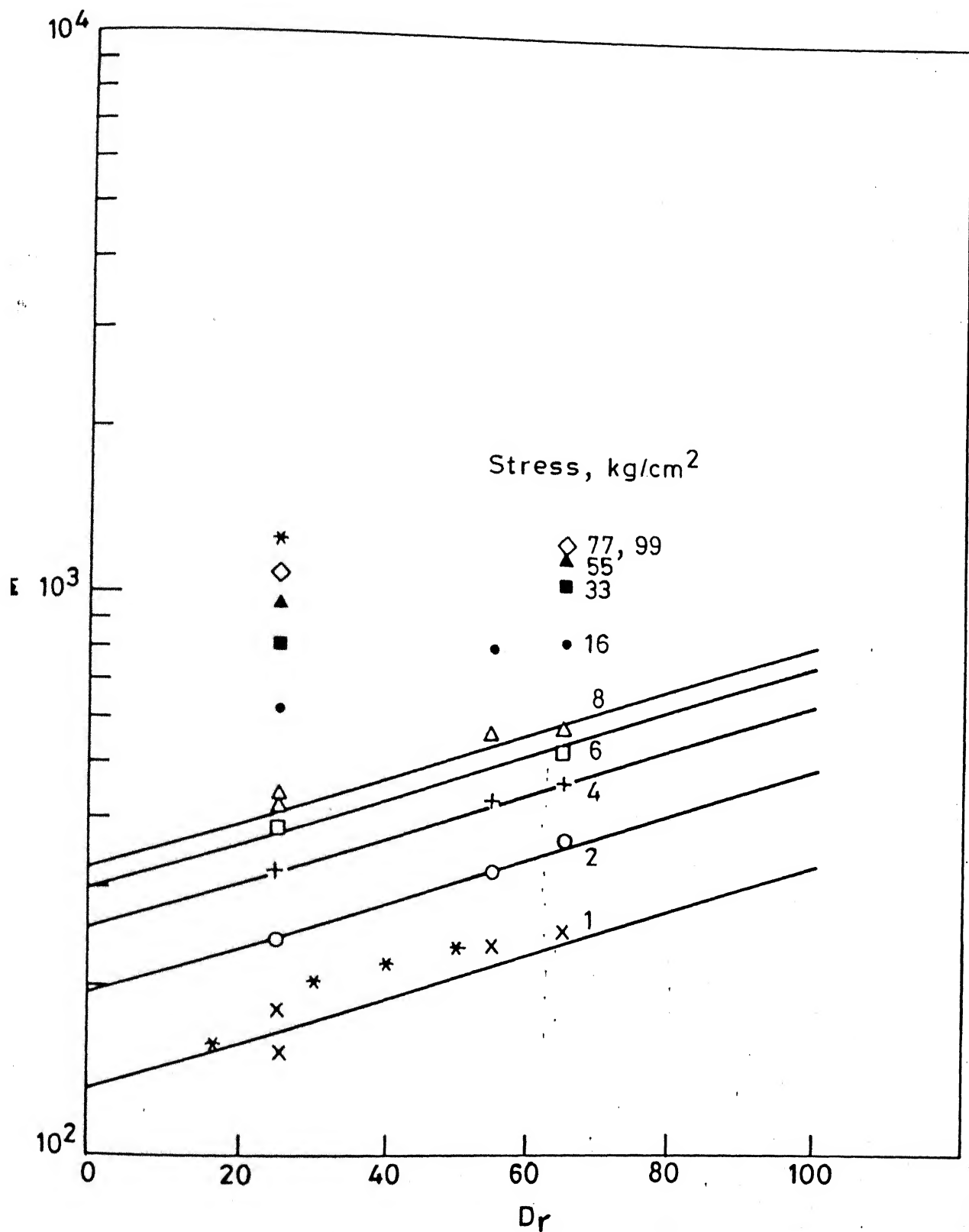


Fig. 5.56 Relationship between M and Dr at different stress levels for Kalpi sand.

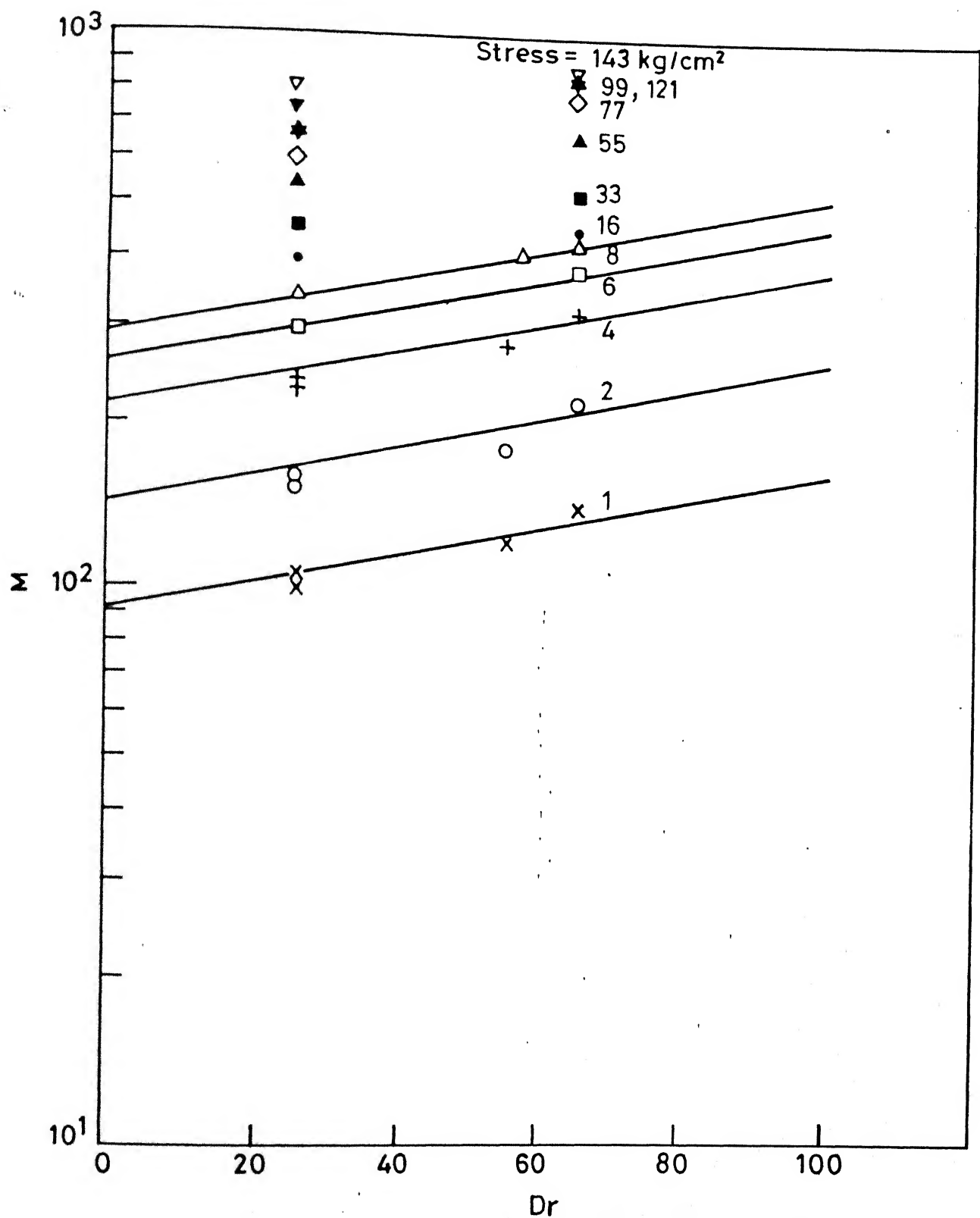


Fig. 5.57 Relationship between M and Dr at different stress levels for Ganga sand.

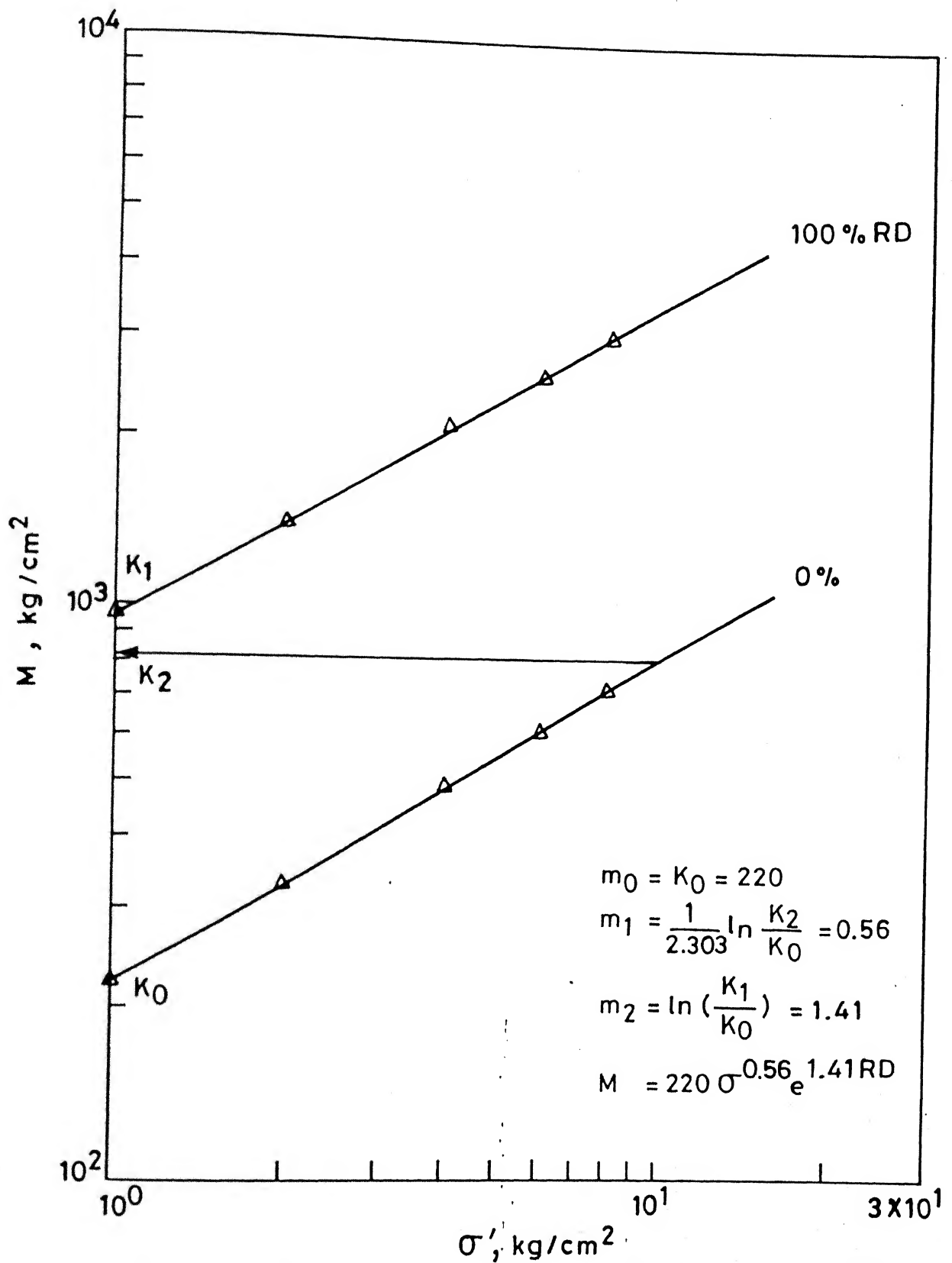


Fig. 5.58 Evaluation of m_0 , m_1 and m_2 coefficients for standard sand.

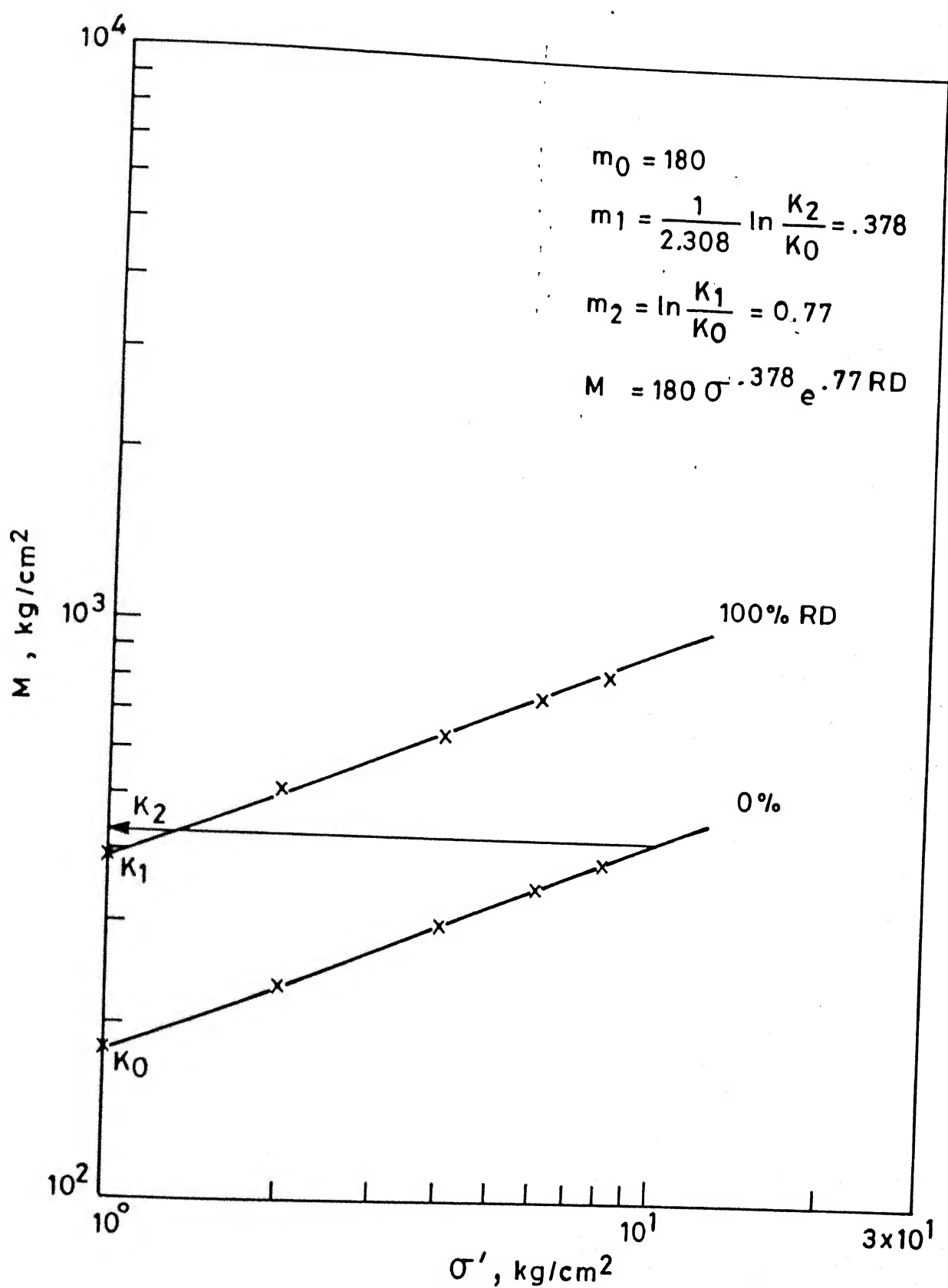


Fig. 5.59 Evaluation of m_0 , m_1 and m_2 coefficients for Calcareous sand.

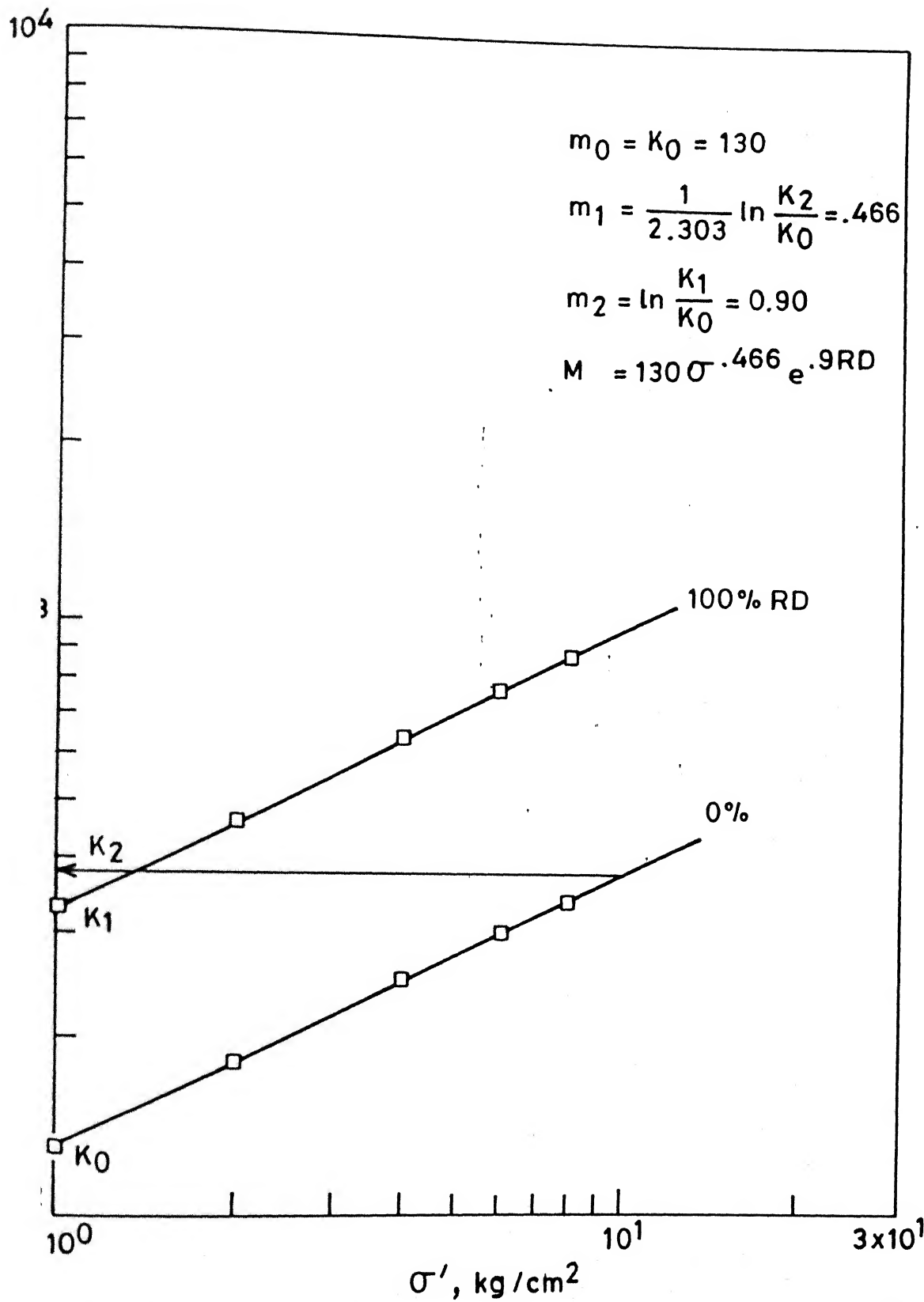


Fig. 5.60 Evaluation of m_0 , m_1 and m_2 coefficients for Kalpi sand.

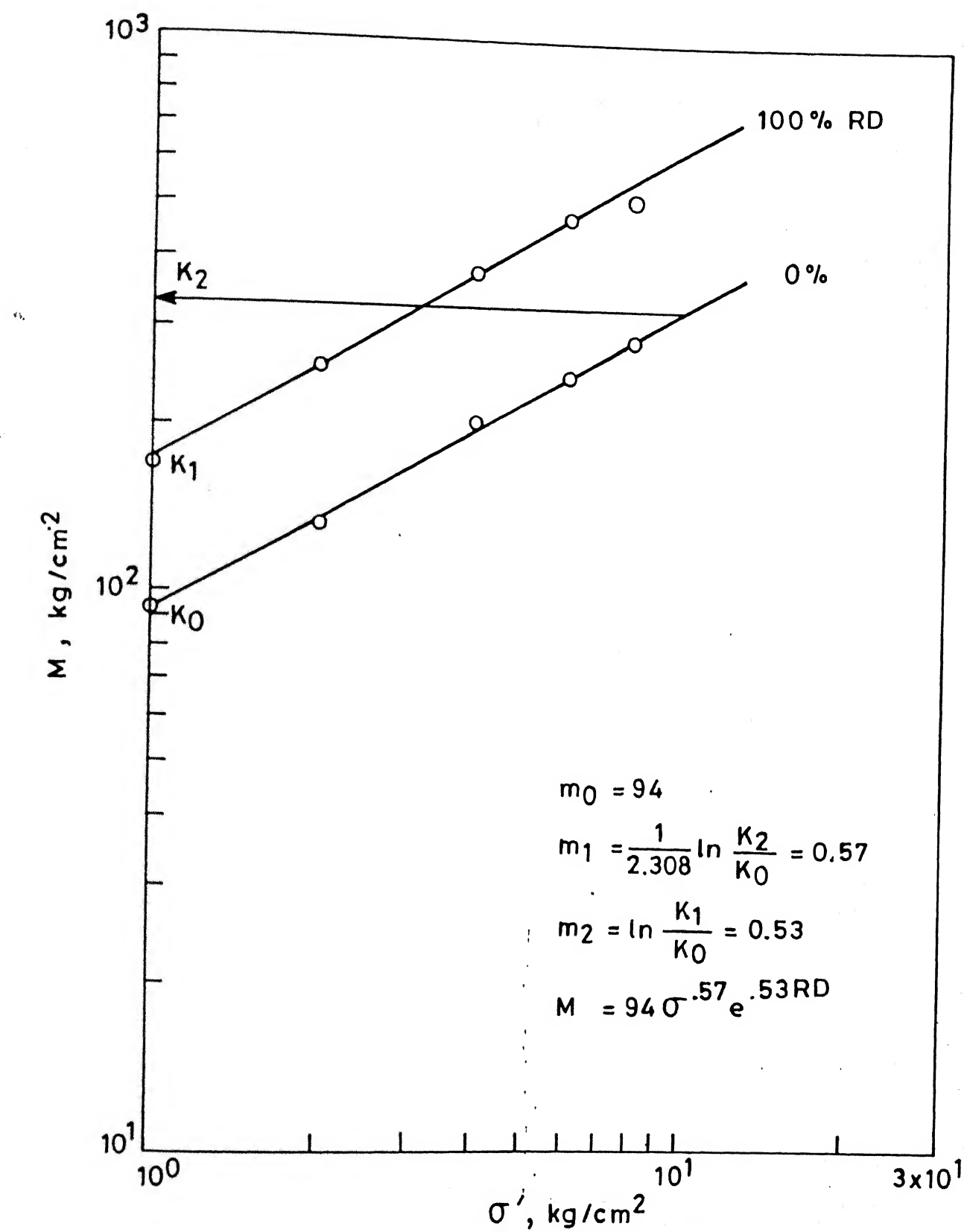


Fig. 5.61 Evaluation of m_0 , m_1 and m_2 coefficients for Ganga sand.

The values of M for relative densities of 0.0 and 1.0 are obtained by extrapolation of test results as in Figs. 5.54 to 5.57. Following this procedure, the values of m_0 , m_1 and m_2 have been worked out for a variety of sands (Figs. 5.58 to 5.61) as shown in Table 5.7.

5.3.2.1 Analysis of Experimental Results

Test results in terms of M versus stress for Standard, Calcareous, Kalpi, Kalpi 2 and Ganga sands are presented in Figs. 5.62, 5.63, 5.64, 5.65 and 5.66 respectively. The results for loose Calcareous sand are also shown in Fig. 5.64 to bring out the fact that upto stress level of 10 Kg/cm^2 , Calcareous and Kalpi Sands show almost similar behaviour. The detail in this stress range is indicated in the inset of the figure. However, for stresses greater than 10 Kg/cm^2 , modulus versus stress relationship for Calcareous sand is markedly different from that of Kalpi and this is mainly due to difference in mineralogy, particle shape and the fact that grain modification in case of Calcareous sand begins at a lower stress level. The results presented are for two relative density values. Also superimposed on these curves are the respective model predictions on the basis of the relationships as in Table 5.7. It has been observed that Standard sand shows more or less a parabolic relationship between modulus and stress, upto quite a high stress level. The agreement between model prediction and experimental data upto $80 - 100 \text{ Kg/cm}^2$ only suggests that experimental coefficients m_0 , m_1 and m_2 have been well determined. In

Table 5.7 : Model Parameters for Modulus of Variety of Sands

Sands	m_0	m_1	m_2	$M = m_0 \sigma^{m_1} e^{m_2}$
Ganga	94	0.573	0.533	$M = 94 \sigma^{0.573} e^{0.533}$
Calcareous	180	0.378	0.773	$M = 180 \sigma^{0.378} e^{0.773}$
Kalpi	130	0.466	0.900	$M = 130 \sigma^{0.466} e^{0.900}$
Standard	220	0.560	1.410	$M = 220 \sigma^{0.560} e^{1.410}$
Ganga (enhanced Mica)	34	0.573	0.593	$M = 34 \sigma^{0.573} e^{0.593}$
Ganga (with mica removed)	120	0.371	0.900	$M = 120 \sigma^{0.371} e^{0.900}$
Ticino	230	0.370	1.470	$M = 230 \sigma^{0.370} e^{1.470}$
Hokksand	208	0.425	1.360	$M = 208 \sigma^{0.425} e^{1.360}$
Ottawa	185	0.750	1.373	$M = 185 \sigma^{0.750} e^{1.373}$
Mine Tailing	128	0.371	0.900	$M = 128 \sigma^{0.371} e^{0.900}$

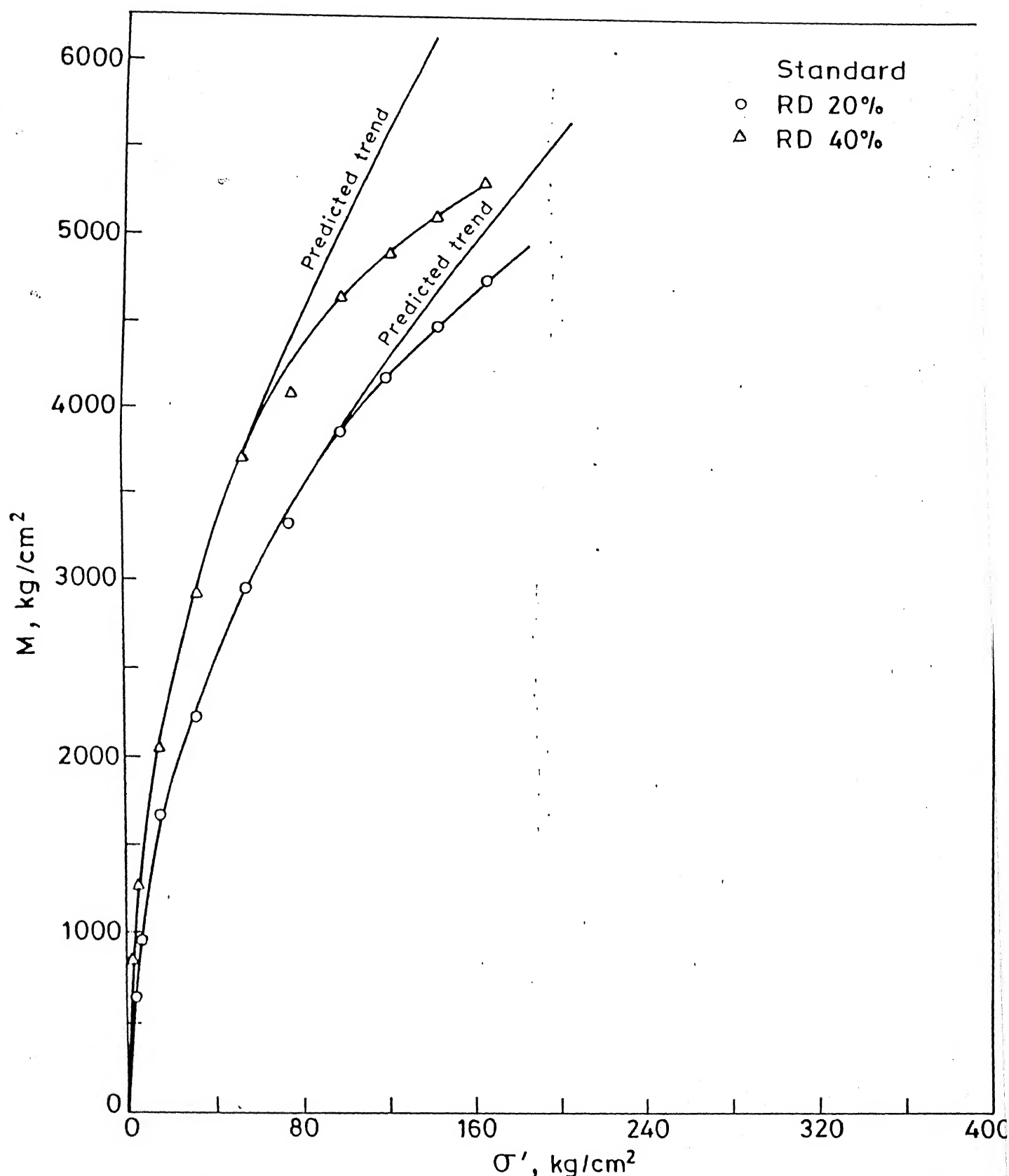


Fig. 5.62 Relationship between constrained modulus (M) and effective confining stress (σ') for Standard sand.

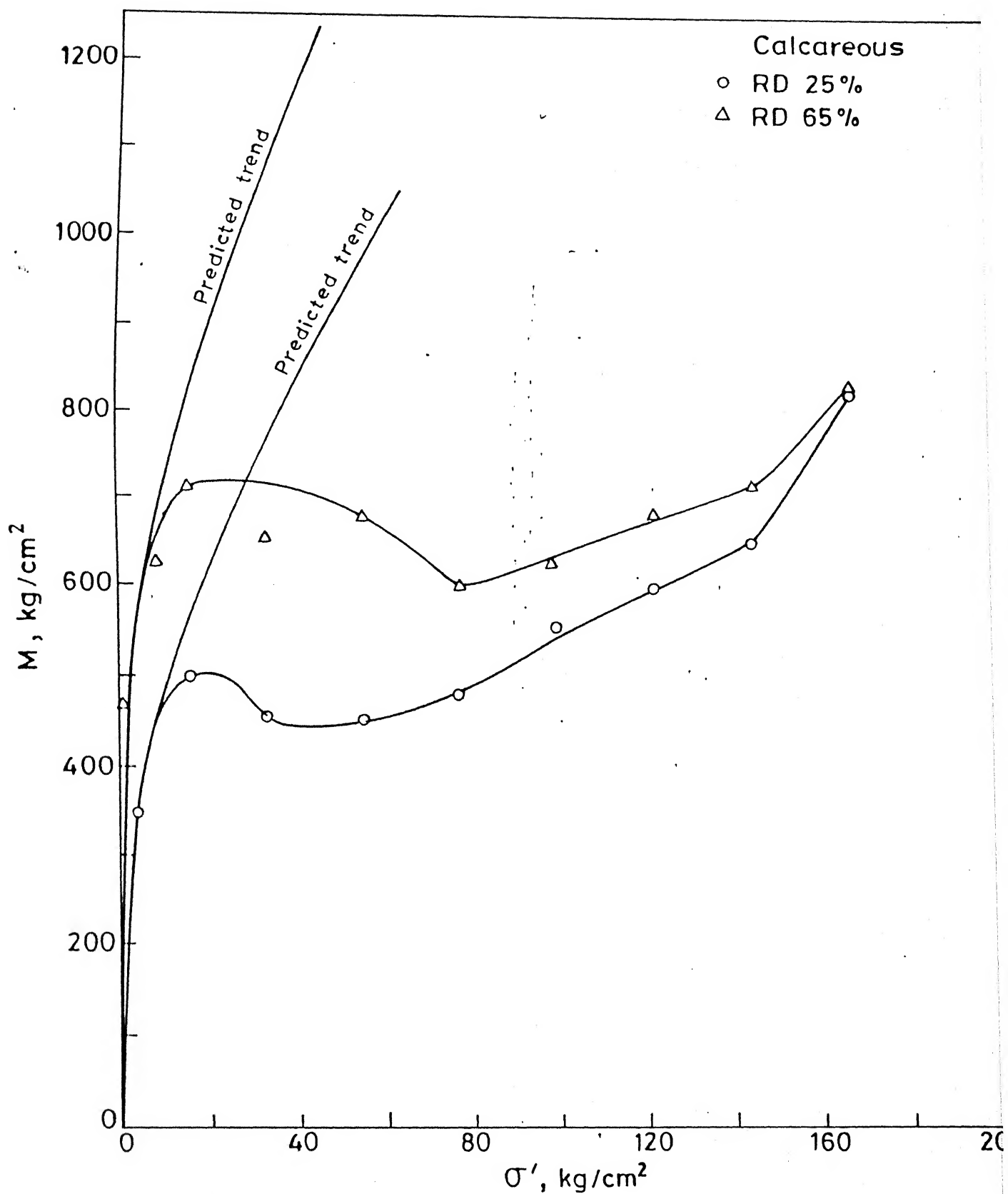


Fig. 5.63 Relationship between constrained modulus (M) and effective confining stress (σ') for calcareous sand.

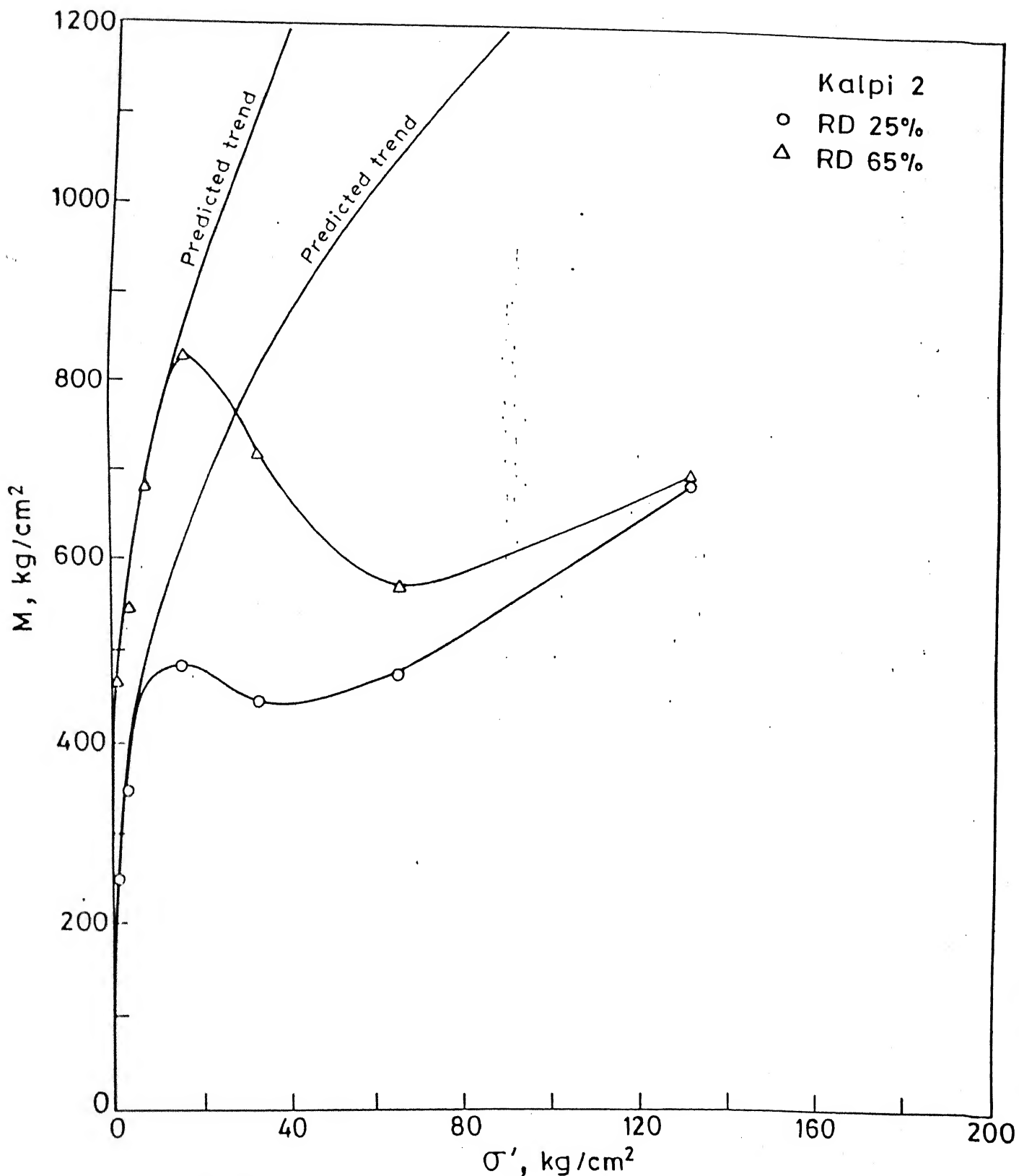


Fig. 5.65 Relationship between constrained modulus (M) and effective confining stress (σ') for Kalpi 2 sand

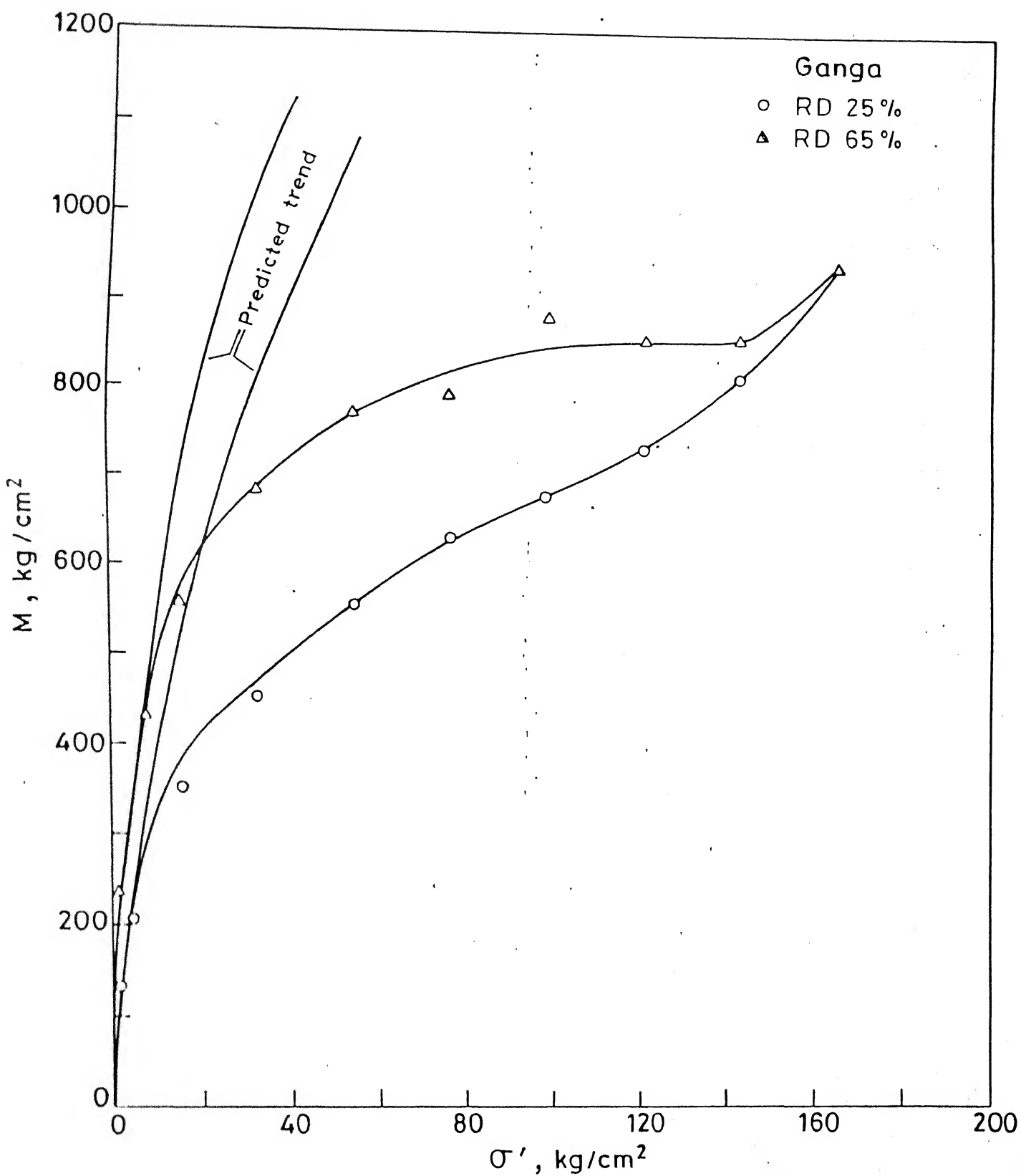


Fig. 5.66 Relationship between modulus (M) and effective confining stress (σ') for Ganga sand.

case of angular sands of medium to high compressibility, the picture is quite different. The values of modulus increase with stress upto a certain stress level (critical stress) and then deviate from the values predicted on the basis of parabolic increase of modulus with stress. The trends for stress values greater than critical stress vary differently for different sands. The value of critical stress also seems to depend on the relative density, particle size, shape, angularity and mineralogy of a sand. While in the case of Standard sand, the range for critical stress is 80-100 Kg/cm², the corresponding ranges for Calcareous, Kalpi, Kalpi-2 and Ganga sands are 9-13, 15-28, 5-13 and 7-12 respectively. Except for the case of Standard sand, which consists of well-rounded quartz grains, the lower values of critical stress are for loose and the higher values are for medium dense states respectively. In case of angular compressible sands, this result is consistent with the fact that they indicate considerable grain modifications at low stress ranges (Fig. 5.35). Harr and Grives (1980) suggested that the product of particle contacts and porosity is constant and they have recommended a value of 3 for the same. In case of loose angular compressible sands, higher porosity would suggest smaller number of particle contacts with consequent higher contact stress concentrations leading to enhanced grain modification and crushing. This would also predict lower critical stress for loose sand as compared to dense sand.

In the case of Standard sand, it is expected that critical stress values for loose and dense states show a similar trend for large differences in relative density. The results in Fig. 5.62 are for a very close range of relative density values. In this case any changes at low stress levels below (200 Kg/cm^2) would be mainly due to particle adjustments. In the case of angular, medium to high compressibility sands, the deviation of experimental trends from the parabolic law is suggested to be due to the changes in the nature of sand with the onset of grain modification. At this low stress level, as indicated earlier, no grain crushing would have taken place and all observed changes in gradation are attributed to grain modification. This procedure to locate the point of deviation of experimental modulus versus stress trends from the predicted parabolic law, and the earlier direct evidence of grain modification (shape and angularity) at low stresses (Fig. 5.35) have been used for defining a critical vertical effective stress level (σ'_c) at which significant grain modification commences. This grain modification leads to significant changes in the sand compressibility (as shown earlier) and therefore the modulus versus stress relationships are observed to be at variance with the parabolic law proposed by Janbu and Bellotti et al. Yudhbir and Rahim (1987) have shown that m_0 and m_1 values upto σ'_c are different from the subsequent behaviour of sand at higher stresses. The laws proposed by Janbu and Bellotti et al are based on test data obtained at stress levels less than $8-10 \text{ Kg/cm}^2$. Results for sand tested

in this stress range are shown in the Fig. 5.67. In this stress range, except for loose, very highly micaceous or very loose carbonate sands, no grain modification is expected. Thus it may be stated that the modulus predictive laws (Eqns. 5.12 and 5.13) tacitly assume no change in the nature of sand during compression. The value of σ'_c indicates a sort of threshold level upto which only the experimental constants m_0 , m_1 and m_2 , as evaluated for low stress level test data, are applicable. On the basis of limited data obtained in this study and the results available in literature, a tentative relationship between critical stress and relative density is proposed (Fig. 5.68). Although trends seen in Fig. 5.68 are consistent with the expected response due to differences in mineralogy and particle angularity, extensive data are required to clearly define these relationships for sands of low, medium and high compressibility.

5.3.2.2 Effect of Grain Mineralogy on the Relationship Between Modulus and Stress

Effect of mineral content on grain modification, crushing, and compressibility has been stressed in the earlier sections. The relationship between modulus and stress for three fractions of Ganga sand with varying percentages of mica content is indicated in Fig. 5.70. All the three samples have practically same d_{50} and comparable gradation curves. It will be seen that as mica content increases, the constrained modulus at a given confining stress decreases. Variation of modulus number m_0 (Eqn. 5.13)

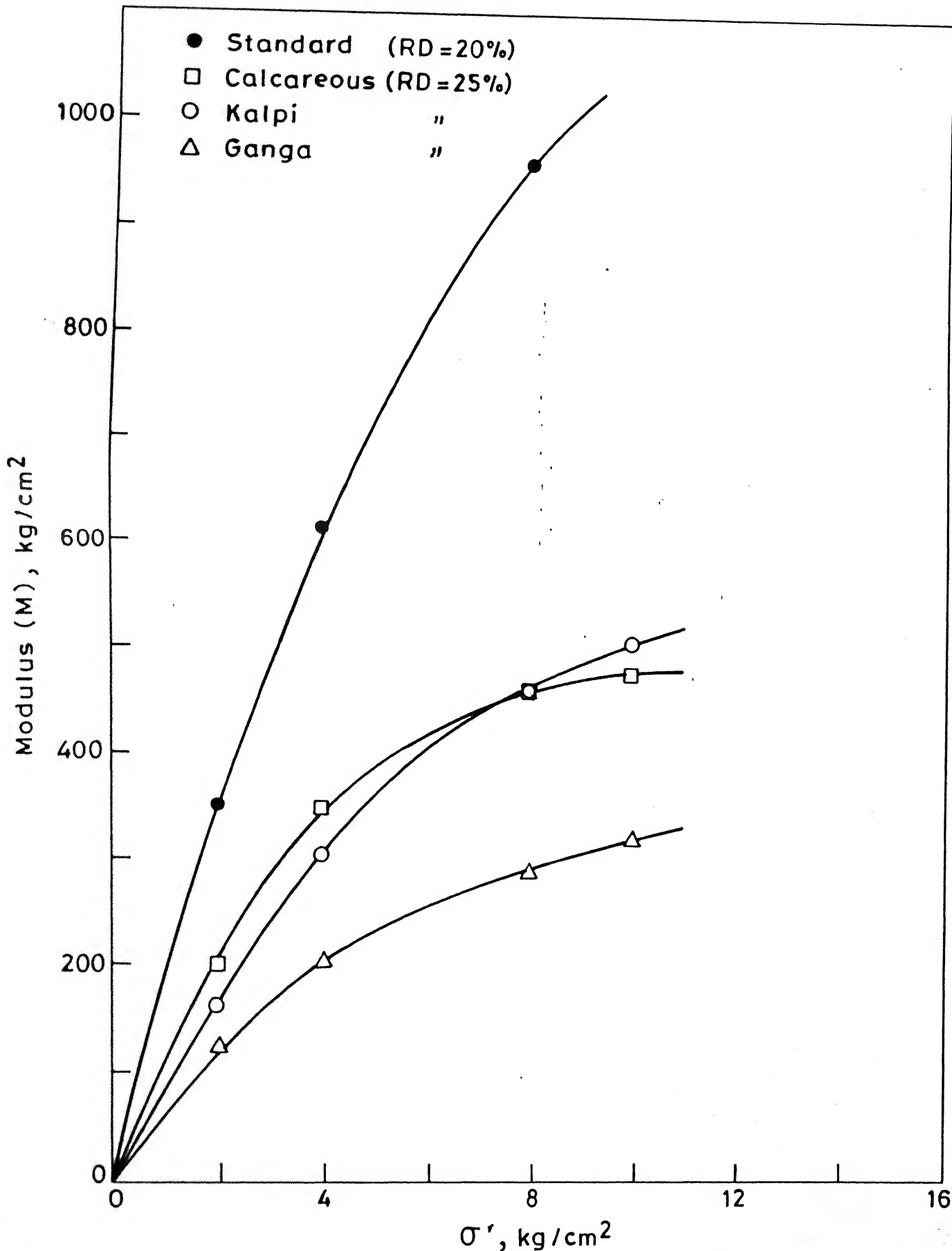


Fig. 5.67 Comparison of M vs σ' relationship at low stress level for Ganga, Kalpi, Calcareous and Standard sands.

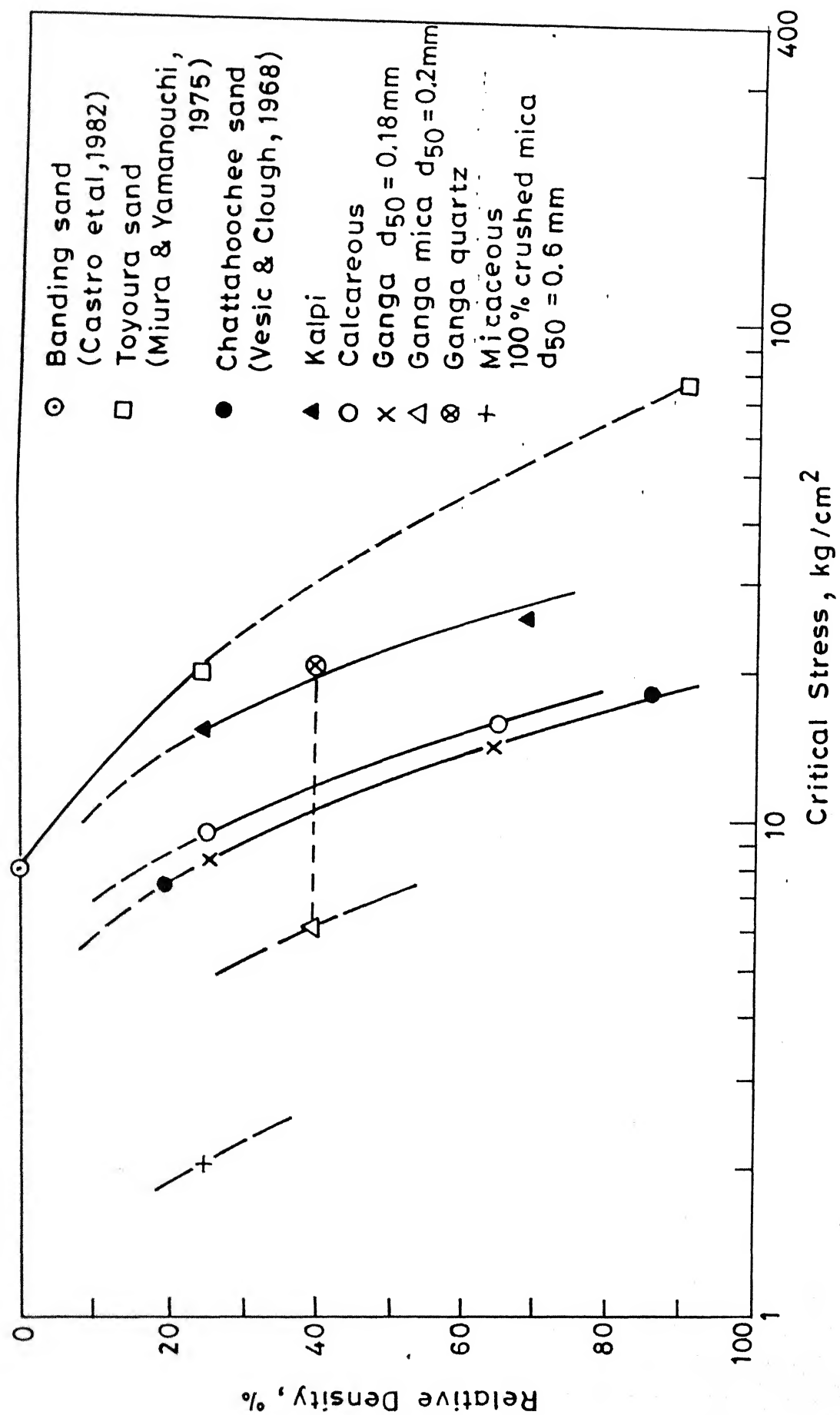


Fig. 5.68 Relationship between critical stress (σ'_c) and relative density (RD) for different sands.

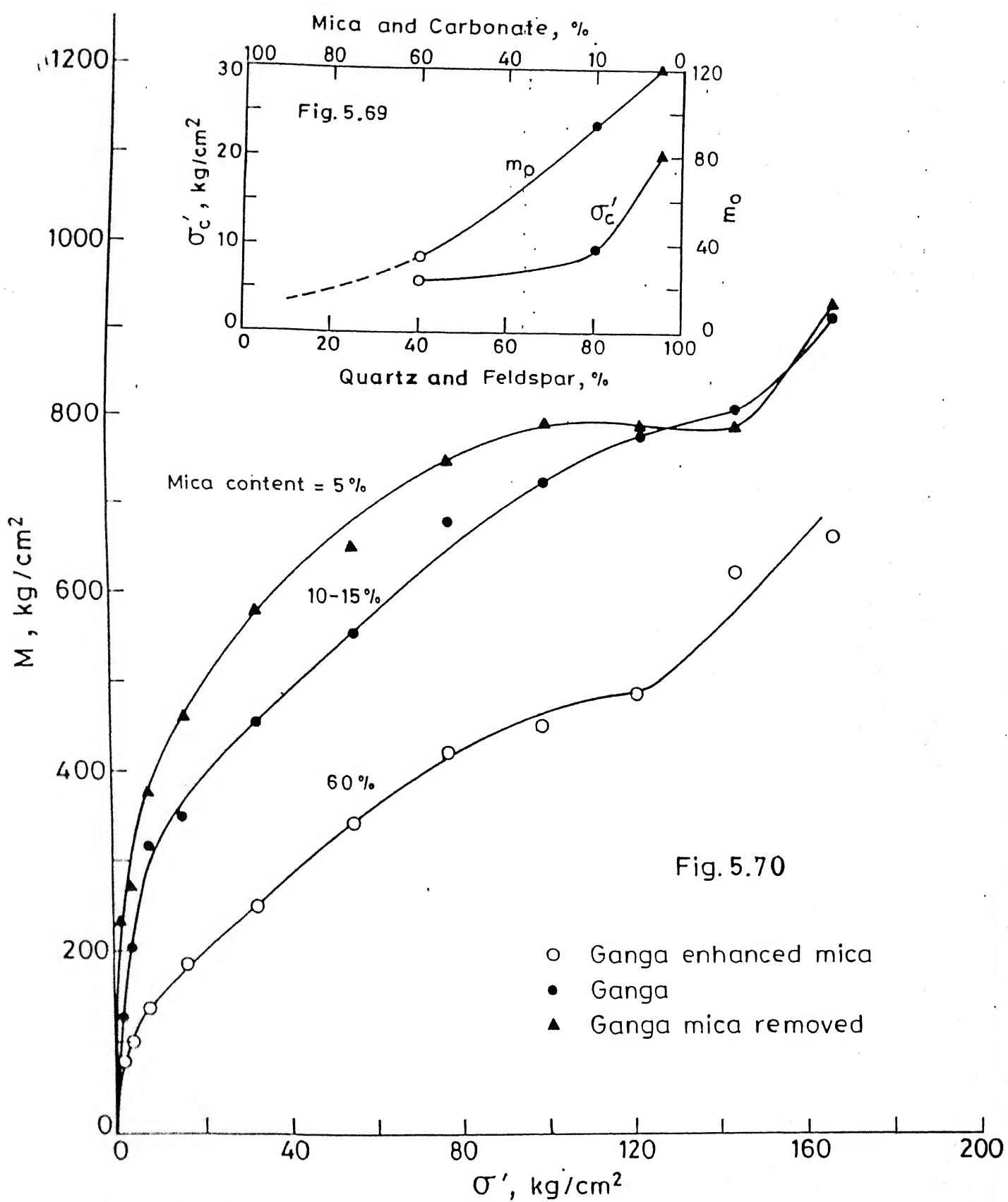


Fig. 5.69 Dependence of σ'_c and m_0 on mineral content.

Fig. 5.70 Effect of mica on M vs σ' relationship for Ganga sand.

and critical stress (Fig. 5.67) with mineral content is illustrated in Fig. 5.69. Additional controlled test data are needed to establish quantitative relationships between constrained modulus and mineral composition for a variety of sands.

5.3.3 Applications of Test Result to The Estimation of Cone Penetration Resistance in Sands

Based on the results of grain shape, angularity, modification, crushing, and compressibility studies discussed earlier and the shear test data on Standard, Kalpi and Ganga sands reported by Phool Chand (1988), it is possible to predict the cone penetration resistance, q_c (measure of ultimate bearing capacity), as a function of relative density and confining effective stress for sands with varying compressibilities. In this section, effect of grain angularity on angle of shearing resistance, reported by Phool Chand (1988) and other workers will be first reviewed and then utilized to predict q_c on the basis of Janbu's theory (1963, 1985). The effect of sand compressibility on the mode of failure will be incorporated in the form of angle β (Fig. 5.71) to compute the appropriate values of bearing capacity factor N_q of a sand based on its angle of shearing resistance.

5.3.3.1 Calculation of q_c for Sands with Varying Degree of Compressibilities

Janbu and Senneset (1974) suggested a value of (-15) for β for sands of low compressibility which exhibit general

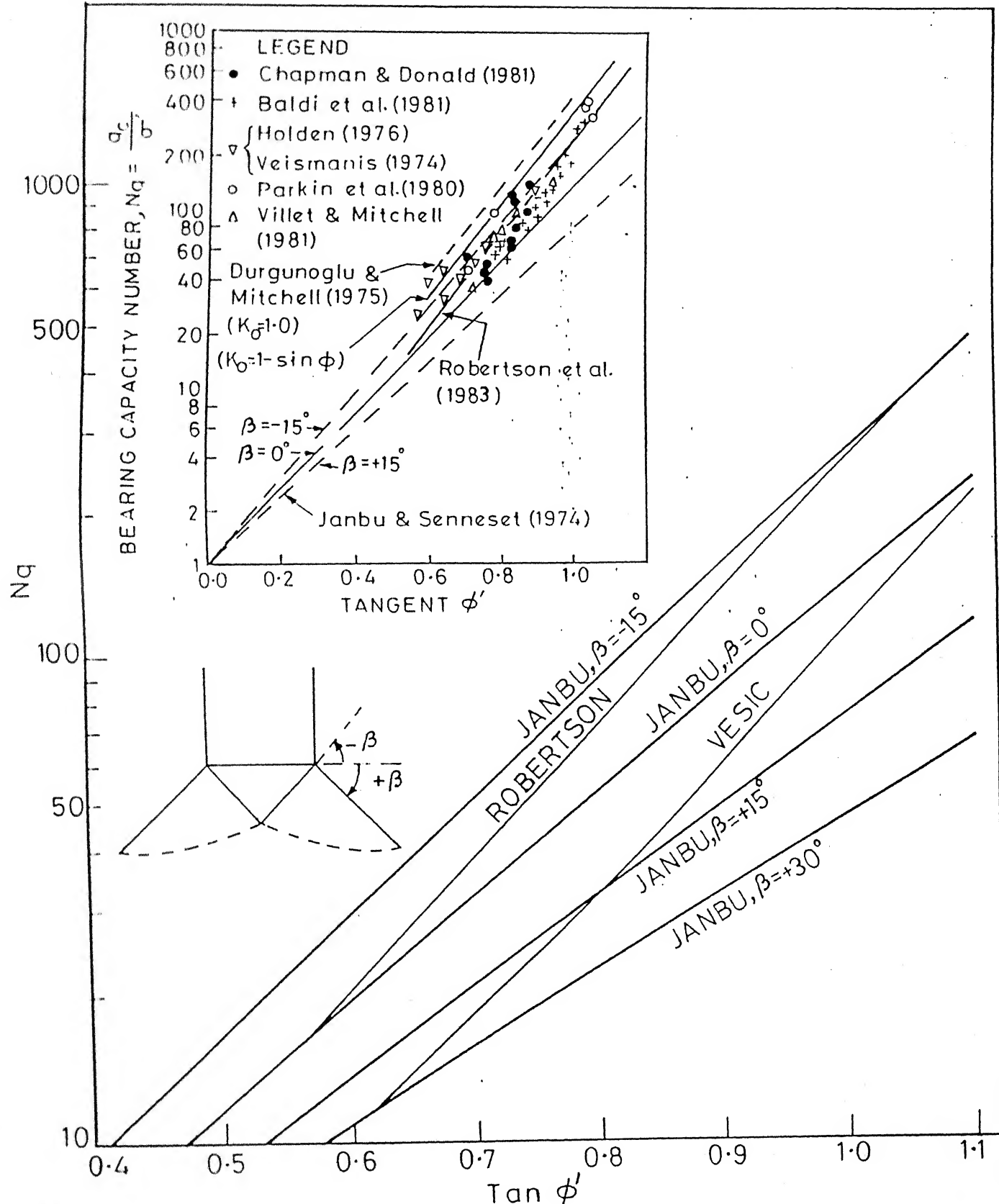


Fig. 5.71 Relationship between bearing capacity number and peak friction angle

shear failure mechanism around the cone. Robertson et al. (1983) (Fig. 5.71-Inset) on the basis of all available data for test chamber studies, concluded that the values for sand of low compressibility (at a given relative density and confining stress) vary from -15° to -32° . For the purpose of computing q_c values, it was assumed that, as a first approximation, $\beta = -15^{\circ}$ to -32° be taken to represent failure in case of rounded quartz sands of low compressibility and $\beta = +15^{\circ}$ be taken to represent the failure mode in case of sands of high compressibility. For sands of moderate compressibility $\beta = 0.0$ was adopted. Ideally in case of compressible sand, variable β values as suggested by Vesic (1963) (Fig. 5.71) would be more appropriate. Since the objective of this exercise is to develop a comparative feel for the overall trends of q_c versus effective stress for sands with low, medium and high compressibility, a constant value of β was chosen. Values of q_c were computed for each of the representative sands (Standard, Kalpi and Ganga) on the basis of ϕ' versus relative density variation at different stress levels as shown in Figs. 5.72 and 5.73 (Phool Chand 1988). The variation of ϕ' with relative density for three sands in the stress ranges investigated is presented in Fig. 5.74. For a given relative density and confining effective stress, angular sand gives higher ϕ' as compared to well-rounded sand. This is consistent with results compiled by Winterkorn and Fang (1986).

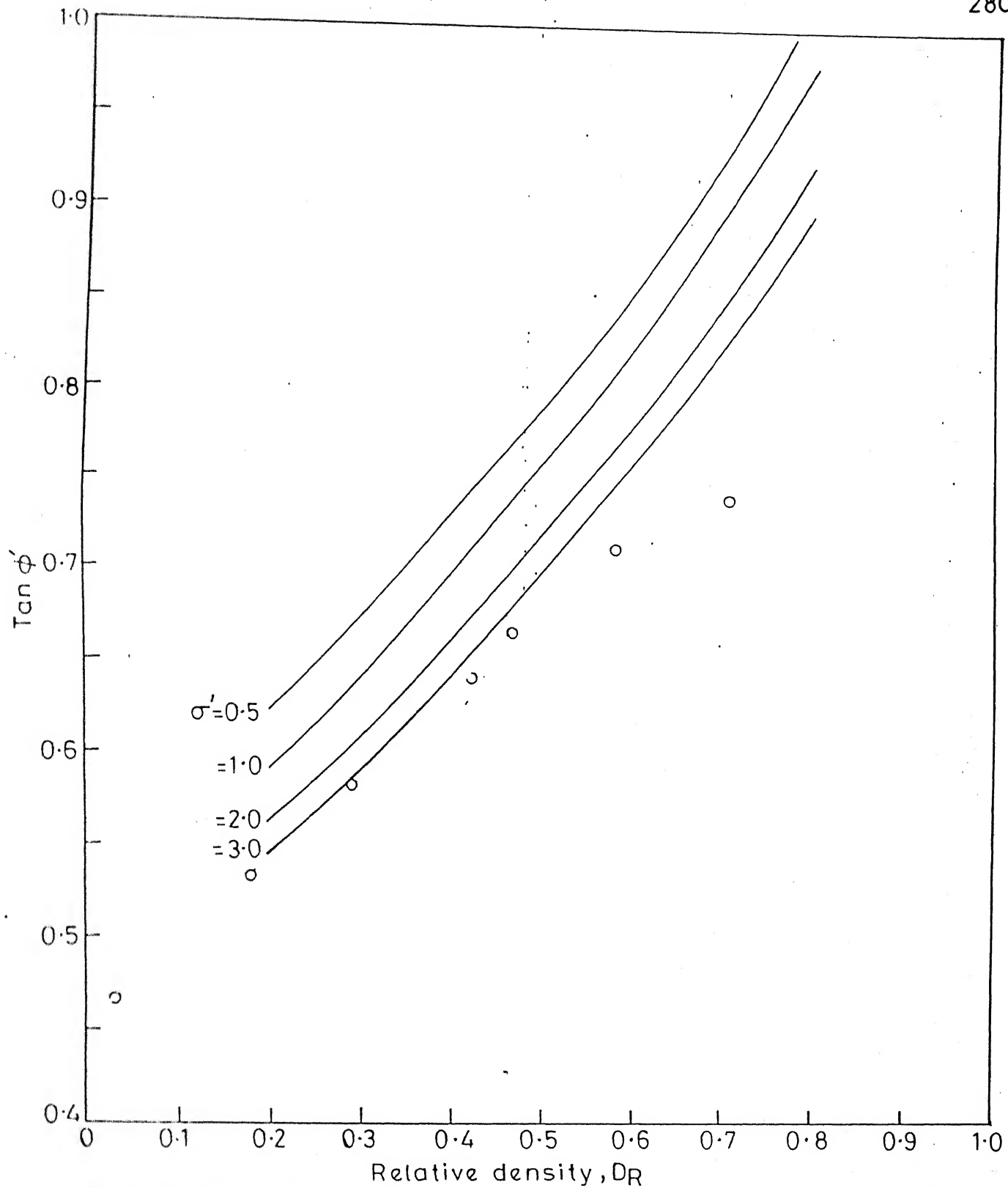


Fig.5.72 Relation between peak friction angle and Relative Density for standard sand at different σ' (Sahu, 1988)

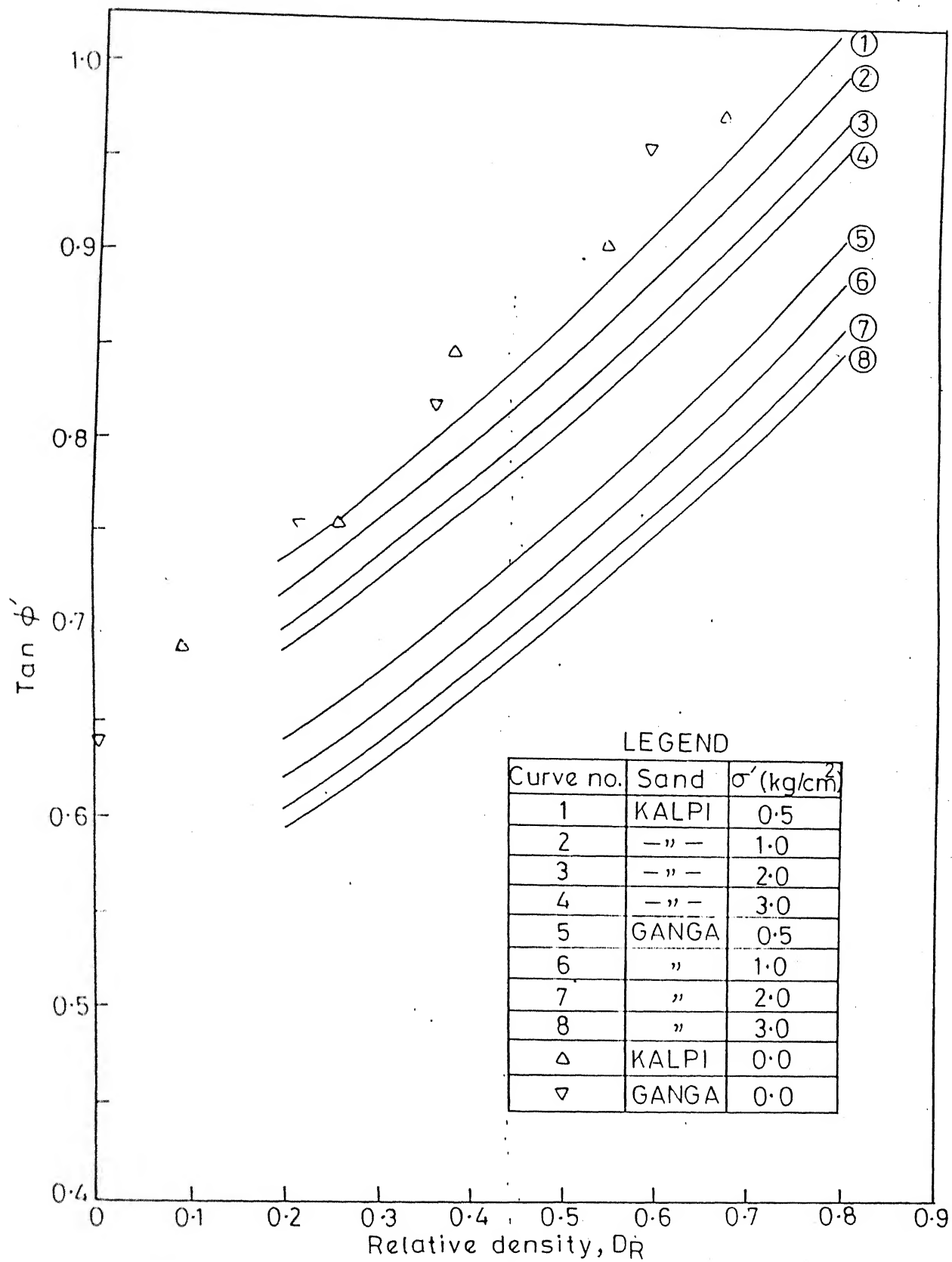


Fig.5.73 Relation between peak friction angle and Relative Density for Ganga and Kalpi at different σ' (Sahu, 1988)

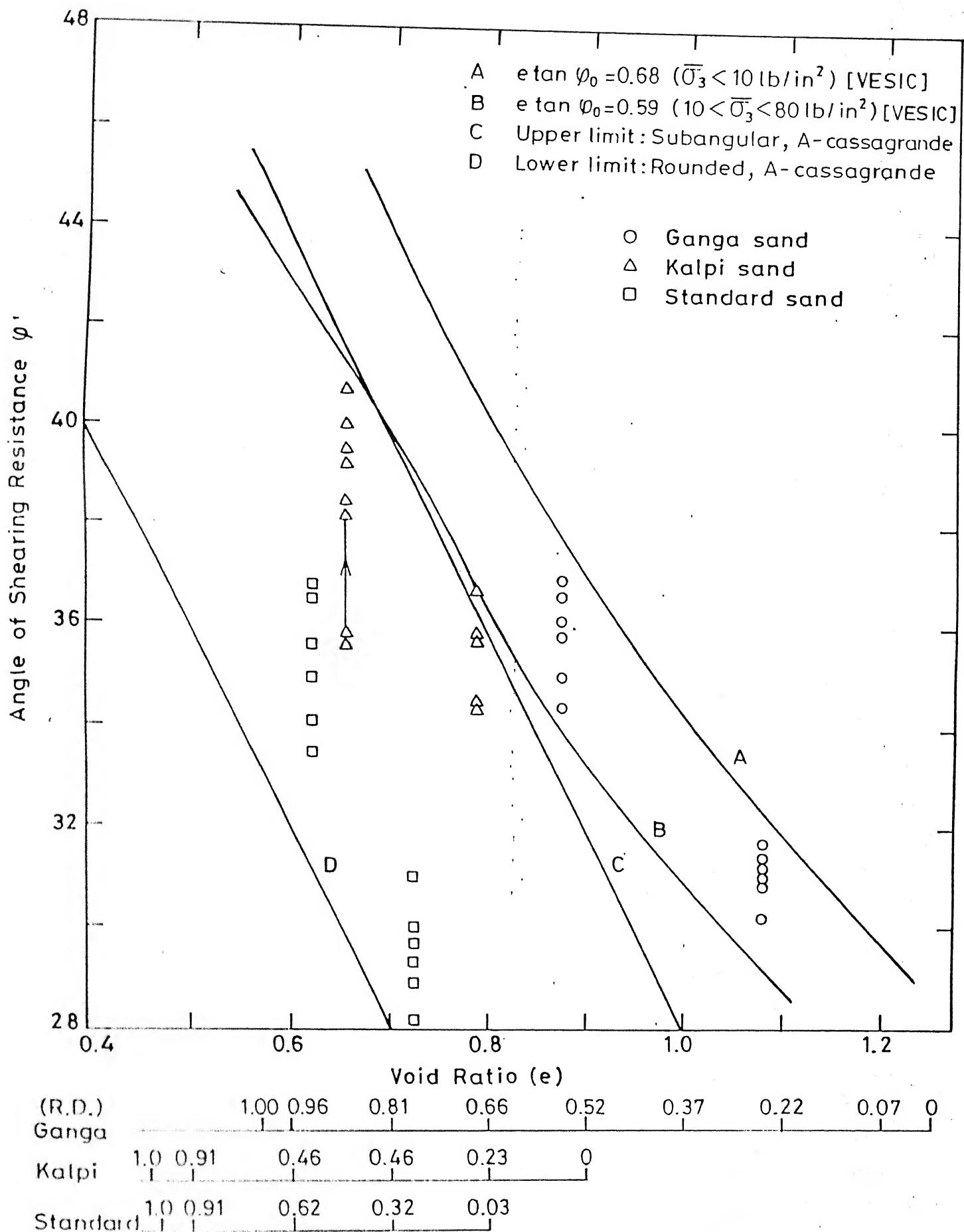


Fig. 5.74 Relation between φ and e or R.D. (Phool Chand, 1988)

Following Bellotti et al (1985), q_c may be expressed in terms of effective stress and relative density in the form

$$q_c = C_0 \sigma^{C_1} \exp (C_2 \cdot D_R) \quad (5.15)$$

where

C_0 , C_1 and C_2 are experimental coefficients.

From the computed q_c values for a range of stress and relative density values, the coefficients C_0 , C_1 and C_2 were evaluated for each of the sands in the same manner as adopted for the computation of m_0 , m_1 and m_2 as detailed earlier. The C_0 , C_1 and C_2 values proposed for sands of low, medium and high compressibility are given in Table 5.8. In addition, the corresponding values of m_0 , m_1 and m_2 characterizing the modulus for these sands are also presented in this Table. The classification of sands in these three categories based on their compressibility is already presented (Table 5.6, Fig.5.53).

5.3.3.2 Comparison Between Predicted and Measured Modulus versus Stress Relationships for Sands

On the basis of predictive laws (Table 5.7), values of modulus at various stress values for a wide range of relative densities were computed for standard, Calcareous, Kalpi and Ganga sands. The predicted and measured results for these four sands are presented in Figs. 5.75 to 5.78. As can be noticed, there is a good agreement between the predicted and the observed values. In Fig.5.79, the behaviour of different sands at comparable relative density value is illustrated. Test data from Phool Chand (1988) are also included. Using

Table 5.8 : Suggested Model Parameter for Constrained
Modulus (M) and Cone Penetration Resistance (q_c)

Type of Sands	Measure of M Kg/cm ²			Measure of q_c Kg/cm ²		
	m_0	m_1	m_2	C_0	C_1	C_2
Low Compressibility Sands	220	0.37	1.41	21	0.51	2.96
Moderate Compressibility Sands	152	0.42	0.84	15	0.64	2.61
High Compressibility Sands	94	0.57	0.53	10	0.87	1.99

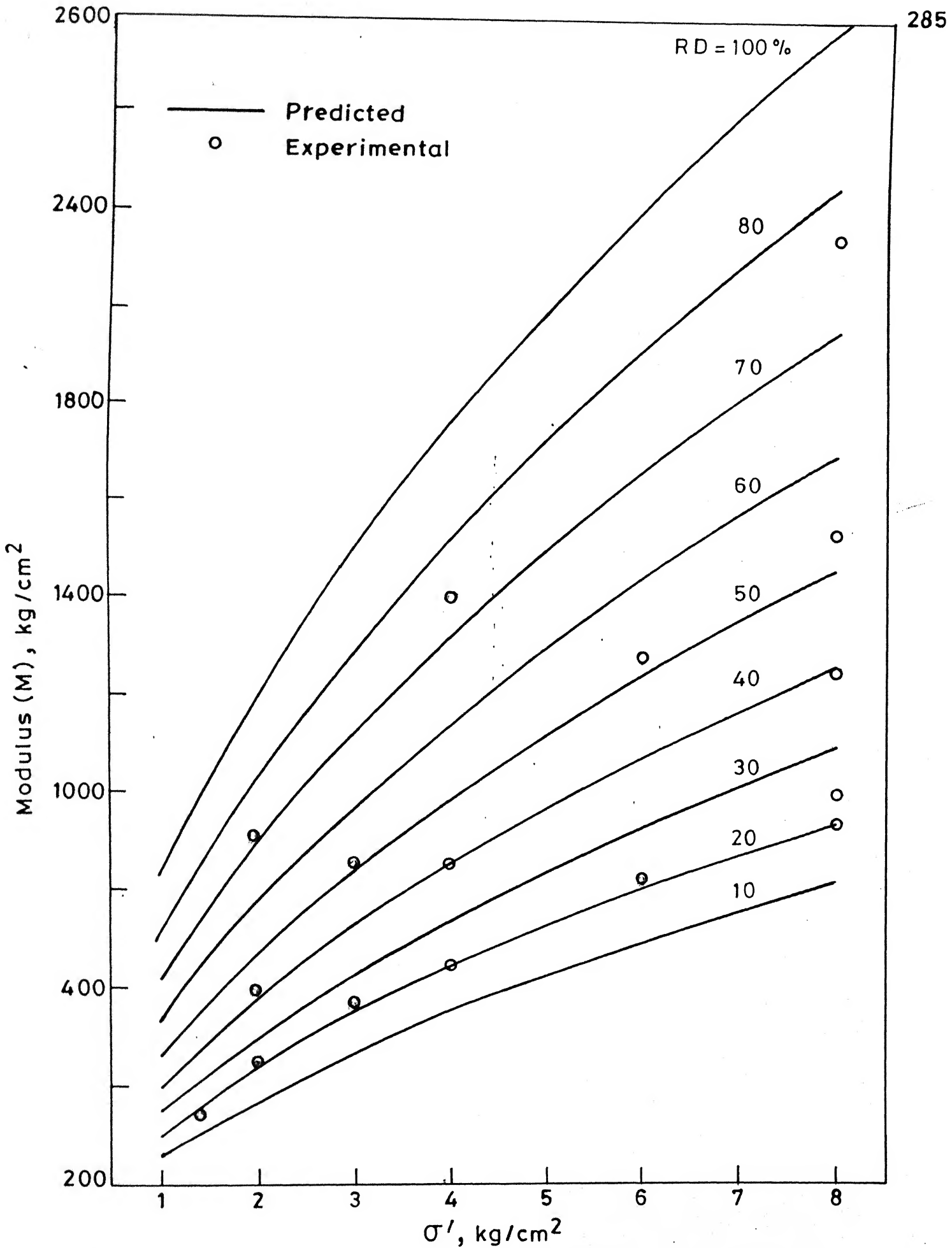


Fig. 5.75 Effect of relative density and σ' on modulus for standard sand.

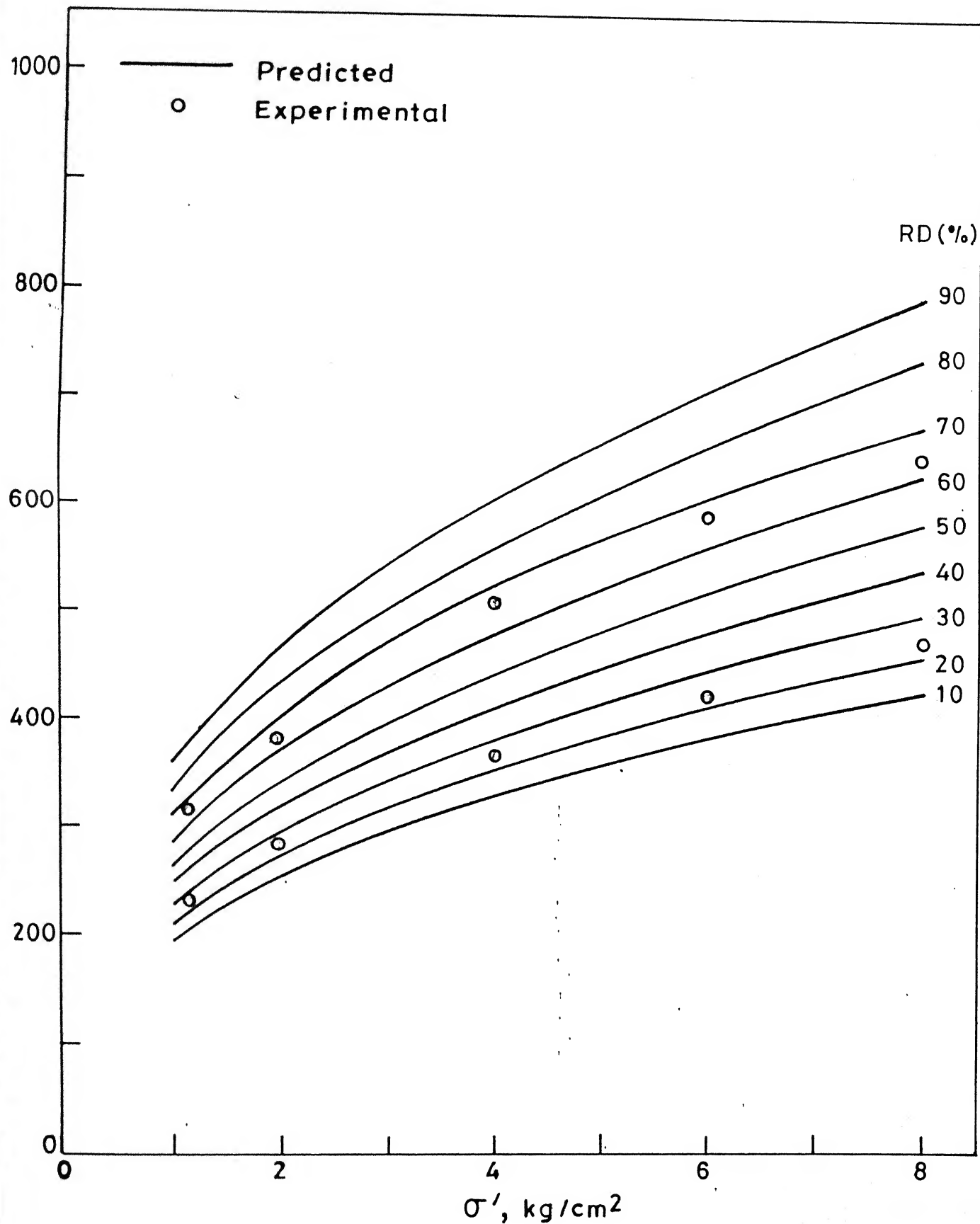


Fig. 5.76 Effect of relative density and σ' on modulus for calcareous sand.

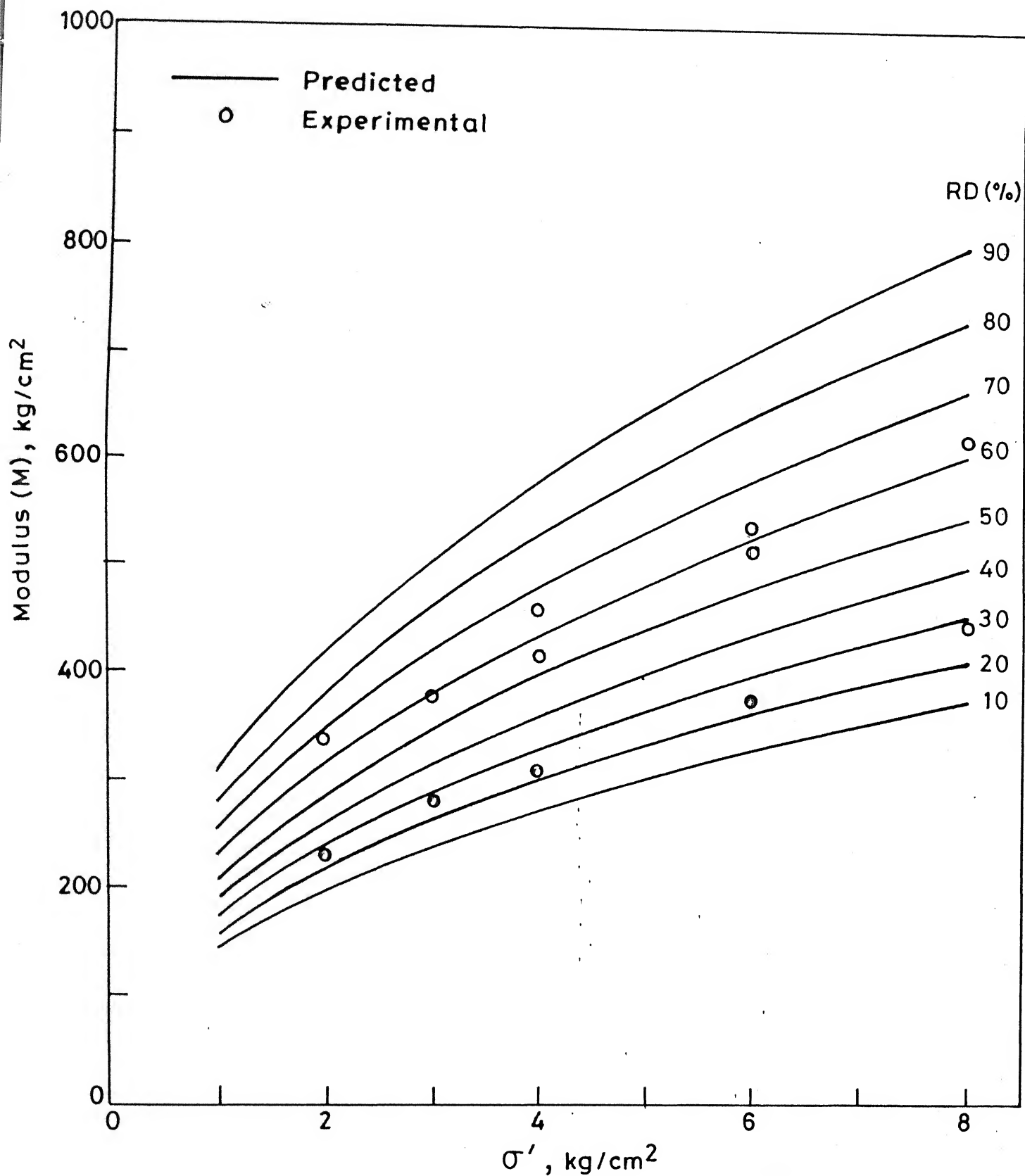


Fig. 5.77 Effect of relative density and σ' on modulus for Kalpi sand.

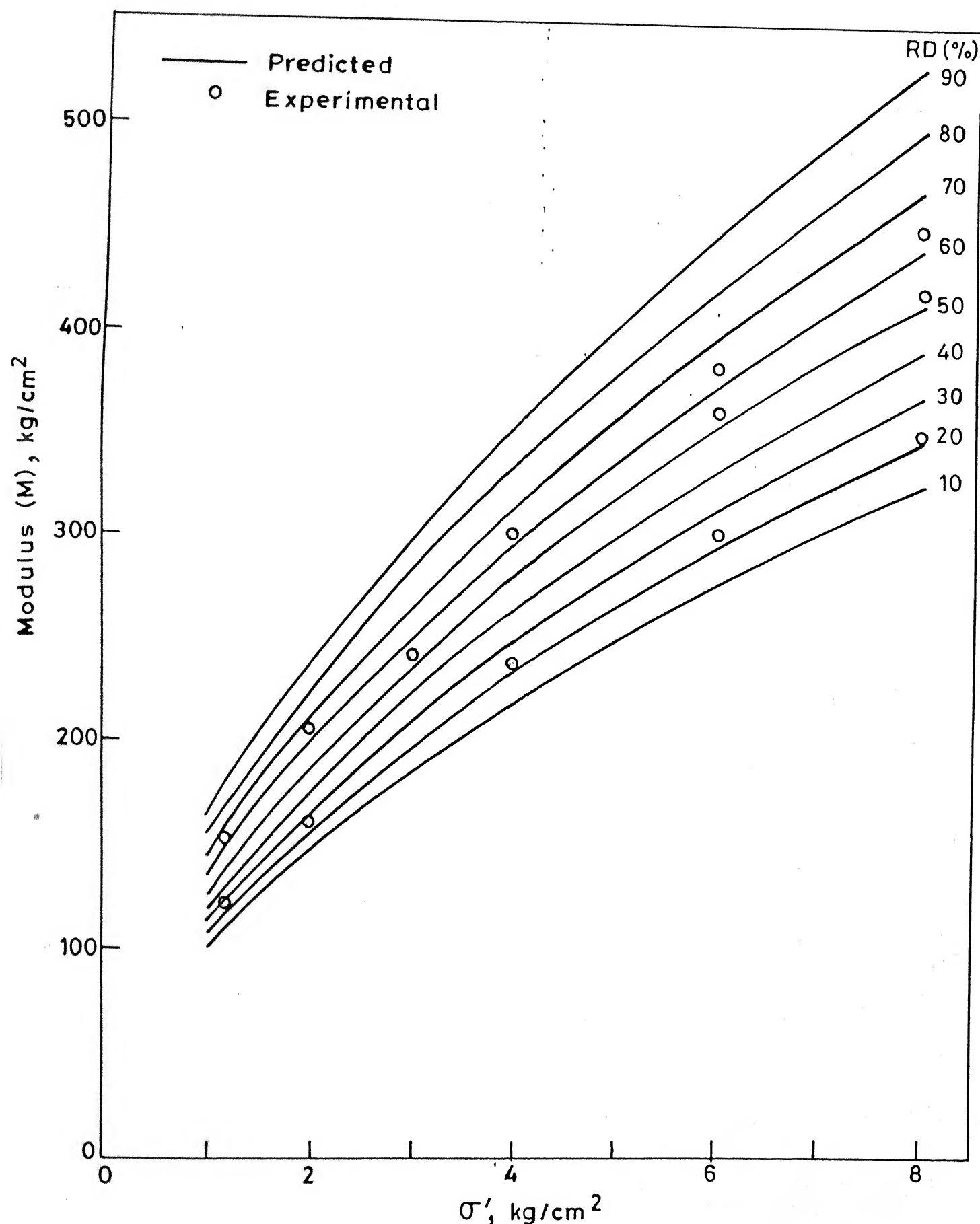


Fig. 5.78 Effect of relative density and σ' on modulus for Ganga sand.

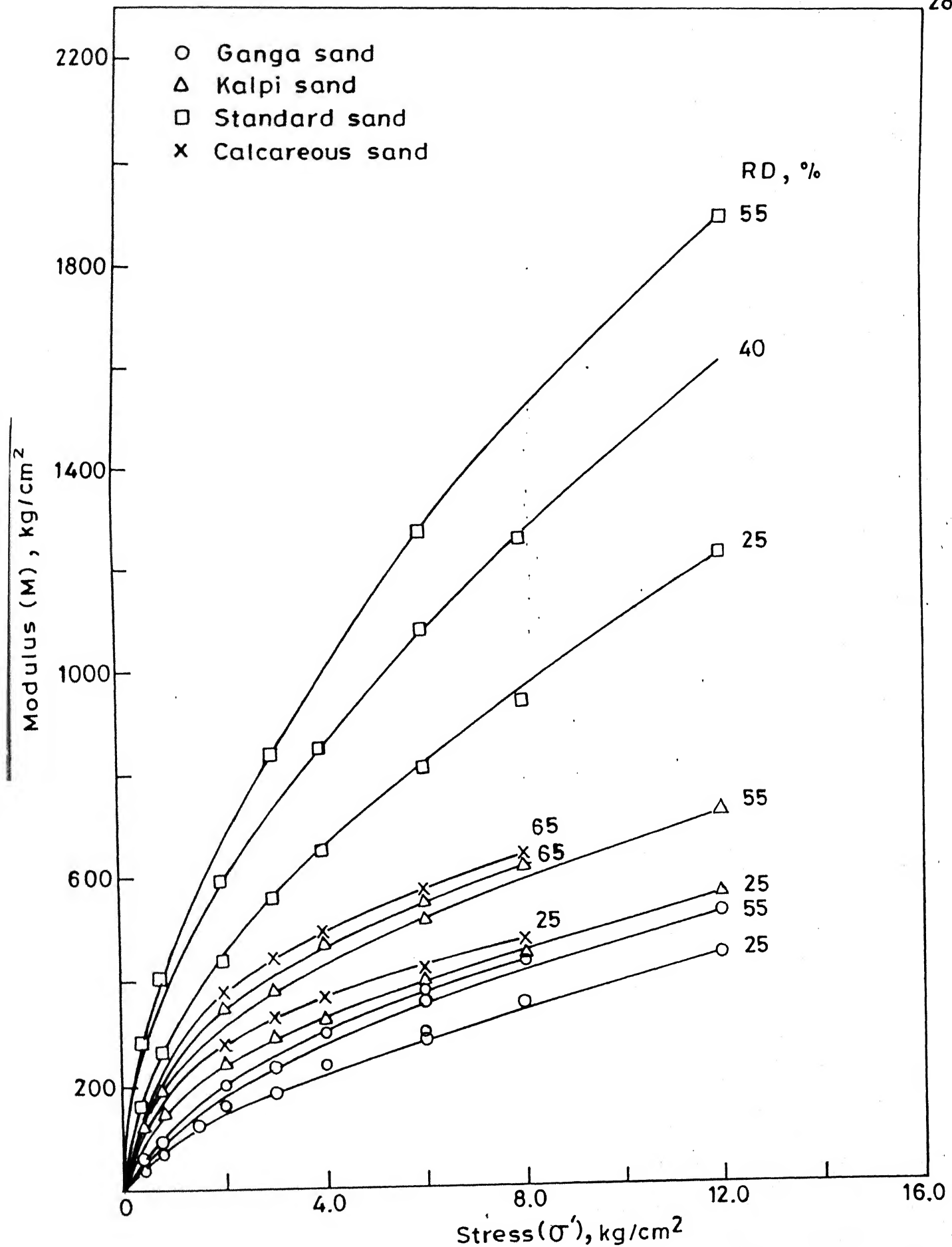


Fig. 5.79 Effect of RD and σ' on modulus for Ganga, Kalpi, standard and calcareous sands.

m_0 , m_1 and m_2 values as recommended in Table 5.8, a generalized comparative relationships of modulus and stress for sands of different compressibilities are presented in Fig. 5.80. Results are compared for relative densities of 0.40 and 0.80 for all the three categories of sands.

Similarly using C_0 , C_1 and C_2 values (Table 5.8), a generalized comparative relationship of q_c and stress for three categories of sands are shown in Fig. 5.81. The relationship as reported by Robertson et al (1983) on the basis of sand compressibility is also shown as insert in this Figure. As can be seen, the patterns as predicted from the present study are in agreement with trends reported by Robertson and coworkers. It may be indicated that the patterns for the trends in Fig. 5.80 and 5.81 in terms of modulus and q_c strikingly similar as influenced by sand compressibility.

The values of m_0 , m_1 and m_2 as well as C_0 , C_1 and C_2 have been correlated with particle angularity. As indicated earlier, low, moderate and high compressibility of sands is directly related to particle angularity (for the same mineral composition). Particle angularity was related to Powers' roundness index (Table 2.2). Relationship between coefficients m_0 , m_1 , m_2 , C_0 , C_1 and C_2 and Powers' roundness index have been presented in Fig. 5.82. Although additional data points would be needed to evolve the exact nature of these relationships, the overall trends are distinct.

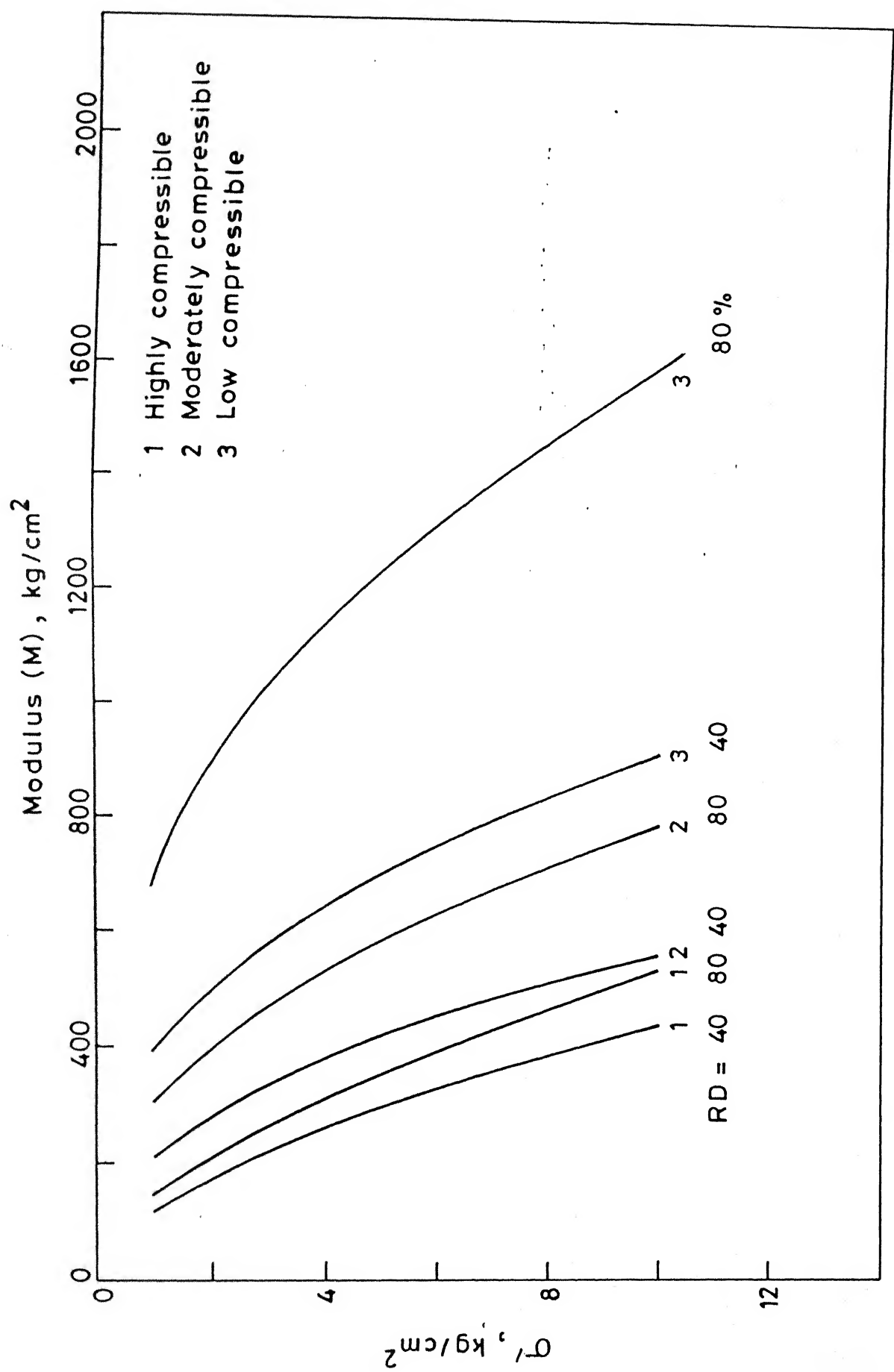


Fig. 5.80 Comparison of M vs σ' for three types of sands at two relative densities.

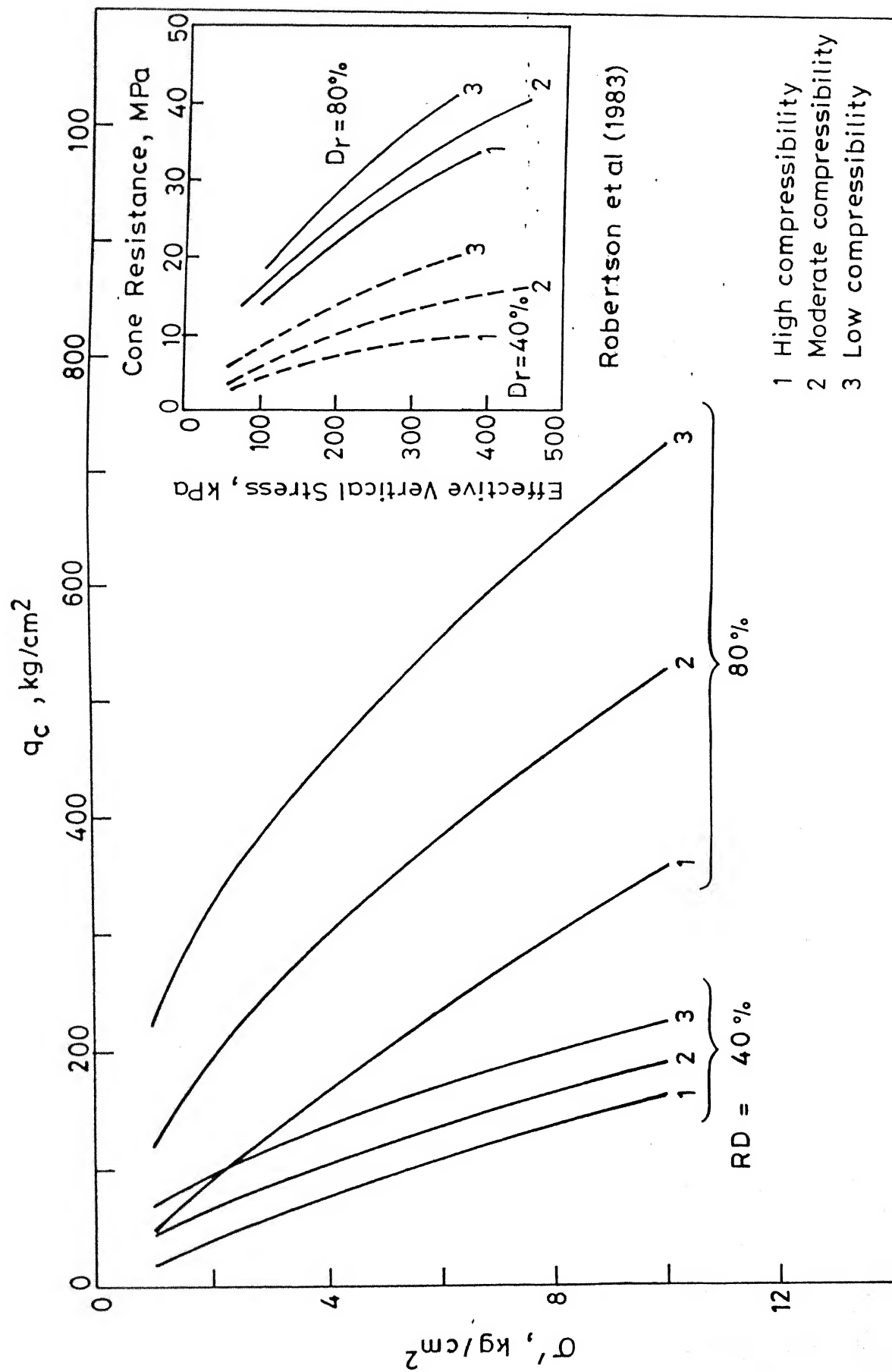


Fig. 5.81 Comparison of q_c vs. σ' for three types of sands at two relative densities.

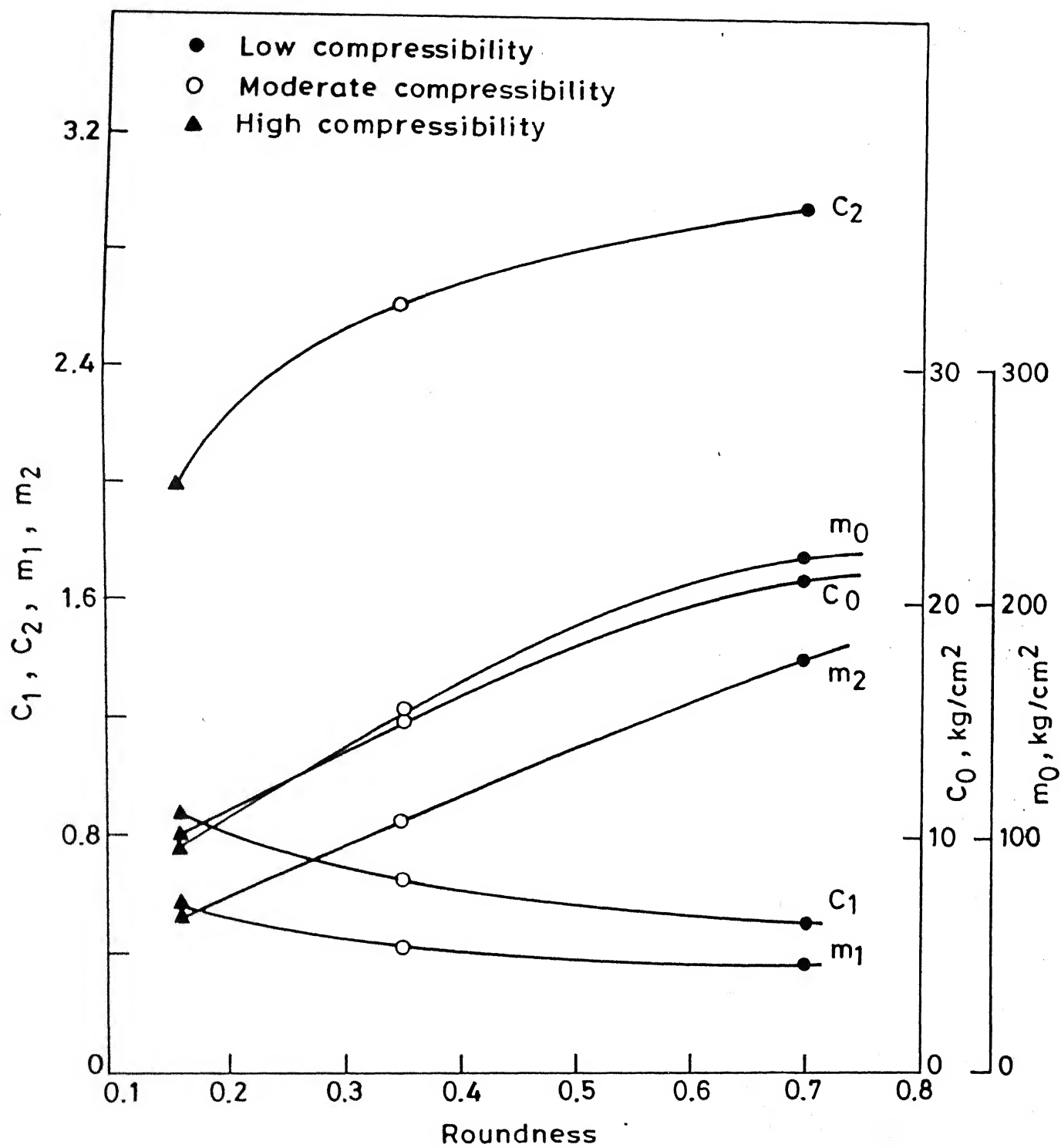


Fig. 5.82(a) Relationship between model parameters for modulus, q_c and particle roundness.

5.3.3.3 Relationship Between q_c and Angle of Shearing Resistance

Broms (1986) has reviewed the available data on various relationships between q_c and ϕ' for sands. The influence of effective overburden pressure and sand compressibility on such a relationship has been indicated. In Fig. 5.82(b), the predicted trends for sands of low and high compressibility from the present study are presented along with the reported values by Meyerhof (1976). The predicted trends are on the basis of the following relationships:

$$\tan \phi' = .64(\sigma')^{-0.04} e^{-5.6 DR} \quad (5.16) \quad \text{For sands of high compressibility}$$

$$q_c = 10(\sigma')^{0.87} e^{1.99 DR} \quad (5.17)$$

$$\tan \phi' = 0.5 (\sigma')^{-0.07} e^{-8.3 DR} \quad (5.18) \quad \text{For sands of low compressibility}$$

$$q_c = 21(\sigma')^{0.51} e^{2.96 DR} \quad (5.19)$$

Relationships (5.16 and 5.18) are based on drained direct shear test data (Phool Chand 1988). The results shown in Fig. 5.82(b) clearly indicate the influence of effective overburden stress and sand compressibility. The relationship proposed by Meyerhof appears to be applicable for sands of medium to low compressibility at low effective stresses. As such there cannot be a unique relationship between q_c & ϕ' irrespective of sand compressibility and effective overburden pressure.

5.3.3.4 Relationship Between M and q_c

The modulus and q_c values as predicted by using m_0 , m_1 , m_2 , C_0 , C_1 , and C_2 recommended for three categories of sands have been compared over a wide range of relative densities.

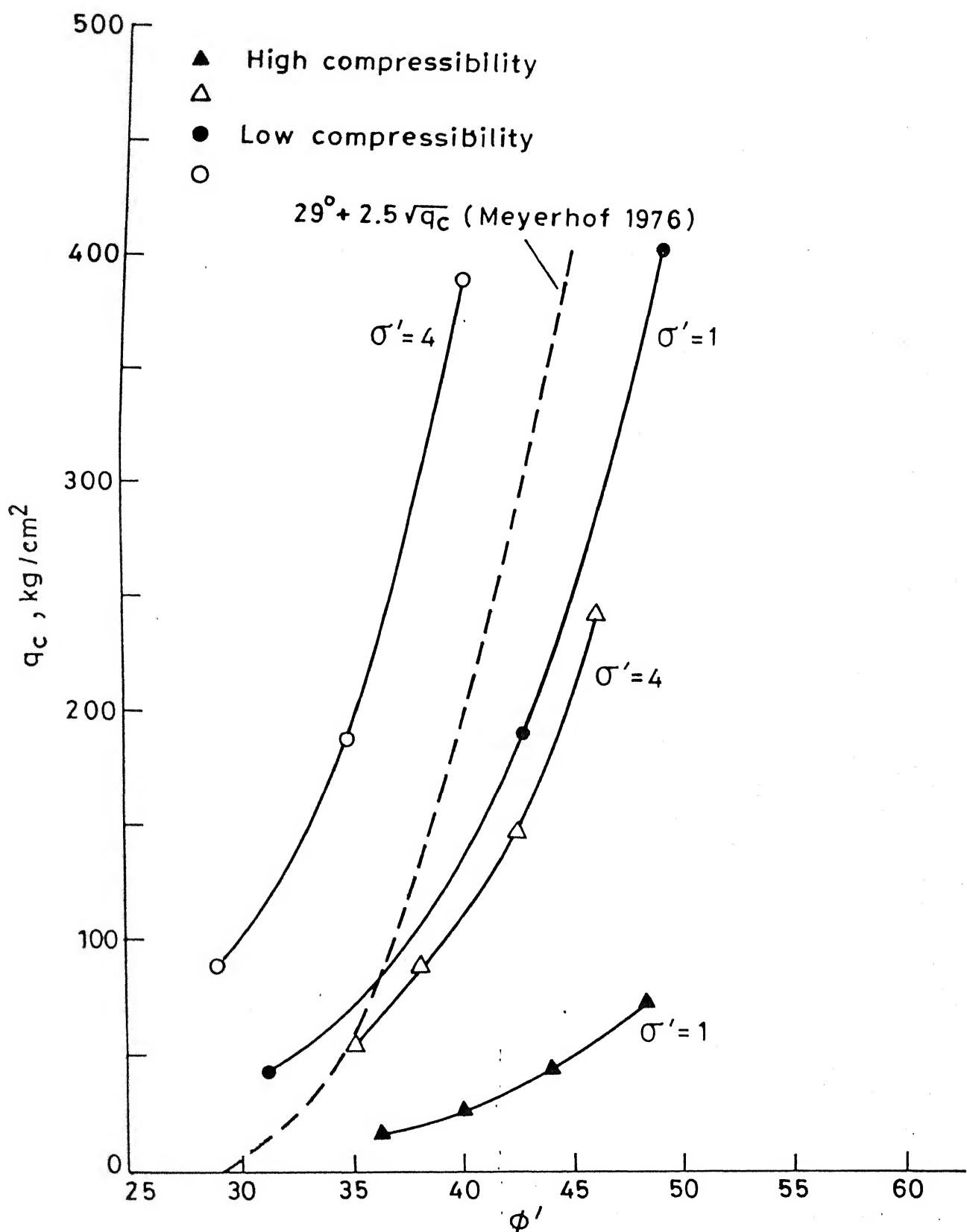


Fig. 5.82(b) Relationship between q_c and angle of shearing resistance (ϕ').

Similar plots have also been reported by Robertson et al. (1983). The relationships for sands for low, moderate and high compressibility are shown in Figs. 5.83 to 5.85 together with the variation of α ($=M/q_c$) versus relative density at stress level of 1 and 10 Kg/cm^2 . Within this stress range, the variation of α values for relative density values of 0.0 and 1.0 is shown in Table 5.9. While q_c versus stress and M versus stress relationships at a given relative density are markedly different for sands of different compressibility, the values of α for all the three categories of sands are within a narrow range for a given relative density. The average curves fitted through the data of α values for all the three categories of sands are presented in Fig. 5.86. The relationship between α and relative density (DR) may be represented as

$$\alpha = 10 \sigma'^{-.22} e^{-(1.6DR)} \quad (5.20)$$

The above expression is valid for normally consolidated sands upto a stress level of 10 Kg/cm^2 and the α values are within the range reported in literature (Mitchell and Gardner 1975). Robertson et al. (1983) suggest the values for α in the range 3-11. The above equation thus appears to define a somewhat unique relationship between α and relative density for normally consolidated sands.

Thus in this section, the following generalizations have been arrived at:

1. Sands, depending on their mineralogy, particle size, shape, angularity and gradation can be grouped into three

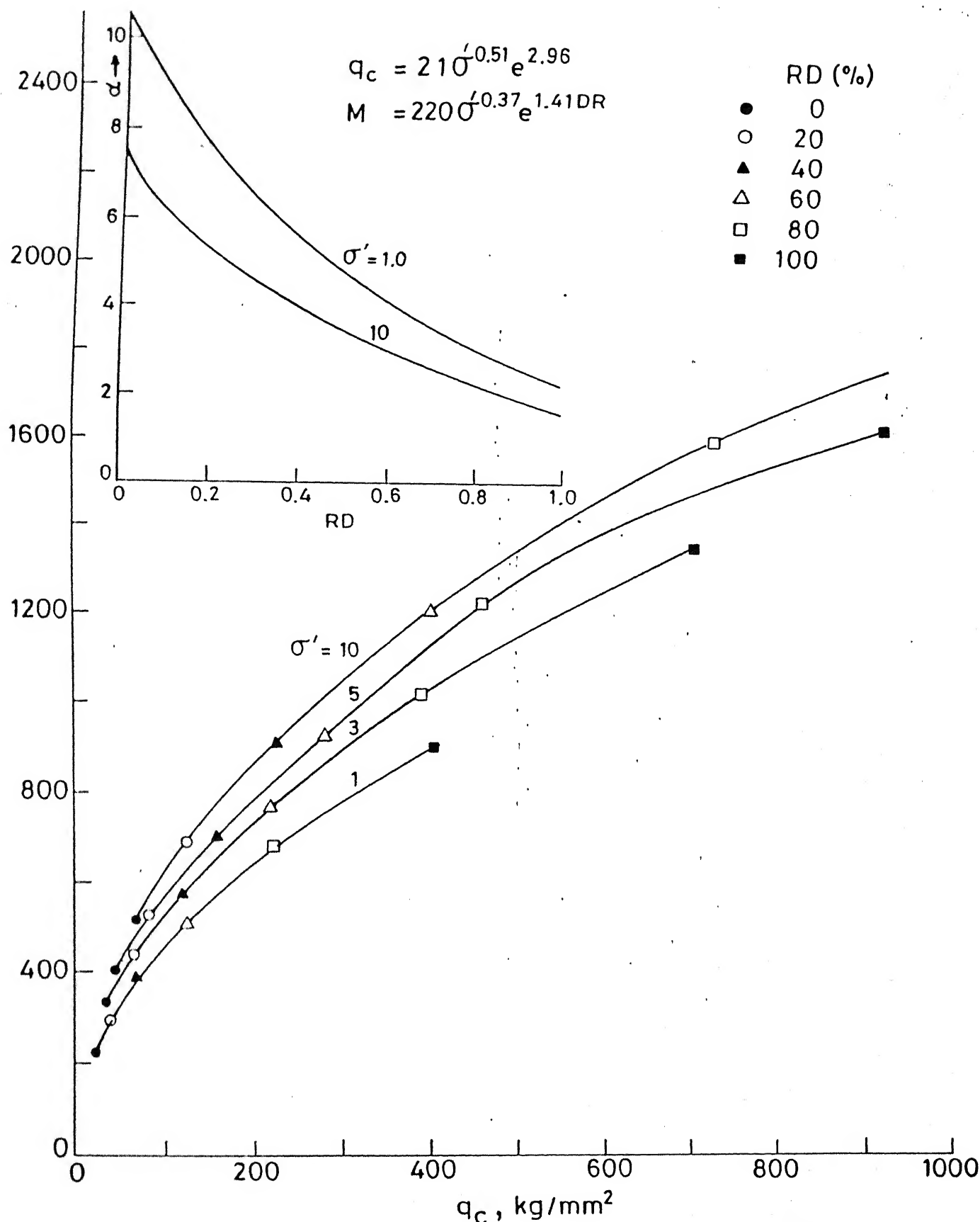


Fig. 5.83 Relationship between M and q_c for sands of low compressibility.

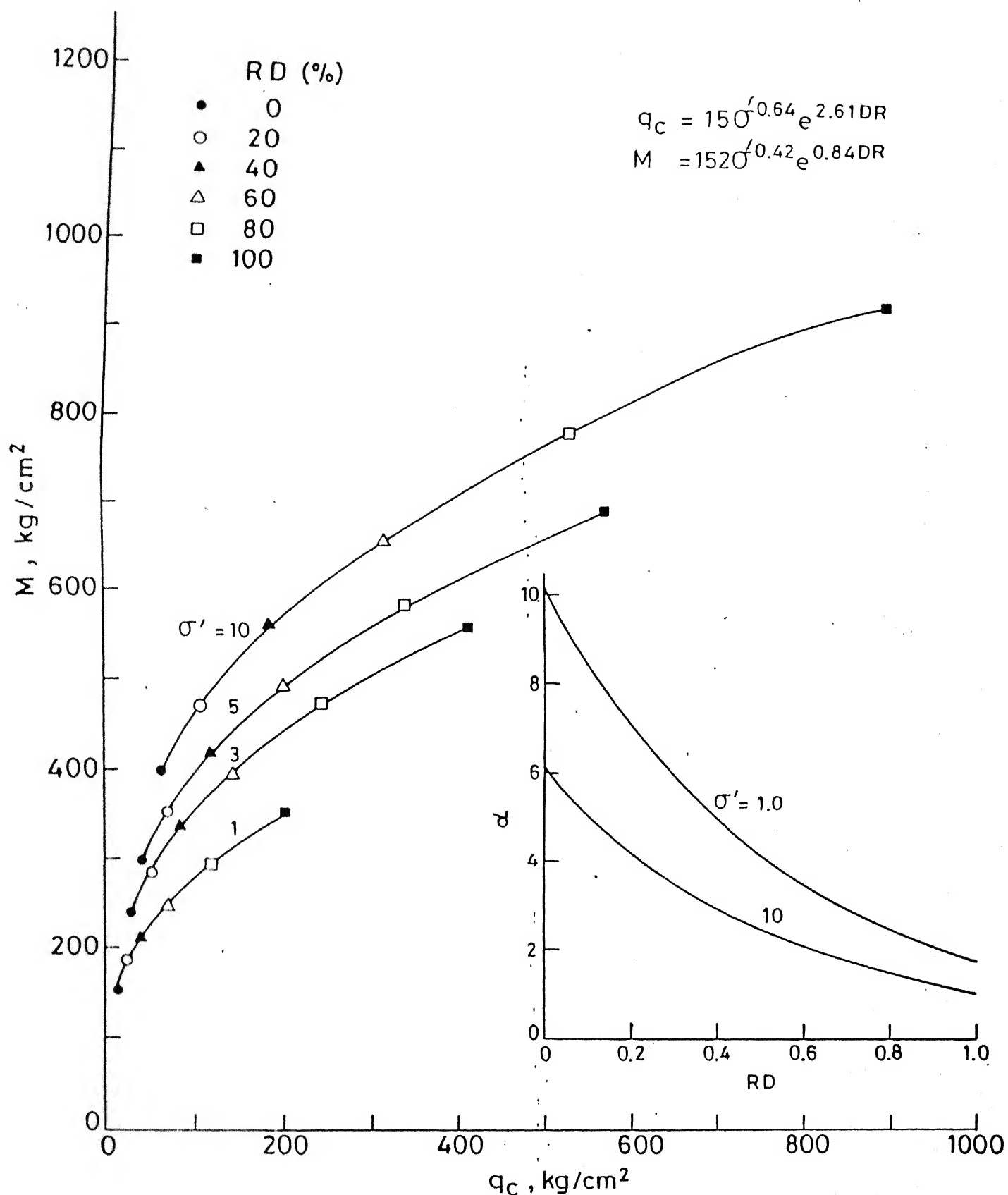


Fig. 5.84 Relationship between M and q_c for sands of moderate compressibility.

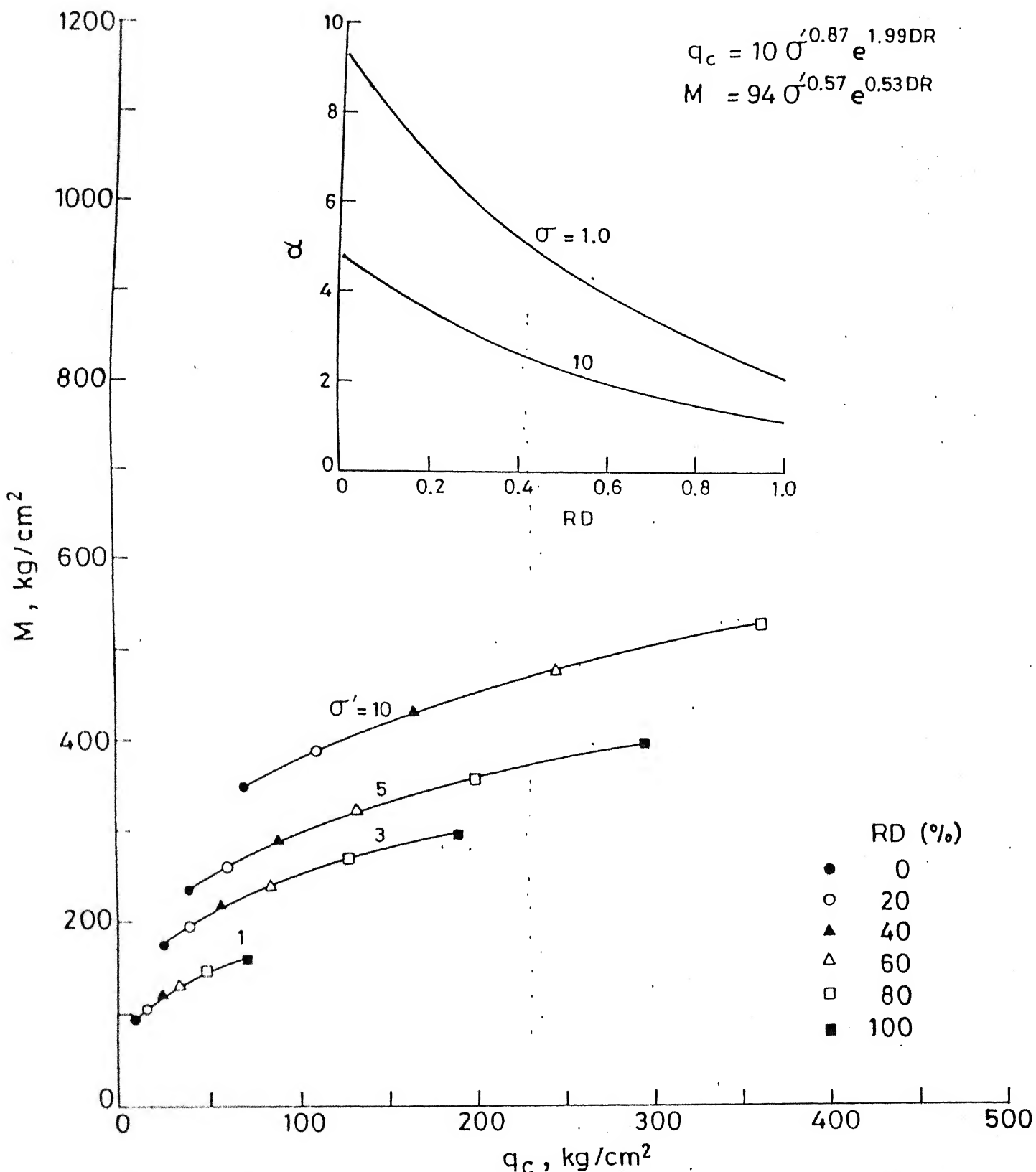


Fig. 5.85 Relationship between M and q_c for sands of high compressibility.

Table 5.9 : Range of α Values for Sands with Ranging
Compressibility

Sand Type	$\sigma' = 1 \text{ to } 10 \text{ Kg/cm}^2$	
	DR = 0	DR = 1.0
Low Compressibility	7.5 - 11.0	1.6 - 2.2
Moderate Compressibility	6.0 - 10.0	1.0 - 1.7
High Compressibility	4.8 - 9.4	1.1 - 2.2

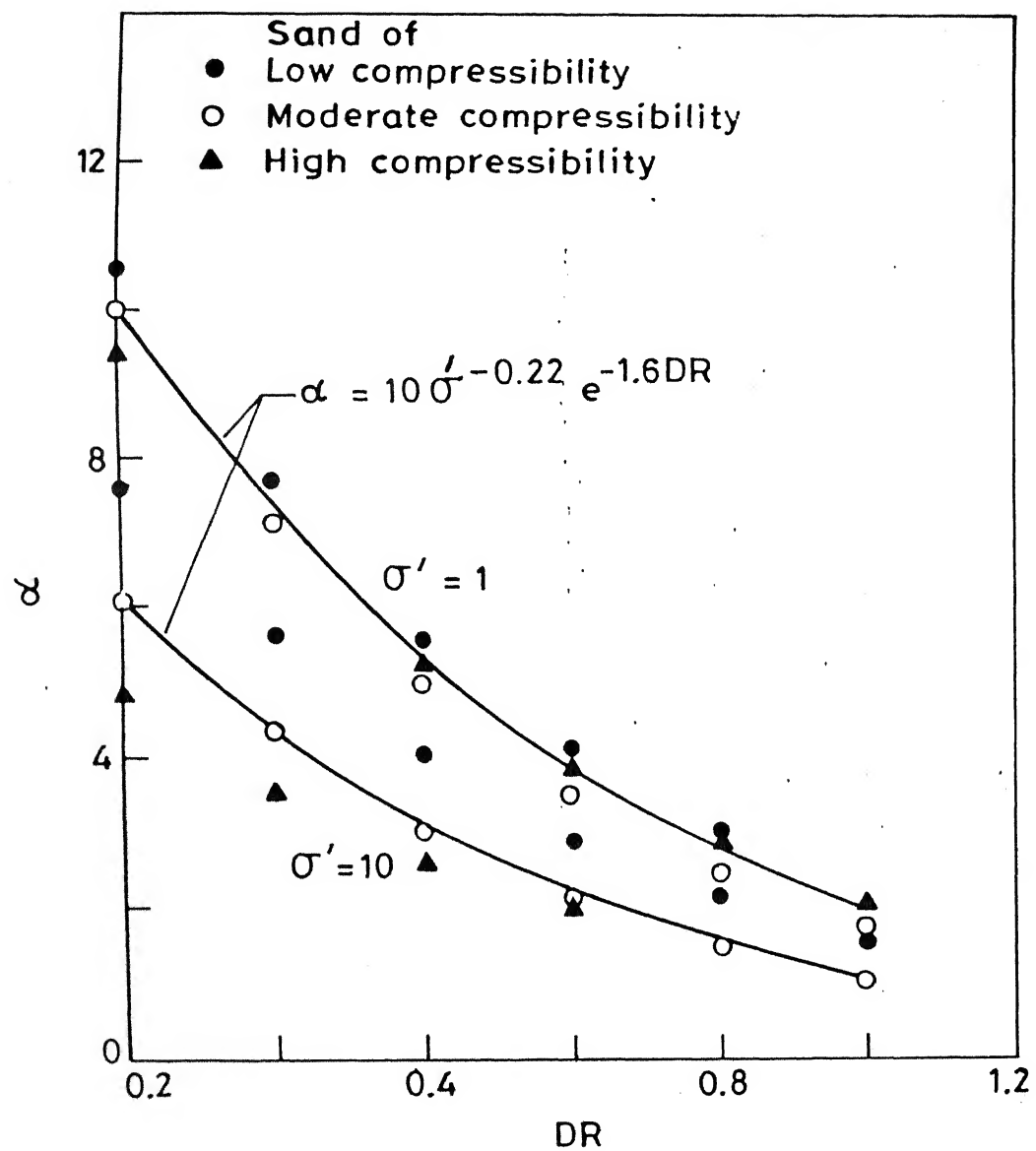


Fig. 5.86 α - DR relationship for sands.

broad categories (Table 5.6) as (i) sands of low compressibility, (ii) sands of moderate compressibility and (iii) sands of high compressibility.

2. Even though factors such as grain size, shape, angularity, gradation, relative density and mineralogy seem to govern the compressibility of sands in a complex manner, the particle angularity and mineral content (for same relative density) appear to be the two most important factors.
3. Stress-strain behaviour of compressible sands is markedly different in low stress ($\sigma' < 10 \text{ Kg/cm}^2$) and high stress ($\sigma' > 30 \text{ Kg/cm}^2$) ranges.
4. Constrained modulus (M) is shown to be related to effective stress and relative density through the expression

$$M = m_0 \sigma'^{m_1} e^{m_2 DR}$$

This is consistent with the model proposed by Bellotti et al (1985). The values of m_0 , m_1 and m_2 are a function of sand compressibility (Table 5.8).

5. The coefficients m_0 , m_1 and m_2 as evaluated are valid for $\sigma' < \sigma'_c$, σ'_c being the critical stress at which significant grain modification begins. Based on limited data, relationship between critical stress and relative density for variety of sands has been proposed. The values of m_0 , m_1 and m_2 will be different for the different stress levels exceeding σ'_c , when grain crushing commences.

broad categories (Table 5.6) as (i) sands of low compressibility, (ii) sands of moderate compressibility and (iii) sands of high compressibility.

2. Even though factors such as grain size, shape, angularity, gradation, relative density and mineralogy seem to govern the compressibility of sands in a complex manner, the particle angularity and mineral content (for same relative density) appear to be the two most important factors.
3. Stress-strain behaviour of compressible sands is markedly different in low stress ($\sigma' < 10 \text{ Kg/cm}^2$) and high stress ($\sigma' > 30 \text{ Kg/cm}^2$) ranges.
4. Constrained modulus (M) is shown to be related to effective stress and relative density through the expression

$$M = m_0 \sigma'^{m_1} e^{m_2 DR}$$

This is consistent with the model proposed by Bellotti et al (1985). The values of m_0 , m_1 and m_2 are a function of sand compressibility (Table 5.8).

5. The coefficients m_0 , m_1 and m_2 as evaluated are valid for $\sigma' < \sigma'_c$, σ'_c being the critical stress at which significant grain modification begins. Based on limited data, relationship between critical stress and relative density for variety of sands has been proposed. The values of m_0 , m_1 and m_2 will be different for the different stress levels exceeding σ'_c , when grain crushing commences.

6. Based on the effect of grain angularity on ϕ' and sand compressibility on mode of failure around static penetration cone, the relation of q_c with the effective stress and relative density is of the following form

$$q_c = C_c \sigma' C_1 e^{C_2 DR}$$

Bellotti et al (1985) proposed a similar form. The values of C_0 , C_1 and C_2 are proposed to be function of sand compressibility (Table 5.8). The values of C_0 , C_1 , and C_2 as evaluated are valid for $\sigma' < 10 \text{Kg/cm}^2$. Coefficients C_0 , C_1 , and C_2 like m_0 , m_1 , and m_2 have been correlated with Powers' roundness index.

7. It has been brought out (Fig. 5.82(b)) that q_c versus ϕ' relationship is governed by sand compressibility and effective overburden stress. There is thus no unique relationship between q_c and ϕ' applicable to all sands as suggested in the literature.

8. Even though modulus versus stress and q_c versus stress (for a given relative density) are shown to be intimately governed by the sand compressibility, their ratio $\alpha = M/q_c$ appears to be uniquely related primarily to relative density and to a lesser degree to the stress. It is proposed that, as a first estimate, α may be evaluated from the expression

$$\alpha = 10 \sigma'^{-.22} e^{-1.6 DR}$$

The value of modulus may thus be estimated using q_c as obtained from the cone test.

CHAPTER VI

CONCLUSIONS

The pattern of deformation of sands under different stress conditions is controlled by several parameters such as the grain size, shape, angularity, state of packing and mineralogy. While earlier studies have emphasized on the grain size and state of packing, importance of grain shape and angularity as well as the mineralogy has not been satisfactorily worked out. On the basis of the detailed investigations undertaken in the present study to examine the interrelationships between various parameters operative during deformation of sands and quantitative evaluation of the same, the following aspects are established:

- 6.1 The particle shape characterization for each of the sand fraction in the sand used in the present study have been carried out using the Zingg diagram and shape factor. On the basis of Zingg diagram and the shape factor versus sphericity relationship (Fig.5.1b), sands can be classified with respect to grain shape.
- 6.2 The tangent count technique, using the image analyzer provides an accurate and highly reliable method to quantify particle surface characteristics of a variety of sands. Typical average tangent count distributions for subrounded to rounded, subangular, angular and very angular grains have been developed (Figs. 5.17 and 5.18) and are recommended as a useful tool for classification of sands in respect of grain angularity. The average tangent count has been employed to provide a systematic

method for evaluation of Powers' roundness index, R (Fig. 5.1c) which can be used to classify sand based on the grain angularity.

6.3 Relationship between angularity and size for a particular alluvial sand can be demonstrated in terms of average tangent count per unit circumferential length of particles for each sieve fraction. An inverse relationship between particle angularity and size has been established in case of alluvial sands (Fig. 5.1a).

6.4 It has been shown that while average tangent count is useful for comparing sands having grains of different angularity, the particle angularity defined as

$$\frac{\text{average number of tangents in a sieve fraction}}{\text{average circumference of the particles in that fraction}}$$

is a good measure of variation of angularity with particle size for a given sand. Particle angularity for alluvial sands is shown to decrease with increase in grain size.

On the basis of these conclusions, it is recommended that in addition to the usual classification tests for sands (e_{\max} , e_{\min} , e , grain size distribution etc.), the shape and angularity characteristics of sand grains should also be evaluated using the technique demonstrated in this study.

6.4 For sands with a wide range of particle gradation characteristics a relationship between total potential for particle breakage (B_p) (Fig. 5.22) and d_{50} (mm) has

been established as:

$$B_p = 1.02 \log d_{50} + 1.15$$

6.6 At low stress levels, ($< 22 \text{ kg/cm}^2$) the total particle breakage (B_T), increases with grain angularity (h/λ) for a wide variety of sands (Fig. 5.26a).

6.7 For same mineralogy and particle angularity, total particle breakage (B_T) (Fig. 5.19) of a sand at a given relative density increases with d_{50} (Fig. 5.26b) over a wide range of stress.

6.8 Based on compression tests at different stress levels (11.02, 22.04, 88.16 kg/cm^2) along with subsequent particle shape analysis (Fig. 5.27), tangent count distribution (Figs. 5.28 to 5.30), smooth edge distribution (Figs. 5.31 to 5.33), particle angularity (Fig. 5.34) and particle breakage analysis (Fig. 5.35), it has been established that there exists a critical stress level, σ'_c at which grains of alluvial sands undergo modification. This critical stress is much less than that required for actual grain crushing and its value depends on mineral composition, size, shape, angularity, gradation and relative density of the sand. On the basis of limited test data available, a tentative relationship between critical stress σ'_c and relative density for a variety of sands has been proposed (Fig. 5.68).

6.9 The grain modification continues upto a stress level of about 80 Kg/cm^2 after which actual particle breakage (crushing) starts. The variation of particle breakage (expressed in terms of B_r) with stress is in general

agreement with the pattern suggested by Terzaghi and Peck (1943) and De Beer (1963). However, the B_r versus σ'_c relationship depends on the nature of the sand.

6.10 For weak sands (Ganga, Kalpi, Calcareous, Crushed Granite and Napa Basalt etc.) the change of B_r with stress may be considered in four phases (Fig. 5.37).

- i) For stress $< 20 \text{ Kg/cm}^2$, the rate of increase of B_r with stress is high and particles undergo modification.
- ii) For stresses between 20 and 100 Kg/cm^2 , the modification continues but B_r increases at a lower rate compared to that in phase (i).
- iii) For stresses greater than 100 Kg/cm^2 , significant particle crushing begins and B_r experiences the highest rate of increase upto a limiting stress which is likely to be smaller than 1000 Kg/cm^2 (Fig. 5.39).
- iv) For stresses greater than the limiting stress, B_r increases at a lower rate than that in phase (iii).

6.11 The variation of B_r with stress in case of strong sands (well rounded quartz, Standard and Mol Sand, etc.) also occurs in four phases (Fig. 5.37)

- I) For stresses upto 200 Kg/cm^2 , the increase of B_r is only marginal, with some modification/crushing in case of subrounded grains.
- II) For stresses between 200 to 400 Kg/cm^2 , B_r increases relatively faster than that in phase I. Grain crushing has started in this phase.

III) The highest rate of increase of B_r occurs for stresses between 400 to 1000 Kg/cm^2 (Fig.5.39).

IV) For stresses greater than a limiting stress (1000 Kg/cm^2) rate of increase of B_r is less than that in phase III.

6.12 The behaviour of subangular to subrounded sands (as in the case of Toyoura Sand) is intermediate to that of weak and strong sands.

6.13 Relative breakage B_r increases with mica content (Fig.5.40a).

6.14 There exist a relationship between B_r and quartz content (also quartz plus feldspar) for different sands (Fig.5.40b).

6.15 Based on the data mainly for Calcareous and Kalpi sands, the effect of carbonate on particle crushing has been evaluated (Fig.5.40c).

6.16 The relative breakage parameter B_r is a much superior index of particle crushing (modification) than some of the other indices available in the literature.

Based on grain size, shape, angularity, mineralogy, gradation and relative density, natural sands' experience particle degradation to varying degrees under stress. Studies related to particle degradation for weak sands under stress should distinguish between grain modification which starts at a critical stress level, and grain breakage (crushing) which commences at a stress level of about 100 Kg/cm^2 . The results of changes in particle gradation under stress should be expressed in terms of Hardin's B_r parameter.

6.17 Based on the test results and comparisons with the predictions from Hardin's Model, the following inferences are made:

- a) The hyperbolic law to predict relative breakage under stress is not unique for all types of sands. The shape of the predicted curve seems to be highly sensitive to the magnitude of the reference breakage stress, σ'_r , (Fig. 5.44a).
- b) Normalization of the test results under different stress paths can be achieved using σ'_1 and σ'_b (Fig. 5.42). The model parameters can as well be worked out in terms of σ'_1 rather than σ'_b which requires reliable values of K_0 for the sand. The ratio σ'_b / σ'_1 varies between 0.9 to 1.5 over the range of K_0 values for normally consolidated sands (Fig. 5.44).
- c) The range of B_r values attainable in practice is likely to be limited to 0.5 (Figs. 5.36, 5.37, 5.38, 5.41, 5.45) even when the stress level is as high as 1000 Kg/cm².

6.18 The shape number (n_s) of Hardin's classification for the computation of reference breakage stress, is correlated with Powers' roundness index (Fig. 5.47). This enables a better classification of grain shape (angularity) which correlates with average number of tangents on grain surface (Table 5.5). Hardin's four part shape (angularity) classification can thus be refined.

Parameters for Hardin's hyperbolic law may as well be worked out in terms of σ'_1 rather than σ'_b . The value of Hardin's

shape number (n_s), for a sand may be obtained from the relationship between n_s and Powers' roundness index (R) (Fig.5.49).

6.19 Stress-strain behaviour of compressible sands is markedly different in low stress ($\sigma' < 10 \text{ Kg/cm}^2$) and high stress ($\sigma' > 30 \text{ Kg/cm}^2$) ranges (Figs. 5.50, 5.51, 5.52).

6.20 Of the factors such as grain size, shape, angularity, gradation and mineralogy that govern the compressibility of sands (for a given relative density) in a complex manner, the particle angularity and mineralogy appear to be the two most important ones (Fig.5.53).

6.21 On the basis of mineralogy, particle size, shape, angularity and gradation, sands can be grouped (Table 5.6) into three broad categories in terms of their compressibility into

- (i) sands of low compressibility,
- (ii) sands of moderate compressibility, and
- (iii) sands of high compressibility.

6.22 The relationship between the constrained modulus (M) and effective stress as proposed by Janbu (1963, 85) and Belotti et al (1985) are valid in the stress range less than the critical stress σ'_c . At stresses beyond this critical value (and less than 100 kg/cm^2), the weak sands undergo significant changes due to grain modification and the relationship between M and effective stress as obtained from experimental data in the present study significantly differs from those that predicted earlier (Figs.5.62 to 5.66).

6.23 At stresses less than the critical stress, M is proposed to be related to effective stress and relative density by the following relationship

$$M = m_0 \sigma'^{m_1} \exp(m_2 D_R)$$

The values of m_0 , m_1 and m_2 for sands of varying compressibility are also estimated (Table 5.7).

6.24 The effect of compressibility on $M - \sigma'$ relationship for sands has been highlighted (Fig. 5.80).

6.25 Based on effect of grain angularity on angle of shearing resistance and sand compressibility on mode of failure around static penetration cone, q_c has been computed at different values of σ' and relative density. The dependence of relationship between q_c and σ' on sand compressibility has been brought out (Fig.5.81a). These trends agree with those presented by Campenella et al. (Fig.5.81 in set).

6.26 A relationship between q_c , relative density and effective stress, is worked out in the present study, is similar to the one reported by Belotti et al (1985) and is of the form

$$q_c = C_0 \sigma'^{C_1} \exp (C_2 D_R)$$

The values of C_0 , C_1 and C_2 are proposed (Table 5.7) for sands of varying compressibility. As ϕ' decreases at high stresses, the proposed relationship and the coefficients C_0 , C_1 and C_2 are applicable strictly for stress levels less than 10 Kg/cm^2 .

6.27 Even though the relation of σ' with M as well as with q_c (at a given relative density) are shown to be intimately governed by the sand compressibility, the

ratio, $\alpha = M/q_c$ however appears to be uniquely related to relative density and effective stress. The range of values of α (3-11) is in agreement with the reported values of Compenella et al.

6.28 It has been brought out (Fig.5.82(b)) that q_c versus ϕ' relationship is governed by sand compressibility and effective overburden stress, and hence no unique relationship between q_c and ϕ' is applicable to all sands as suggested in the literature.

6.29 It is proposed that as a first estimate, α may be evaluated from the following relationship:

$$\alpha = 100'^{-0.22} \exp (-1.6 DR)$$

The value of M thus can be estimated on the basis of q_c obtained from the cone test.

The compressibility of sands is strongly controlled among other factors by mineralogy and grain angularity. At low stresses, the stress-strain behaviour of weak sands is mainly governed by grain interlocking. At higher stress (>30 Kg/cm^2), the stress-strain behaviour is significantly different from that at low stresses due to the grain modification and crushing. This distinction should be clearly recognized.

The power relationship of modulus with stress and relative density tacitly assumes that the sand remains unchanged (without any change in its stress-strain behaviour) during loading to high stresses. The fact that the stress-strain behaviour of the sand undergoes changes due to

particle modification and crushing at high stresses, these power laws and the suggested coefficients m_0 , m_1 and m_2 are strictly applicable for stress levels less than critical stress. Both q_c versus σ' and M versus σ' relationships are strongly controlled by the compressibility of the sand. Therefore any relationship developed for a particular sand is only applicable for sands of similar compressibility characteristics. Correlation developed for relatively incompressible rounded to subrounded artificial quartz sands is therefore not to be applicable to natural sands which are as a rule subangular to angular in character and therefore compressible in behaviour.

The expression $\alpha = 100'^{-0.22} \exp(-1.6 DR)$ may be employed to estimate the value of M on the basis of cone penetration resistance value (q_c) commonly obtained as part of soil investigation program.

REFERENCES

Aga, J.G. Morgenstern, N.R. and Scott, J.D. (1987), "Shear Strength and Stress-Strain Behaviour of Athabasca Oil Sand at Elevated Temperature and Pressures" Canadian Geotechnique Vol.24, No.1, pp. 1-10.

Al Hussain, M. (1983), "Effect of Particle Size and Strain Condition on the Strength of Crushed Basalt" Canadian Geotechnique Vol. 4, pp.707-717.

Bellotti R. et al, (1985), "Laboratory Validation of in Situ Tests," Geotechnical Engineering in Italy. An Overview, Published on Occasion of ISSMFE Golden Jubilee.

Beringen, F.L., Kolk, H.J. and Windle, D. (1982), "Cone Penetration and Laboratory Testing in Marine Calcareous Sediments ASTM, STP 777, pp. 179-209.

Billam J. (1971), "Some Aspects of the Behaviour of Granular Material at High Pressures" Proceedings Rescoe Memorial Symposium.

Blatt, H, Middleton, G. & Murray, R. (1971), "Origin of Sedimentary Rocks," Prentice Hall Inc. Englewood Cliff, New Jersey, USA.

Bolton, M.D. (1984), "The Strength and Diltancy of Sands", Cambridge University Reports.

Broms, B.B. (1986), "Penetration Tests" Fourth International Geotechnical Seminar, Singapore.

Burmister, M.D. (1936), "The Grading-Density Relations of Granular Materials", Bulletin No.6, Civil Engineering Research Laboratory, Columbia University.

Burmister, M.D. (1946), "The Importance and Practical Use of Relative Density in Soil Mechanics", Presented at the Meeting of Committee D-18 on Soils for Engineering Purpose Held During the Fifty First, Annual Meeting of Society Detroit, Mich.

Burmister, M.D. (1962), "Physical-Stress-Strain & Strength Response of Granular Soils" Symposium on Field Testing of Soils, Special Technical Publication Vol. 322, ASTM.

Castro, G. (1969), "Liquefaction of Sands," Harvard Soil Mechanics Series, No. 8, Pierce Hall, Cambridge Massachusetts.

Clayton, C.R.I., et al. 1985), "Dynamic Penetration of Resistance and the Prediction of the Compressibility of Fine Grain Sand - A Laboratory Study," Geotechnique Vol.35, No.1, pp. 19-31.

Datta, M., Gulhati, S.K. and Rao, G.V. (1979), "Crushing of Calcareous Sands During Drained Shear", Society of Petroleum Engineering.

Datta, M., Gulhati, S.K. and Rao, G.V. (1980), "Engineering Behaviour of Carbonate Soils of Indian and Some Observations of Such Soils", ASTM, STP, 777.

EL Sohby, M.A. (1969), "Deformation of Sands Under Constant Stress Ratio", Proc. of 7th I.C.O. SMFE, Mexico, Vol. 1, pp. 111-119.

EL Sohby M.A. and Andrews, K.Z. (1972), "Deformation Characteristics of Granular Material Under Hydrostatic Compression", Canadian Geotechnique, Vol. 4, pp. 323-338.

Frassoni, A. (1982), "Large Scale Laboratory Tests for the Mechanical Characteristics of Granular Material", Int. Conf. on Large Dam-RIO-DE-JANARO.

Grives, D.A. and Harr, M.E. (1980), "Particle Contacts in Discrete Materials," Technical Note, J. of Geotechnical Engg. Div. ASCE, GT5, pp. 559-564.

Hardin, B.O., (1985), "Crushing of Soil Particles" Journal of Geotechnical Engineering Division, ASCE, Vol. No. 10, pp.1177-1192.

Haruyama, M. (1977), "Deformation Characteristics of Highly Compressible Sand-Shirasu", Soil and Foundation, Vol.17, No.1, pp.39-52.

Hilf, J.W. (1957), "Compacting Earth Dam with Heavy Jumping Rollers", Journal of ASCE, Vol. 83, SM2, No. 1205.

Hirschfeld, R.C. and Poulos, S.J. (1963), " High Pressure Triaxial Tests on a Compacted Sands and an Undisturbed Silt", Laboratory Shear Testing of Soils, Special Technical Publication, ASTM, No. 361.

Holubec, I. and D'Appolonia, E. (1973), "Effect of Particle Shape on the Engineering Properties of Granular Soils", Evaluations of Relative Density and Its Role in Geotechnical Projects Involving Cohesionless Soils, ASTM, STP 523 pp. 304-318.

Ishihara, K and Watanabe, T. (1976), "Sand Liquefaction through Volume Decrease Potential", Soils & Foundation, JSSMFE. Vol.16, No.6, pp. 61-70.

Junbu, N. (1985), "Soil Models in Offshore Engineering", Geotechnique Vol. 35, No.3, pp. 241-281.

Janbu, N. and Senneset, K. (1974), "Effective Stress Interpretation of In-situ Static Penetration Tests", Proceedings of European Symposium on Penetration Testings ESCOPT 1, Stockholm, Sweden, Vol.22, pp. 181 - 193.

Kapoor, J.K. (1985), "Compressibility and Frictional Resistance of a Variety of Sands", M.Tech. Thesis, Department of Civil Engineering, IIT Kanpur, India.

Koerner, R.M. (1970), "Effect of Particle Characteristics on Soil Strength", Journal of SMFE, Vol. 96, SM4, pp.1221-34.

Kolbuszeweski, J.J. (1948), "An Experimental Study of the Maximum and Minimum Porosities of Sands", Proc. 2nd, I.C.O. SMFE, Vol.1 Rotterdom.

Kolbuszeweski, J.J. and Frederick, M.R. (1963), "The Significance of Particle Shape and Size on the Mechanical Behaviour of Granular Materials", Proc. of European Conference on SMFE. Wiesbanden, Vol. 1 pp. 253-263.

Krumbein, W.C. (1941), "Measurement of Geological Significance of Shape and Roundness of Sedimentary Particles", Jour. Sedimentary Pet. Vol. 11, pp. 64-72.

Lambe, T.W. and Whitman, R.V. (1969), "Soil Mechanics" John Wiley and Son Inc. New York.

Lee, K.L. and Farhoomand, I. (1967), "Compressibility and Crushing of Granular Soils in Anisotropic Triaxial Compression", Canadian Geotechnical Journal Vol. 4, No. 1, pp. 68-99.

Lee, K.L. and Seed, H.B. (1967), "Drained Strength Characteristics of Sands", Journal of SMFE Division, ASCE, Vol. 93, No. SME, pp. 117-141.

Lee, K.L. and Seed, H.B. (1970), "Undrained Strength of Anisotropically Consolidated Sands", Journal of ASCE, Vol. 96, pp. 411-428.

Leps, T.M. (1970), "Review of Shearing Strength of Rockfill", Journal SMFE, ASCE, Vol. 96, No. SM4, pp. 1159-1170.

Marachi, N.D., Chan, C.K. and Seed, H.B. (1972), "Evaluation of Properties of Rockfill Materials", Journal SMFE, ASCE Vol. 98, No. SM1, pp. 95-114.

Marsal, R.J. (1967), "Large Scale Testing of Rockfill Materials", Journal of SMFE Division, ASCE, Vol. 93, No. SM2, pp. 271-430.

Mayne, P.W. and Kulhaway, F.H. (1982), "Ko-OCR Relation in Soil" Proc. 2nd Pan American Conference, SMFE, Brazil, Vol. 1, pp. 183-202.

Meyerhof, G.G. (1976), "Bearing Capacity and Settlement of Pile Foundations" ASCE, Vol. 102, No. GT3 pp. 197-228.

Miura, N. and Yamanouchi, T. (1973), "Compressibility and Drained Shear Characteristics of a Sand under High Confining Pressure", Reprint from Technology Report of the Yamaguchi University, Vol. 1, No. 2, pp. 271-290.

Miura, N. and Yamanouchi, T. (1975), "Effect of Water on the Behaviour of a Quartz Rich Sand under High Stresses", Soil & Foundation, JSSMFE, Vol. 15, No. 4, pp. 23-34.

Miura, N. and Sukeo-o-Hara (1979), "Particle Crushing of Decomposed Granite Soil Under Shear Stresses", Soil and Foundation, JSSMFE, Vol. 19, No. 3, pp. 1-14.

Moore, C.A. (1971), "Effect of Mica on K_0 Compressibility of Two Sands", Journal of SMFE Div., ASCE, Vol. 97 No. SM9 pp. 627-640.

National Research Council (1985), "Liquefaction of Soils During Earthquakes", National Academy Press, Washington, D.C.

Oda, M. (1972), "Initial Fabric and their Relations to Mechanical Properties of Granular Material", Soils and Foundation JSSMFE, Vol. 12, No. 1, pp. 17-36.

Oda, M. (1972), "The Mechanism of Fabric Changes During Compressional Deformation of Sand", JSSMFE, Vol. 12, No. 2, pp. 1-18.

Oda, M., Minami, K., and Onoder, T. (1976), "Shear Strength of Undisturbed Sample of Decomposed Granite Soil", JSSMFE, Vol. 16, No. 1, pp. 17-26.

Phool Chand (1988), "Effect of Stress History on Strength and Compressibility of Sands", M.Tech. Thesis, Department of Civil Engg., IIT Kanpur, India

Powers, M.C. (1953), "A New Roundness Scale for Sedimentary Particles", Journal Sedimentary Pet. Vol.23, No.2, pp. 117-119.

Ramamurthy, T. (1969), "Crushing Phenomenon in Granular Soil," Journal of INS of SM&FE, Vol.8, No.1-4, pp.67-86.

Ramamurthy, T. and Lal R.S. (1970), "Influence of Crushing on Properties of Badarpur Sands", Journal of INS. of SM & FE Vol. 9, No. 1-4, pp. 305-322.

Ramamurthy, T. and Kanitkar, V.K. (1972), "Elastic Compression of Sands Under High Isotropic Consolidation Stresses", Proc. Symposium on Strength and Deformation Behaviour of Soils, Bangalore, pp. 115-120.

Robertson, P.K. and Campanella, R.G. (1983), "Interpretation of Cone Penetration Tests. Part I: Sand", Canadian Geotechnical Journal, Vol.20, pp. 718-733.

Robertz, J.E. and De Souza, J.M. (1958), "The Compressibility of Sands", Proc. ASTM, Vol. 58, pp. 1269-77.

Sahu, J. (1988), "Model Studies on Sands with Different Angularity and Mineralogy", M. Tech. Thesis, Department of Civil Engineering, IIT Kanpur.

Singh, P. (1981), "The Stress Strain Behaviour of Anisotropically Consolidated Ganga Sand", M. Tech, Thesis, Department of Civil Engineering, I.I.T. Kanpur, India.

Terzaghi, K. (1925), "Principal of Soil Mechanics: VI - Elastic Behaviour of Sand and Clay", Engineering News Record, Vol. 95, No. 25, pp. 987-90.

Terzaghi, K. (1931), "The Influence of Elasticity and Permeability on Swelling of the Two Phase Systems", in Colloidal Chemistry (J. Alexander Ed.) Vol. III, Chemical Catalog Co. New York pp. 65-88.

Terzaghi, K. and Peck, R.B. (1948), "Soil Mechanics in Engineering Practice", John Wiley and Sons, Inc. New York.

Twenhofel (1950), "Principles of Sedimentation", Mc Graw-Hill Book Co. Inc. New York, pp. 302-311.

Uesugi, M. and Kishida, H. (1986), "Influential Factors of Frictional Between Steel and Dry Sands", Soil and Foundation, JSSMFE, Vol. 26, No. 2, pp. 36-46.

Vaid, Y.P., Chern, T.C. and Tumi, H. (1985), "Confining Pressure Grain Angularity and Liquefaction", ASCE Journal of Geotechnical Engineering, Vol. 111 No. 10, pp. 1229-1235.

Vesic, A.B. (1963), "Bearing Capacity of Deep Foundation in Sand", Highway Research Record, No. 39, HRB, Washington, D.C. pp. 112-153.

Vesic, A.B. and Barksadale, L.D. (1963), "On Shear Strength of Sand at High Pressure", Report of Soil Mechanics Laboratory, Georgia Institute of Technology.

Vesic, A.B. and Clough, G.W. (1968), "Behaviour of Granular Material Under High Stresses", Journal SMFE, ASCE Vol. 94, No. SM3, pp. 661-688.

Wadell, H. (1932), "Volume Shape and Roundness of Rock Particles" Journal Geol. Vol. 40, pp. 443-451.

Winterkorn, H.F. and Fang, H.Y. (1986), "Foundation Engineering Handbook", Galgatia Book Source Publishers, New Delhi.

Youd, T.L. (1973), "Factors Controlling Maximum and Minimum Densities of Sands", ASTM, STP 523, pp. 98-112.

Yudhbir (1978), "Engineering Geology Aspects of Earth Structures", Proc. of GEOCON - India, Conf. on Geotechnical Engineering, Vol. II, pp. 9-21.

Yudhbir and Rahim A. (1987), "Compressibility Characteristics of Sands", Proc. 9th South East Asian Geotechnical Conference, Bangkok, Thailand, Vol. 1, pp. 483-494.

BIBLIOGRAPHY

Aschembrenner, B.C. (1956), "A New Method of Expressing Particle Sphericity" Journal of Sed. Pet. Vol. 26, pp. 75-89.

Bardon, L. and Proctor, D.C. (1971), "The Strength of Granular Material" Canadian Geotechnical Journal, Vol. 8, pp. 372-383.

Bishop A.W. and Henkel, D.J. (1962), "The Measurement of Soil Properties in the Triaxial Test", Edward Arnold Ltd. London, Second Edition.

Bishop, A.W. (1965), "Triaxial Tests on Soil at Elevated Cell Pressures", Proc. 6th Int. Conf. on SMFE, Montreal Vol. 1, pp. 170-174.

Bishop, A.W. (1966), "The Strength of Soils as Engineering Materials", Geotechnique, Vol. 16, No.2, pp.21-128

Bowden, F.P. and Tabor, D. (1950), "The Friction and Lubrication of Solids", 1st Ed. Clarendon Press, Oxford.

Bridgeman, P.M. (1918), "The Failure of Cavities in Crystals and Rocks Under Pressures", American Journal of Science, Vol. 45, pp. 243-268.

Bridgeman, P.M. (1953), "Studies in Large Plastic Flow and Fracture", London, McGraw Hill Publication Co.Ltd.

Charles J.A. and Watts, K.S. (1980), "The Influence of Confining Pressure on the Shear Strength of Compacted Rockfill", Geotechnique Vol. 30, Vol. 4, pp. 353-367.

Conforth, D.H. (1974), "Prediction of Drained Strength of Sands from Relative Density Measurements", Evaluation of Relative Density and its Role in Geotechnical Projects Involving Cohesionless Soils, ASTM, STP 523, pp. 281-303.

Cox, E.P. (1927), "A Method of Assigning Numerical and Percentage Values to the Degree of Roundness", Journal Paleon, Vol. 1, pp.179-183.

De Beer (1963), "The Scale Effect in the Transposition of the Results of Deep Sounding Tests on the Ultimate Bearing Capacity of Piles and Caisson Foundation," Geotechnique Vol. 13, No.1.

Dikin, E.A. (1973), "Influence of Grain Shape and Size Upon the Limiting Porosities of Sands", ASTM, STP, 523.

Dobkin, J.E., Jr. and Folk, R.L. (1970), "Shape Development on Tahitei-Nui" Journal Sed. Pet. Vol. 40, pp. 1167-1203.

Folk, R.L. (1955), "Student Operator Error in Determination of Roundness, Sphericity and Grain Size", Journal Sed. Pet. Vol. 25, pp. 297-301.

Griggs, D.T., Turnner, F.J. and Heard, H.C. (1960), "Deformation of Rocks at 500 to 800°C," Rock Deformation Memoir 79, Geological Society of America.

Griffith, J.C. (1967), "Scientific Method in Analysis of Sediments", New York, McGraw Hill Book Co.

Hall, E.B. and Gordon, B.B. (1963), "Triaxial Testing Using Large Scale Pressure Equipment, ASTM, No. 361, pp. 315-328.

Hardin, J., Borg, I., Fredman, M. and Higgs, D.V. (1960), "Experimental Deformation of St. Peter Sand: A Study of Cataclastic Flow", Rock Deformation Memoir 79, Geological Society of American.

Hentengi, M. and Mc Donald, P.H. Jr. (1958), "Contact Stresses Under Combined Stresses and Twist," Journal of Appl. Mech. Vol. 25, pp. 360-401.

Hendron, A.J. Jr. (1963), "The Behaviour of Sand in One-Dimensional Compression", Ph.D. Thesis, Department of Civil Engg. University of Illinois (Urbana), USA.

Holtz, W.G. and Gibbs, H.J. (1956), "Triaxial Shear Test on Previous Gravely Soils," ASCE, Jour. of SMFE Division, Vol. 82, SM1.

Kjaernsli, B and Sande, A. (1963), "Compressibility of Some Coarse Grained Material", Proc. of European Conf. on SMFE, Vol. 1, pp. 245-251.

Koerner, R.M. (1968), "The Behaviour of Cohesionless Soils Formed From Various Minerals", Ph.D. Thesis Duke University.

Lees, G. (1964), "The Measurement of Particle Shape and Its Influence in Engineering Materials," Journal of British Granite and Whinstone Federation, Vol. 4, No. 2.

Leslie, D.D. (1963), "Large Scale Triaxial Tests on Gravity Soils", Proc. 2nd Pan American Conference on Soil Mechanics and Foundation Engineering, Sao Paulo, Brazil Vol. 1.

Leslie, D.D. (1975), "Shear Strength of Rockfill", Physical Properties and Engineering Study, No. 526, South Pacific Division, Corps of Engineer Laboratory, Sausalito, California.

Lo, K.Y. and Roy, M. (1973), "Response of Particulate Materials at High Pressures", Soils and Foundations, JSSMFE, Vol. 13, No.1, pp. 61-76.

Lowrison, G.C. (1974), "Crushing and Grinding, The Size Reduction of Solid Materials", Butterworth and Co. (Publishers) Ltd. London.

Marsal, R.J. (1965), "Discussion of Shear Strength", Proc. of 6th Int. Conf. on SFE, Montreal Vol. 3, pp. 310-316.

Mindlin, R.D. and Deresiewics, H. (1953), "Elastic Sphere in Contact Under Varying Oblique Forces", Journal of Appl. Mech. Vol. 20, pp. 327-344.

Pentland, A. (1922), "A Method of Measuring the Angularities of Sands", Royal Society Canada Proc. and Trans. (Ser.3), Vol. 21, Appendix C, Title and Abstracts.

Pettijohn, F.J. (1949), "Sedimentary Rocks", Harpers and Brothers, New York.

Rowe, P.W. (1955), "A Stress-Strain Theory for Cohesionless Soil with Application to Earth Pressure at Rest and Moving Walls", Geotechnique Vol. 4, pp. 70-80.

Russel, R.D. and Taylor, R.E. (1937), "Roundness and Shape of Mississippi River Sands", Journal of Geology, Vol. 45, pp. 225-267.

Schultz, E and Mousa, A. (1961), "Factors Affecting the Compressibility of Sands", Proc. 5th Int. Conf. SMFE, Vol.1, pp. 335-340.

Smith, J.C. and Liu, C.K. (1953), "Stresses Due to Tangential and Normal Loads on an Elastic Solid with Application to Some Contact Stress Problem", Journal of Appl. Mech, Vol. 20, pp. 157-166.

Sneed, E.D. and Folk, R.L. (1958), "Pebbles in the Lower Colorado River, Texas, a study in Particle Morphogenesis", Journal of Geol. Vol. 66, pp. 114-150.

A 141992



A141992